5-1978

Autecology of Selected Genera of Mississippian, Permian and Triassic Ammonoids: Analysis of Coiling Geometries

Edward Ellis Chatelain
Utah State University

AUTECOLOGY OF SELECTED GENERA OF MISSISSIPPIAN, PERMIAN AND TRIASSIC AMMONOIDS: ANALYSIS OF COILING GEOMETRIES

by

Edward Ellis Chatelain

A thesis submitted in partial fulfillment
of the requirements for the degree

of

MASTER OF SCIENCE

in

Geology

UTAH STATE UNIVERSITY
Logan, Utah

1978

ACKNOWLEDGMENTS

The writer wishes to thank Dr. Richard R. Alexander for his aid in the reconnaissance, research, and preparation of this study. Dr. Alexander, along with Dr. Peter Kolesar and Dr. Robert Q. Oaks Jr., reviewed the manuscript and presented suggestions for its improvement. The writer also wishes to thank Dr. Donald Fiesinger and Bill Perkins for their extensive work in determinations of phosphate percentages, Dr. Peter Kolesar for his patient assistance of x-ray-diffraction technique, and Dr. Clyde T. Hardy for his timely encouragement.

Special thanks go to my family: my father, for his immeasurable patience in field collecting, supplying transportation, and critical suggestions toward this study; my mother, for typing into all hours of the night and morning; my sister and her husband, for the use of their collections of fossils; my brother, who aided in compilation and plotting of the data; and to Margie Baird, for typing, field collecting, encouragement, and moral support.

Edward Ellis Chatelain

TABLE OF CONTENTS

LIST OF TABLES

LIST OF FIGURES

LIST OF FIGURES (Continued)

LIST OF FIGURES (Continued)

LIST OF FIGURES (Continued)

LIST OF FIGURES (Continued)

LIST OF FIGURES (Continued)

ABSTRACT

Autecology of Selected Genera of Mississippian, Permian and Triassic Ammonoids: Analysis of Coiling Geometries

by

Edward Ellis Chatelain, Master of Science

Utah State University, 1978

Major Professor: Dr. Richard R. Alexander
Department: Geology

Ammonoids were collected from the Chainman Formation (Mississippian) of southeastern Nevada and southwestern Utah, the Phosphoria Formation (Permian) of southeastern Idaho and westernmost Wyoming, and the Thaynes Formation (Triassic) of northeastern Nevada and southeastern Idaho. The collections are interpreted to represent unwinnowed, untransported death assemblages of ammonoids which were subject to chemical conditions of the nekto-benthic environment. Associated lithologies were sampled and geochemically analyzed for content of phosphate and organic matter. Ammonoid fossil collections, combined with ammonoids illustrated in the literature, were subjected to the graphical W and D analysis of Raup (1967). The basic parameters involved in the description of shell-coiling geometry are whorl expansion rate, W, and the distance of the generating curve from the axis of coiling of the shell, D. Values of W determined range from 1.32 to 3.96, which correspond to slight and rapid increases in whorl height during coiling. Values of D determined

range from 0.02 to 0.55, which correspond to extremes of involute and evolute coiling geometries, respectively.

Body chamber length corresponds with shell coiling geometry. Values determined in this study range from 10° to 540°. Corresponding W values are 3.96 and 1.50, whereas corresponding D values are 0.02 and 0.40, respectively. Average body chamber length in analyzed ammonoids is observed to decrease from 297° to 209° from Mississippian to Triassic time. Increase in apertural area accompanied this trend, and a possible consequence was that a greater range of prey sizes was afforded ammonoids with shorter body chambers.

Life-orientation, described as the angle between the apertural plane and the gravitational vector, is calculated entirely on shell form and other geometrical considerations. Recent observations concerning Nautilus, combined with fossil evidence of epizoan encrustation suggest that ammonoids had an ability to control orientation, which is not observed from preservable morphology.

From Mississippian to Triassic time, no trends in reconstructed life-orientation can be substantiated, based solely on W and D values.

Rotational stability during directed locomotion is important for conservation of the energy budget of this nektonic carnivorous organism. This property is calculated by the distance between the center of buoyancy and the center of gravity of the ammonoid. Values determined range from .04 (very unstable) to .16 (very stable). Corresponding W values are 1.50 and 4.00 where corresponding D values are 0.20 and 0.02, respectively. A trend toward increasing average rotational stability (.07 to .10) is noted for ammonoids from Mississippian to Triassic time.

Efficiency in the utilization of calcium carbonate is the ratio of internal volume of the shell to volume of shell material. Values determined range from 5.80 to 7.25. Corresponding W values are 4.00 and 1.50, corresponding D values are 0.02 and 0.54, respectively. Abundant ammonoids found in black, phosphatic limestones rich in organic matter have an average efficiency value of 6.2. Abundant ammonoids from corresponding light-colored crystalline carbonates have an average efficiency value of 6.02, and indicate no correlation between efficiency and abundance.

Size-frequency distributions are utilized in recognition of opportunistic species of ammonoids. High numerical abundance, high mortality rate of juveniles, small size and conservation of calcium carbonate typifies the paleo-opportunistic species Cravenoceras, Psuedogastrioceras and Ophiceras.

Biovolume-relative abundance distributions are useful in discerning the carrying capacity of the habitat both in number of individuals and species diversity. A large area under the biovolume-relative abundance profile indicates diversification under optimum environmental conditions; a small area under the profile indicates colonization of a stressful habitat. The Chainman, Phosphoria and Thaynes (Columbites Zone) Formations have ammonoid assemblages which show small areas under the biovolume-relative abundance profile, characteristic of anoxic environmental stress. The Permian stratigraphic units correlative with the Phosphoria Formation have ammonoid assemblages which show large areas under the profile and the associated lithologies, i.e., light-gray, crystalline carbonates, suggest environments which could support a

diversified ammonoid fauna, including large-sized species. Ontogenetic variation produces changes in the body chamber length, life orientation, rotational stability, and utilization of calcium carbonate of the analyzed genera of ammonoids. These ontogenetic variations usually resulted in the development of more involute shell-coiling geometries. Corresponding size-frequency distributions suggest increased mortality rates during ontogeny for some genera (Paracravenoceras, Medlicottia) which show decreasing efficiency in the utilization of calcium carbonate.

(182 pages)

INTRODUCTION

Ammonoids are found in lithologies which represent a wide variety of sedimentary environments (Miller and others, 1957, p. L 22). Although classified as nekto-benthos, fossil evidence suggests that ammonoids did come in contact with the sea floor during life. Fenton and Fenton (1958, p. 194) regarded broad, smooth, spheroidal shells of the Mississippian and Permian as typical crawling forms. Thus, the chemical environment of the sea floor could influence selection in the morphology of these nekto-benthic organisms. Recognition of the possible influence of the substrate on the ammonoid morphology allows ammonoid assemblages to be compared with their associated lithology with the intention of establishing correlations between former bottom environment and preserved shell form.

The Mississippian Chainman Formation of Nevada and Utah contains prolific numbers of Cravenoceras, with very rare occurrences of other associated ammonoid genera. The Chainman Formation is a gray to black shale, with thin beds and stringers of black limestone, which are often high in phosphate and organic matter.

The Permian Phosphoria Formation of Idaho and Wyoming contains prolific numbers of small Pseudogastrioceras, Spirolegoceras and uncommon, small representatives of Medlicottia. The Meade Peak Phosphatic Shale Member, which contains these ammonoids, is a black, phosphatic shale with black, phosphatic, dolomitic limestone nodules and concretions.

The Triassic Thaynes Formation of Idaho and Nevada contains a thin layer of black, very fine-grained limestone, with a significant amount of phosphate. Within this layer, designated the Columbites Zone (Smith, 1832, A11) are prolific numbers of small Ophiceras, common species of Columbites, and uncommon specimens of Meekoceras and Celtites.

Each of the above ammonoid assemblages are similar, in that large numbers of small ammonoids are found, usually belonging to a one or two species. Furthermore, the associated lithologies have a black color indicative of a high organic content and display weight loss when bleached with 3% hydrogen peroxide. Ammonium molybdenate tests reveal appreciable concentrations of a mineral identified as fluorapatite by X-ray diffraction.

Under similar paleoecological conditions, different ammonoid genera were able to dominate an assemblage. One obvious and common denominator among these dominant but different taxa is the development of similar ammonoid coiling geometries. In his analysis of ammonoid shell-coiling geometries, Raup (1967) evaluated several ammonoid characteristics, namely the body-chamber length, life orientation, rotational stability of the conch, and the efficiency of calcium-carbonate utilization in construction of the shell. Chamberlain (1976) also calculated the relative drag coefficients of shells utilizing various shell-coiling geometries. These investigations foster the hypothesis that advantages afforded a particular coiling geometry should correlate directly with relative abundances of the preserved taxa.

To test this hypothesis, ammonoid genera with distinct coiling geometries were examined from a spectrum of lithologies, and relative abundances noted. The quantitative techniques formulated by Raup (1967) facilitate evaluation of the adaptive significance of various coiling geometries. In combination with environmental inferences from the associated lithologies, his quantitative techniques are employed in this investigation with the objective of reconstructing the functional morphology and varying adaptive values of a spectrum of coiling geometries among ammonoids from the formations mentioned above.

PARAMETERS DESCRIBING COILING GEOMETRIES OF AMMONOID SHELLS

Ammonoid shells display a wide variation in shape and size. Raup (1967), however, was able to simulate by computer (Figures 1 and 2) the entire field of known planispiral ammonoids, based on only a few, simple parameters. Only planispiral ammonoids were studied, because variations in shape are due mostly to dimensional differences within the coiling which is confined to one plane.

Four parameters completely describing the total range of variation in planispiral ammonoid coiling geometries were obtained using the different linear dimensions of the ammonoid shell as variables (Raup, 1967, p. 44).

These variables are defined as follows and will hereafter be referred to by their lower case designation: a--height of last whorl; b--width of last whorl; c--distance to umbilicus from apertural whorl shoulder; d--distance from umbilicus to the shell venter of the apertural whorl; e--distance from umbilicus to the shell venter of the preceding whorl; f--distance to umbilicus from preceding whorl shoulder and g--the height of the preceding whorl. Only a, b, d and e will be utilized in this study. Umbilicus width, utilized in some investigations, also will be ignored.

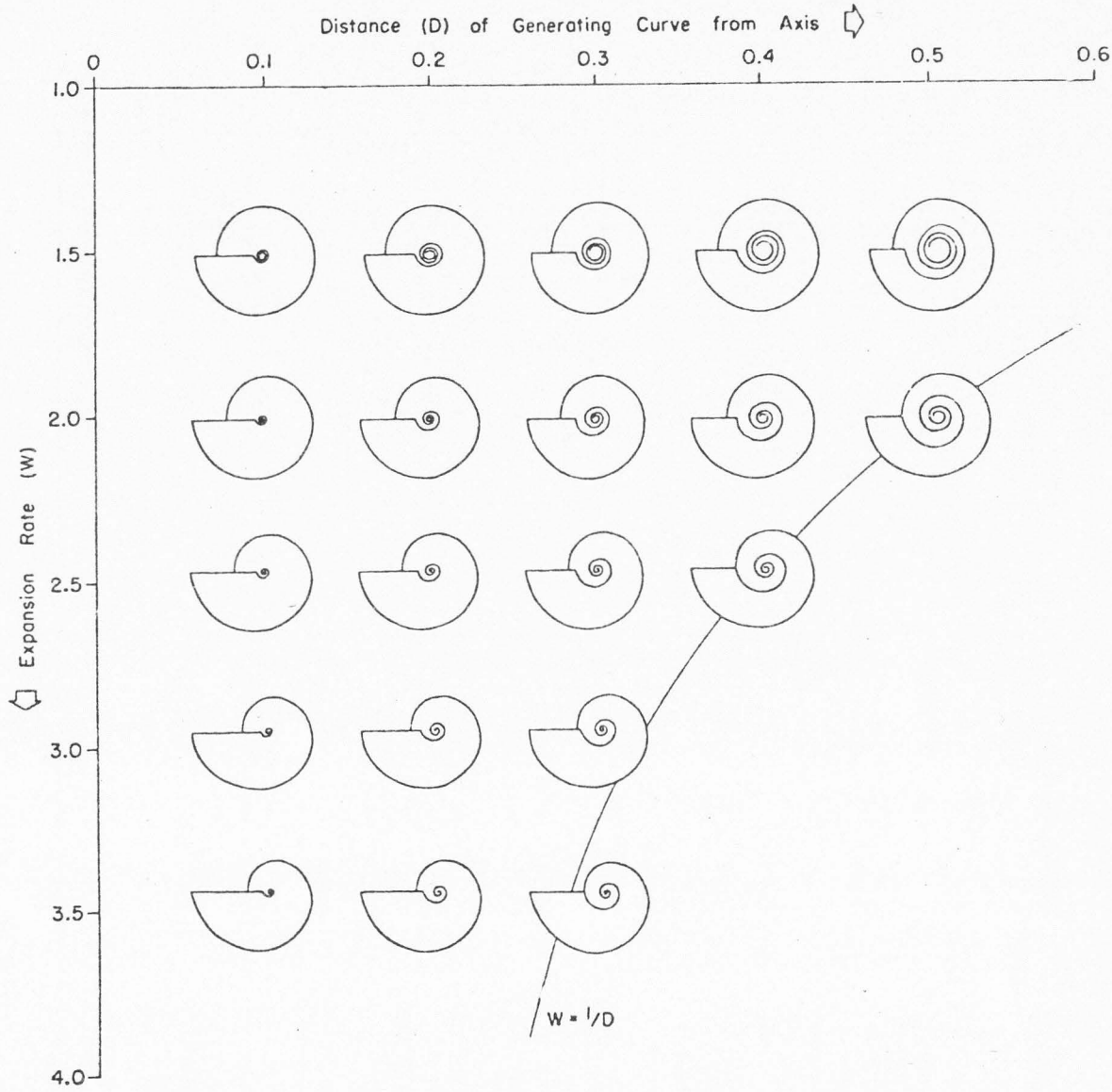

Figure 1. The ammonoid field of shell-coiling geometries, umbilical view. (After Raup, 1967, p. 47, Figure 3)

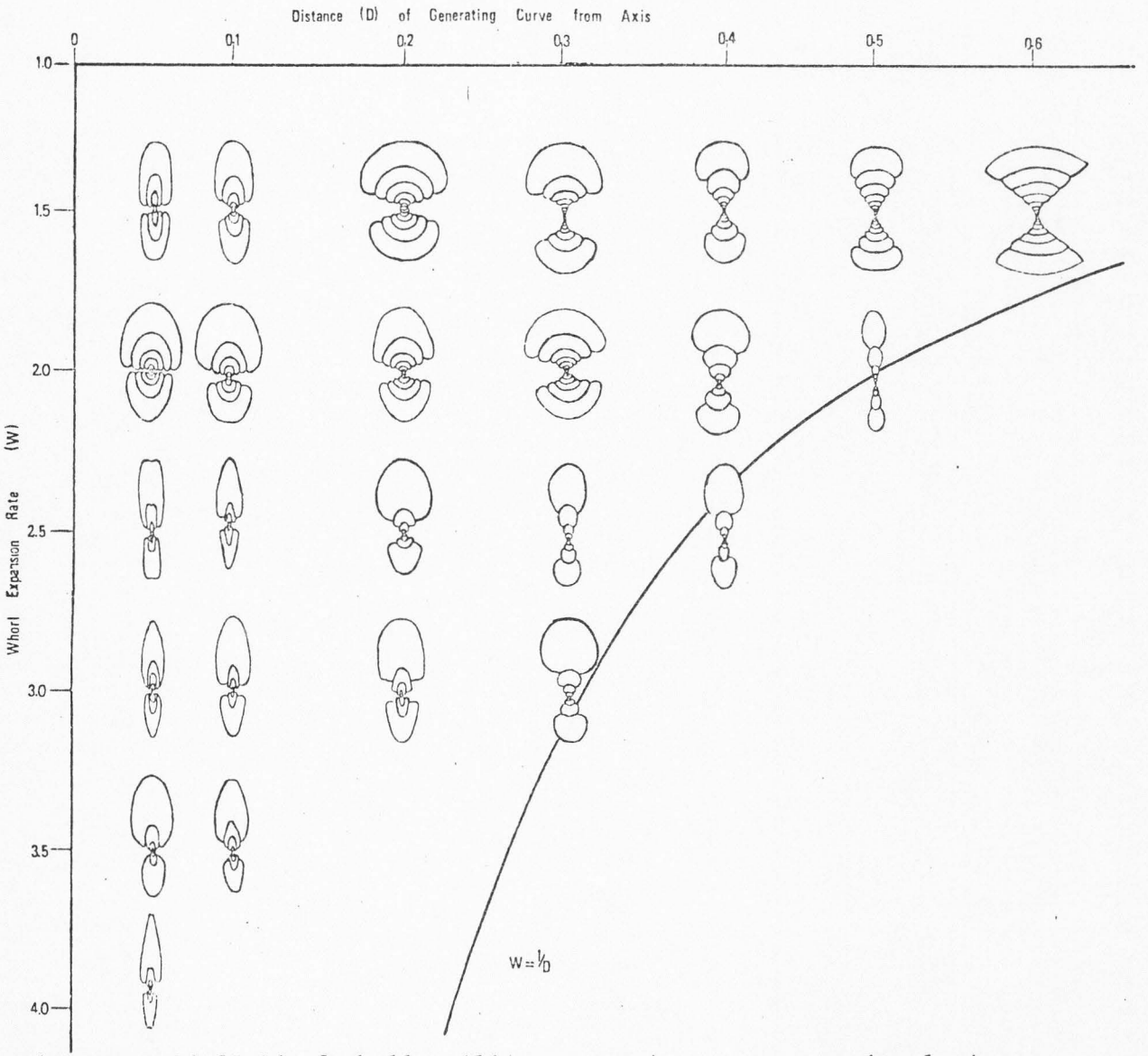

Figure 2. The ammonoid field of shell-coiling geometries, cross-sectional view.

Whorl expansion rate (Raup, 1967, p. 45), W, is defined as the quantity $(d/e)^2$ (see Figure 3). The quantity is squared so as to emphasize the expansion rate differences between the two halves of the shell (e.g., Figure 4A). The visual appearance of the shell is altered only gradually by changes in W (Figures 1, 2, 4). Shells with a nearly circular outline to the venter and many volutions characteristically have low W values, whereas shells with huge apertures and disproportionately small preceding whorls characteristically have high W values.

The distance of the generating curve from the axis of coiling, D, is the other important parameter defining the coiling geometry (Raup, 1967, p. 44). D is computed as $\frac{d \text{ minus } a}{d}$ (Figure 3). The calculation measures expansion of the apertural whorl relative to that of the entire whorl expansion from the apertural shell venter to umbilical center. Variations in D are visibly apparent (Figure 4B). Low values are characteristic of involute shells, which have short body chambers and more buoyant shells (Moore et al., 1952, p. 386). High D values describe evolute shells, in which body chamber length can approach a volution and one-half (= 540 degrees).

The cross-sectional-whorl inflation or depression, S (Raup, 1967, p. 46), and the height of the umbilical shoulder at its greatest width, F (Chamberlain, 1976, p. 540), are correlated (Figure 3). S is computed as the ratio of the apertural whorl width to apertural whorl height, $\frac{b}{a}$. F is computed as the distance from the apertural whorl venter to the greatest apertural whorl width divided by the total shell

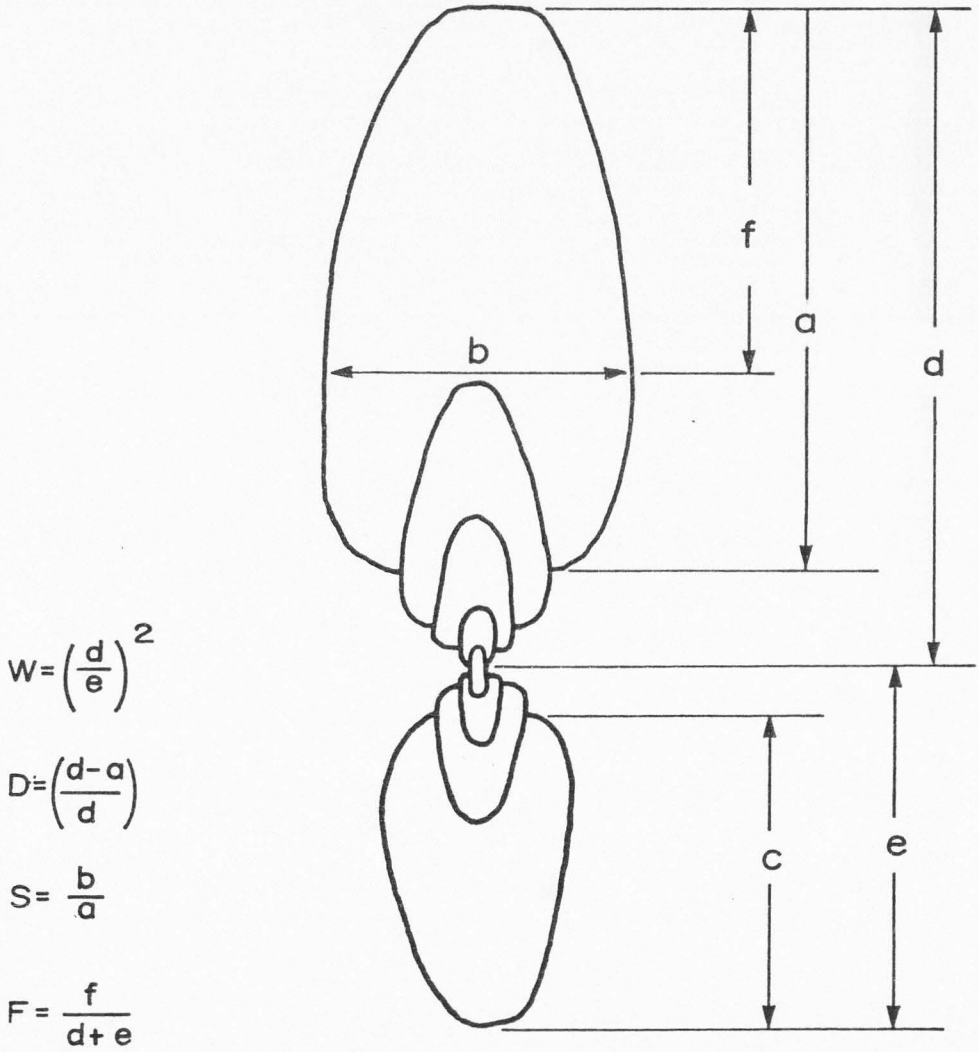

Figure 3. Parameters of the ammonoid shell Trachyceras lecontei (After Smith, 1927, p. 182, Plate 45). (W, D, and S parameters after Raup, 1967, Figure 1, p. 44; F parameter after Chamberlain, 1976, Figure 1, p. 542.)

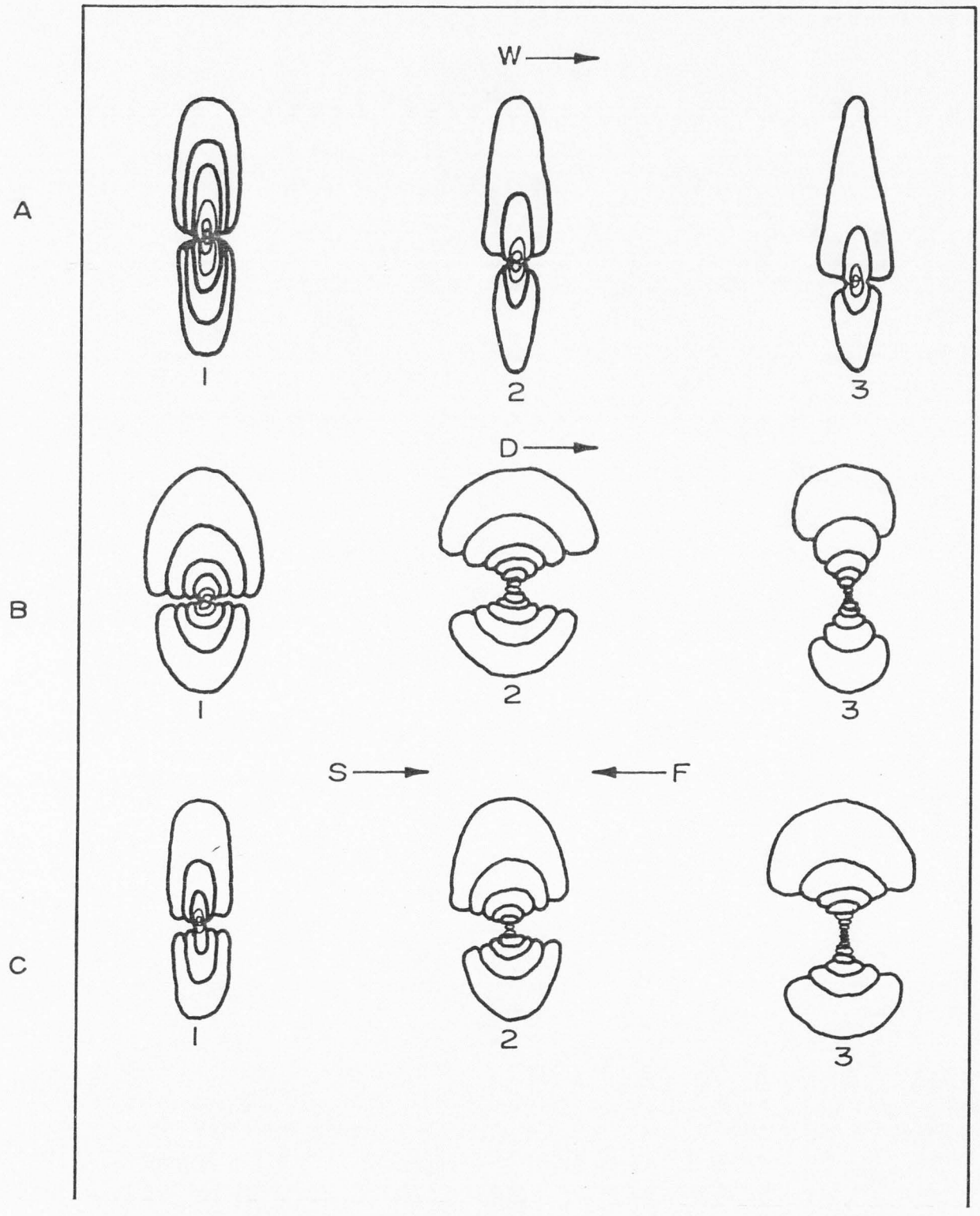

Figure 4. Variations in the parameters W, D, and S (After Miller and Furnish, 1940; Nassichuk and Others, 1965; Peterson, 1975; Saunders, 1973; and McCaleb, 1968)

diameter, f/d + e. S and F are observed to be inversely proportional, although the relationship is not linear (Figure 4C). Each possible W and D value has a great many possible S and F values.

Because a coordinate system plotting S and F values as well as W and D values would require a four-dimensional representation, and because of the lack of data on S and F, the two-dimensional diagram of Raup (1967, p. 47, Figure 3), which has W as the abscissa and D as the ordinate, is utilized in this investigation.

ANALYZED AMMONOID ASSEMBLAGES

Ammonoids were collected from several different localities from Mississippian, Permian, and Triassic beds exposed in Nevada, Utah, Idaho and Wyoming. A wide range of associated lithologic types are represented. The W, D, and S shell-coiling geometry parameters were calculated from shell measurements and plotted, size-frequency diagrams were constructed, and biovolume-species abundance distributions were calculated and graphed. Associated matrix was analyzed by x-ray diffraction (Table 1). Organic matter content, fluorapatite (phosphate) content, and insoluble residue content were also determined. In addition, a comprehensive literature search was undertaken to supply the same kinds of information as above for collecting localities which were either of secondary importance or too remote to facilitate field examination by the author. The following is a description of these localities, their representative ammonoid faunas and associated lithologies. Accessibility of visited collecting localities can be gleaned from the respective locality maps.

Mississippian

Mississippian ammonoid collecting localities in the western United States are restricted areally and numerically (Figure 5), although the Chainman Shale of Nevada and Utah, and equivalent Perdido Formation of California contain prolific assemblages of *Cravenoceras*.

Table 1. Key for lithologies associated with analyzed ammonoid genera

Geologic Period	Lithologic Number	% Organic	% $Ca_3(PO_4)_2$	Lithologic Description	Stratigraphic Unit
Miss.	1	ND	23.50*	Black, phosphatic, nodular limestone	Chainman Formation
Miss.	2	0.74*	0.70*	Black,fine-grained,coquinoid limestone	Chainman Formation
Miss.	3	ND	ND	Dark gray,fine-grained,coquinoid limestone	Perdido Formation
Miss.	4	ND	4.5*	Arenaceous,ferruginous,claystone concretions	Chainman Formation
Permian	5	ND	ND	Dark gray,coarsely crystalline limestone	Wolfcamp Formation
Permian	6	ND	ND	Interbedded, fossiliferous shales and ls.	Florena, Neva Fms
Permian	7	ND	ND	Shales, marls, and limestones	Admiral, Clyde Fms
Permian	8	ND	ND	Gray, thick-bedded limestone	Hueco Formation
Permian	9,13	0.95*	2.50*	Black,phosphatic,dolomitic limestone	Phosphoria Formation
Permian	10	0.73	0.13[a]	Black,nodular,granular limestone	Bone Spring Formation
Permian	11	ND	ND	Shaly and marly ls, sandy to conglomeratic limestone	Leonard Formation
Permian	12	ND	ND	Marly dolomite	Blaine Formation
Permian	14	ND	ND	Light gray,oolitic,cherty limestone	Word Formation

Table 1. Continued

Geologic Period	Lithologic Number	% Organic	% $Ca_3(PO_4)_2$	Lithologic Description	Stratigraphic Unit
Permian	15	ND	ND	Blue-gray, massive & nodular limestone	Beds 10-17, Difunta section
Permian	16	ND	ND	Silicified, bioclastic limestone and argillaceous, dolomitized, bioclastic limestone	Cache Creek Series (near top)
Permian	17	ND	ND	Thin-bedded cherty ls, sandy ls, and ciliceous shale	Capitan Formation
Permian	18	0.34[b]	None	Thin to thick-bedded, fine-grained to granular ls. Gray to dary gray	Bell Canyon Formation
Permian	19	ND	ND	Black shale with hard, black limestone concretions	Beds 4-7 Difunta section
Permian	20	ND	ND	Black shale and conglomeratic graywacke	La Colorado Beds
Triassic	21	ND	1.50*	Thick-bedded, fine to coarsely crystalline, coquinoid limestone	Thaynes Formation
Triassic	22	0.75*	1.70*	Black, very fine-grained, nodular to concretionary limestone	Thaynes Formation

*determined in this investigation
ND not determined in this investigation

[a]Phillip B. King, 1948, Geology of the Southern Guadalupe Mountains, Texas, U. S. Geological Survey Professional Paper 215, p. 14.

[b]Ibid, p. 55

Figure 5. Mississippian ammonoid-collecting localities in Nevada and Utah.

Nearest ammonoid-bearing correlative units of this age are the Barnett Formation of Texas, and the Heath Formation of Montana (Miller and others, 1949, p. 611).

The Chainman Formation (Shale) was examined in detail by the author at two localities. At Kane Springs Wash in southeastern Nevada (Figure 6) (see also Section A of Webster, 1969, p. 56), two levels of ammonoids were sampled. From phosphatic limestone nodules, abundant crushed specimens of Cravenoceras merriami together with numerous nuculanoid pelecypods and some gastropods were found. One immature specimen of Pronorites sp. was found, but specimens of Eumorphoceras as reported by Webster (1969, p. 5) were not recovered. These sampled strata constitute Lithology 1 (Table 1). A bed in the upper level of the Chainman Shale of section A (Webster, 1969, p. 56) contains many large specimens of Cravenoceras hesperium, either entirely free of matrix, or as centers of quartz-claystone concretions. A poorly preserved specimen of Anthracoceras sp. also was recovered. The sampled strata of the upper level constitute Lithology 4 (Table 1). This level is readily traceable for one half mile or more at the original locality, and was found again several miles to the northeast along the front of the Meadow Valley Mountains (Figure 6).

Because of the high phosphate content observed (approximately 23%) in Lithology 1, the large average diameters of individuals recovered from Lithology 4, and the prolific number of specimens recovered from each, the Kane Springs Wash locality was selected for detailed analysis.

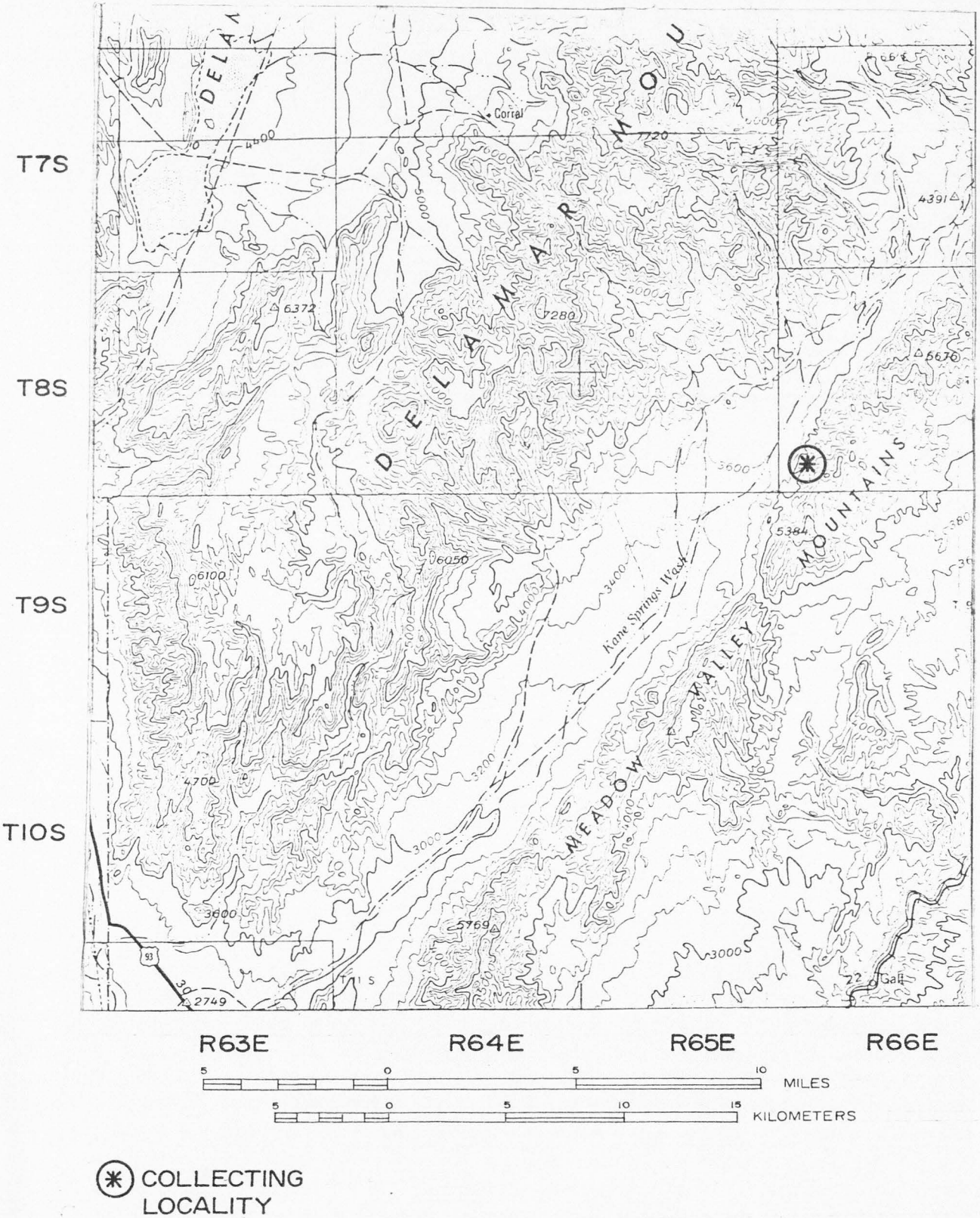

Figure 6. Ammonoid-collecting locality in the Mississippian Chainman Formation near Kane Springs Wash, Nevada.

The Confusion Range in central southwestern Utah (Figure 7) contains large outcrops of the Chainman Formation. Northeast of the Foote Range (Figure 7) a six inch layer of black, fine-grained, coquinoid limestone crops out discontinuously for about one-quarter mile. This layer is Lithology 3 (Table 1). Specimens of the rhynchonellid brachiopod Leiorhynchus dominate, but small specimens of ammonoids are found abundantly. These genera of ammonoids comprise the upper Eumorphoceras zone of Gordon, Hose and Repenning (1957 p. 1737) and include:

Cravenoceras merriami
C. hesperium
C. cf. C. friscoense
Pronorites sp.
Dimorphoceras sp.
Girtyoceras sp.

Eumorphoceras bisulcatum

This assemblage was chosen for analysis on the basis of abundance, and small average diameters of the ammonoids, as well as the fine-grained, black, carbonate lithology.

In the Panamint Range northwest of Death Valley (Figure 5), Gordon (1964, p. A2) found a similar but better preserved assemblage near Rest Spring. From a gray, fine-grained bed of limestone not over six inches thick (Lithology 2, Table 1) he obtained:

Cravenoceras merriami
C. richardsonium
Eumorphoceras paucinodom
Prolecanites (Rhiepicantes) sp.
Anthracoceras macalleristi
Delpinoceras californicum

Cravenoceras inyoense

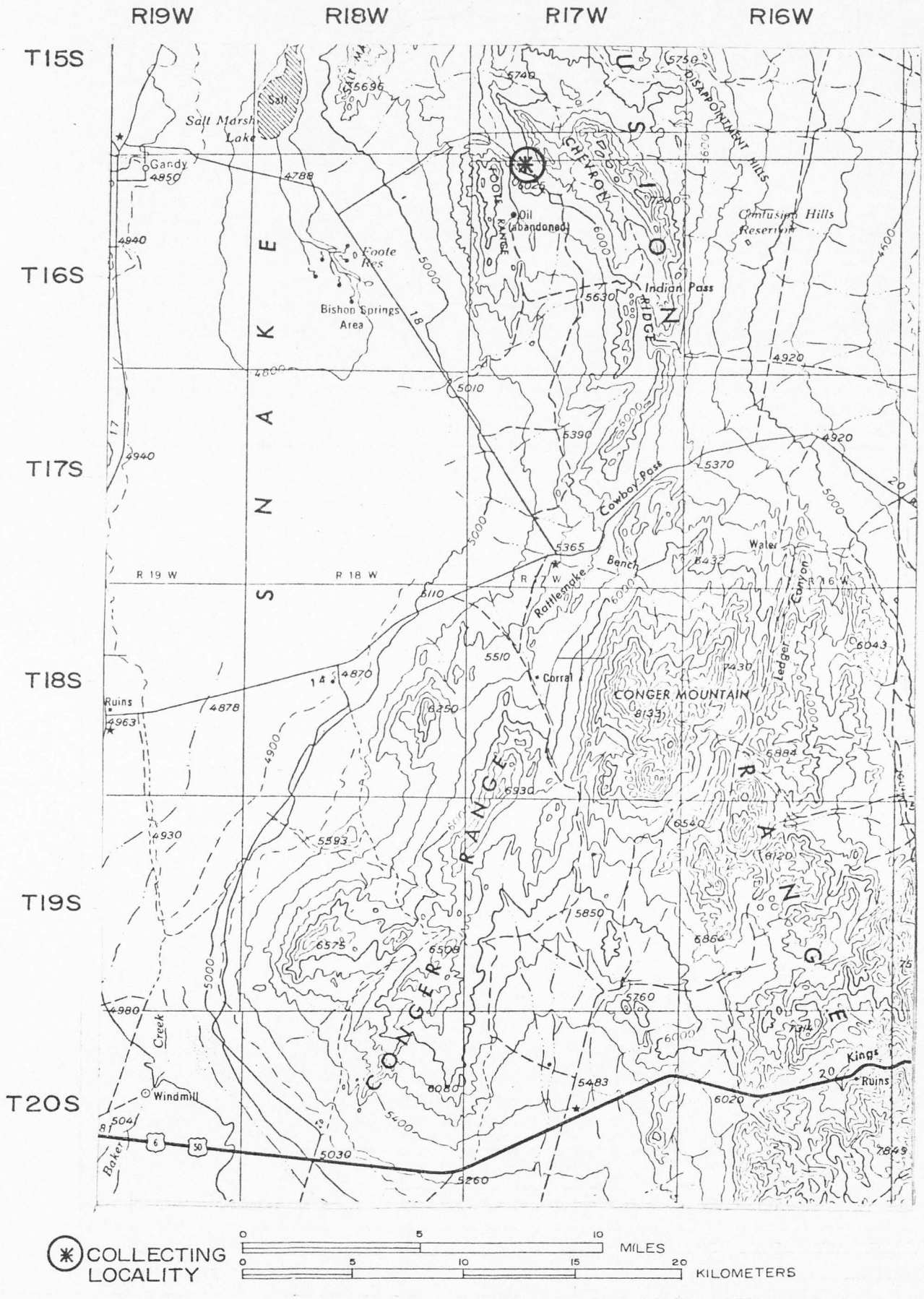

Figure 7. Ammonoid-collecting locality in the Mississippian Chainman Formation in the Confusion Range, Utah.

Higher in the section, presumably within the base of the Rest Spring Shale, Cravenoceras hesperium was recovered probably from ferruginous, claystone concretions. This locality is rather inaccessible, and because Gordon (1964) provided sufficient information, collecting at this locality was deemed unnecessary.

In east-central Nevada, Youngquist (1949a, p. 282; 1949b, p. 613) recorded a prolific ammonoid assemblage from three important localities. The associated lithology is reported to consist of limestone stringers, ribs, and nodules. The following were obtained from these localities (Figure 5):

Cravenoceras hesperium
C. merriami
C. richardsonium
C. nevadense
C. scotti
C. kingi
Eumorphoceras bisulcatum
Dimorpoceras humphreyi
Goniatites choctawensis
Girtyoceras meslerianum
Anthracoceras columbrellus
Epicanites cf E. loeblichi

Because of previous exhaustive collecting (over 3000 specimens sampled), these localities were not revisited. It is important to note, however, that relative abundances of the dominant taxon, Cravenoceras, in these assemblages are similar and all other faunal species are uncommon to rare. Although Goniatites choctawensis was collected in appreciable numbers (90 specimens), it is not a consistent element of the Cravenoceras assemblages elsewhere.

Permian

Permian ammonoid localities are scattered in the western United States. Miller and others (1957, p. 1057) described these localities in some detail. As mentioned in the Treatise (Miller and others, 1957, p. L22), scattered and singular occurrences of ammonoids can be indicative of post-mortem drift, and thus do not constitute an indigenous assemblage. These scattered and singular occurrences are not plotted on Figure 8. According to Miller and Cline (1957, p. 1057) the only abundant ammonoid faunas in the western United States are found in the Meade Peak Phosphatic Shale Member of the Phosphoria Formation of Idaho and Wyoming, and equivalent strata of Utah (Figure 9). From phosphatic, dolomitic limestone (Lithology 9, Table 1) they compiled the following composite list:

Stacheoceras bransonum	Peritrochia girtyi
S. sexolobatum	Spirolegoceras fischeri

Pseudogastrioceras simulator

Field collections from Coal, Layland and Raymond Canyons, Sublette Range, Wyoming, have enlarged this list, although representatives of Peritrochia and Stacheoceras were not recovered. From these localities in the Sublette Range, Wyoming (Figure 9), representatives

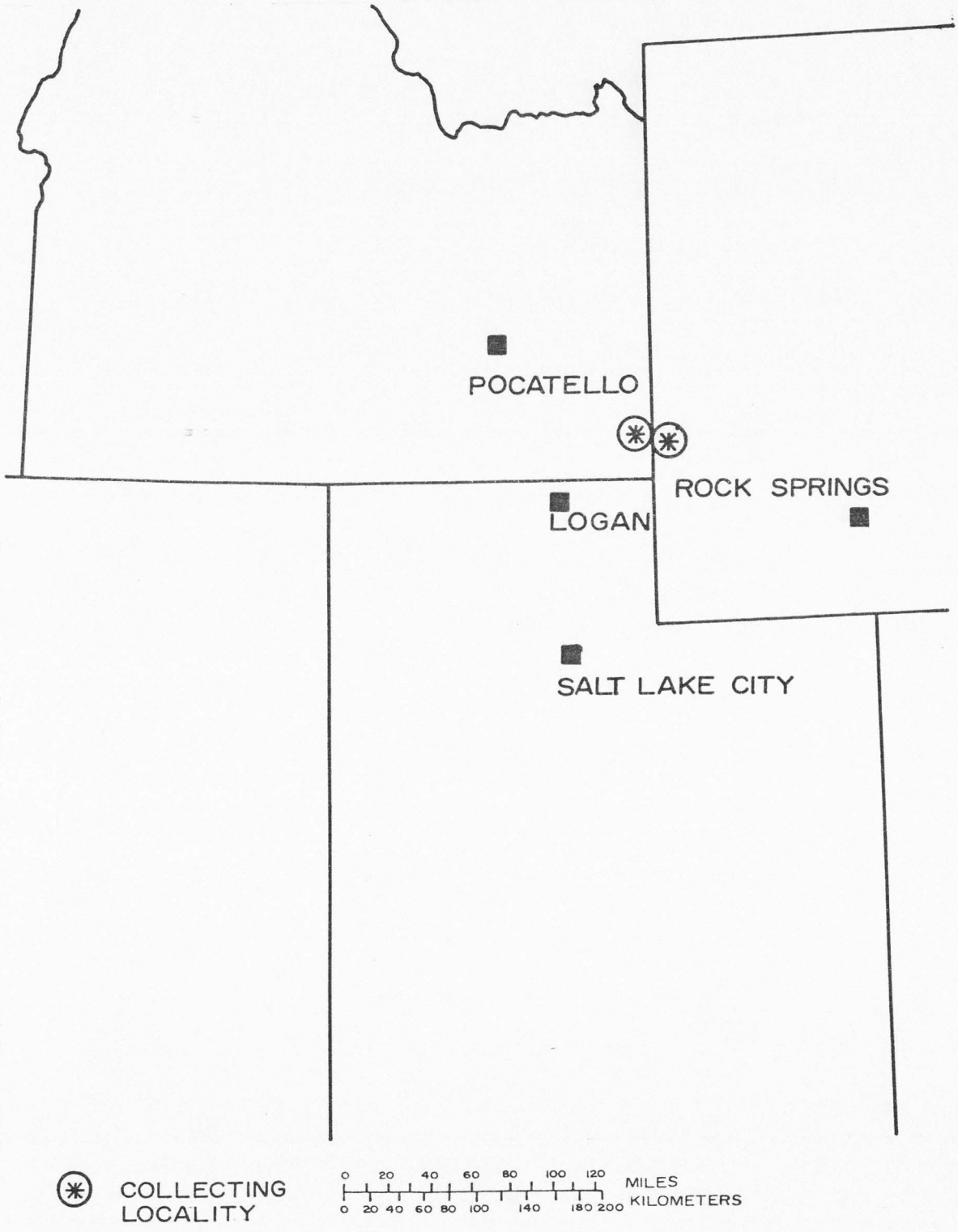

Figure 8. Permian ammonoid-collecting localities in Idaho and Wyoming.

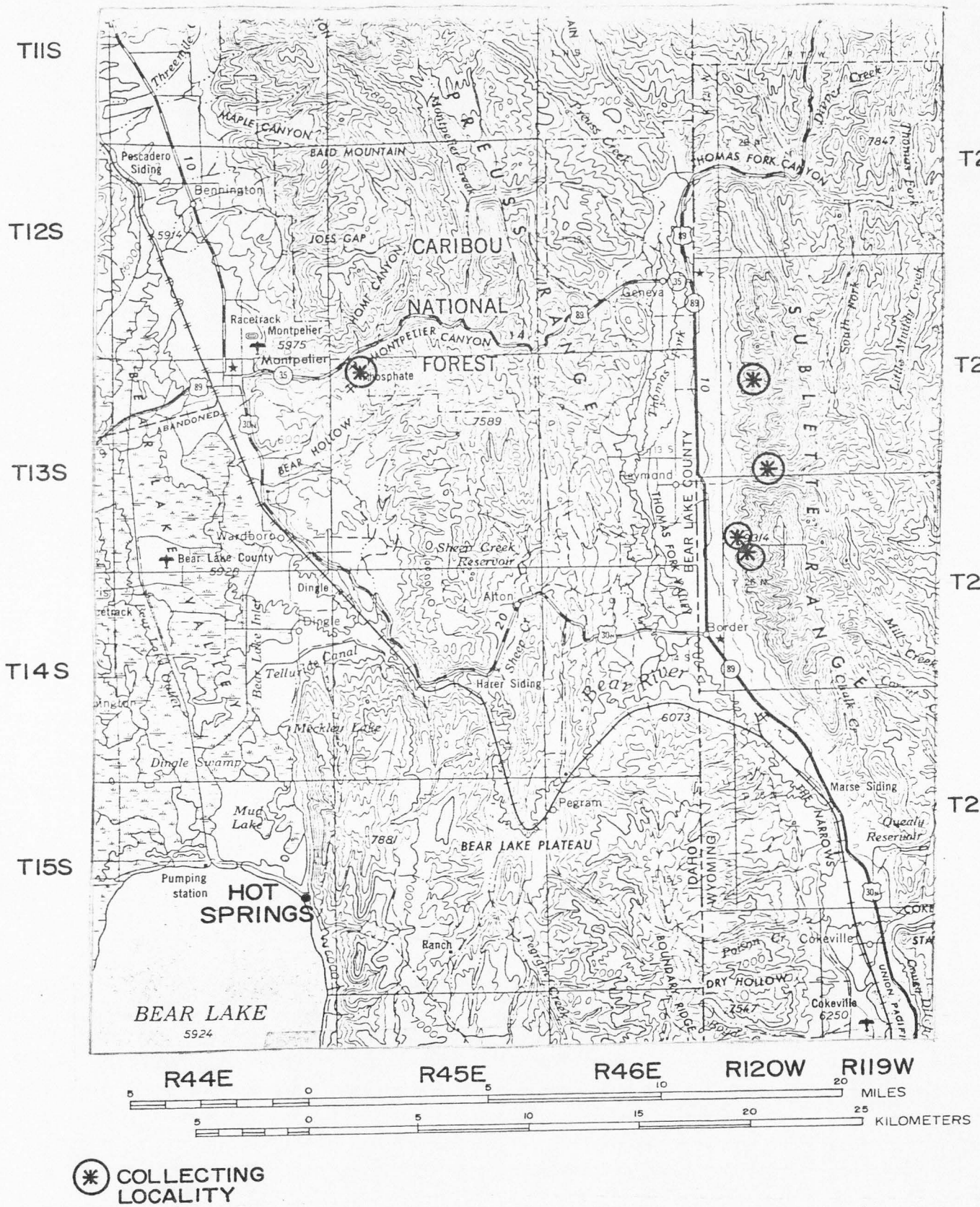

Figure 9. Ammonoid-collecting localities in the Permian Phosphoria Formation near Montpelier, Idaho, and in the Sublette Mountains, Wyoming.

of Medlicottia c.f. M. whitneyi and one large individual of Paragastrioceras c.f. P. serratum (Layland Canyon only) were discovered from the bed described by Girty (1910, p. 18), from Coal Canyon Section, bed 19, as "black and brown, thin-bedded, phosphatic shale, with limestone layers and large nodules at top; Gastrioceras simulator." At the old mine east of Montpelier, Idaho (Figure 9), associated with dark brown to black, phosphatic limestone nodules, Paragastrioceras sp. and Adrianites sp. were found along with numerous specimens of Spriolegoceras fischeri. The comparative abundances of these different genera, together with the high organic and phosphate content of their associated lithologies, warranted detailed analysis of this Permian assemblage.

Other Permian faunal assemblages subjected to the W-D analysis, which were not collected in the Phosphoria Formation outcrops, are described entirely from the literature. These assemblages are from outcrops in British Columbia, Canada, Coahuila, Mexico, and the southwestern United States (Figure 10). They were similarly selected on the basis of abundance, diversity and a wide variety of associated lithologies (Table 1).

Representing the Wolfcampian (Lower Permian) Series, is Lithology 5 (Table 1) consisting of a hard, brown-weathering, coarsely crystalline, dark gray limestone about three inches thick as described by

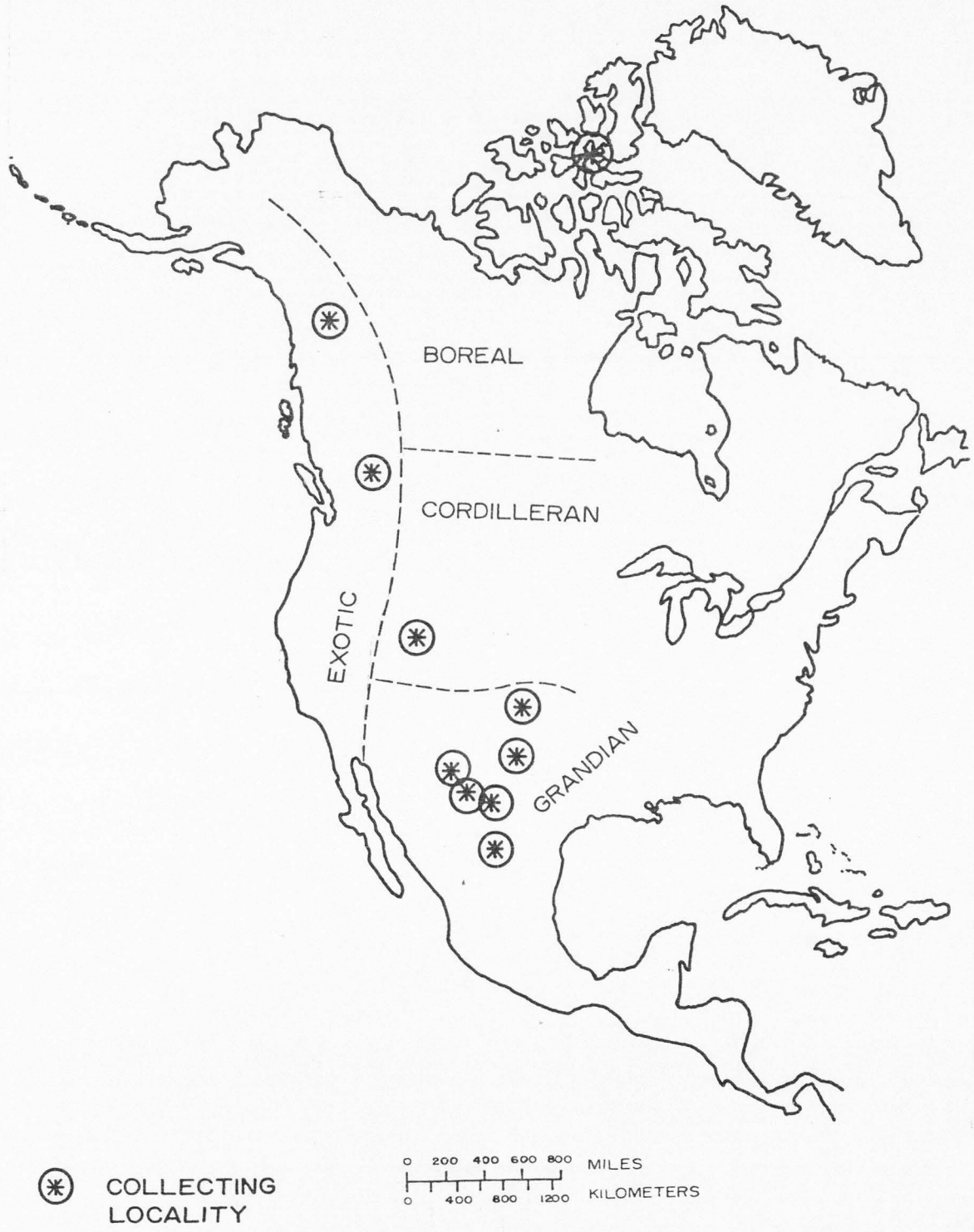

Figure 10. Permian ammonoid-collecting localities in North America. (Provincial boundaries after Yancey, 1975, Figure 1, p. 760.)

King (1937, pp. 95-97). This unit crops out near the top of the Wolfcamp Formation in the Glass Mountains of Texas, and contains the following ammonoid species, according to Miller and Furnish (1940, p. 13):

Neopronorites bakeri
Artinskia huecoensis
Daraelites kingi
Eosianites deciensis
E. modestus
Thalassoceras welleri
Metalegoceras aricki
Peritrochia subquadratum
P. sellardsi
Properrinites bakeri

Lithology 6 (Table 1) consists of fossiliferous, gray shales and thin limestones of the Florena Shale, and interbedded limestones and shales of the Neva Limestone in southern Kansas. Artinskia whortani and Properrinites plummeri are found in the Florena Shale whereas Metalegoceras sp. is found in the Neva Limestone (Moore and others, 1951, p. 47). Lithology 7 (Table 1) is represented by thick-bedded limestones in the middle part of the Hueco Limestone exposed at the southern end of the Hueco Mountains of Texas as described by Miller and Furnish (1940, p. 15). They listed many ammonoid species, some of

which are also found in southeastern New Mexico from alternating green, silty shales, buff siltstones, and dolomitic limestones in the lower part of the same formation (Miller and Parizek, 1948, p. 350). Miller and Furnish (1940) listed the following:

Neopronorites bakeri	Metalegoceras c.f. M. colemanense
Eosianites deciensis	Agathiceras c.f. A. girtyi
E. modestus	Pernitrochia sellardsi
E. ruzhencevi	Artinskia huecoensis

Properrinites bosei

Lithology 8 (Table 1) consists of the Indian Creek Shale Member of the Admiral Formation and shale and limestone of the Clyde Formation exposed in north-central Texas. Miller and Furnish (1940, p. 18) listed the following forms from the Indian Creek Shale Member (left column) and from the Clyde Formation (right column):

Artinskia adkinsi	Artinskia electraensis
Pseudogastrioceras admiralense	Agathiceras contractum
Metalegoceras colemanense	Peritrochia electraensis
Agathiceras applini	Properrinites cumminsi
Peritrochia sellardsi	Medlicottia coepi
Properrinites bosei	Metalegoceras baylorense
	Popanoceras walcotti

Lithology 10 (Table 1) is represented by the Bone Spring Limestone in the Guadalupe Mountains of Texas. It consists of black laminated limestone with granular nodules, according to King (1948, pp. 14-21). Ammonoids reported by Miller and Furnish (1940, p. 9) are:

Paraceltites elagans
Texoceras texanum
Perrinites hilli
Peritrochia erebus
Agathiceras c.f. *A. girtyi*
Propinacoceras knighti

Lithology 11 (Table 1) is represented by the Leonard Formation in the Glass Mountains of Texas. It is described by King (1930, pp. 65-66) as shaly limestone; brown, calcareous, coarse-grained sandstone; marly limestone; and fine-grained, sandy, gray limestone grading to conglomeritic limestone; with pebbles of rounded chert in the limestone layers. *Perrinites sp.* is very abundant in the shaly and marly limestone layers. From these layers Miller and Furnish (1940, pp. 13-14) listed the following:

Propinacoceras knighti
Medlicottia costellifera
M. whitneyi
Daraelites leonardensis
Metalegoceras schucherti
Eothinites hessensis
Perrinites hilli
Thalassoceras sp.
Adrianites defordi
A. newelli
Agathiceras girtyi
Peritrochia dunbari
Stacheoceras rothi
Popanoceras sp.

Lithology 12 (Table 1) is found in the Blaine Formation of north-central Texas. The main rock type is a soft dolomite according to Sellards and others (1932, p. 178). The unit contains ammonoids in great numbers, among which Miller and Furnish (1940, p. 19) listed:

Propinacoceras knighti
Medlicottia whitneyi
Metalegoceras sp.
Stacheoceras sp.
Perrinites hilli

The Wordian (Lower Guadalupian) Series, is represented by Lithology 13 (Table 1) which is the same as Lithology 9 (Table 1). It is repeated here because the precise age of the fauna is still somewhat in doubt. Miller and others (1957, p. 1057) designated the age as Leonardian, but the Phosphoria is also regarded as being Guadalupian (Dunbar and Waage, 1969, p. 289).

Lithology 14 (Table 1) is the famous Word Formation in the Glass Mountains of Texas. Most ammonoids are found in the "Third" limestone of King (1930, pp. 71-72), which consists of light gray, oolitic limestone with masses of chert. The "Second" limestone, which is made up

of gray, fine to coarse-crystalline limestone in thick ledges, also contains some ammonoids. Miller and Furnish (1940, p. 14) listed the following, mostly from the "Third" limestone:

Medlicottia burckhardti
M. kingorum
Paraceltites multicostatus
P. ornatus
P. sellardsi
Cibolites uddeni
Popanoceras bowmanni
Agathiceras girtyi
Pseudogastrioceras altudense
P. roadense
P. serratum
Atsabites multiliratus
A. williamsi
Adrianites adamsi
A. marathonensis
Waagenoceras dieneri

Lithology 15 (Table 1) consists of beds 10-17 in the Difunta section of King and others (1944, pp. 14-15) at Las Delicias, Coahuila, Mexico. These beds consist of blue-gray, massive and nodular limestone, with interbedded shale, graywacke, and lava. Miller and Furnish (1940, p. 17) listed ammonoids recovered from these beds as:

Medlicottia burckhardti
M. girtyi
Paraceltites ornatus
Pseudogastrioceras roadense
Epithalassoceras ruzhencevi
Pseudoagathiceras sp.
Agathiceras girtyi
Stacheoceras sp.
Waagenoceras guadalupense
W. dieneri
Adrianites sp.

Lithology 16 (Table 1) is a composite of two separate lithologies. In southwestern British Columbia, Canada, is the Cache Creek Series, which contains ammonoids that Nassichuk (1977, p. 558) described from a bed of slightly argillaceous, partly dolomitized, bioclastic wackestone. In northwestern British Columbia, near Atlin, the Horsefeed Formation also has an ammonoid-bearing layer of slightly silicified, bioclastic grainstone. From the Cache Creek Series the following ammonoids are listed by Nassichuk (1977, p. 561):

Propinacoceras beyrichi
Agathiceras suessi
Daubichites sp.
Neocrimites warreni
Paraceltites c.f. *P. rectangularis*
Waagenoceras c.f. *W. girtyi*

From Horsefeed Formation, Nassichuk (1977, p. 561) listed:

Eumedlicottia burckhardti
Agathiceras girtyi
Hyattoceras c.f. *H. geinitzi*
Adrianites sp.
Martoceras saundersi
Paraceltites c.f. *P. rectangularis*
Stacheoceras mediterraneum
S. gemmellaroi
S. mangeri
Waagenoceras canadensis
W. dieneri
W. girtyi

The Guadalupian (Upper Guadalupian) Series, is the youngest Permian interval examined. Lithology 17 (Table 1) is the Altuda Member of the Captian Formation which is exposed in the Glass Mountains of Texas.

According to King (1930, p. 80), thin-bedded, cherty limestone, sandy limestone, and siliceous shale are the predominant rock types. From this unit, Miller and Furnish (1940, p. 15) found examples of Paraceltites altudensis, Pseudogastrioceras roadense, P. altudense, and Timorites uddeni.

Lithology 18 (Table 1) is from the Bell Canyon Formation in the Guadalupe Mountains of Texas. Dark-gray, fine-grained to granular, thin-bedded limestones make up the unit, according to King (1948, pp. 55-57). Ammonoids recovered from these layers and listed by Miller and Furnish (1940, p. 11) included:

Medlicottia girtyi
Paraceltites altudensis
Cibolites uddeni
Xenaspis skinneri
Timorites c.f. T. schucherti
Pseudogastrioceras altudense
P. beedi
P. roadense
Waagenoceras guadalupense
W. dieneri

Hoffmannia fisheri was found by Plummer and Scott (1937, p. 363) from the same formation.

Lithology 19 (Table 1) is represented by beds 4-7 in the Difunta section of King and others (1944, pp. 13-14). These strata crop out near Las Delicias, Coahuila, Mexico, and consist of black shales with hard, black, limestone concretions. Ammonoids and other fossils form

the nuclei of the concretions. Ammonoids from this unit listed by Miller and Furnish (1940, p. 18) included:

Propinacoceras sp.
Paraceltites altudensis
Cibolites sp.
Xenodiscites sp.
Pseudogastrioceras roadense
Strigogoniatites sp.
Adrianites dunbari
Stacheoceras toumanskyae
Waagenoceras dieneri
Timorites schucherti

Lithology 20 (Table 1) is thought by many to be the youngest ammonoid-bearing Permian strata in the western Hemisphere. This lithology is described by Newell (1957, p. 1573) as black shale and conglomeratic graywacke. The bed is interpreted as a turbidite deposit and thus includes a transported fauna. Spinosa and others (1970, p. 731) listed the following ammonoids from these layers, which they term the "La Colorado beds":

Neocrimites sp.
Stracheoceras c.f. S. tridens
Timorites n. sp.
Propinacoceras n. sp.
Episageceras c.f. E. nodosum
Kingoceras kingi
Eoaroxoceras ruzhencevi
Xenodiscus wanneri

Triassic

The Sycthian (Lower Triassic) Series contains several ammonoid assemblages, but only two were analyzed. They represent the most varied lithologies and prolific collections obtainable. Both are contained in

the Thaynes Formation of Nevada and Idaho (Figure 11). Lithology 21 (Table 1) is the Meekoceras layer, in which the abundance of ammonoids is prolific near Montello, Nevada (Figure 12). Near Montello, Kummel and Steele (1962, p. 639, Unit "a") collected from a light-gray, fine to coarse-crystalline, thick-bedded, coquinoid limestone, nearly four hundred ammonoids, which included the following species:

Dieneroceros spathi
D. knechti
D. subquadratum
Hemiaspenites obtusus
Flemingites russelli
Anaflemingites siberlingi
Xenoceltites youngi
Preflorianites toulai
Psuedoaspidites wheeleri
Owenites koeneni
Paranannites aspenensis
Prosphigites slossi
Juvenites septentrionalis
J. thermarum
Paraussuria compressum
Lanceolites compactus
Aspenites acutus
Meekoceras gracilitatus
Wyomingites whiteanus
Arctoceras tuberculatum
Arctoprionites sp.
Pseudosageceras multiobatum

The Columbites layer is abundantly fossiliferous only in northern Bear Lake Valley of Idaho (Figure 13). In Nevada, Collinson (1968, p. 35) reported finding several specimens of Columbites sp. and one of

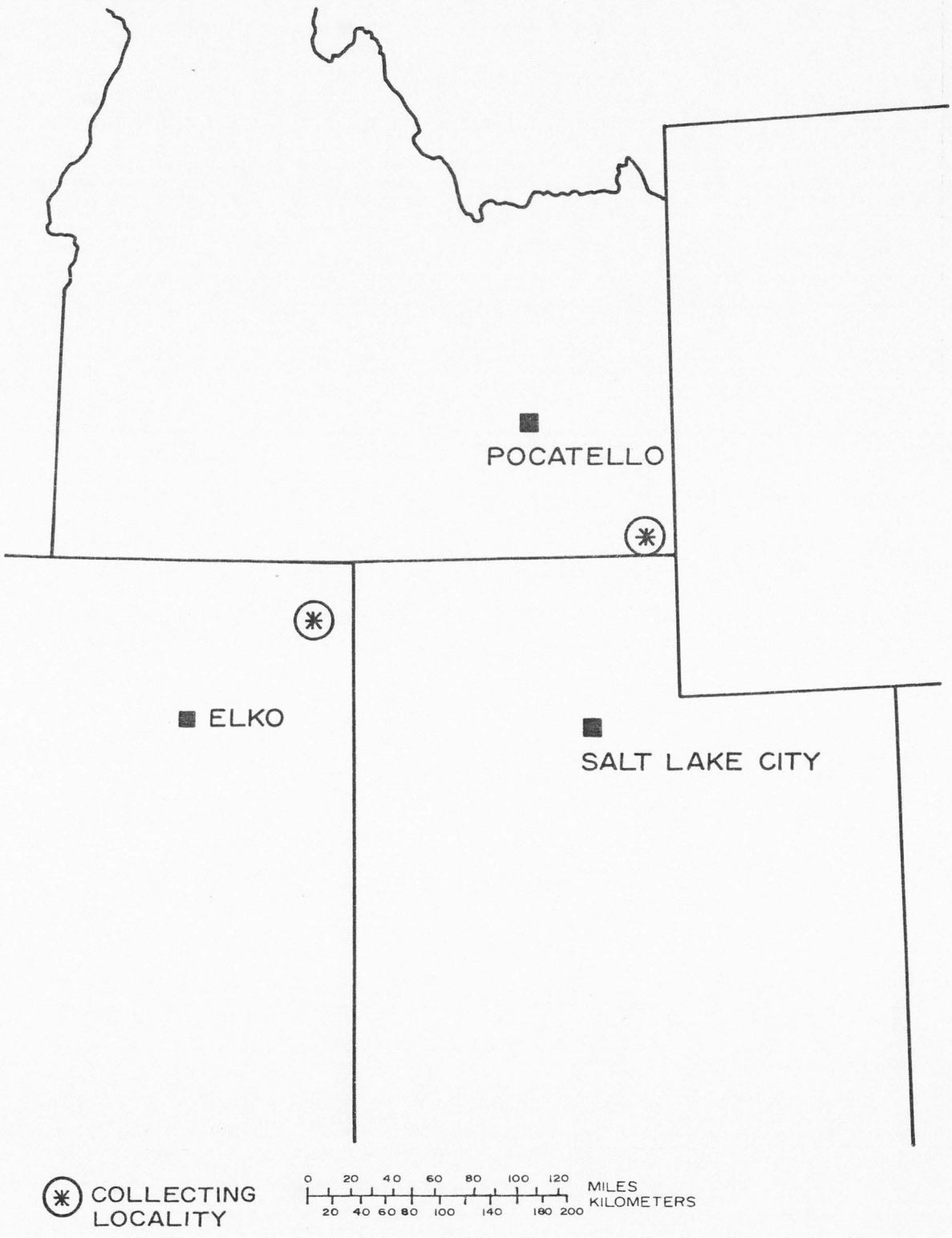

Figure 11. Triassic ammonoid-collecting localities in Idaho and Nevada.

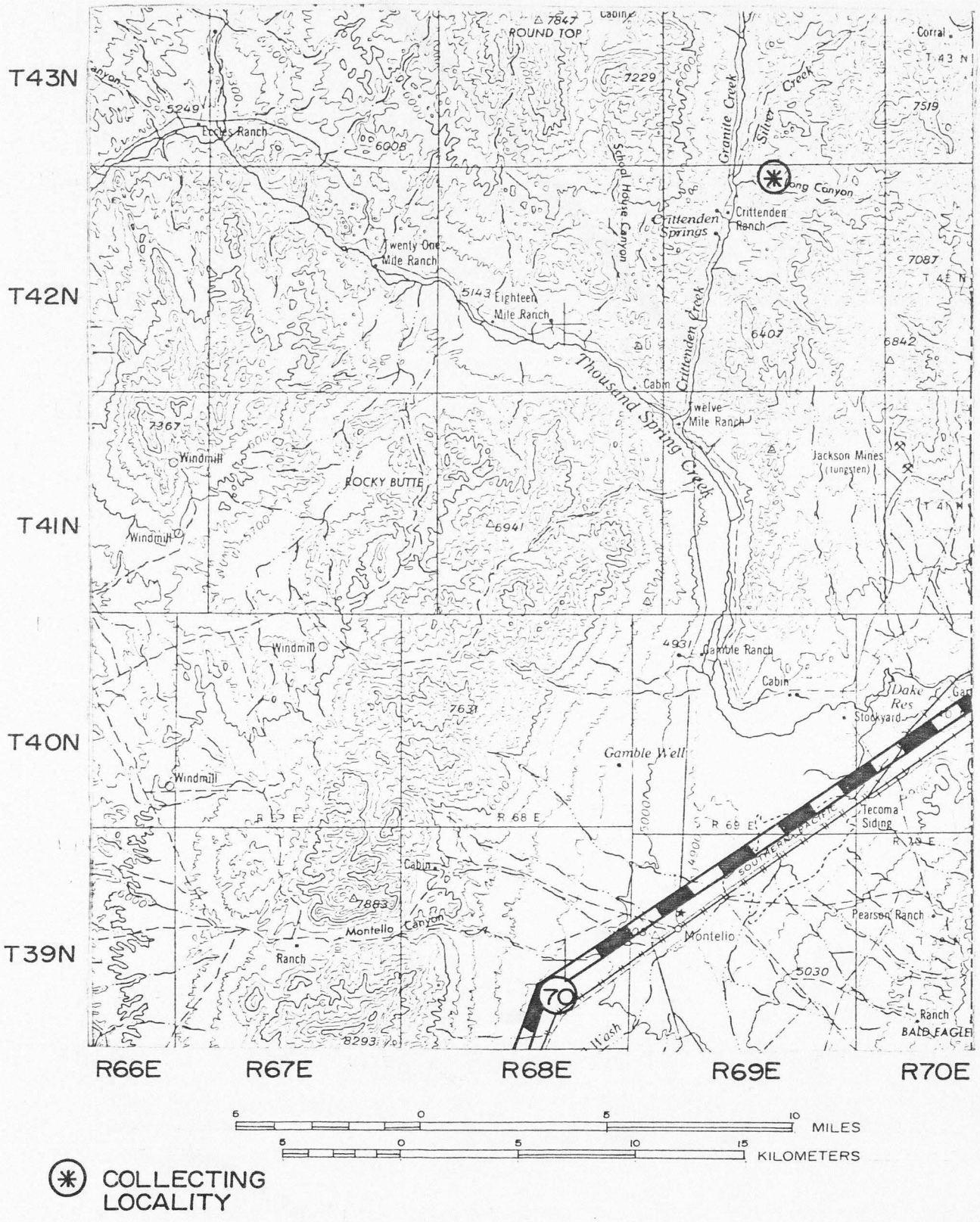

Figure 12. Ammonoid-collecting locality in the Triassic Thaynes Formation near Crittenden Springs, Nevada.

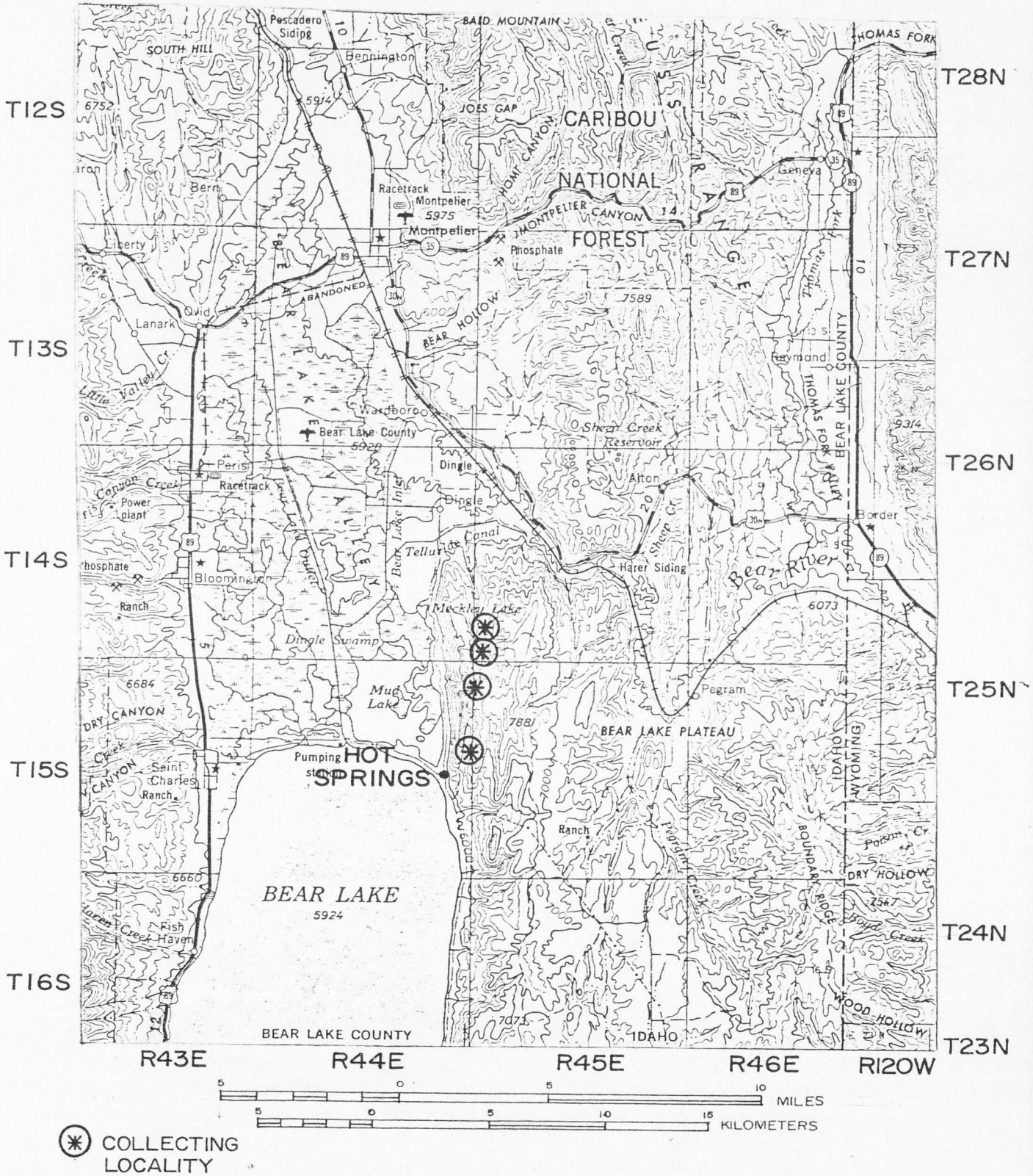

Figure 13. Ammonoid-collecting locality in the Triassic Thaynes Formation near Hot Springs, Idaho.

Tirolites c.f. T. illyricus. One and one-half miles west of Paris, Idaho, Smith (1932, p. 11) collected, from a bituminous layer of brown limestone not over 6 inches thick, the following ammonoids:

Ophiceras jacksoni
O. spenci
Meekoceras curticostatum
Meekoceras micromphalus
M. pilatum
M. sanctorum
Pseudoharpoceras (Hellenites) idahoense
Tirolites c.f. T. illyricus
Pseudosageceros multlobatum
Celtites apostolicus
C. planovolvis
C. ursensis
Columbites consanguineus
C. ligatus
C. minimus
C. ornatus
C. parisianus
C. spenci

Because of the exhaustive collecting of Smith (1932) and more recent investigations (Kummel, 1957), the author judged that this locality would not provide sufficient numbers of additional ammonoids to improve the data for this study. Thus, this locality was not visited.

On the eastern shore of Bear Lake, about one and one-half miles northeast of Bear Lake Hot Springs, the Columbites layer crops out again (Figure 13). The layer strikes northeast along the crest of a ridge for approximately six miles. The same fauna as reported by Smith (1932) is found, with the added appearance of a Cordillerites sp. The lithology, however, is very different from the Paris Canyon

exposure. Kummel (1957, p. 453) described the lithology at Hot Springs as a black, very fine-grained limestone, with small amounts of detrital quartz. The stratum at Hot Springs is Lithology 22 (Table 1), from which have been secured over three thousand ammonoids. I do not recognize as many species as Smith (1932), or Kummel (1954) did. My faunal list includes the following:

Columbites sp. (and varieties)
Ophiceras sp. (and varieties)
Meekoceras sp. (widely umbilicate)
Meekoceras sp. (narrowly umbilicate)
Celtites sp. (and varieties)
Tirolites illyricus
Pseudosageceras multilobatum
Cordillerites n. sp.

W, D, AND S PARAMETER VALUES OF SELECTED AMMONOID GENERA

Dimensions of selected Mississippian (Chesterian) ammonoid genera were obtained entirely by measuring photographs of Miller and others (1957), Gordon (1964), and Saunders (1973), with a vernier calipers. These dimensions are recorded in Table 2, and the distribution of these ammonoid coiling geometries is shown in Figure 14, umbilical view. W varies from 1.53 in Cravenoceras to 2.50 in Anthracoceras. D varies from 0.02 in Delpinoceras to 0.50 in juvenile Pronorites, and S varies from 0.82 in Anthracoceras to 1.82 in Cravenoceras.

Dimensions of selected Permian ammonoid genera were obtained entirely by measuring photographs of Miller and Furnish (1940), Plummer and Scott (1937), Miller and others (1957), Spinosa and others (1970), Spinosa and others (1975), and Nassichuk (1977). These dimensions are recorded in Table 3, and the distribution of these ammonoid coiling geometries is shown in Figure 15. Xenodiscus, labeled Ot in the figure, is outside the ammonoid field of Raup (1967, p. 47, Figure 3). This is because the sample of ammonoid genera used to delimit Raup's W-D field for ammonoids contains only 400 genera; there are thousands of ammonoid species described. W varies from 1.32 in Adrianites to 3.87 in Thalassoceras. D varies from 0.04 in Medlicottia to 0.58 in Metalegoceras, and S varies from 0.32 in Medlicottia to 3.10 in Metalegoceras.

Table 2. Parametric values for coiling geometries of selected ammonoid genera from the Mississippian *Cravenoceras hesperium* Zone

No.	Genera	d	e	W	a	D	b	S	Sf abr[a]	Lithology No.
1	*Cravenoceras*	22.3	18.05	1.53	17.84	.200	32.46	1.82	Go	1,2,3,4, White Pine Shale[b]
2	*Eumorphoceras*	17.3	11.66	2.20	11.66	.326	13.87	1.19	Go	2,3, White Pine Shale[b]
3	*Anthracoceras*	28.0	18.00	2.40	27.00	.038	22.00	0.82	Go	2,4, White Pine Shale
4	*Delpinoceras*	19.3	13.60	2.01	19.01	.015	16.35	0.86	Di	2
5	*Prolecanites* (Rhiepicanites)	6.7	4.65	2.06	4.00	.400	3.36	0.84	Pr	2
6	*Pronorites*	11.0	8.00	1.87	5.50	.500	7.00	1.27	Me	1,3
7	*Dimorphoceras*	4.4	3.08	2.03	2.64	.027	3.19	1.21	Di	3, White Pine Shale
8	*Epicanites*	5.8	4.06	2.06	3.50	.400	1.96	0.84	Pr	White Pine Shale
9	*Girtyoceras*	14.5	10.02	2.09	11.44	.211	11.21	0.98	Go	3, White Pine Shale

After Gordon (1964), and Saunders (1973).

[a]Superfamilial abbreviations are explained in Figure 14.

[b]White Pine Shale of Youngquist (1949).

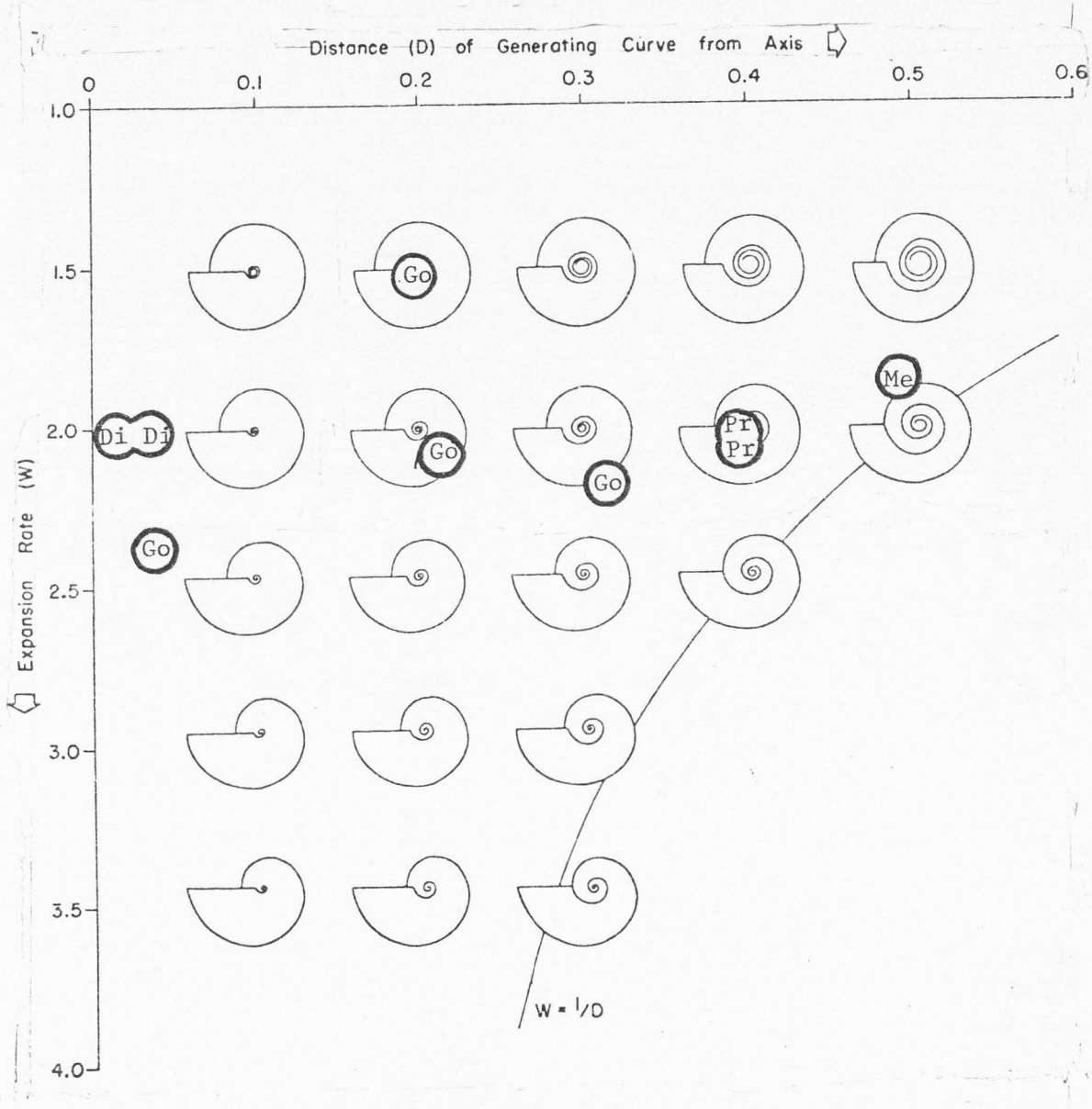

Figure 14 Field of ammonoid-shell-coiling geometries of genera from the Mississippian Chainman Formation, Cravenoceras Zone.

Table 3. Parametric values for coiling geometries of selected Permian ammonoid genera

No.	Genera	d	e	W	a	D	b	S	Sf Abr[a]	Lithology No.
1	Propinococeras	48.5	29.6	2.68	45.5	.062	18.5	0.41	Me	10,11,12,16,19,20
2	Artinskia	34.1	20.4	2.79	32.1	.058	11.0	0.34	Me	5,6,7,8
3	Medlicottia	41.1	23.2	3.14	39.5	.039	12.5	0.32	Me	8,9.11,12,13,14,15,18,20
4	Daraelites	39.2	19.2	2.32	22.9	.218	19.5	0.85	Pr	5,11
5	Epithalassoceras	35.0	23.0	2.32	32.7	.066	ND[b]	ND[b]	Di	15
6	Thalassoceras	23.6	12.0	3.87	20.4	.136	17.0	0.83	Di	5,11
7	Texoceras	16.9	12.4	1.86	13.8	.183	16.7	1.21	Ad	10
8	Adrianites	17.0	14.8	1.32	14.1	.171	19.8	1.40	Ad	9,11,13,14,15,16,19,20
9	Pseudoagathiceras	18.7	14.0	1.78	11.7	.374	22.3	1.91	Ag	15
10	Metalegoceras	20.8	16.0	1.69	8.7	.582	27.0	3.10	Go	5,6,7,11,12
11	Strigogoniatites	67.2	45.2	2.21	51.8	.229	48.0	0.93	Go	19
12	Pseudogastrioceras	31.7	22.3	2.02	24.1	.239	26.0	1.08	Go	8,9,13,14,15,16,17,18,19
13	Waagenoceras	19.0	14.3	1.77	16.4	.179	31.1	1.90	Cy	14,15,16,18,19
14	Timorites uddeni	39.0	29.8	1.71	24.8	.364	37.3	1.50	Cy	17,20
15	Peritrochia	21.1	16.3	1.67	19.4	.081	27.6	1.42	Cy	5,7,8,9,10,11,13
16	Stacheoceras	29.4	24.2	1.48	24.2	.177	28.8	1.19	Cy	9,11,12,13,15,16,19,20
17	Popanoceras	34.4	27.6	1.55	32.6	.052	16.7	0.50	Cy	17,20
18	T. schucherti	47.3	39.2	1.46	37.1	.216	36.4	0.98	Cy	18,19
19	Hyattoceras	28.6	19.8	2.09	27.1	.052	20.1	0.74	Cy	16
20	Perrinites	52.2	36.0	2.10	47.4	.092	46.9	0.99	Ag	10,11,12
21	Properrinites	25.5	19.5	1.71	21.5	.157	27.6	1.28	Ag	5,6,7,8

Table 3. Continued

No.	Genera	d	e	W	a	D	b	S	Sf abr[a]	Lithology No.
22	Agathiceras	18.9	13.0	2.11	18.0	.048	19.4	1.08	Ag	7,8,10,11,14,15,16
23	Atsabites	25.5	19.6	1.69	10.5	.392	12.8	1.22	Go	14
24	Eosianites	19.5	16.2	1.45	10.0	.487	28.0	2.80	Go	5,7
25	Eothinites	24.1	18.6	1.68	12.8	.469	16.5	1.29	Go	11
26	Spirolegoceras	27.5	19.8	1.93	22.3	.189	25.0	1.12	Go	9,13
27	Paragastrioceras	35.4	30.0	1.44	21.4	.344	43.5	2.03	Go	9,13
28	Paraceltites	23.6	17.1	1.90	11.2	.525	5.8	0.52	Ot	10,14,15,16,17,18,19
29	Xenaspis	27.7	18.4	2.26	17.3	.375	7.8	0.45	Ot	18
30	Cibolites	28.7	18.8	2.33	16.8	.415	7.0	0.42	Ot	14,18,19
31	Kingoceras	36.4	25.0	2.12	23.7	.349	11.0	0.46	Ot	20
32	Xenodiscus	40.5	25.5	2.52	22.0	.457	14.0	0.41	Ot	20
33	Xenodiscites	29.5	21.0	1.97	19.0	.356	11.0	0.58	Ot	19
34	Eoaraxoceras	47.5	33.0	2.07	31.0	.347	24.0	0.73	Ot	20
35	Hoffmania	12.0	9.0	1.77	6.4	.466	6.6	1.03	Ad	18
36	Neopronorites	23.9	15.2	2.47	18.4	.230	15.0	0.82	Me	5,7
37	Episageceras=Medlicottia									20
38	Neocrimites=Adrianites									20,16
39	Martoceras=Stacheoceras									16

After Miller and Furnish (1940), Plummer and Scott (1937), Miller and others (1957), Spinosa and others (1970), Spinosa and others (1975), and Nassichuk (1977).

[a]Superfamilial abbreviations are explained in Figure 15.
[b]ND-Not determined from available information

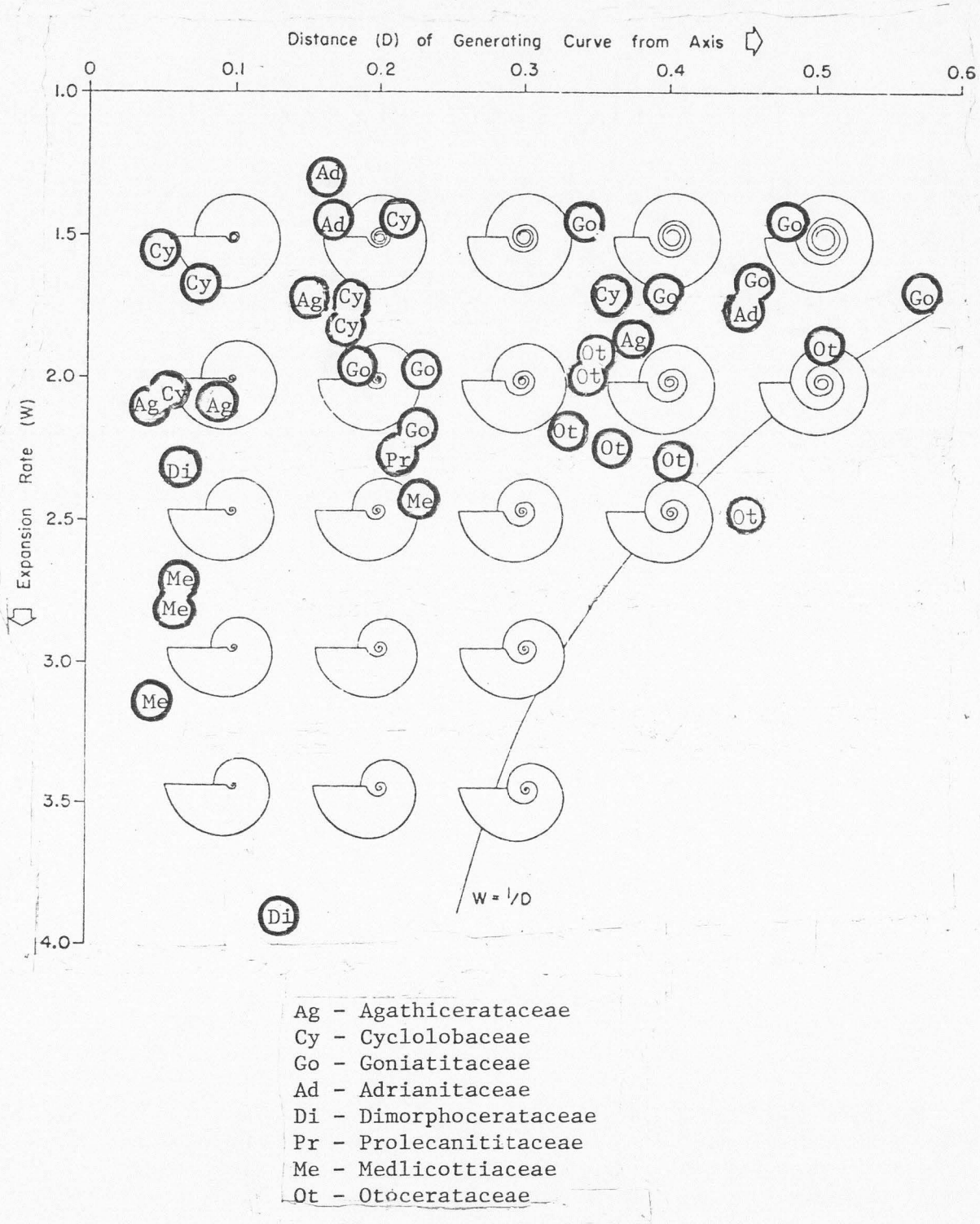

Figure 15. Field of ammonoid-shell-coiling geometries of selected Permian genera.

Dimensions of selected Lower Triassic (Scythian) ammonoid genera were obtained entirely by measuring photographs of Miller and others (1957), Smith (1932), Kummel and Steele (1962) and Tozer (1965). These dimensions are recorded in Table 4 for the Meekoceras Zone, and Table 5 for the Columbites Zone. The corresponding distributions of ammonoid coiling geometries are shown in Figure 16 for the Meekoceras Zone ammonoids and Figure 17 for the Columbites Zone ammonoids. W varies from 1.44 in Juvenites to 3.03 in Pseudoaspidites. D varies from .05 in Lanceolites to .40 in Dieneroceras, and S varies from 0.35 in Aspenites to 1.44 in Prosphingites for ammonoids of the Meekoceras Zone. For ammonoids of the Columbites Zone W varies from 1.40 in Protropites to 3.96 in Cordillerites. D varies from .03 in Pseudosageceras to .54 in Celtites, and S varies from 0.28 in Sageceras to 1.38 in Protropites.

Specimens collected were not measured for their W, D and S parameter values here, because of the mechanical difficulties of different diameters. It was assumed that photographs would provide an accurate, measurable representation of the average adult diameter of each genus which are plotted for all W and D graphs.

Table 4. Parametric values for coiling geometries of selected ammonoid genera from the Triassic *Meekoceras gracilitatus* Zone

No.	Genera	d	e	W	a	D	b	S	Sf abr[a]	Lithology No
1	*Lanceolites*	18.0	14.50	1.54	17.00	.050	9.50	0.54	No	21
2	*Paraussuria*	22.2	12.77	3.02	20.84	.061	9.29	0.46	No	21
3	*Pseudoaspidites*	25.5	14.65	3.03	23.72	.070	13.06	0.55	No	21
4	*Aspenites*	15.5	9.90	2.45	14.04	.094	4.90	0.35	No	21
5	*Arctoceras*	22.3	13.88	2.58	19.40	.130	11.83	0.61	No	21
6	*Owenites*	17.0	13.88	1.50	14.35	.156	10.47	0.73	No	21
7	*Meekoceras*	31.5	21.28	2.19	26.65	.154	11.99	0.45	No	21,22
8	*Prosphingites*	22.0	16.92	1.69	18.08	.178	26.04	1.44	No	21
9	*Parannites*	12.8	9.99	1.64	10.01	.218	9.31	0.93	No	21
10	*Flemingites*	20.0	13.21	2.29	14.56	.272	10.34	0.71	No	21
11	*Anaflemingites*	24.6	17.22	2.04	17.69	.281	12.38	0.70	No	21
12	*Xenoceltites*	10.9	7.59	2.06	7.49	.312	5.25	0.70	No	21
13	*Preflorianites*	17.5	11.18	2.45	10.50	.400	3.67	0.35	No	21
14	*Juvenites*	14.5	12.08	1.44	9.06	.375	11.69	1.29	No	21
15	*Wyomingites*	20.0	13.50	2.19	12.50	.375	7.00	0.56	No	21
16	*Pseudosageceras*	35.0	20.20	3.00	33.80	.032	14.56	0.43	Me	21,22
17	*Dieneroceras*	18.0	12.11	2.21	12.00	.333	8.04	0.67	Ot	21

After Smith (1932), and Kummel and Steele (1962).

[a]Superfamilial abbreviations are explained in Figure 15.

Table 5. Parametric values for coiling geometries of selected ammonoid genera from the Triassic *Columbites parisianus* Zone.

No.	Genera	d	e	W	a	D	b	S	Sf abr[a]	Lithology No.
1	*Columbites*	30.6	24.2	1.60	16.3	.467	13.7	0.84	No	22, Albania
2	*Arnautoceltites*	13.6	10.5	1.68	8.1	.404	10.4	1.28	No	Albania
3	*Isculites*	17.0	14.0	1.47	12.9	.241	10.6	0.82	No	Albania, Timor
4	*Protropites*	13.5	11.4	1.40	8.2	.393	11.3	1.38	No	Albania
5	*Prosphingites*	18.9	11.7	2.61	13.6	.280	9.9	0.73	No	21, Albania
6	*Meekoceras*	30.2	20.4	2.19	24.7	.182	12.8	0.52	No	21,22, Olenek
7	*Proptychites*	23.4	14.9	2.47	19.9	.150	13.4	0.67	No	Albania, Timor
8	*Procarnites*	16.0	11.2	2.04	14.2	.113	10.0	0.70	No	Albania, Timor
9	*Hedenstroemia*	28.0	17.4	2.59	26.9	.039	11.5	0.43	No	Albania
10	*Albanites*	15.9	9.7	2.69	12.7	.201	9.4	0.74	No	Albania, Timor
11	*Pseudoharpoceras*	23.0	15.0	2.35	13.7	.404	14.8	1.08	Ce	22
12	*Sibirites*	19.4	13.6	2.03	10.6	.454	10.7	1.00	Ce	Olenek
13	*Olenekites*	11.8	8.2	2.07	8.4	.290	7.2	0.86	Ce	Olenek
14	*Tirolites*	28.0	17.3	2.62	19.4	.307	9.0	0.46	Ce	22, Albania
15	*Keyserlingites*	21.4	13.6	2.48	15.4	.280	18.1	1.18	Ce	Olenek
16	*Celtites*	17.0	13.0	1.71	7.8	.541	7.9	1.01	Tr	22
17	*Ophiceras*	30.0	21.5	1.95	21.0	.300	11.6	0.55	Ot	22, Albania, Olenek
18	*Leiophyllites*	14.9	10.7	1.94	7.3	.510	7.0	0.96	Ph	Timor, Albania
19	*Sageceras*	40.5	20.6	3.86	37.2	.081	10.5	0.28	Me	Albania
20	*Pseudosageceras*	51.6	29.5	3.06	50.0	.031	14.7	0.29	Me	21,22, Albania
21	*Cordillerites*	23.0	11.6	3.96	22.5	.020	8.6	0.38	Me	22

After Smith (1932), Miller and others (1957), and Tozer (1965).

[a]Superfamiliar abbreviations are explained in Figure 17

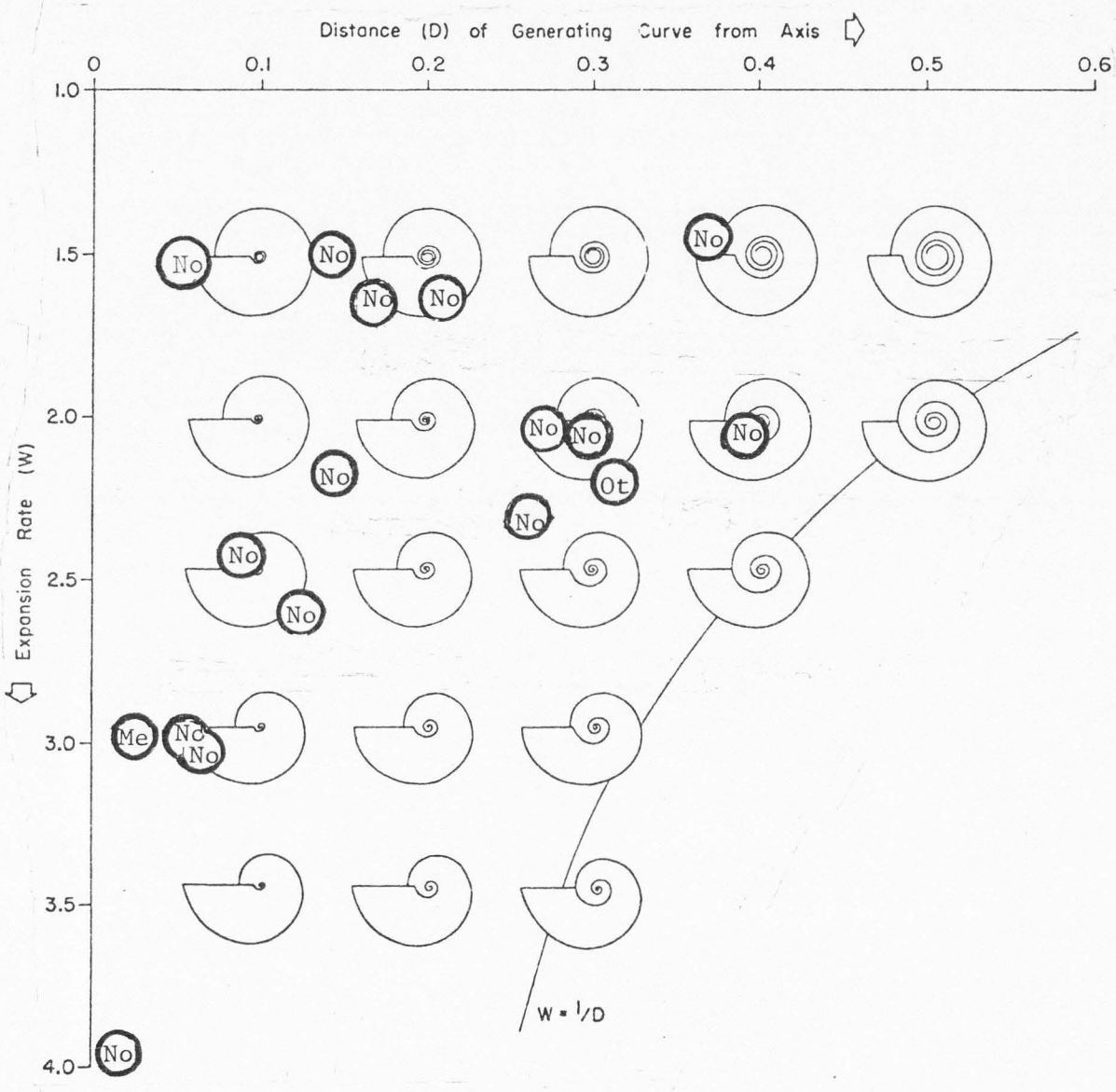

No - Noritaceae
Tr - Tropitaceae
Ce - Ceratitaceae
Ph - Phylloceratataceae
Me - Medlicottiaceae
Ot - Otoceratataceae

Figure 16. Field of ammonoid-shell-coiling geometries of genera from the Triassic Thaynes Formation, Meekoceras Zone.

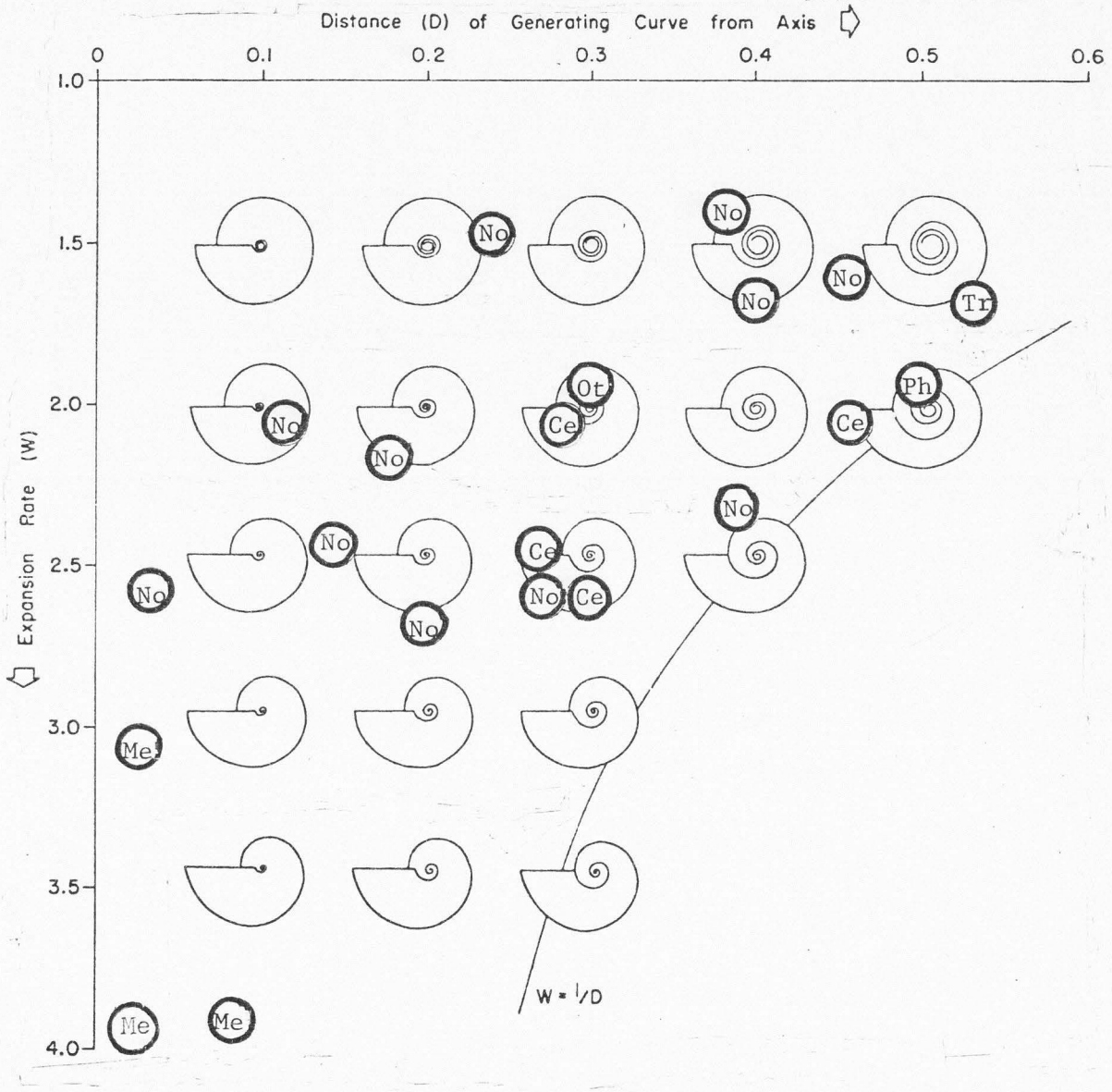

No- Noritaceae
Tr- Tropitaceae
Ce- Ceratitaceae
Ph- Phylloceratáceae
Me- Medlicottiaceae
Ot- Otoceratáceae

Figure 17. Field of ammonoid-shell-coiling geometries of genera from the Triassic Thaynes Formation, Columbites Zone.

LENGTH OF BODY CHAMBER

Length of body chamber, or the arc encompassed by the volutions of the body chamber, has been calculated by Raup (1967, p. 59). These calculations involved balancing animal tissue in the body chamber whorl against the buoyancy afforded by the remaining empty chambers of the shell. Raup assumed that combined, the empty chambers plus the tissue of the body chamber, and weight of the total shell resulted in neutral buoyancy for the ammonoid in the water column. Values include an assumed constant shell thickness of 0.08 times the radius of the generating curve, a water density of 1.03, a shell density of 2.94, a tissue density of 1.07, and three whorls of shell material. Assuming these values are constant for all ammonoids, body chamber length is computed as a function of W and D (Raup, 1967, p. 58). Possible body chamber lengths derived by this method are shown (in degrees) superimposed upon the field of ammonoid shell-coiling geometries in both umbilical and cross sectional view (Figures 18 and 19).

Changes in W values effect drastic changes in body chamber length which can approach a maximum value of a volution and one half (low W) and a minimum value of one quarter volution (high W). When D is varied with constant W, only slight changes in body chamber length are noted, though the maximum value of 540 is found in the medial D range.

Selected Mississippian (Chesterian) ammonoid genera show (Figure 20) a weighted (10^3 abundance = 4 x body chamber length value,

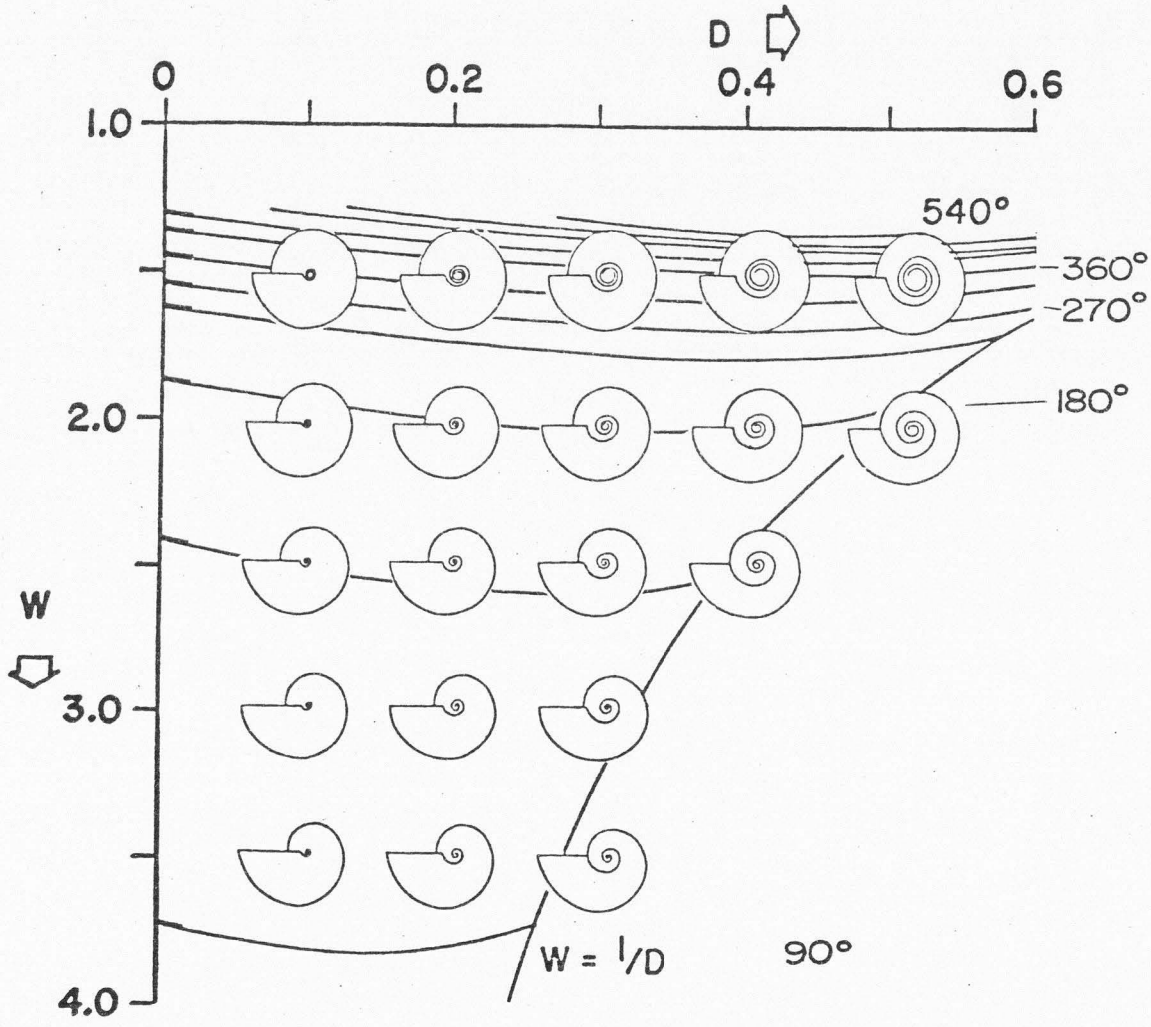

Figure 18. Length of the body-chamber isopleths (in degrees) superimposed upon the ammonoid field of coiling geometries, umbilical view. (After Raup, 1967, Figure 16, p. 60)

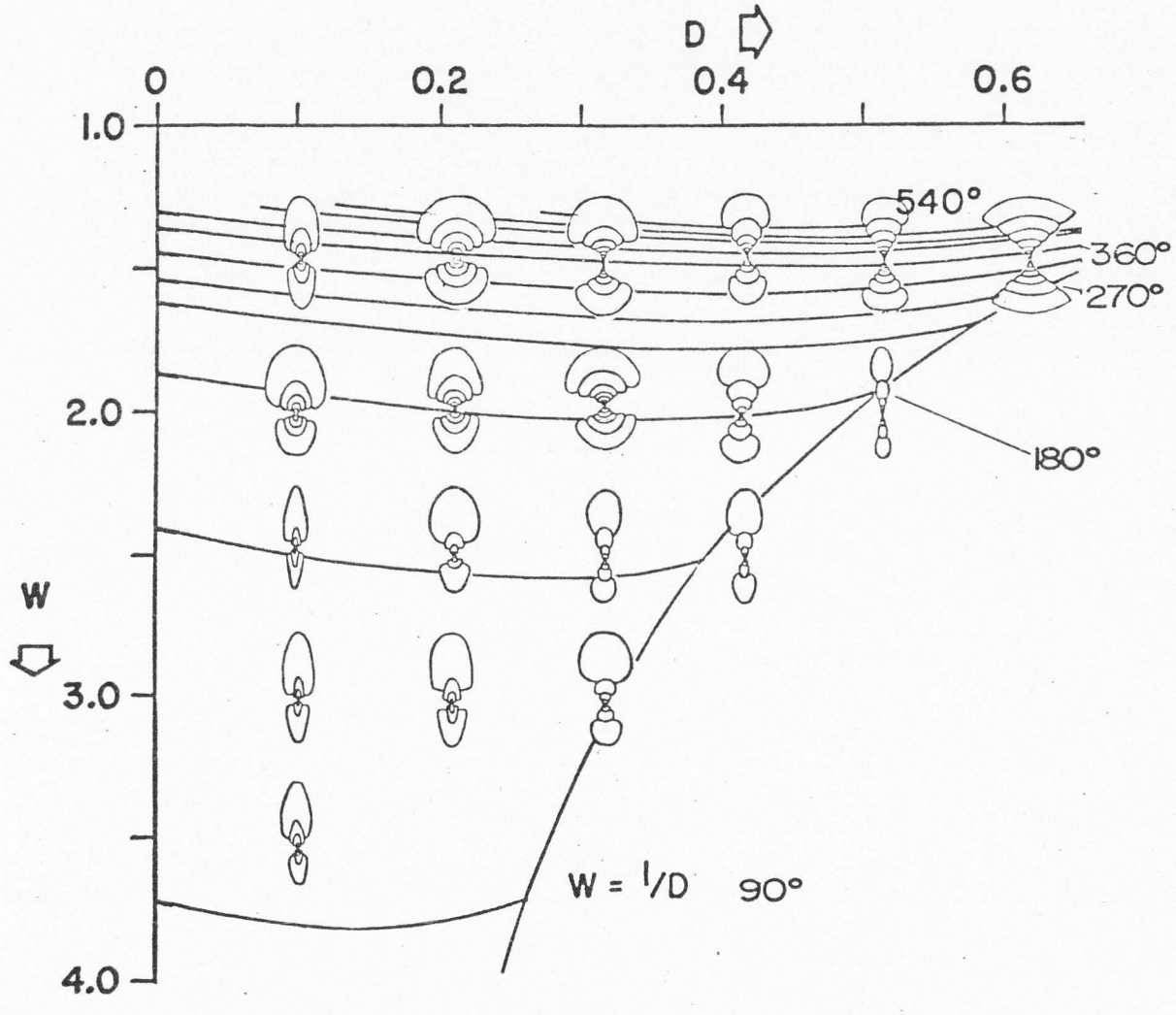

Figure 19. Length of the body-chamber isopleths (in degrees) superimposed upon the ammonoid field of coiling geometries in cross-sectional view.

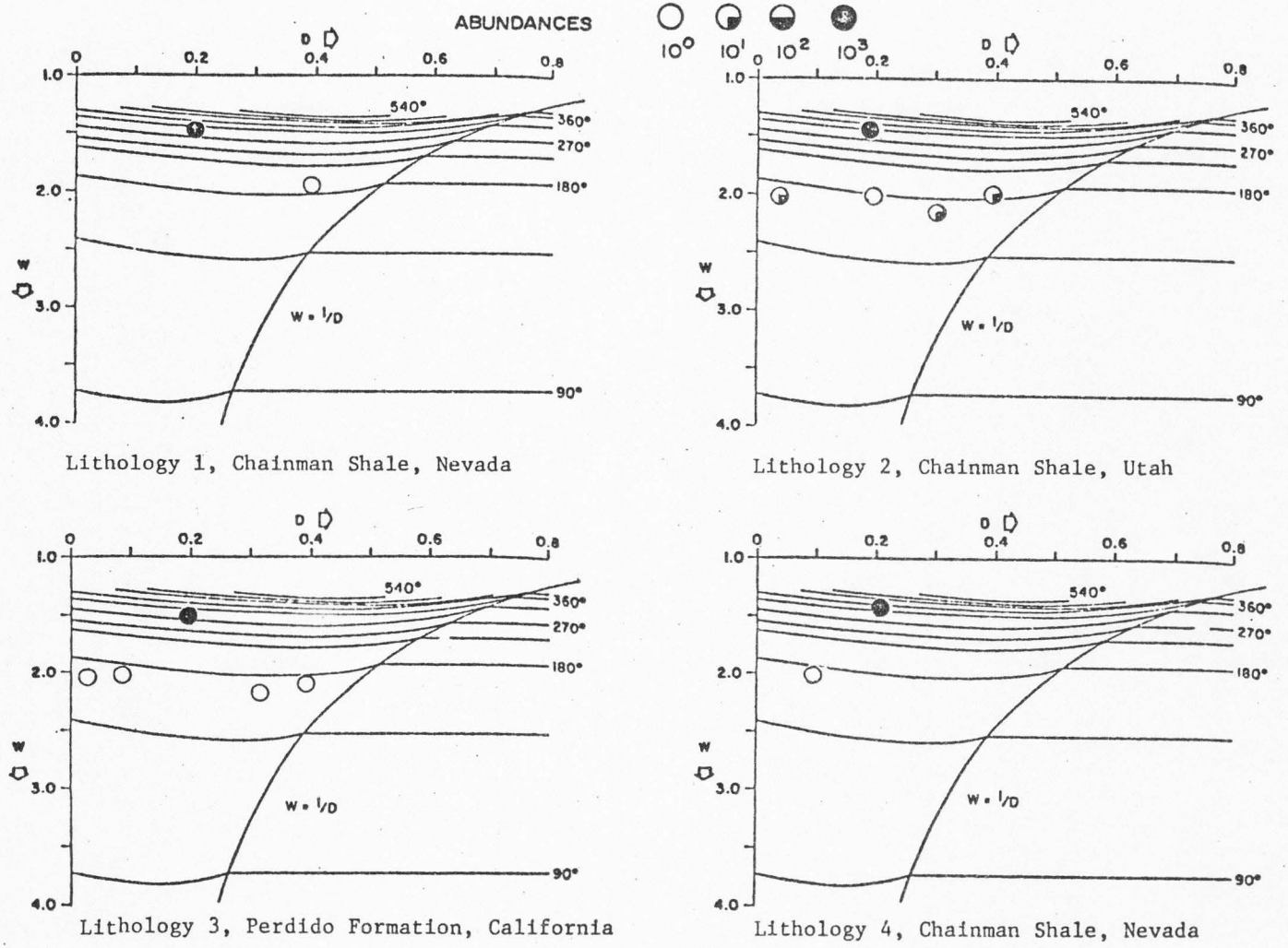

Figure 20. Body-chamber lengths, selected Mississippian (Chesterian) ammonoid genera.

10^2 abundance = 3 x body chamger length value, 10^1 abundance = 2 x body chamber length value, 10^0 abundance = body chamber length value read from graph) average body chamber length of 297°, with a range between 170°-360°. Cravenoceras, with a body chamber length of 360° and the greatest abundance among this group, greatly influences the weighted average. Selected Lower Permian (Wolfcampian) ammonoid genera show (Figure 21) a weighted average body chamber length of 219°, with a range between 110°-405°. Appearance of medlicottid forms significantly decrease the modal value in comparison to the previous genera studies. Selected Middle Permian (Leonardian) ammonoid genera show (Figure 22) a weighted average body chamber length of 195° with a range between 110°-540°. Continued presence of medlicottids, plus the first appearance of Perrinites contribute to the reduced average body chamber length, in comparison to earlier analyzed ammonoid assemblages. Selected Upper Permian (Lower Guadalupian) ammonoid genera show (Figure 23) a weighted average body chamber length of 209°, with a range between 110°-540°. The slight increase is due to prolific numbers of Waagenoceras, a genus not previously encountered. Selected Upper Permian (Upper Guadalupian) ammonoid genera show (Figure 24) a weighted average body chamber length of 213°, with a range between 110°-450°. This value is comparable to that for the Lower Guadalupian. Waagenoceras, Stacheoceras, and Adrianites affect a slight increase in body chamber length. Selected Lower Triassic (Scythian) ammonoid genera show (Figure 25) a weighted average body chamber length of 205°, with a range between 110°-540°. Ammonoids of the Columbites Zone alone have an

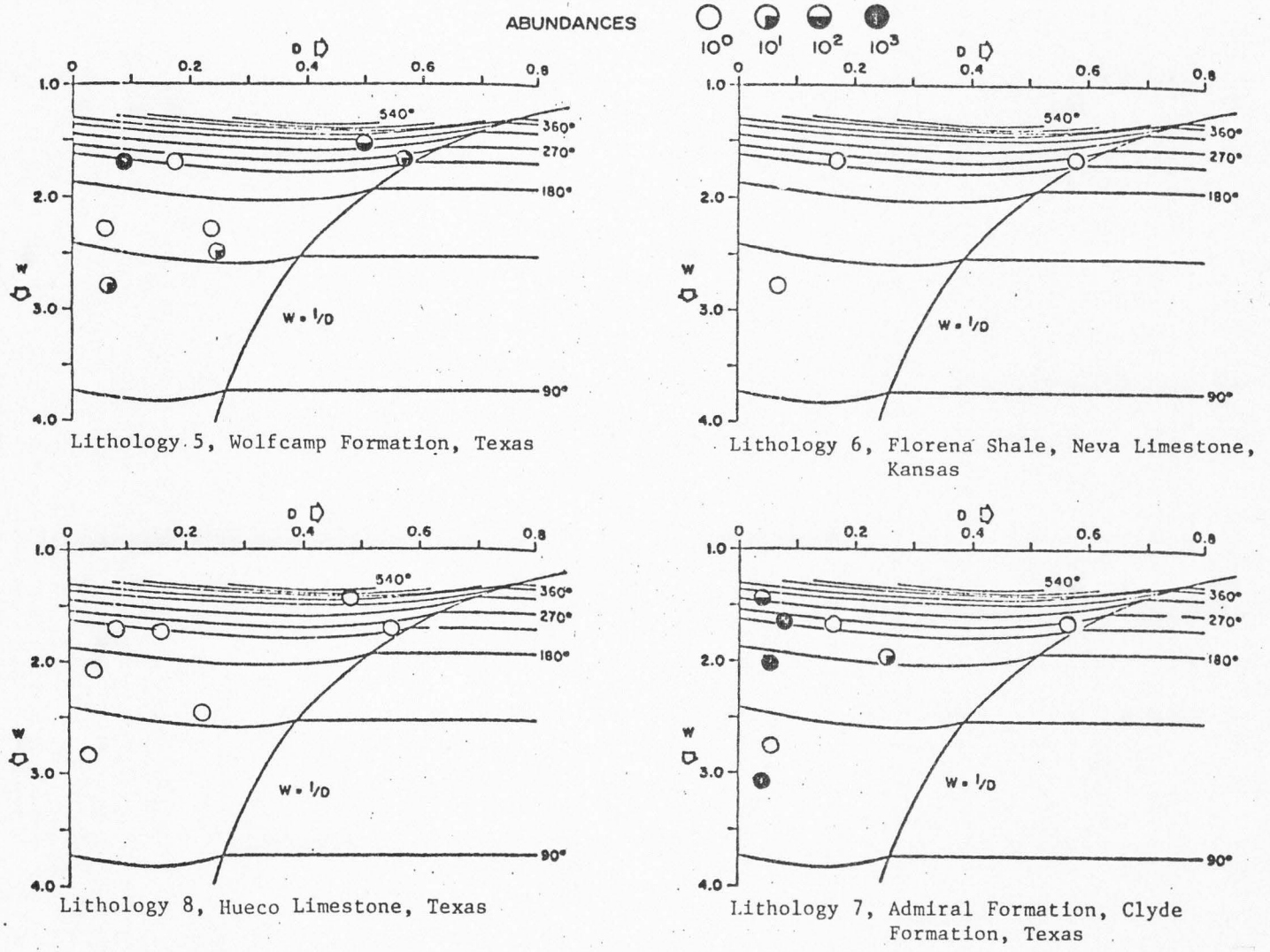

Figure 21. Body-chamber lengths, selected Lower Permian (Wolfcampian) ammonoid genera.

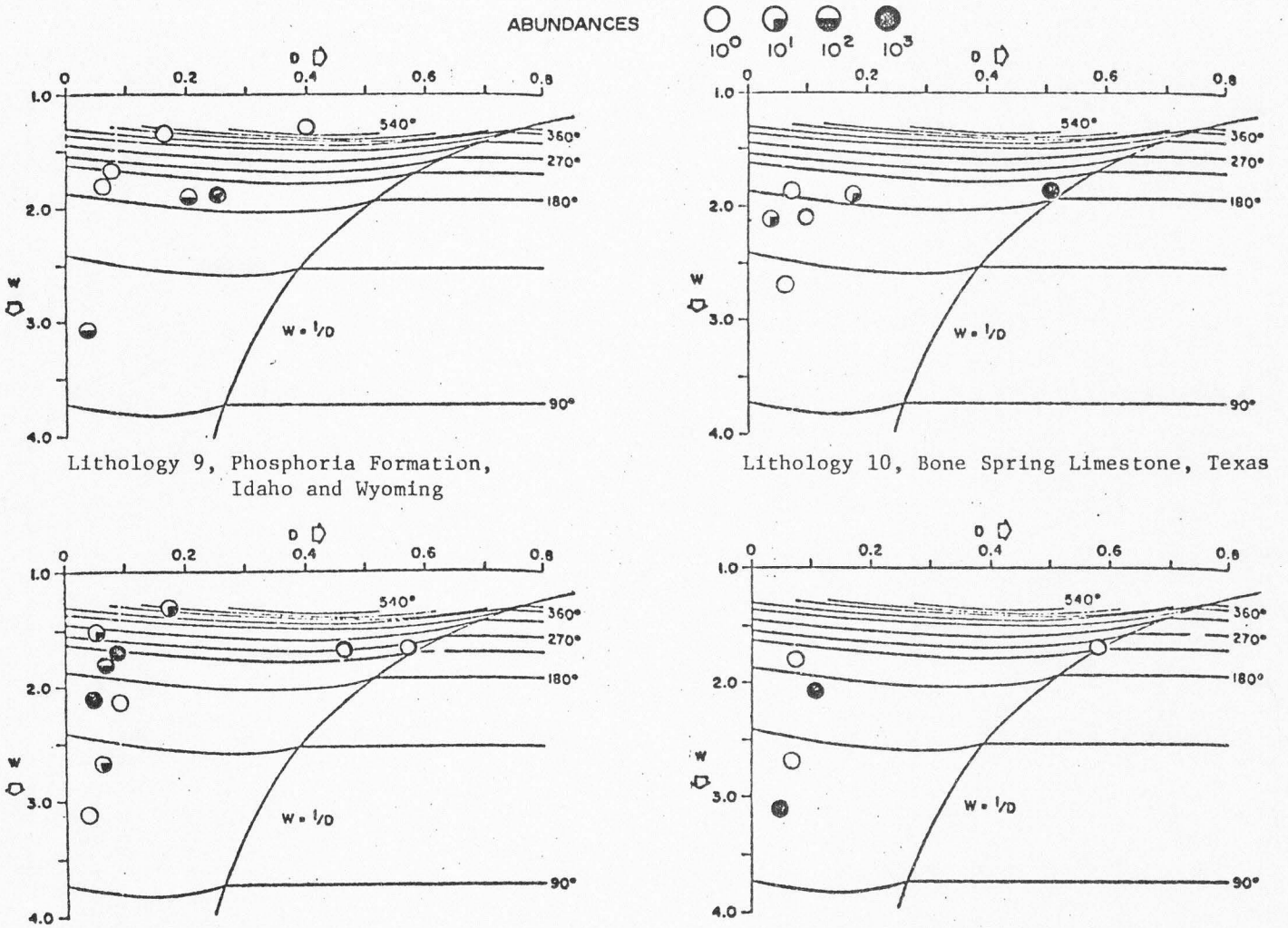

Lithology 9, Phosphoria Formation, Idaho and Wyoming

Lithology 10, Bone Spring Limestone, Texas

Lithology 11, Leonard Formation, Texas

Lithology 12, Blaine Fomation, Texas

Figure 22. Body-chamber lengths, selected Middle Permian (Leonardian) ammonoid genera.

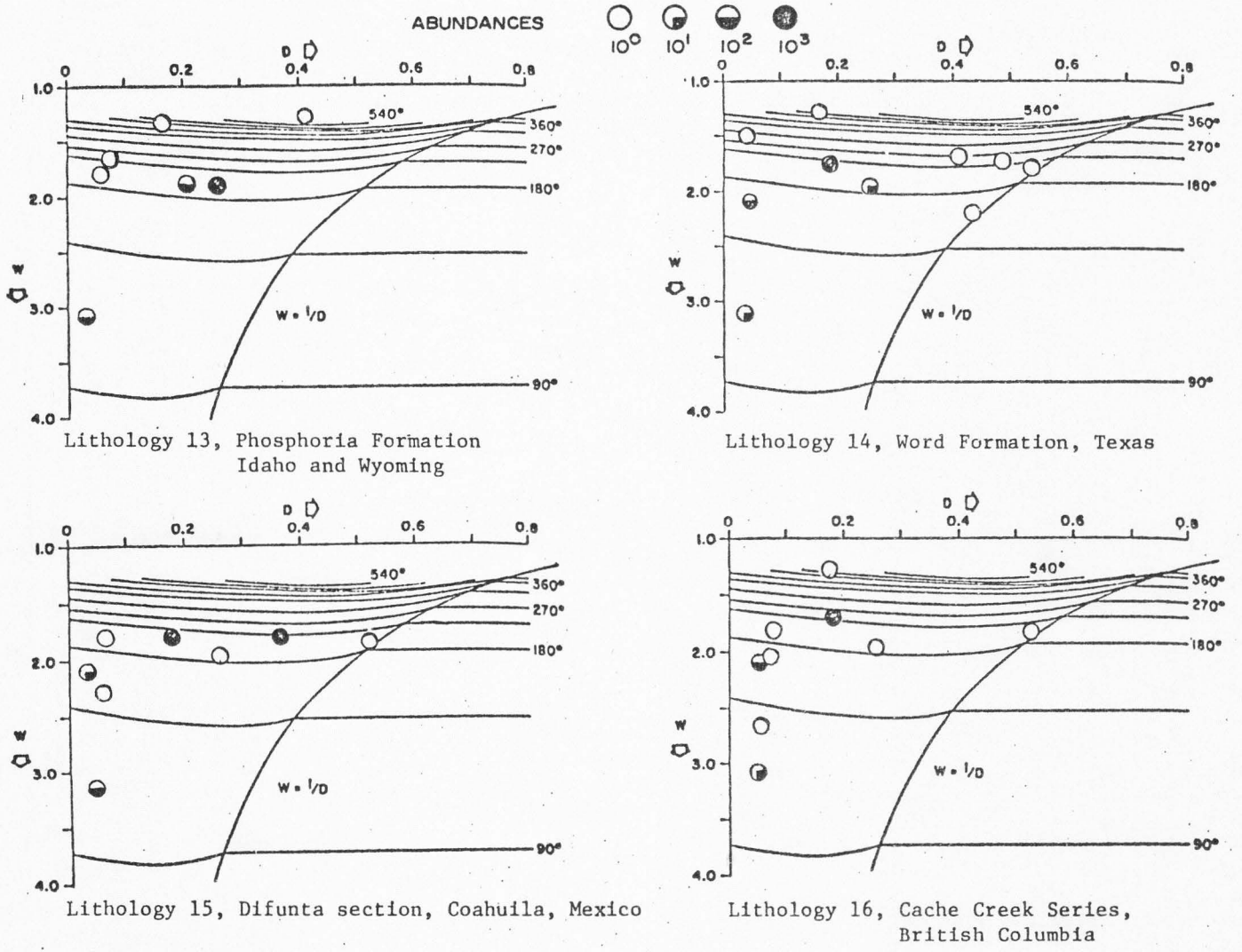

Lithology 13, Phosphoria Formation
Idaho and Wyoming

Lithology 14, Word Formation, Texas

Lithology 15, Difunta section, Coahuila, Mexico

Lithology 16, Cache Creek Series,
British Columbia

Figure 23. Body-chamber lengths, selected Upper Permian (Lower Guadalupian) ammonoid genera.

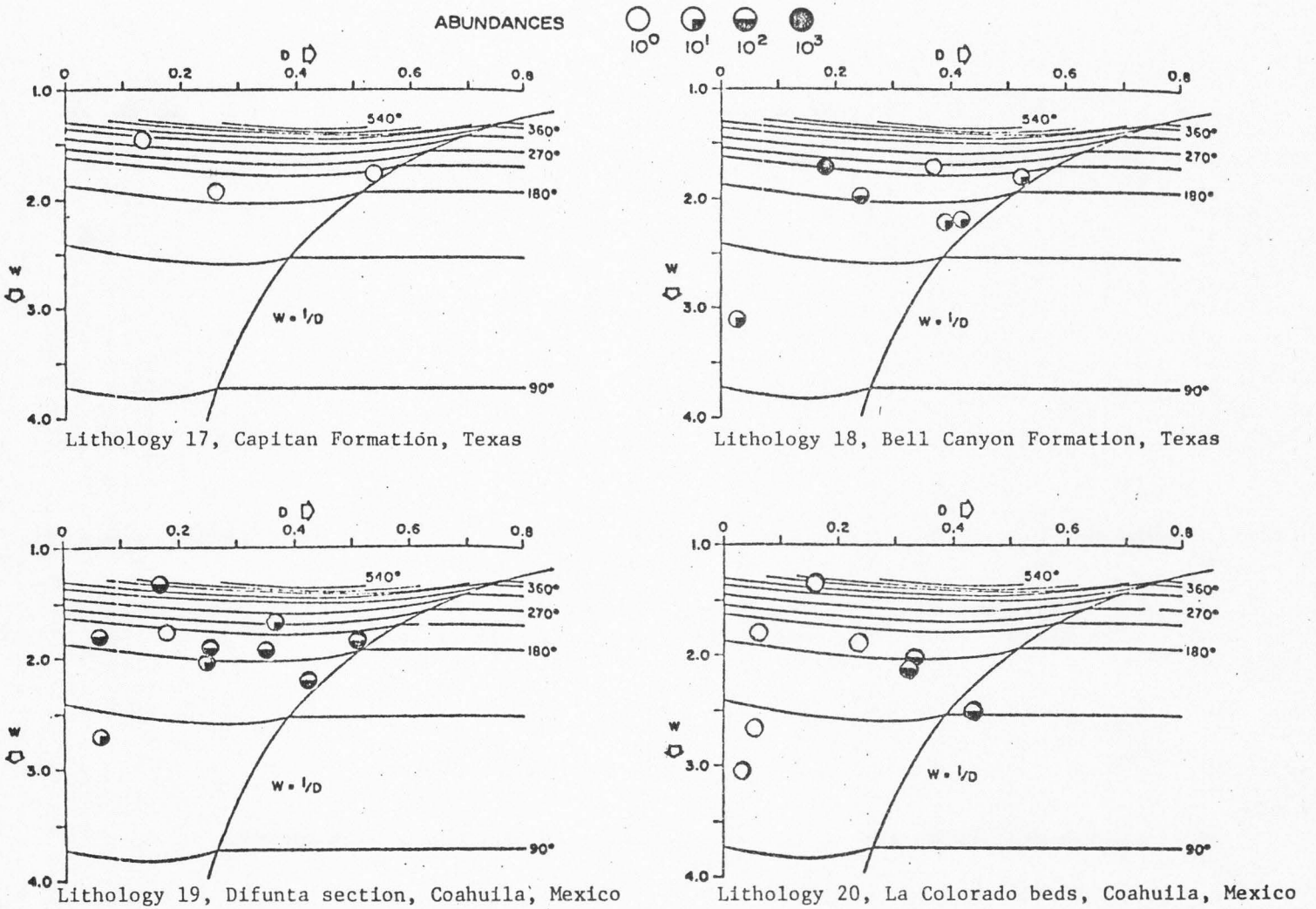

Figure 24. Body-chamber lengths, selected Upper Permian (Upper Guadalupian) ammonoid genera.

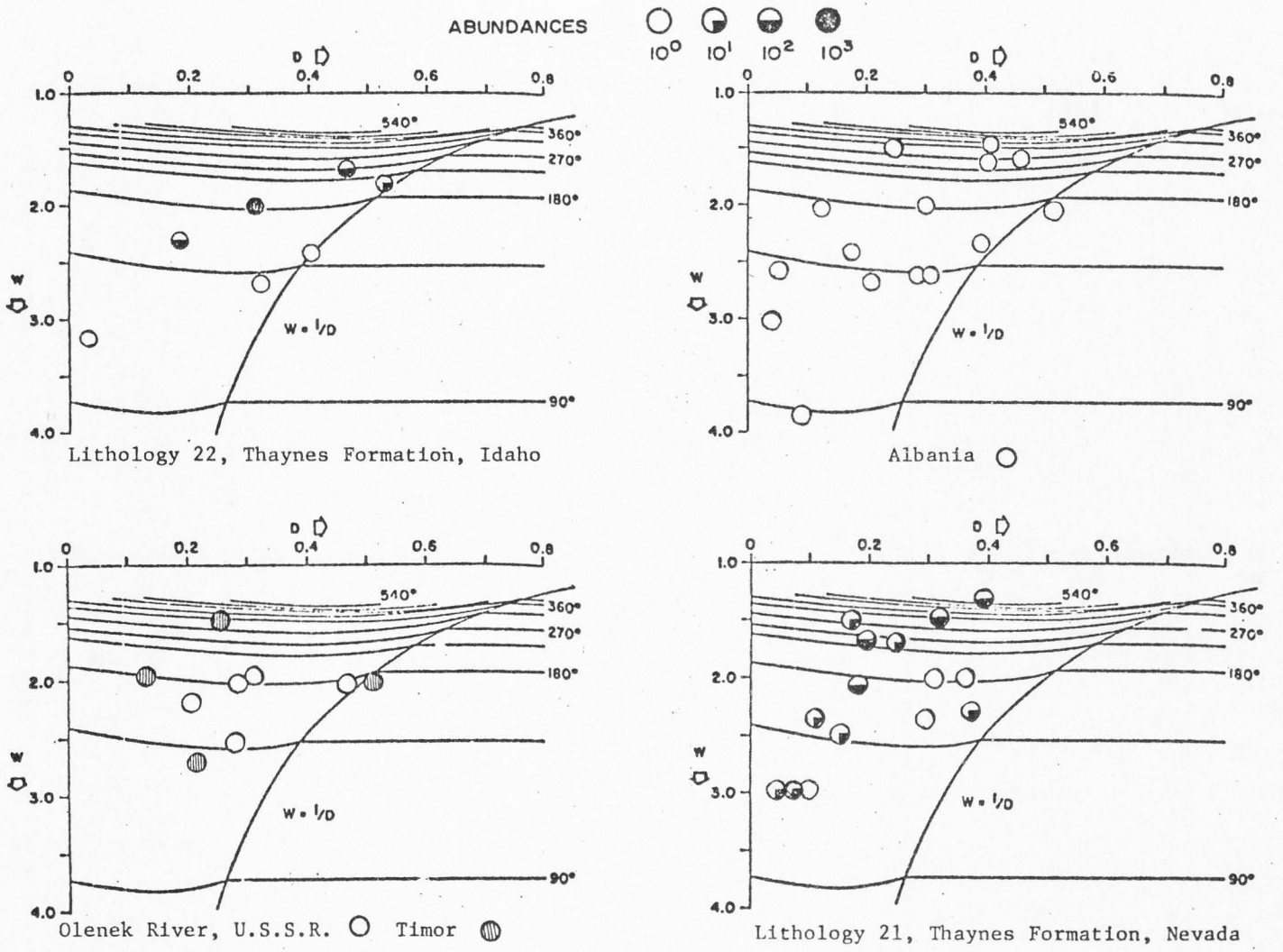

Figure 25. Body-chamber lengths, selected Lower Triassic (Scythian) ammonoid genera.

average body chamber length of 183°, with a narrow range of between 110°-270°. Ammonoids of the Meekoceras Zone have an average body chamber length of 227°, with a wider range of between 110°-540°. Albanian, Russian, and Timorese ammonoid abundances are not reported in the literature, and thus computations of weighted average body chamber lengths for these assemblages cannot be made. Interestingly, the distribution of values cluster in the moderate W range.

Raup (1967, p. 59) noted that body chamber length in itself is not an autecological factor, but that it was indirectly important concerning the form of the ammonoid body and the rotational stability of the animal in the water column. The latter consideration becomes crucial because as more weight of the animal is distributed above the chambers, the center of gravity of the ammonoid is displaced dorsally. This displacement has the effect of decreasing the distance between the center of buoyancy and the center of gravity of the ammonoid. Consequently, rotational stability of the ammonoid decreases.

A correlation between body chamber length and apertural area is observed among the analyzed ammonoids. With respect to W and D, as W increases apertural area increases, as D increases apertural area decreases. A corresponding increase in the size of the anatomical parts related to food capture is assumed with increasing apertural area. Consequently, range of potential prey sizes increase with increasing apertural area. It is the interpretation of the author that long body chambers, with corresponding small apertural areas, restricted the prey size of the ammonoid. These genera, i.e., Popanoceras, Adrianites, Paragastrioceras, and Stacheoceras are not abundant in the analyzed

assemblages (Figures 21-24). Dominant Paleozoic forms: such as Cravenoceras, Perrinites, Pseudogastrioceras, Waagenoceras, and Medlicottia display a general trend of decreasing body chamber length, i.e., from 360° to 110° respectively. In Triassic assemblages, Ophiceras averages 180°, while Meekoceras a widespread form, averages about 160°. This trend suggests the directional selection for decreased body chamber lengths and corresponding increase of apertural area of ammonoids, which utilized the availability of larger prey in the seas progressively from Mississippian to Triassic time. Inferred increased diversification of available prey is congruent with observed diversification of ammonoid genera during the same interval of time (Treatise, 1957, p. L126). Increased diversification of prey, with associated expansion of range of prey size, could account for the trend toward decreased modal body chamber length, increased apertural area, and increased diversification of ammonoids.

LIFE-ORIENTATION

According to Raup (1967, p. 60, Figure 16) it is possible to reconstruct the approximate life-orientation of an ammonoid by computing the angle between the aperture and the gravitational vector in rest position. Raup (1967) based his analysis of life-orientation on the important contribution of Trueman (1941). These calculations of life-orientation assume the attitude of the shell (in rest position) is due primarily to shell form and other geometrical considerations, ignoring the ability of the surviving cephalopod Nautilus to adjust its attitude by fluid secretion in the chambers. Again, the critical assumptions made by Raup (1967, p. 61) included constant shell thickness, a density of 1.07 for the soft body of the animal, and a density of 2.94 for the shell material. Raup (1967, p. 61) followed the calculations of Trueman by using the center of gravity of the body chamber to estimate the center of gravity of the entire shell. This is because the body chamber plus animal soft parts constitutes the bulk of the weight of the animal. The center of buoyancy is, however, calculated by the center of gravity of the volume of water displaced by the entire shell. Raup then proposed a wide variety of different life-orientations according to respective shell-coiling geometries (Figures 27 and 27) seen both in umbilical and cross sectional view.

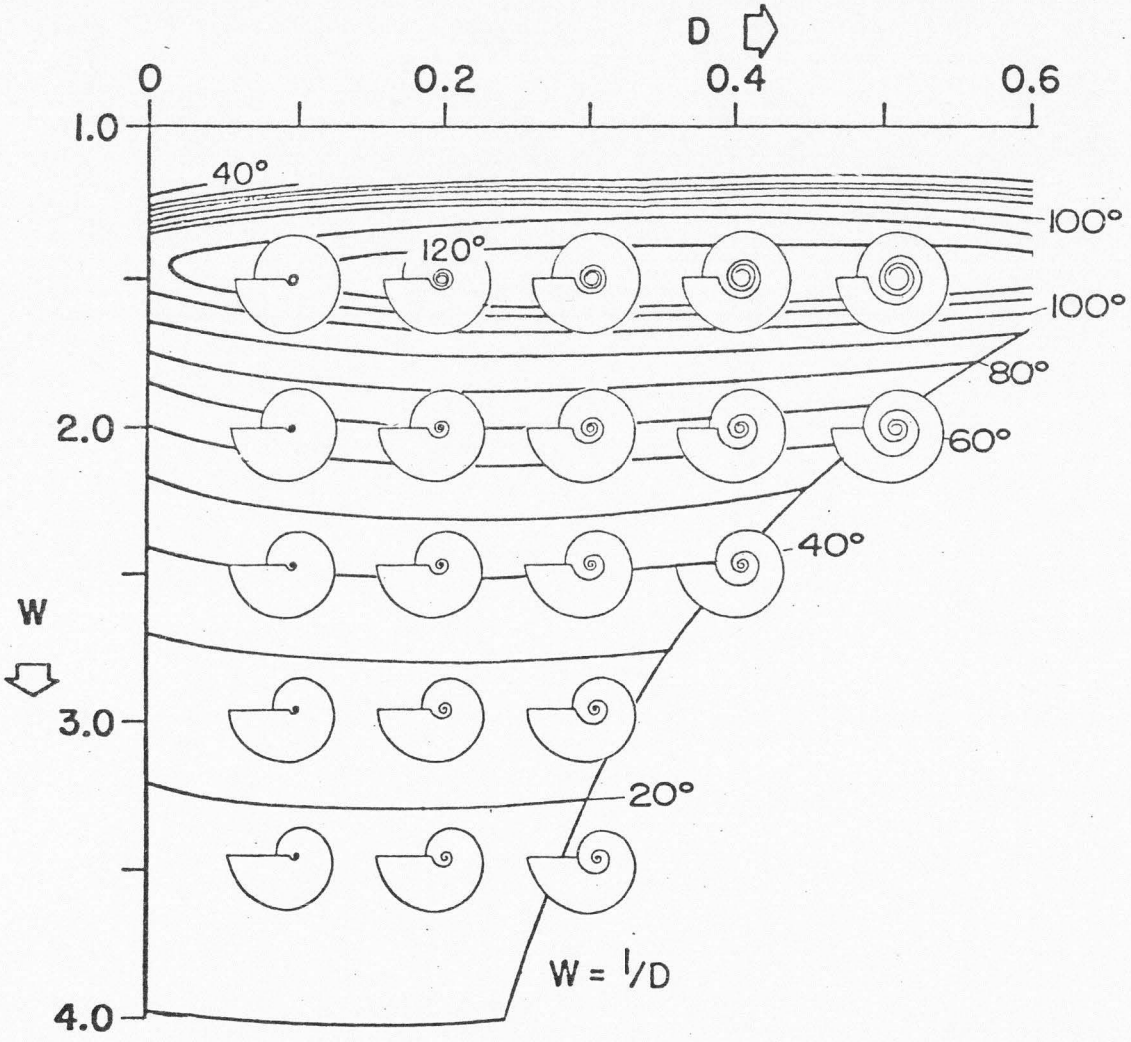

Figure 26. Life-orientation isopleths superimposed upon the ammonoid field of coiling geometries, umbilical view. (After Raup, 1967, Figure 18, p. 62)

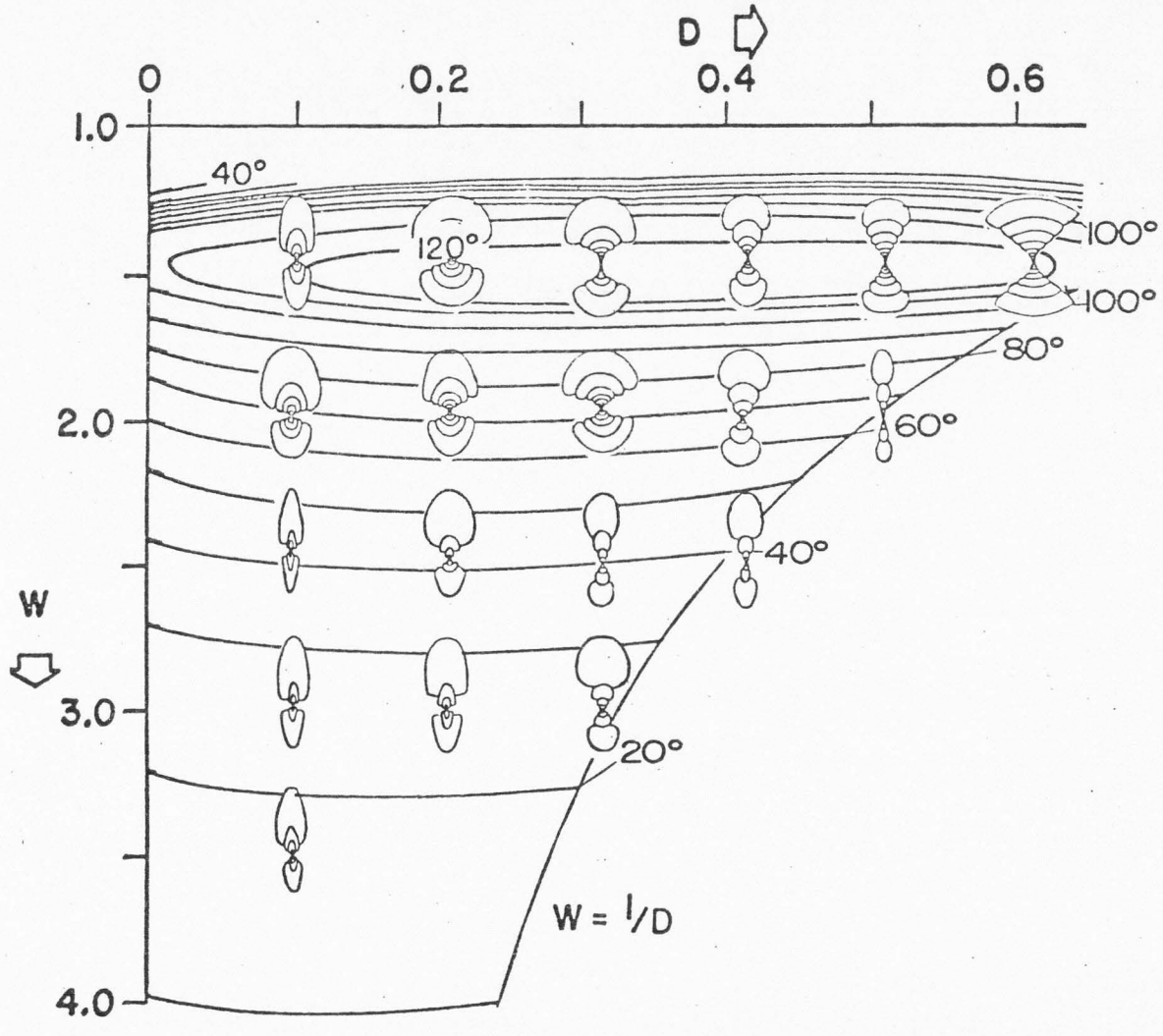

Figure 27. Life-orientation isopleths superimposed upon the ammonoid field of coiling geometries, cross-sectional view.

Selected Mississippian (Chesterian) ammonoid genera show (Figure 28) a weighted (10^3 abundances = 4 x orientation value, 10^2 abundances = 3 x orientation value, 10^1 abundances = 2 x orientation value, 10^0 abundances = original orientation value) average life-orientation angle of 99° from the gravitational vector, with a range between 60°-120°. Selected Lower Permian (Wolfcampian) ammonoid genera show (Figure 29) a weighted average life-orientation angle of 72° from the gravitational vector, with a range between 20°-120°. The appearance of medlicottids with their corresponding small life-orientation angles (average approximately 25°) influences the observed decrease in the weighted average.

Selected Middle Permian (Leonardian) ammonoid genera show (Figure 30) a weighted average life-orientation angle of 66° from the gravitational vector, with a range between 20°-120°. Selected Upper Permian (Lower Guadalupian) ammonoid genera show (Figure 31) a weighted average life-orientation angle of 70° from the gravitational vector, with a range between 20°-120°. Selected Upper Permian (Upper Guadalupian) ammonoid genera show (Figure 32) a weighted average life-orientation angle of 72° from the gravitational vector, with a range between 20°-120°. Selected Lower Triassic (Scythian) ammonoid genera show (Figure 33) a weighted average life-orientation angle of 72° from the gravitational vector, with a range between 10°-120°. The ammonoid genus Cordillerites has a life-orientation angle of 10°, the lowest among all analyzed genera.

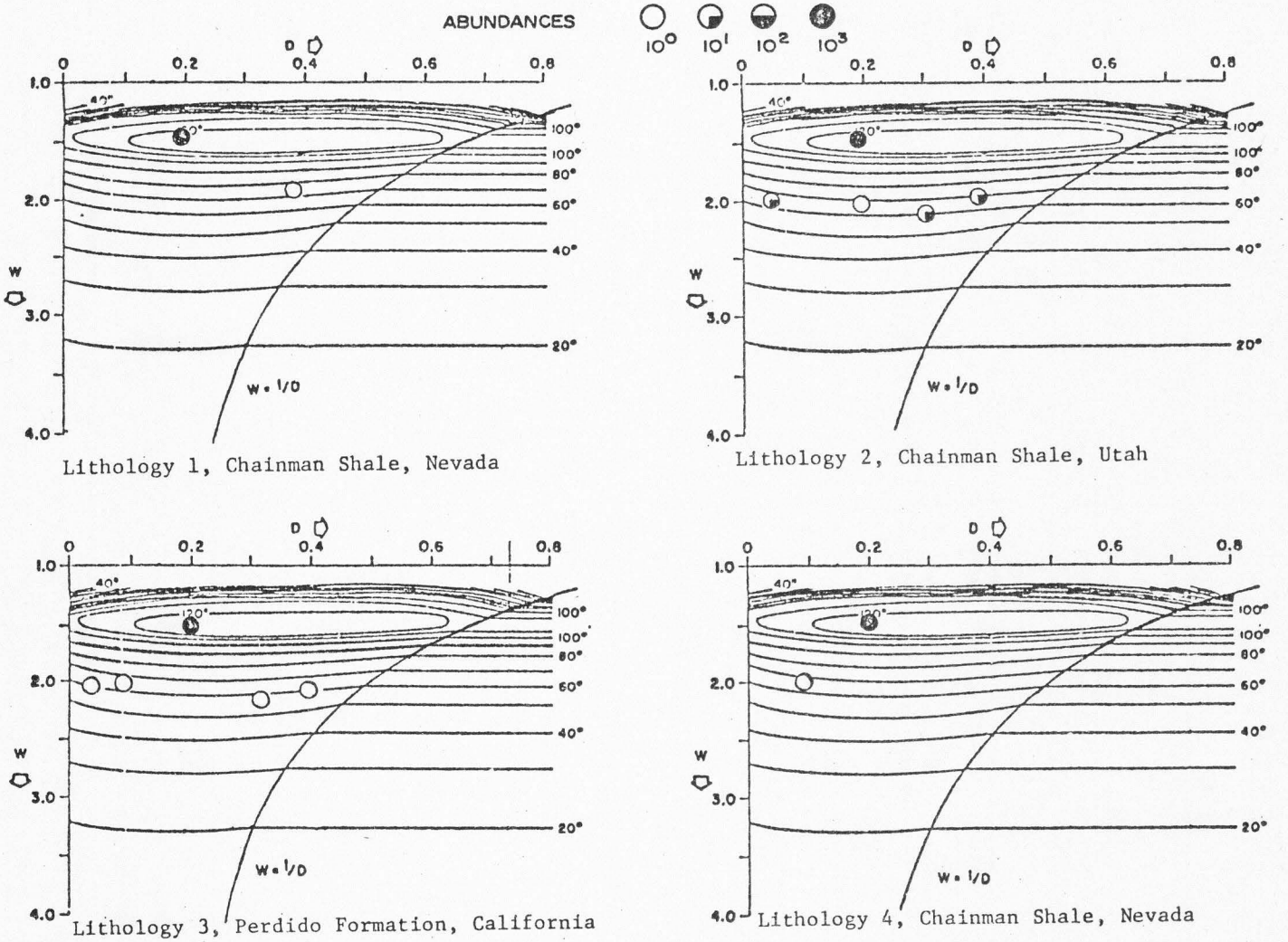

Figure 28. Life-orientations, selected Mississippian (Chesterian) ammonoid genera.

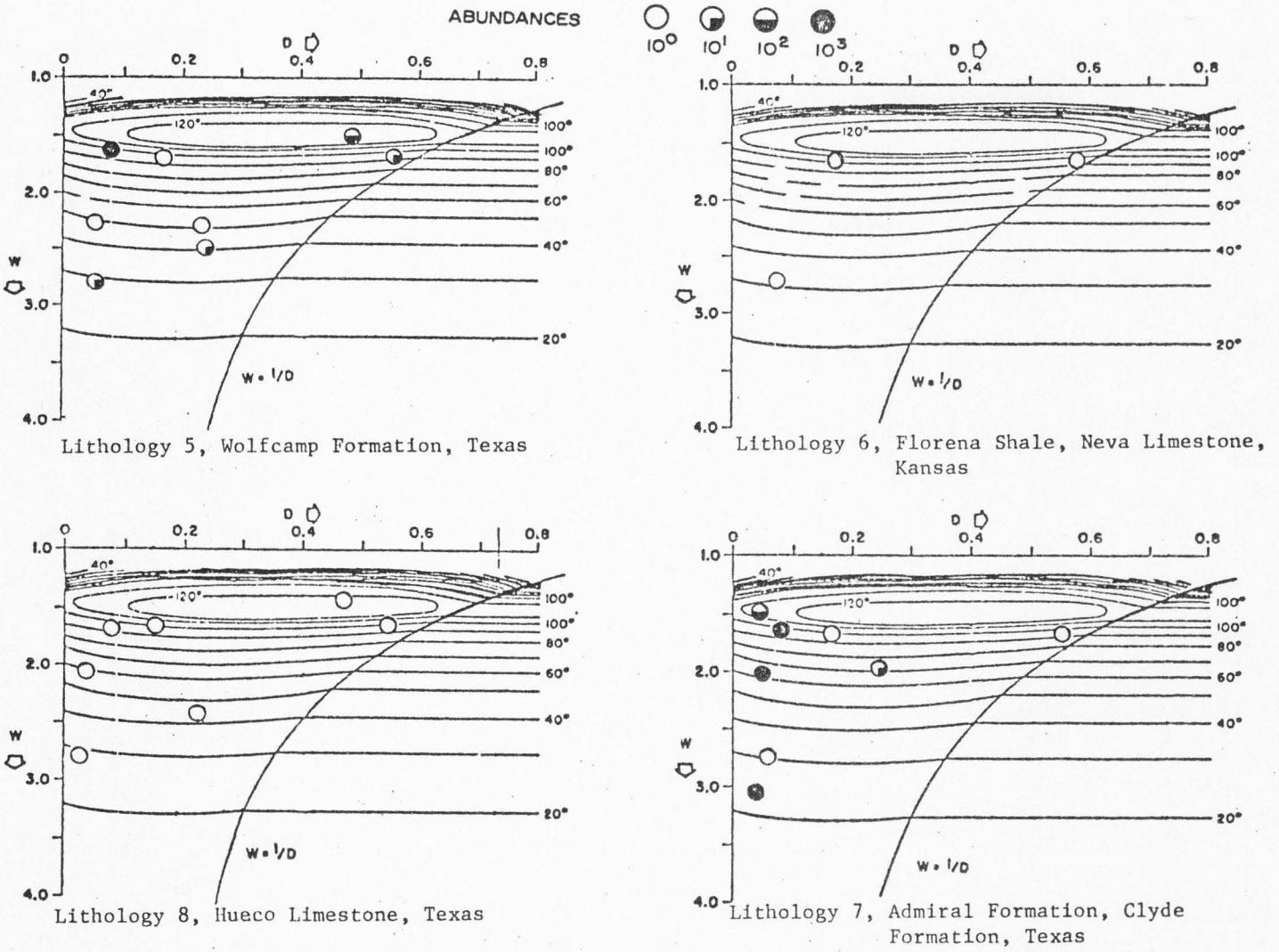

Lithology 5, Wolfcamp Formation, Texas

Lithology 6, Florena Shale, Neva Limestone, Kansas

Lithology 8, Hueco Limestone, Texas

Lithology 7, Admiral Formation, Clyde Formation, Texas

Figure 29. Life-orientations, selected Lower Permian (Wolfcampian) ammonoid genera.

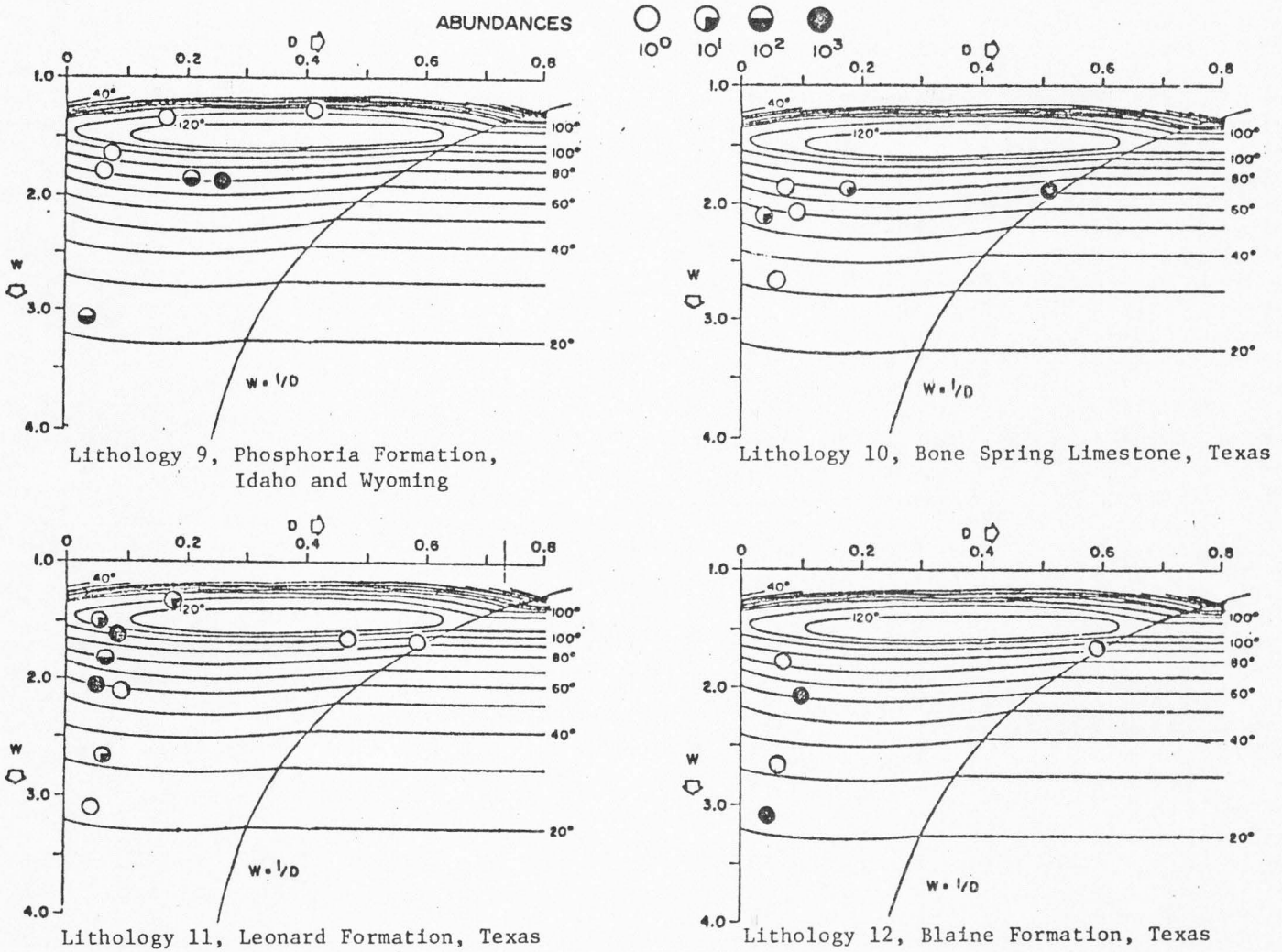

Lithology 9, Phosphoria Formation, Idaho and Wyoming

Lithology 10, Bone Spring Limestone, Texas

Lithology 11, Leonard Formation, Texas

Lithology 12, Blaine Formation, Texas

Figure 30. Life-orientations, selected Middle Permian (Leonardian) ammonoid genera.

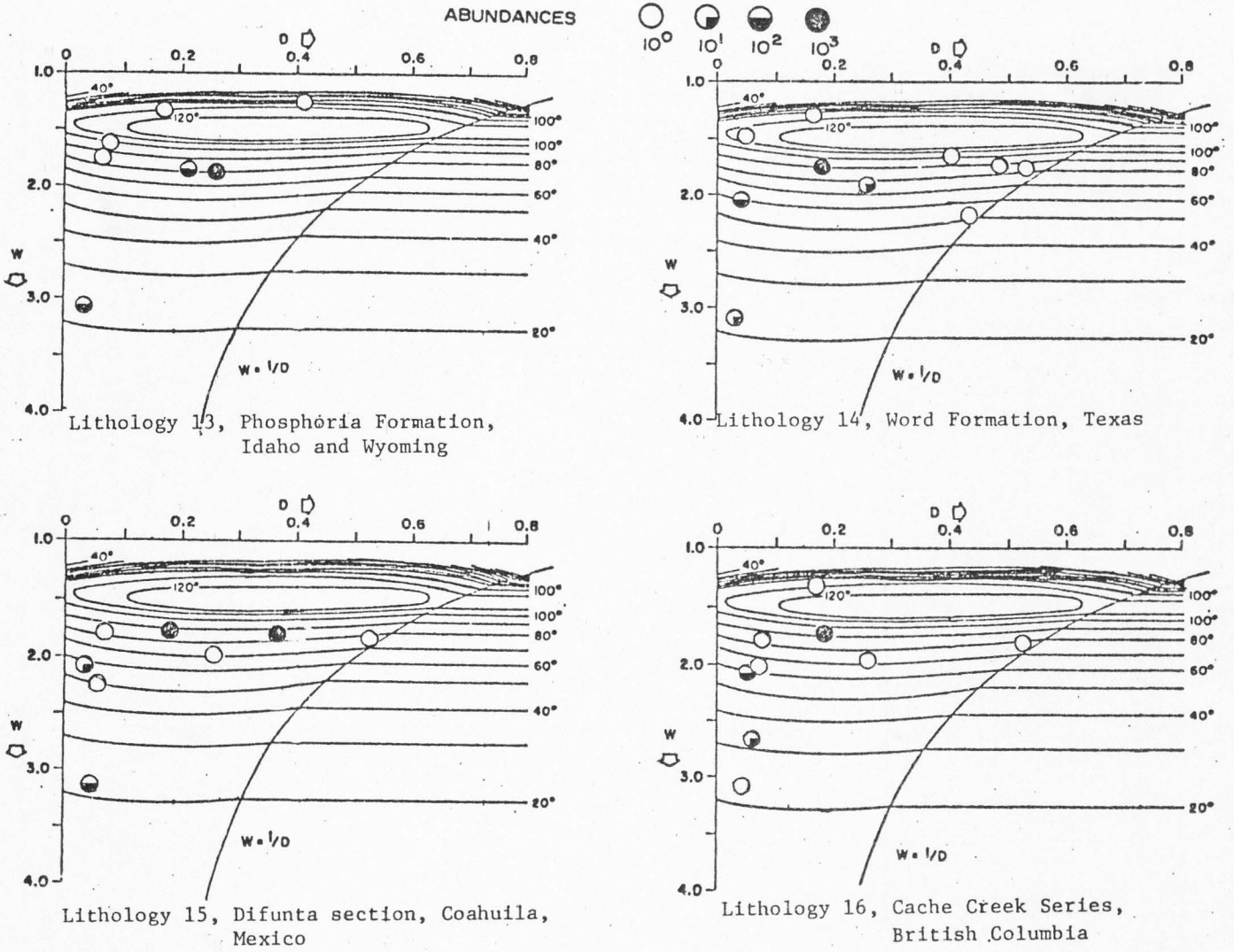

Lithology 13, Phosphoria Formation, Idaho and Wyoming

Lithology 14, Word Formation, Texas

Lithology 15, Difunta section, Coahuila, Mexico

Lithology 16, Cache Creek Series, British Columbia

Figure 31. Life-orientations, selected Upper Permian (Lower Guadalupian) ammonoid genera.

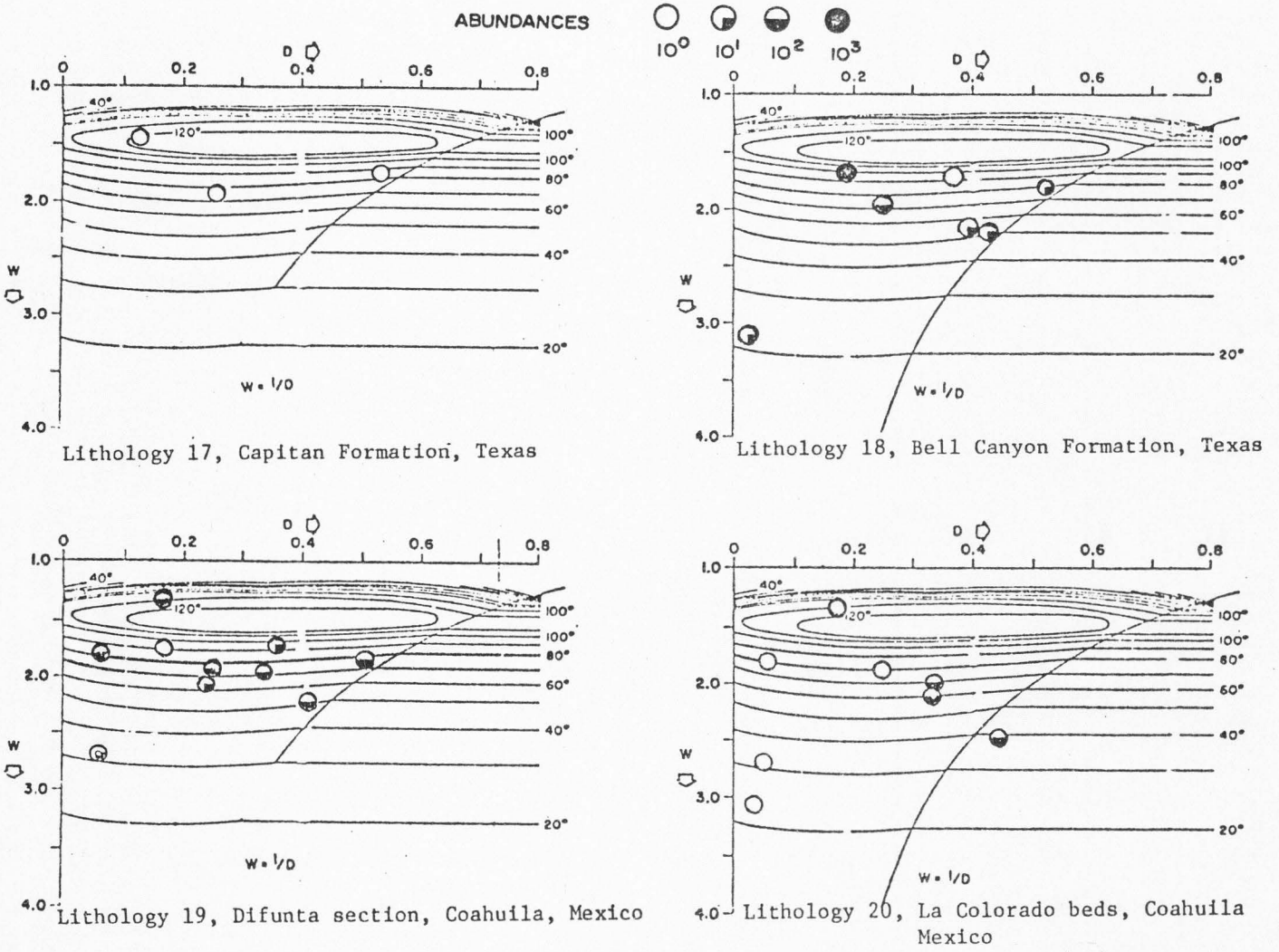

Lithology 17, Capitan Formation, Texas

Lithology 18, Bell Canyon Formation, Texas

Lithology 19, Difunta section, Coahuila, Mexico

Lithology 20, La Colorado beds, Coahuila Mexico

Figure 32. Life-orientations, selected Upper Permian (Upper Guadalupian) ammonoid genera.

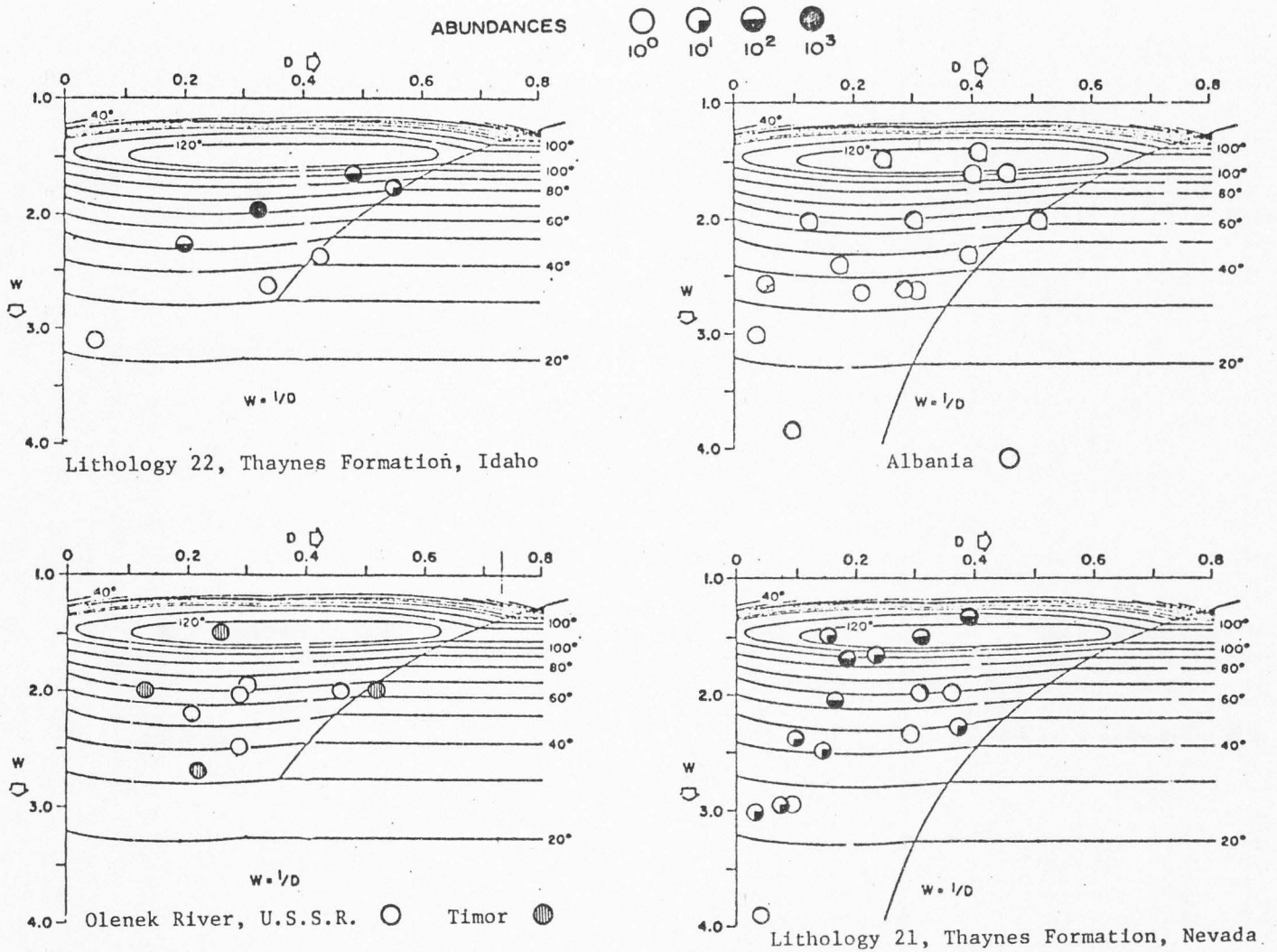

Figure 33. Life-orientations, selected Lower Triassic (Scythian) ammonoid genera.

In view of the recent findings available on Nautilus and Spirula concerning the use of fluid in the chambers for the purpose of posture and buoyancy control (Denton, 1974, pp. 286, 291), I disagree with Raups' exclusive focus on W and D values as an accurate means of reconstructing life orientation. Evidence from epizoan encrustation on a Cretaceous Buchiceras specimen from Peru (Seilacher, 1960, pp. 191-193) deserves mention (Figures 34 and 35). This example was further studied by Heptonstall (1973, pp. 319-321), who estimated the epizoans added between 8 and 24 g of additional weight to the ammonoid (5-10% total weight) which, by the distribution, orientation, and size of the encrusting oysters, was inferred to have maintained its original life attitude for some time after the initial encrustation. Despite the fact that this example was considered pathologic, and that modern Nautilus is rarely encrusted, this evidence suggests the consideration of life orientation based entirely on the geometry of the shell is oversimplified. Furthermore, I have observed live Nautilus pompilius at the Golden Gate Park Aquarium in San Francisco, California and noted an attendant rocking motion resulting from each burst of the hyponome; in a particularly stable form such as Nautilus this amounts to a variation in attitude of approximately 10°. In forms displaying less stability, however, much larger variation would be expected. Because of these complexities and lack of consistent trends in the data, inferences about life-orientation reconstructed solely on the basis of the W and D variables of ammonoids are not reliable, given the suspected ability of the organism to adjust its orientation.

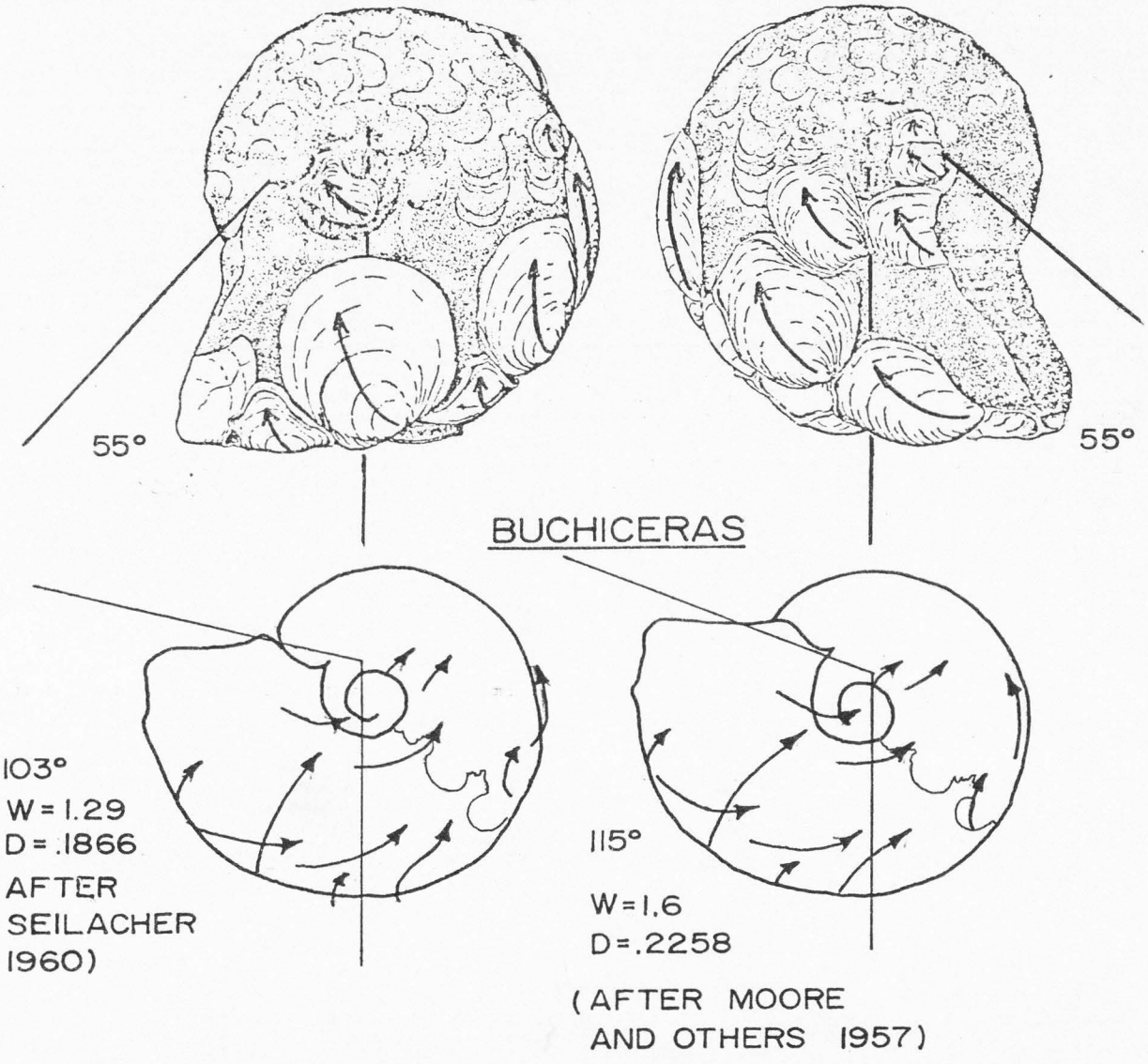

Figure 34. Examples of discrepancies in reconstructions of life-orientations: W-and-D analysis versus epizoan encrustation.

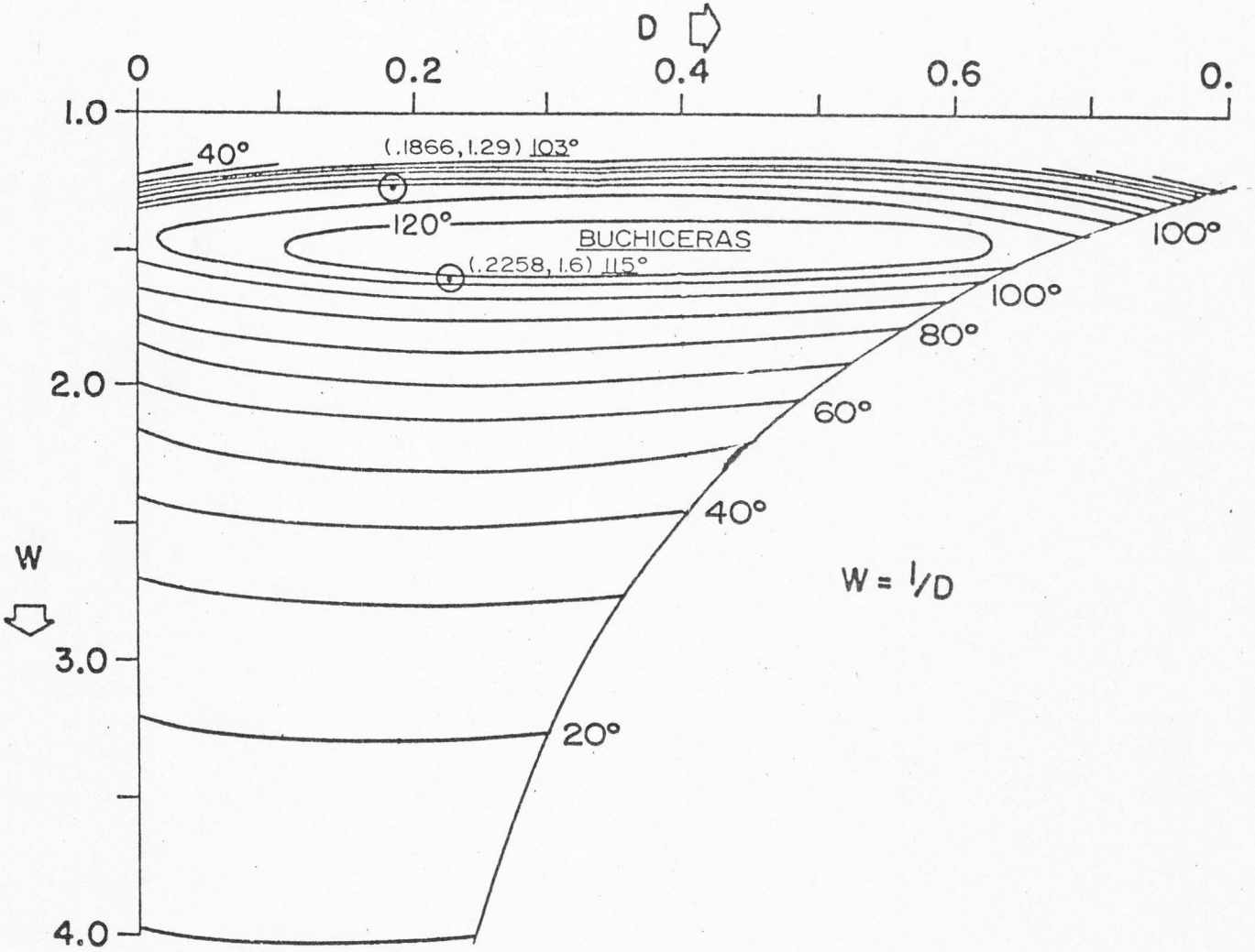

Figure 35. Extremes of life-orientations based on W-and-D shell-coiling parameters.

HYDRODYNAMIC STABILITY

According to most reconstructions of the life habit of coiled cephalopods, based primarily on observations of living Nautilus, it is assumed that the chambers within the shell contained gases (slightly more nitrogen than normally occurs in the atmosphere) which are observed to be at slightly less than atmospheric pressure. Water, being more dense than air (62.43 lb/ft^3 to .08071 lb/ft^3) exerts an upward pressure on all surfaces of the shell proportional to the depth. This is because the inside of the shell is being maintained at a comparatively low pressure. Pressure adjustments, made by adding or removing amounts of liquid (Tasch, 1973, pp. 409-410) within the chambers facilitate passive vertical movement within the water column. Thus, the buoyant force is described as acting with a magnitude equal to the weight of water displaced by the volume of the shell, applied at the center of that volume. The line of this force will always pass through that point, no matter what the orientation of the shell.

Gravity opposes the buoyant force, and this downward pull can also be resolved collectively into a single point of application, the center of gravity. The line of this force will also pass through the same point at any orientation. These opposing forces (see Figure 36) will, however, balance at a specific orientation of the shell, and the hydrodynamic stability of this particular orientation is determined by

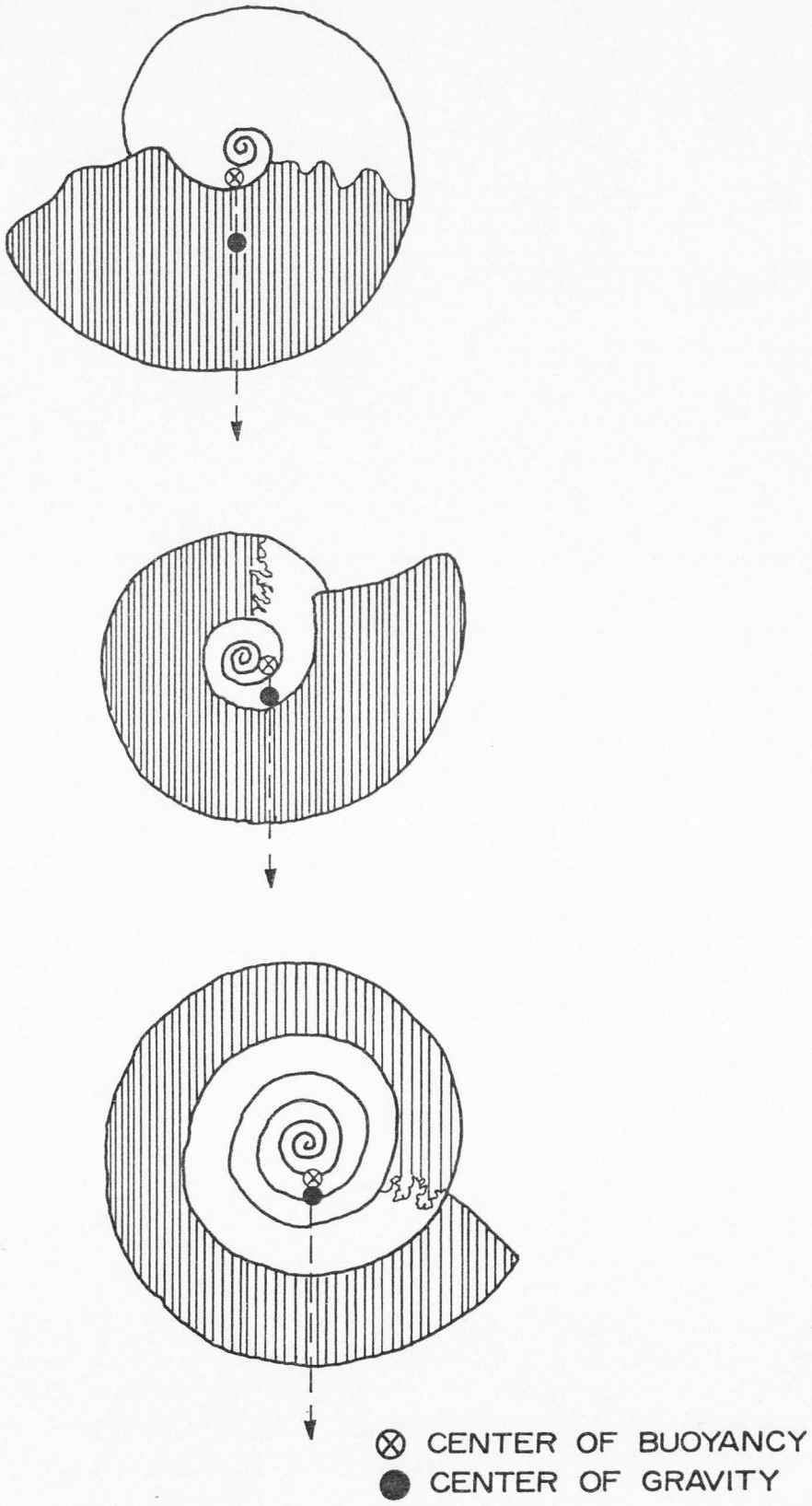

Figure 36. Stabilities of rest attitudes for various coiling geometries of ammonoids (After Trueman, 1941).

the distance separating the points of application of the two vectors. The greater the distance between these two points, the greater the magnitude of the restoring force to return the shell to its original orientation, when acted upon by an external force, e.g., the water bursts of the hyponome, currents, etc. Rotational stability isopleths are shown superimposed upon the field of ammonoid shell-coiling geometries in umbilical and cross-sectional view (Figures 37 and 38).

Selected Mississippian (Chesterian) ammonoid genera show (Figure 39) a weighted (10^3 abundances = 4 x stability value, 10^2 abundances = 3 x stability value, 10^1 abundances = 2 x stability value, 10^0 abundance = original stability value) average rotational stability value of .07, with a range between .04-.10. Selected Permian ammonoid genera show (Figures 40-43) a range of weighted average rotational stability values between .09-.12, with a mean value of .11. The extreme values are found in Wolfcampian and Leonardian time, respectively. Selected Triassic (Scythian) ammonoid genera show (Figure 44) a weighted average rotational stability value of .10, with a range between .04 and .14. Though some genera have stability values which approach .04 (the low stability field), they rarely fall in the .04 isopleth. It is the interpretation of the author that the void area represents rotational stability too low to insure survival of the ammonoid, even though, as will be shown later, this is the area of most efficient utilization of calcium carbonate. In contrast, Medlicottia (Figures 41-42) occupies an area of inefficient calcium carbonate utilization, yet both its stability value and abundance are high. Under anoxic conditions, ammonoids would be forced to conserve energy expended in locomotion.

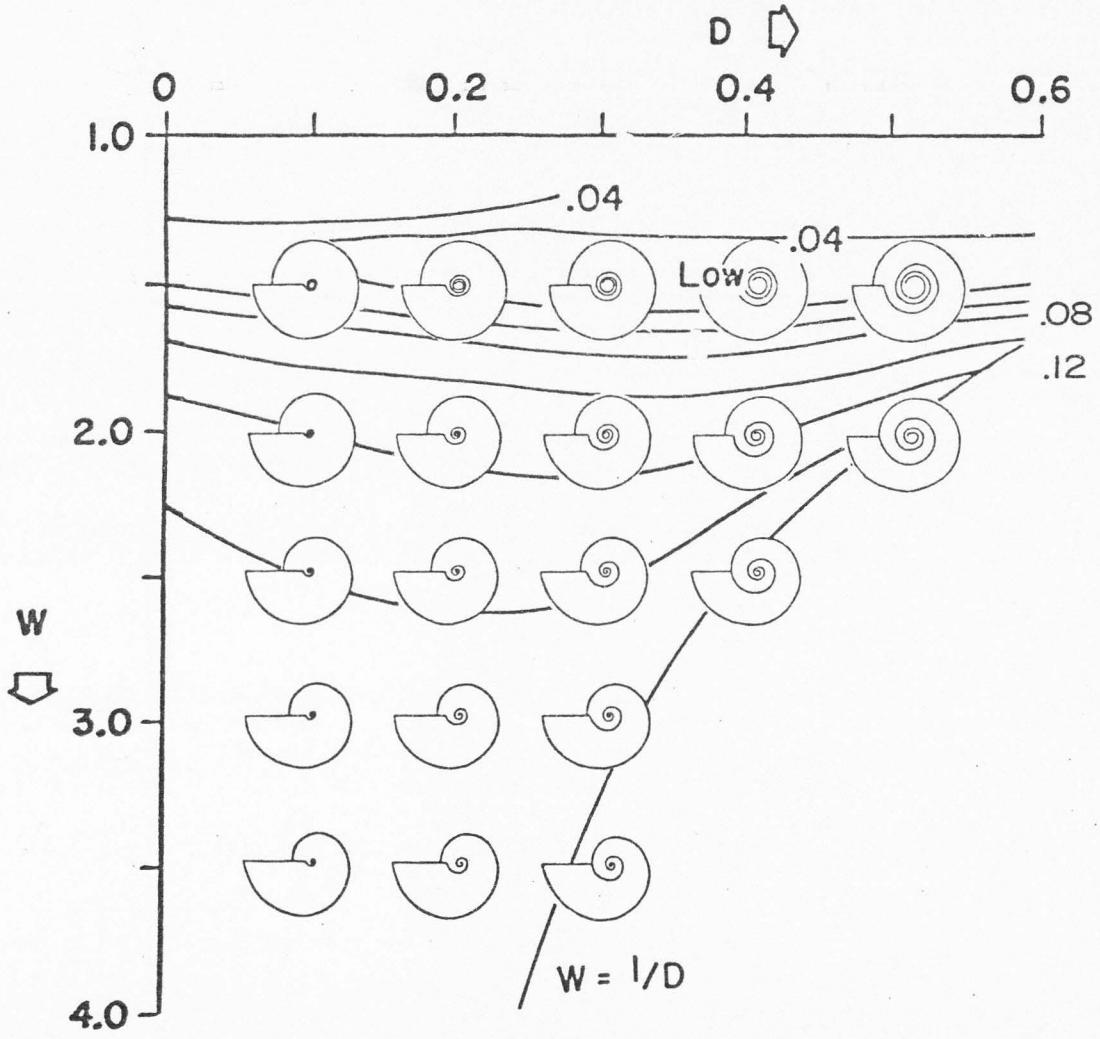

Figure 37. Stability isopleths superimposed upon the ammonoid field of coiling geometries, umbilical view. (After Raup, 1967, Figure 19, p. 63)

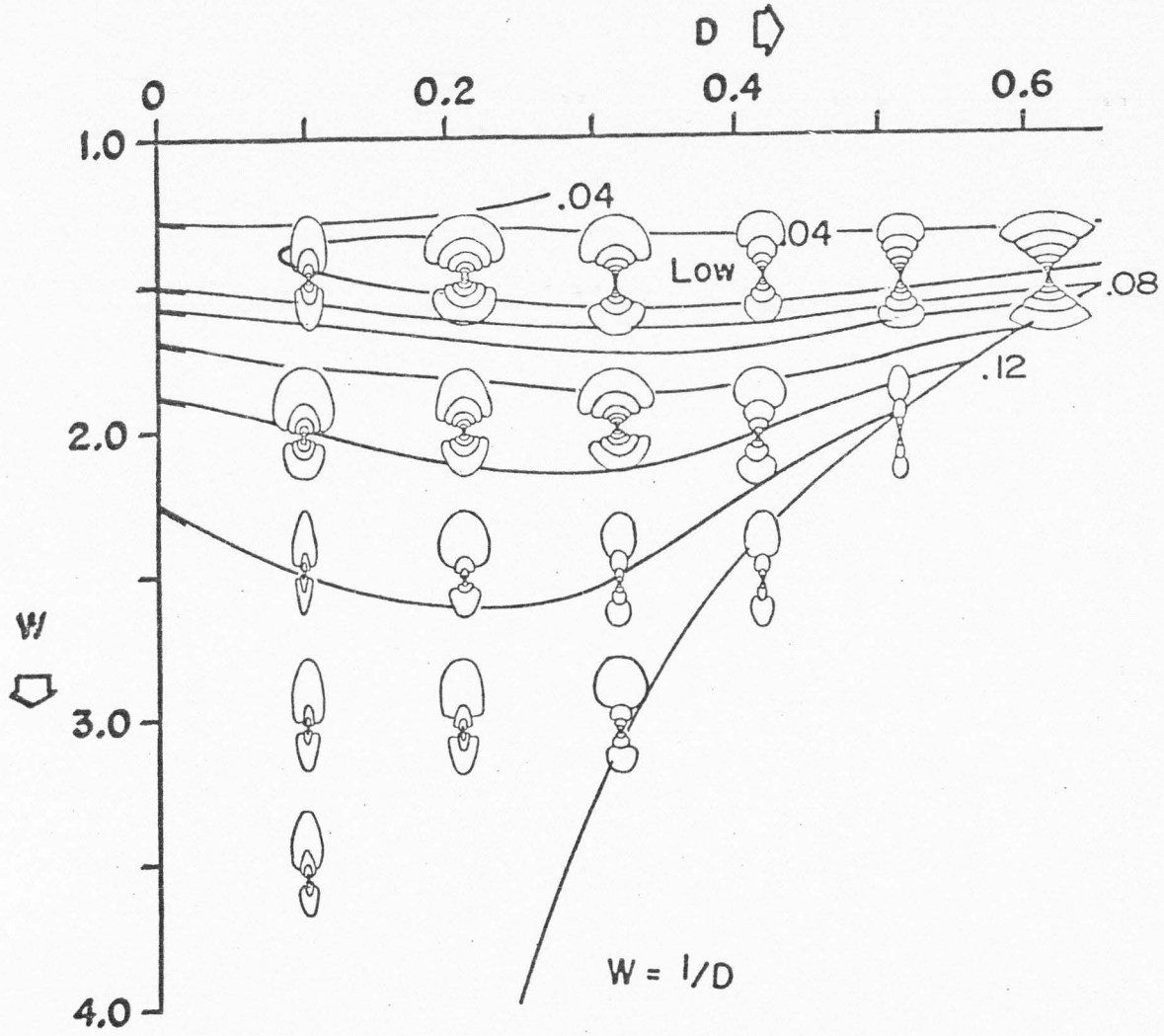

Figure 38. Stability isopleths superimposed upon the ammonoid field of coiling geometries, cross-sectional view.

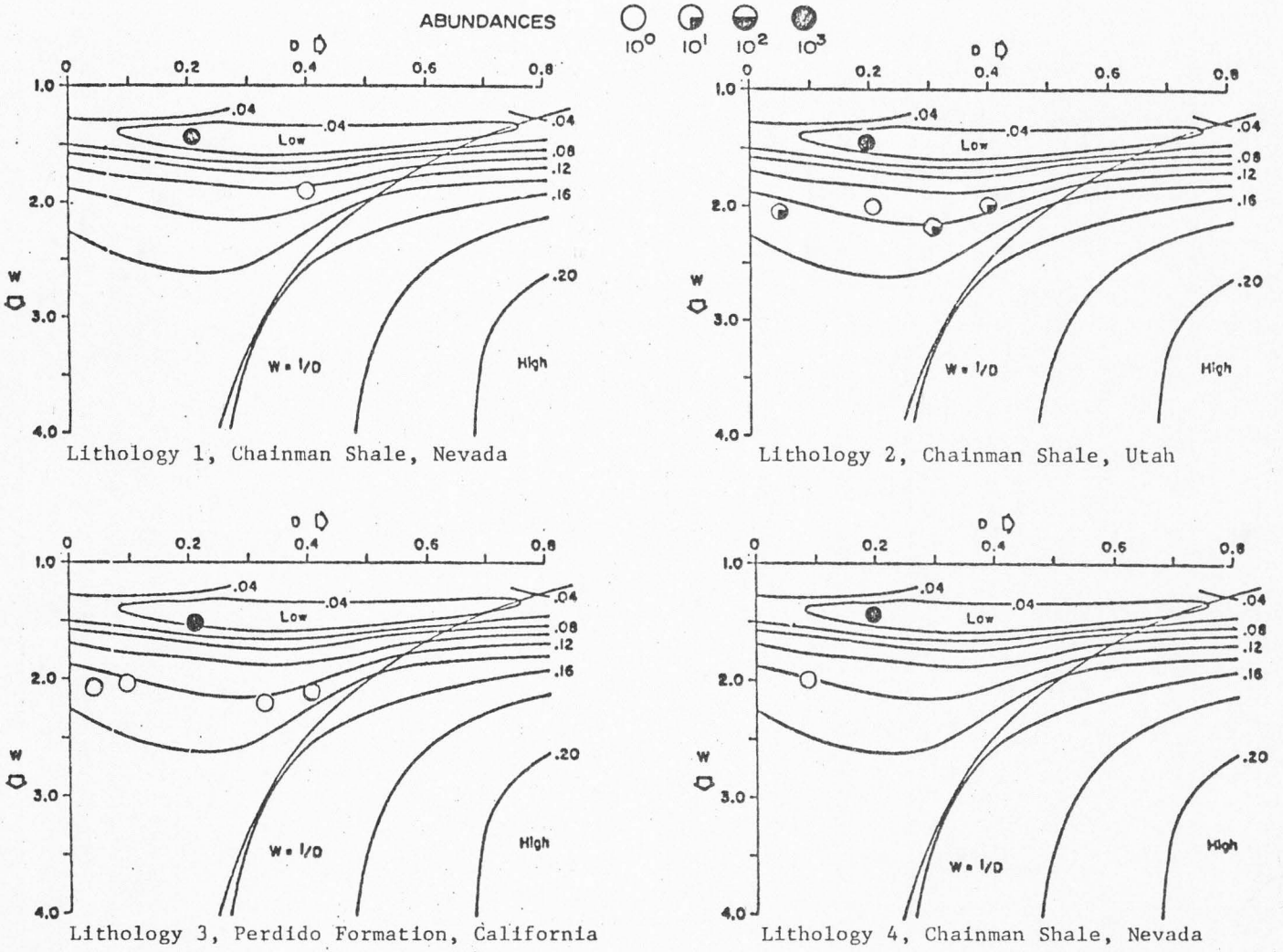

Figure 39. Stability values, selected Mississippian (Chesterian) ammonoid genera.

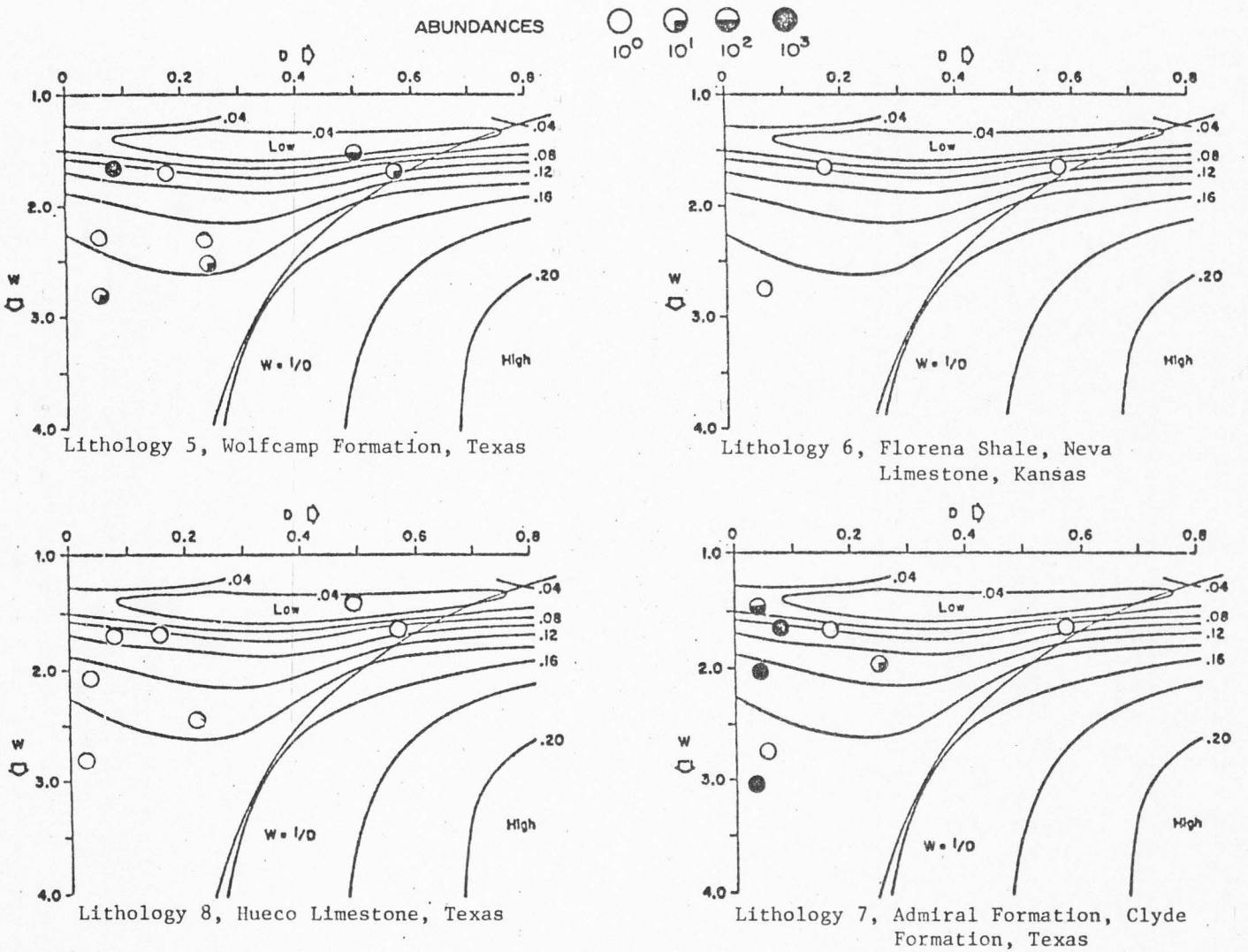

Lithology 5, Wolfcamp Formation, Texas

Lithology 6, Florena Shale, Neva Limestone, Kansas

Lithology 8, Hueco Limestone, Texas

Lithology 7, Admiral Formation, Clyde Formation, Texas

Figure 40. Stability values, selected Lower Permian (Wolfcampian) ammonoid genera.

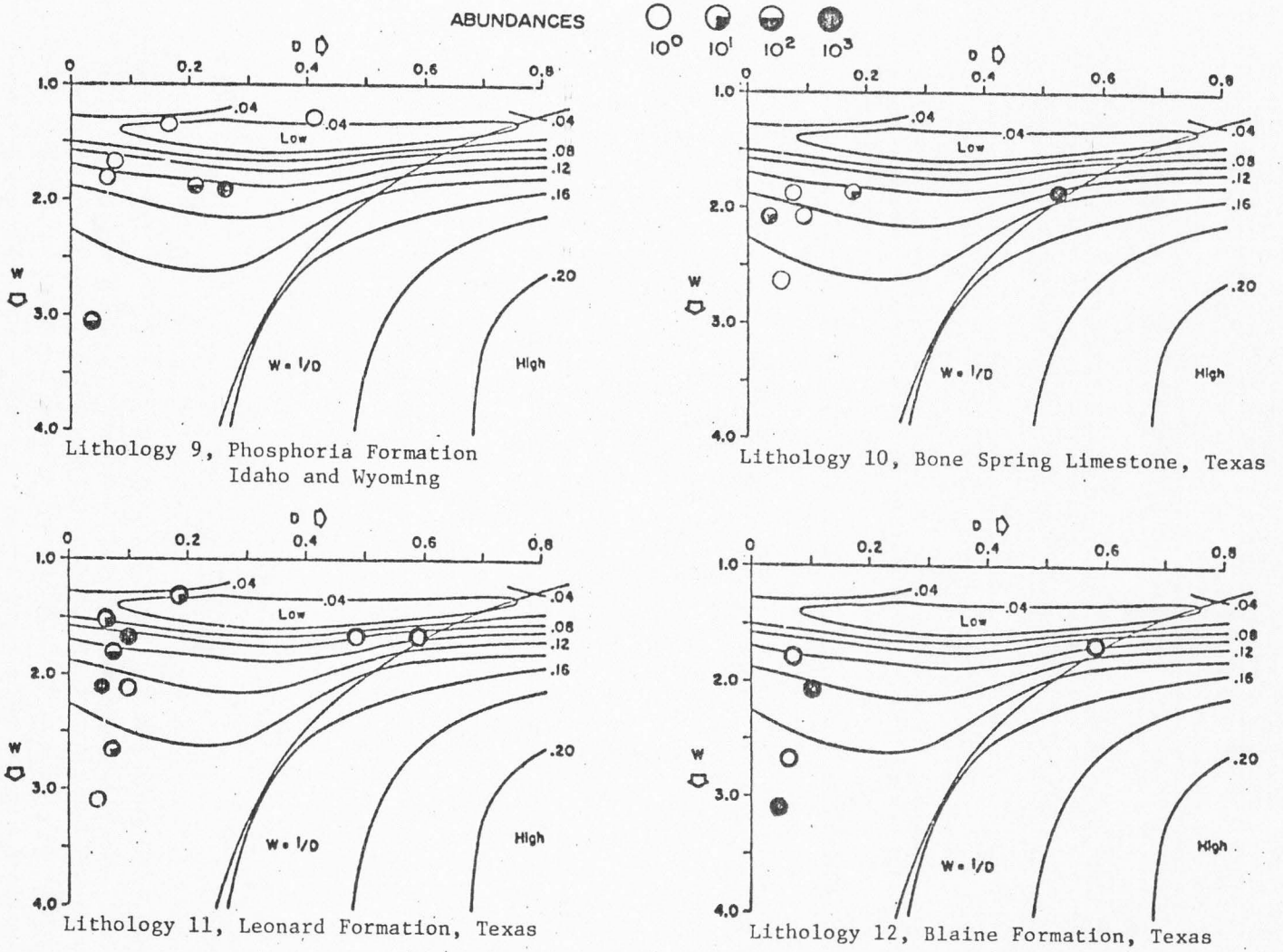

Figure 41. Stability values, selected Middle Permian (Leonardian) ammonoid genera.

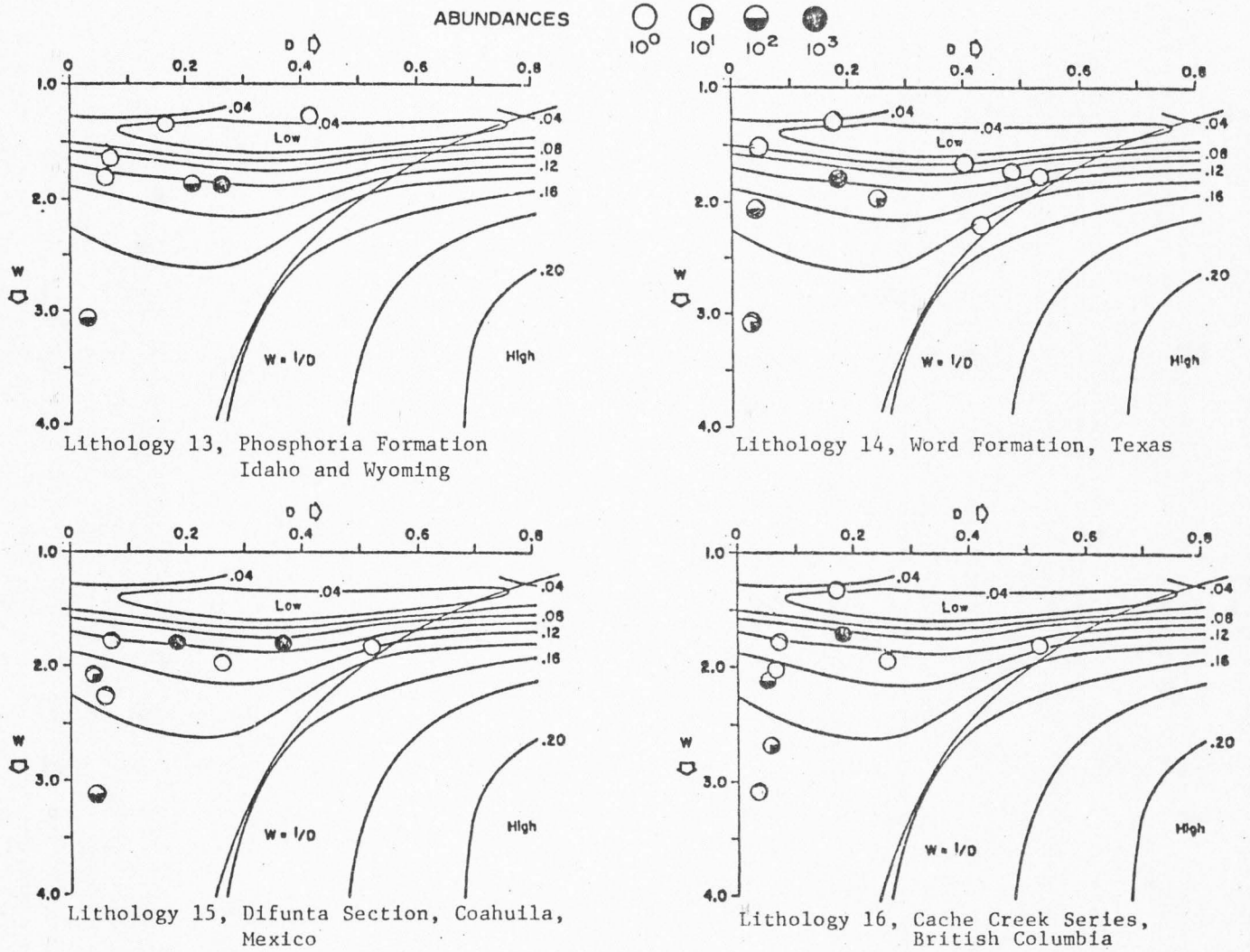

Figure 42. Stability values, selected Upper Permian (Lower Guadalupian) ammonoid genera.

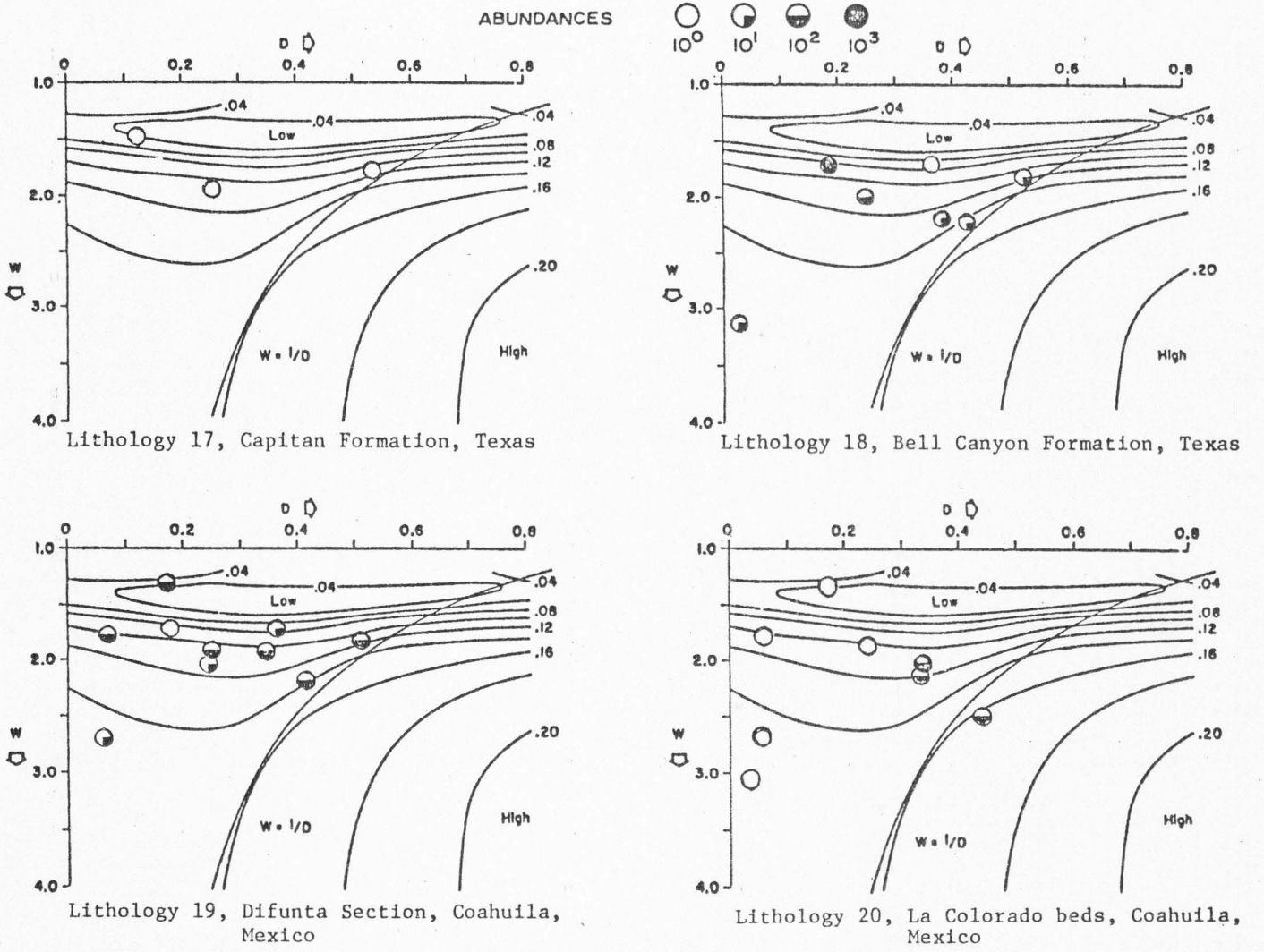

Figure 43. Stability values, selected Upper Permian (Upper Guadalupian) ammonoid genera.

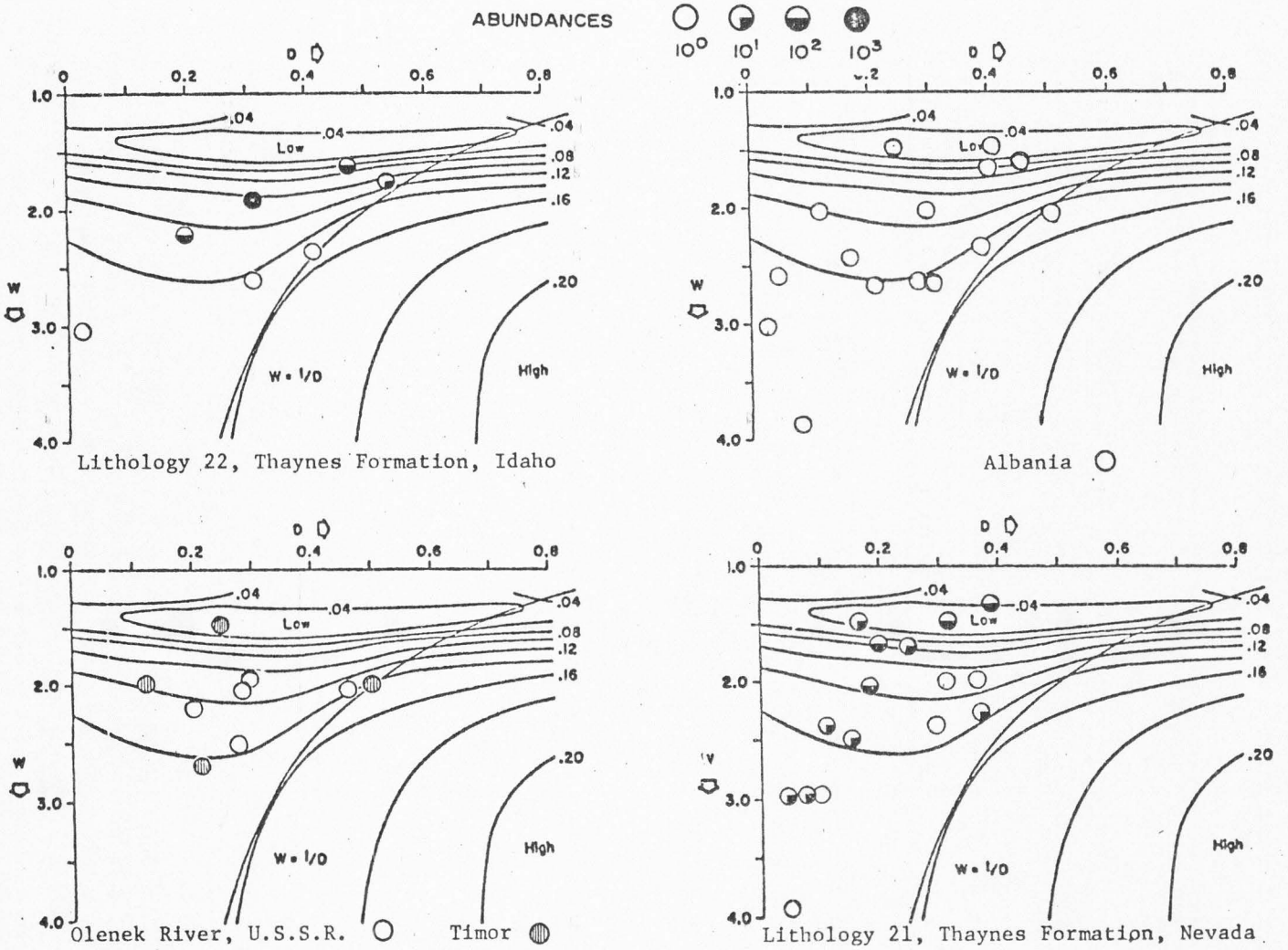

Figure 44. Stability values, selected Lower Triassic (Scythian) ammonoid genera.

The metabolic rate of these carnivorous animals was probably high, which necessitated a constant search for prey (one experimental subject of Nautilus consumed 70 grams of fish bait in one meal, which is about 15-20% of the animal's entire weight (Ward and others, 1977, p. 380). A premium would be placed on coiling geometries which were less prone to rotational instability, thereby minimizing energy wasted in attitude adjustment while searching for prey. Stability also contributed to the progressive adaptive radiation of ammonoids between Mississippian and Triassic times.

EFFICIENCY IN THE UTILIZATION OF CALCIUM CARBONATE

Efficient utilization of calcium carbonate as shell material is similar to the previous consideration of body-chamber lengths in that it is an inherent property of the ammonoid shell-coiling geometry. Efficiency, in the abbreviated sense, is defined (Raup, 1967, p. 58, Figure 15) as the computed ratio of internal shell volume to volume of shell material. Higher values of this ratio describe forms more efficient in constructing a shell with the least possible amount of material. Efficiency (Figures 45 and 46) varies directly with the coiling-geometry parameter D. Correlations with the W, S and F parameters are not readily discernable. To emphasize variation in efficiency with changing D values, it must be remembered that shells with low D values (involute) have considerable overlapping of whorls (onlap) which requires secreting practically the entire aperture circumference in each whorl. High D values, however, require a much smaller portion of construction for each new whorl, as the surface of the previous whorl is used as a floor for the succeeding whorl (Figure 47).

Ammonoid coiling geometries studied occupy a very broad area of the W and D field, irrespective of taxonomic subdivisions (Figures 48-53).

Selected Mississippian (Chesterian) ammonoid genera from lithologies 1 and 2 (Figure 50)(Phosphatic, nodular limestone rich in organic matter) have a weighted (10^3 abundances = 4 x efficiency value,

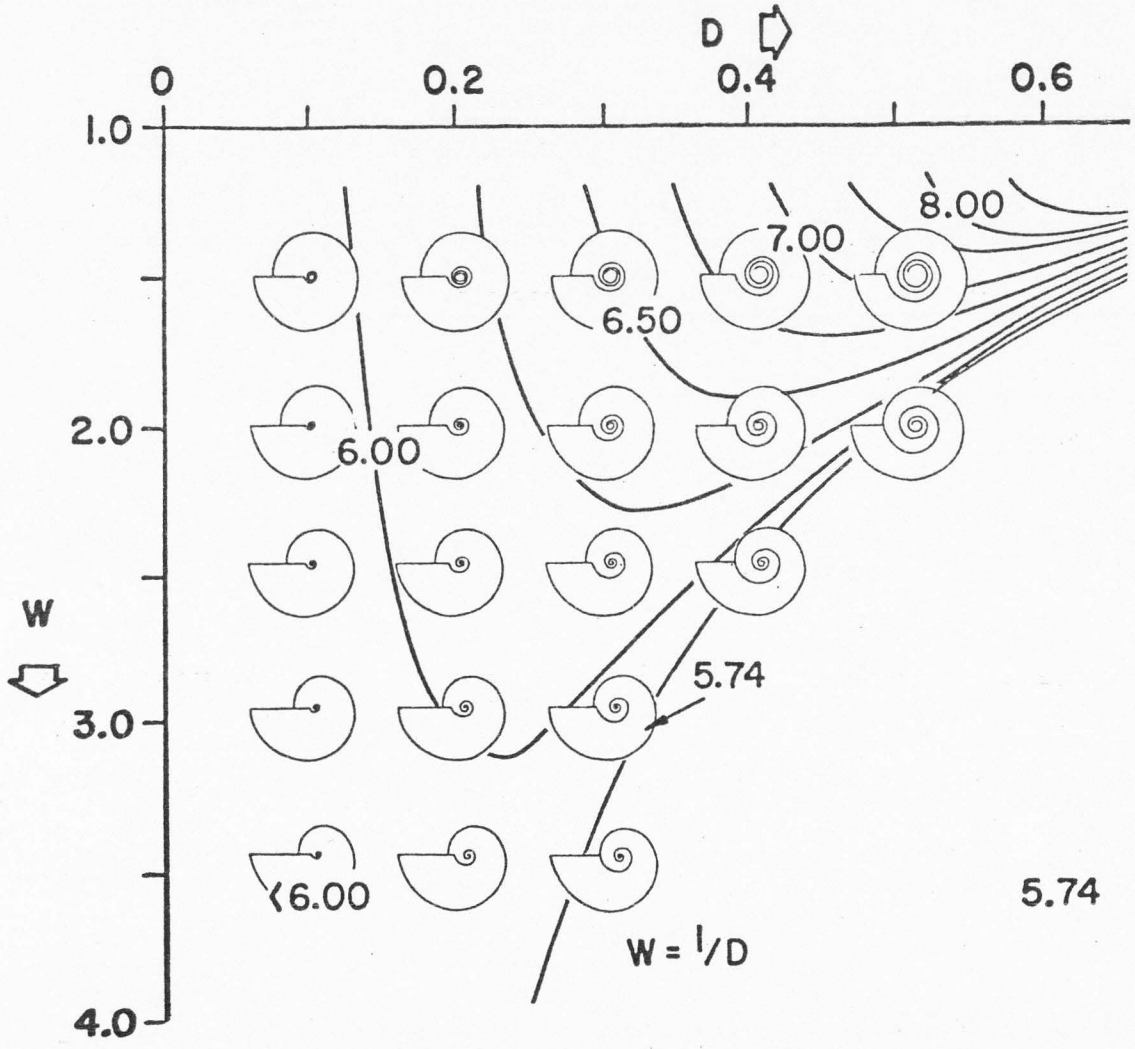

Figure 45. Isopleths for calcium-carbonate efficiency superimposed upon the field of coiling geometries, umbilical view. (After Raup, 1967, Figure 15, p. 58)

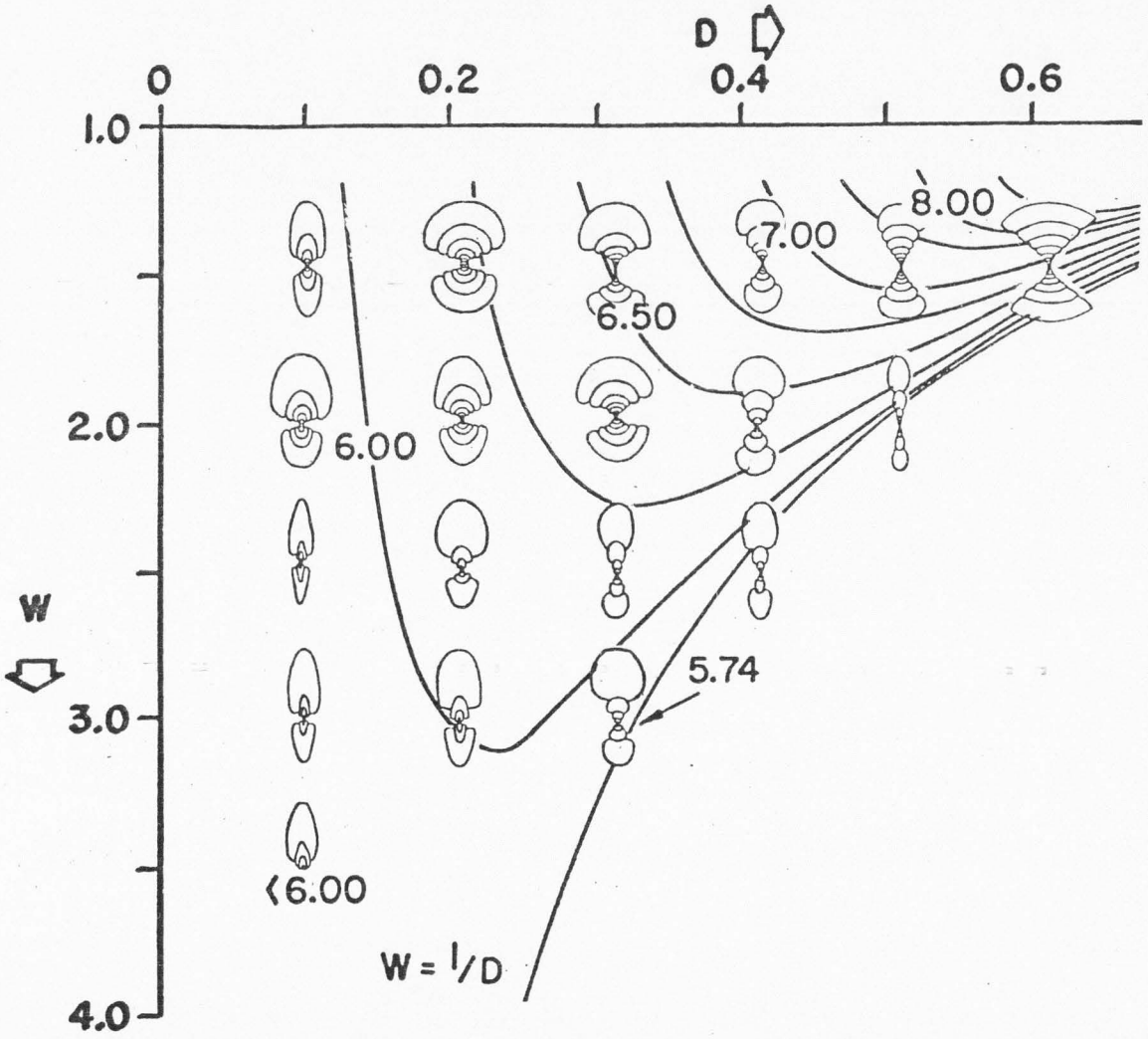

Figure 46. Isopleths for calcium-carbonate efficiency superimposed upon the ammonoid field of coiling geometries, cross-sectional view.

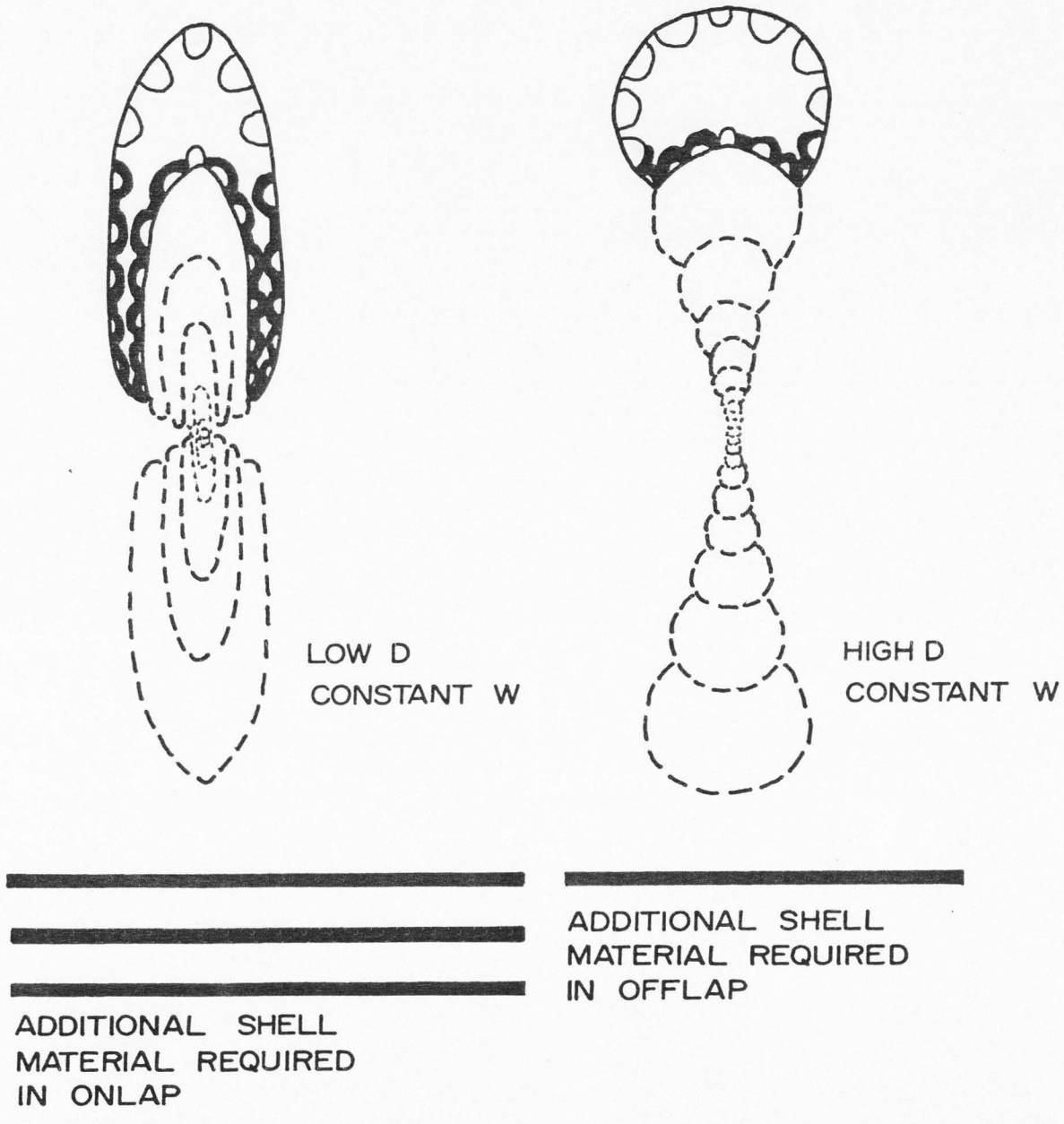

Figure 47. Efficiency in utilization of calcium carbonate in shell-coiling geometries of ammonoids, onlap versus offlap.

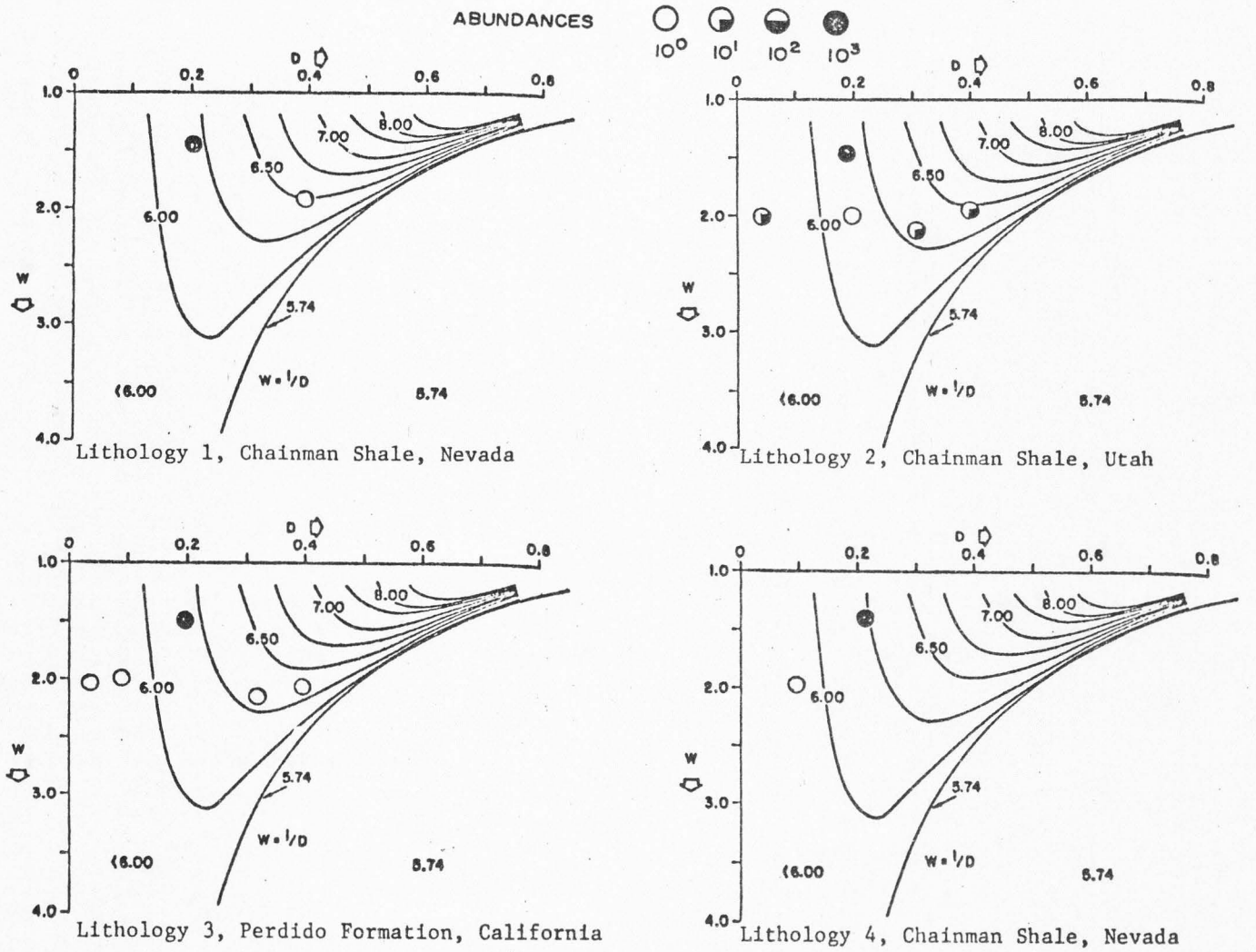

Figure 48. Calcium carbonate efficiency, selected Mississippian (Chesterian) ammonoid genera.

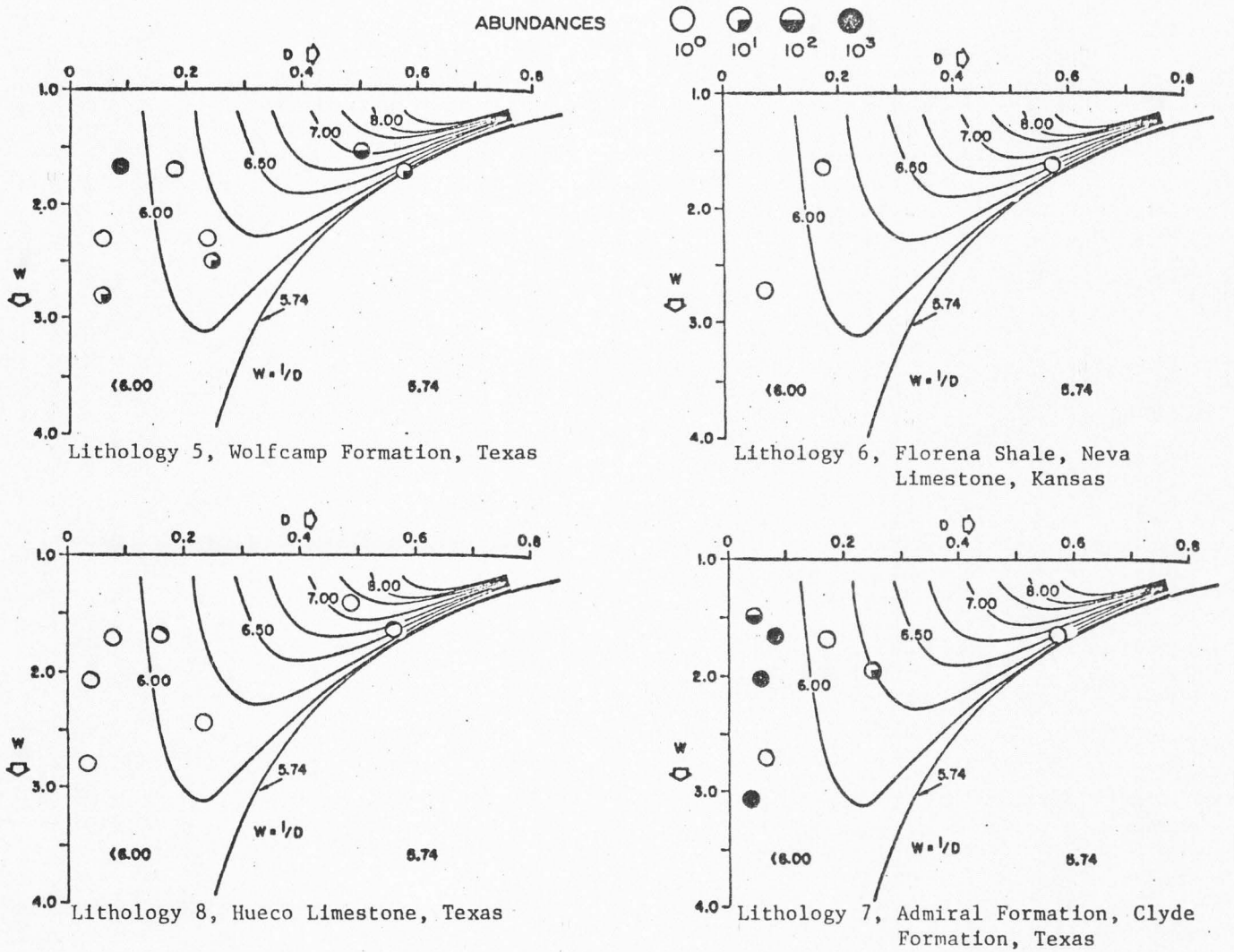

Figure 49. Calcium carbonate efficiency, selected Lower Permian (Wolfcampian) ammonoid genera.

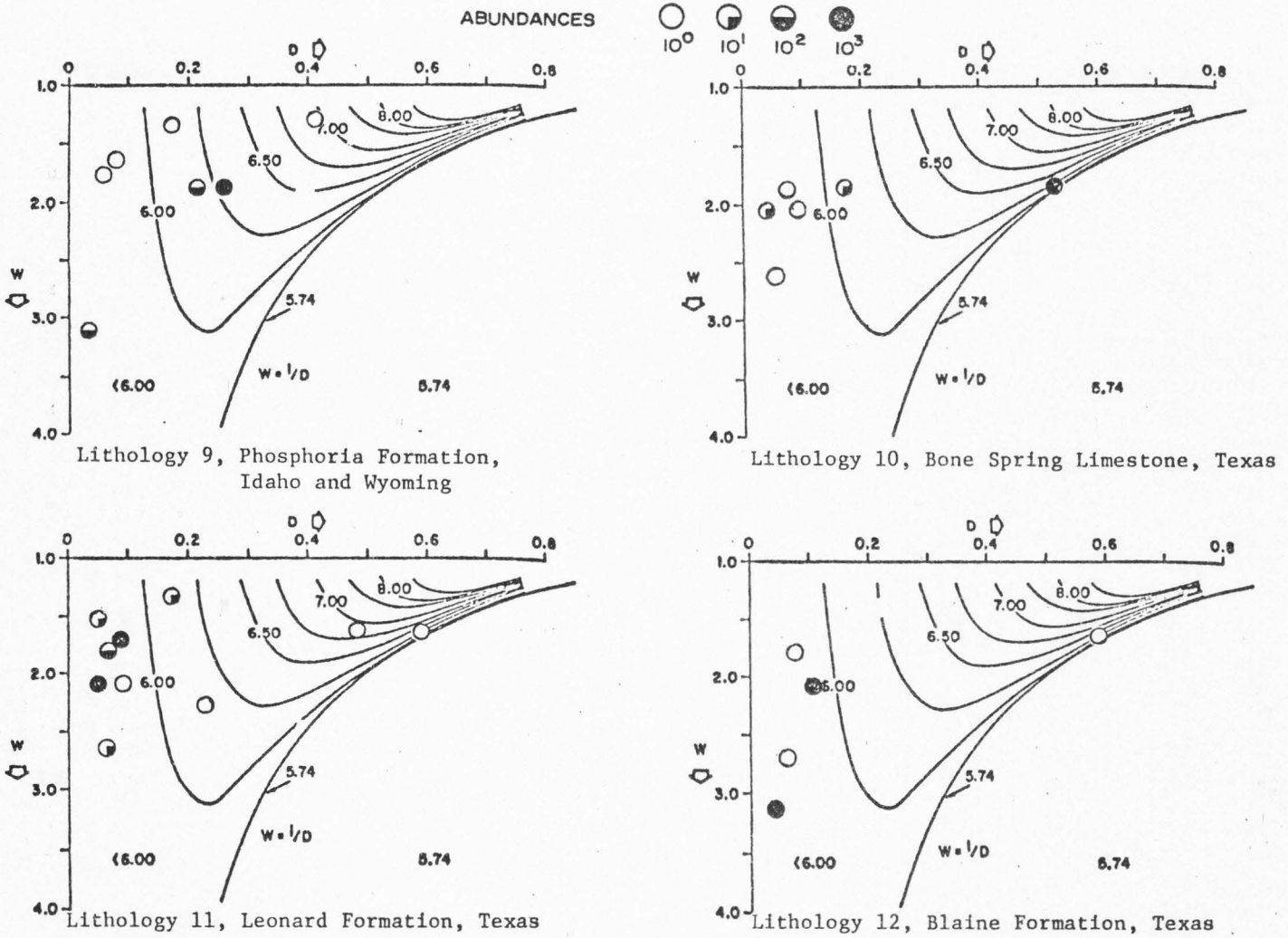

Figure 50. Calcium carbonate efficiency, selected Middle Permian (Leonardian) ammonoid genera.

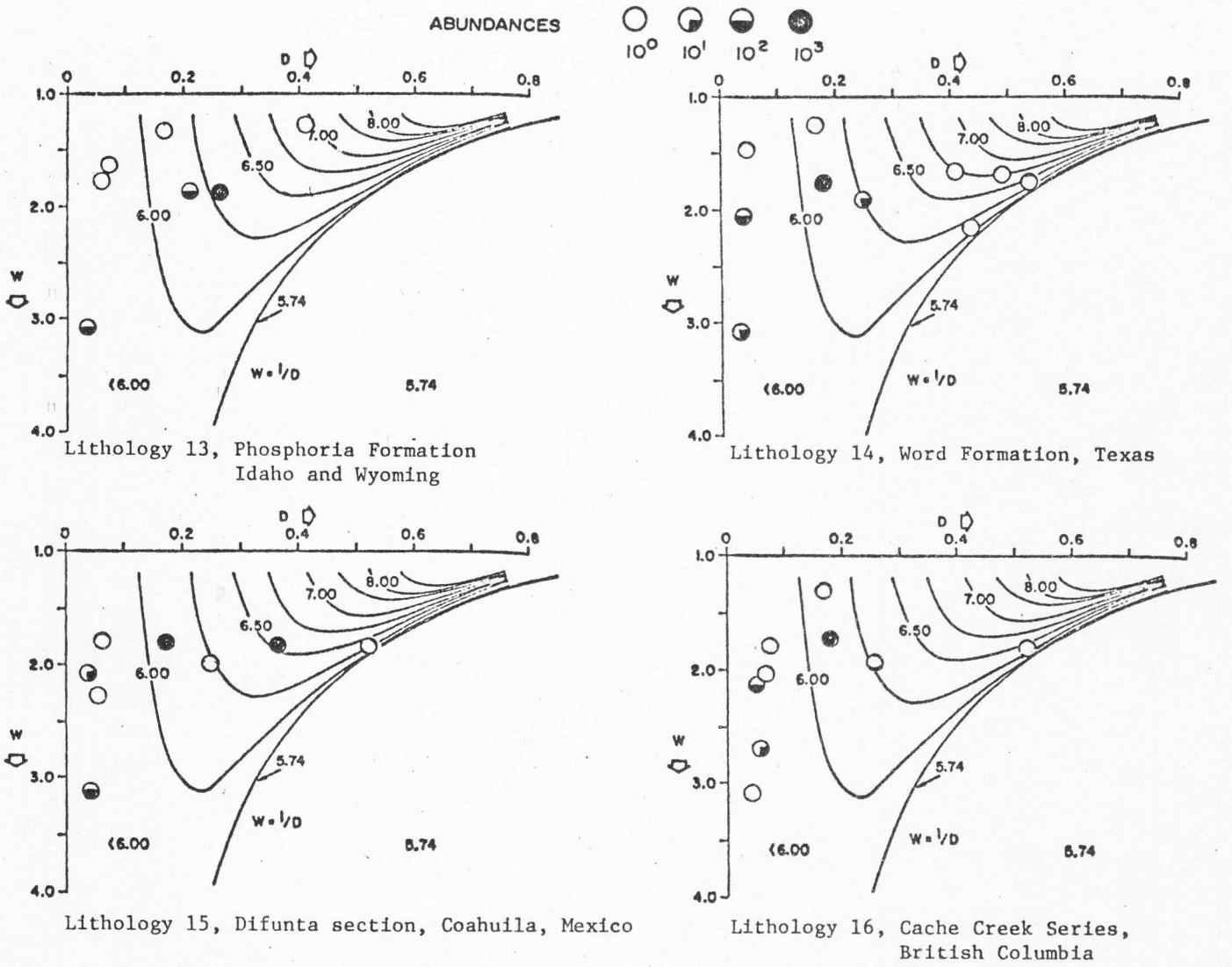

Figure 51. Calcium carbonate efficiency, selected Upper Permian (Lower Guadalupian) ammonoid genera.

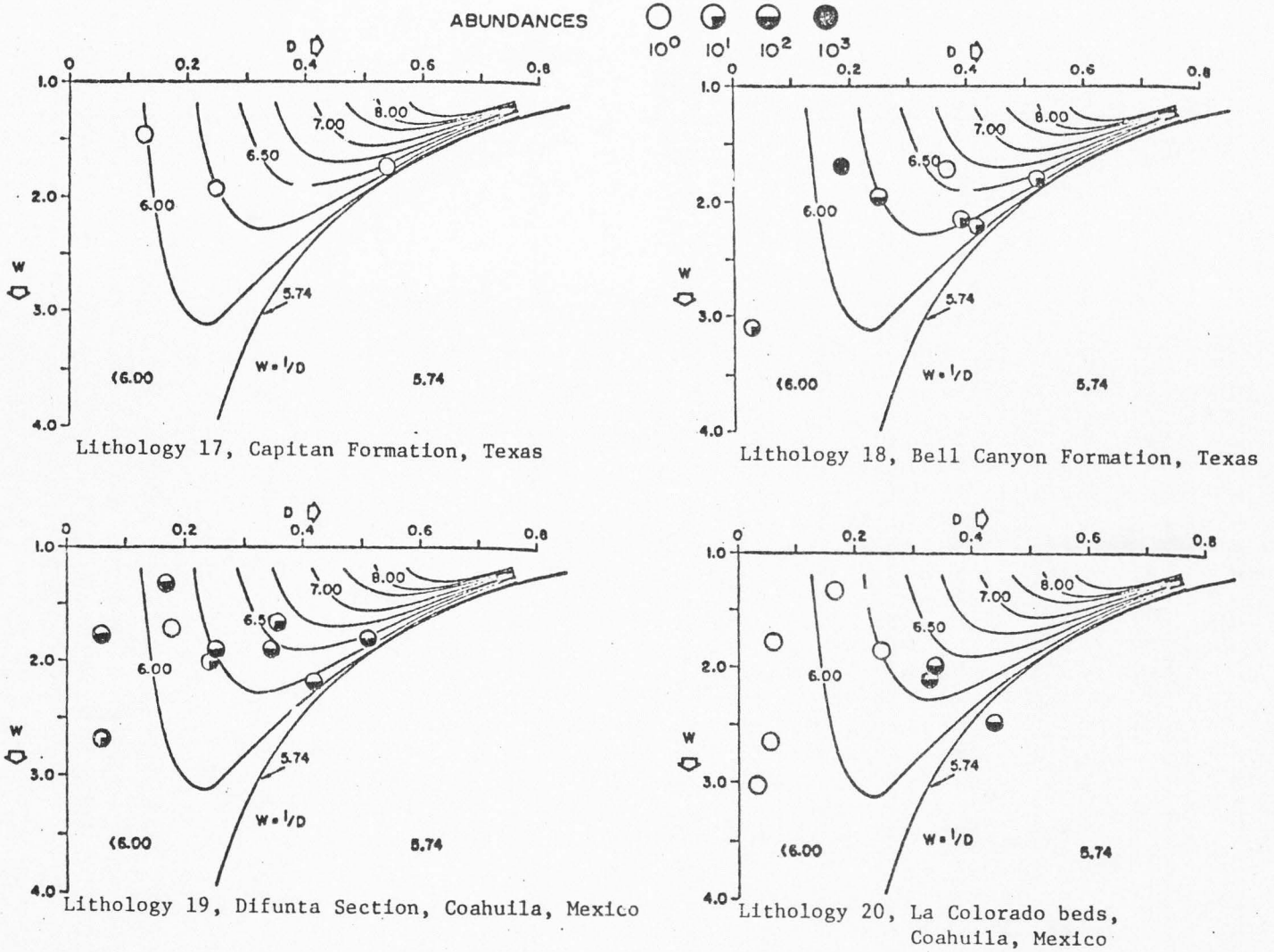

Figure 52. Calcium carbonate efficiency, selected Upper Permian (Upper Guadalupian) ammonoid genera.

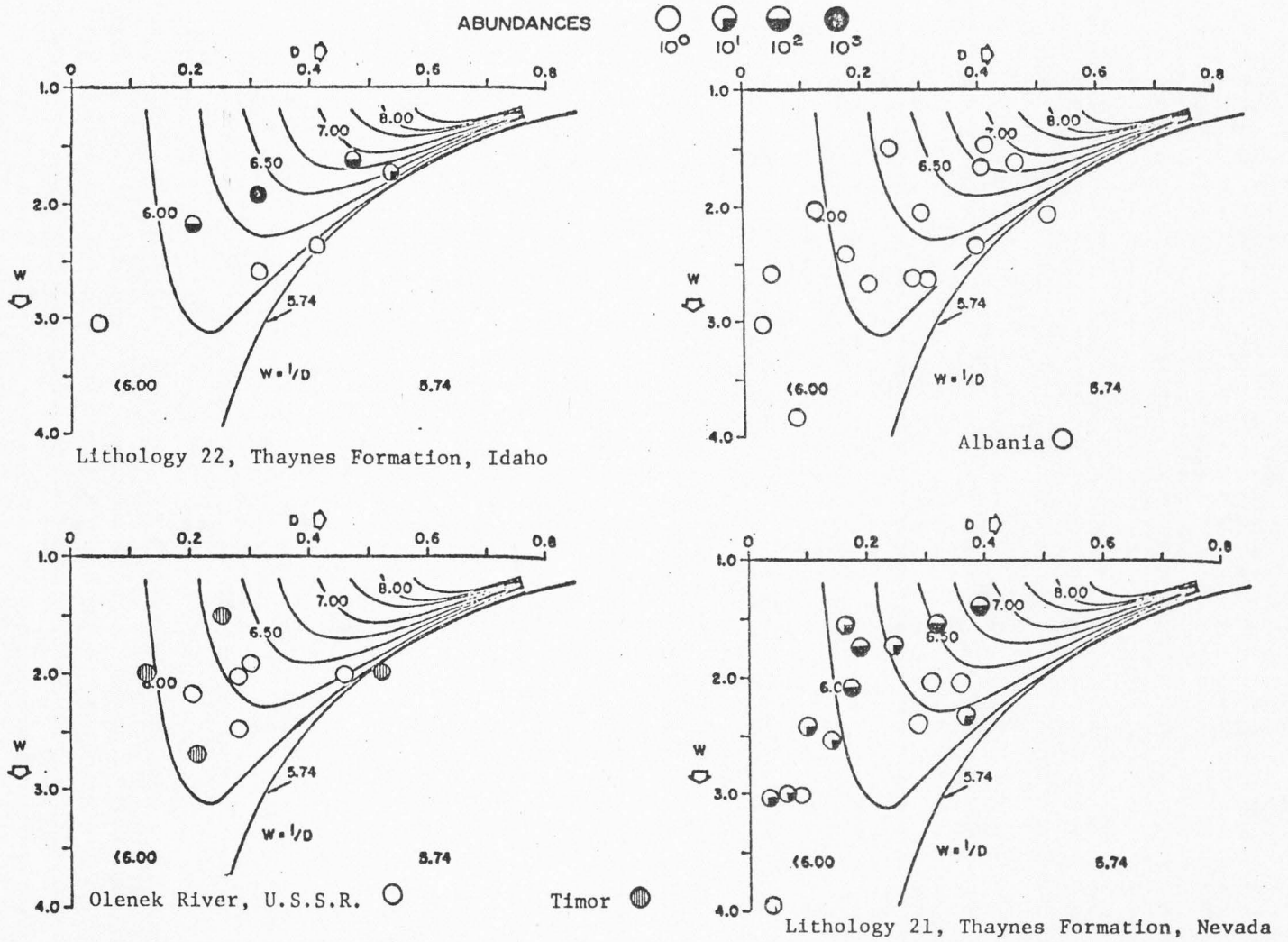

Figure 53. Calcium carbonate efficiency, selected Lower Triassic (Scythian) ammonoid genera.

10^2 abundances = 3 x efficiency value, 10^1 abundances = 2 x efficiency value, 10^0 abundances = original efficiency value) average efficiency value of 6.21. Lithology 3 (Perdido Formation) has not been geochemically analyzed, but it is suspected to be low in organic matter and phosphate minerals (less than .1% and 1% respectively). Together with Lithology 4 (which has appreciable phosphate, 4.5%, but no perceptible organic matter), ammonoids from these lithologies have a weighted average efficiency value of 6.14.

Selected Permian ammonoid genera from the Phosphoria Formation (Lithologies 9, 13, Figures 51 and 52) have a weighted average efficiency value of 6.21 (Table 6). These ammonoid assemblages are found in phosphatic, dolomitic limestone nodules in phosphatic shale. The weighted average efficiency values for all other Permian lithologies (numbers 5, 7, 10-12, 14-19 excluding numbers 6, 8, 17 and 20 for reasons of deficient sample size) is 6.07, but because no precise geochemical analyses are available for these lithologies, the extent to which anoxic conditions prevailed in these environments cannot be reconstructed accurately. However, interpretation of lithologic descriptions (Table 1) suggest that Lithologies 10, 18 and 19 can be included among examples of phosphatic limestones rich in organic matter. The formations in which each of the latter two lithologies are situated have been subjected to geochemical analysis (King, 1948), but the strata sampled and analyzed may not coincide with the ammonoid-bearing beds. When ammonoid assemblages from Lithologies 9, 10, 13, 18, 19, are averaged and compared against the ammonoid assemblages of

Table 6. Comparison of $CaCo_3$ efficiency values with various lithologies

Geologic period	Lithology number	Weighted average $CaCO_3$ efficiency value	% $Ca_3(PO_4)_2$	% organic matter
Mississippian	1	6.26	23.50	ND
Mississippian	2	6.16	0.70	0.74
Mississippian	3	6.14	NR	NR
Mississippian	4	6.13	4.50	ND
Permian	5	6.16	NR	NR
Permian	6	too few specimens	NR	NR
Permian	7	5.94	NR	NR
Permian	8	too few specimens	NR	NR
*Permian	9,13[a]	6.15	1.85	0.90
*Permian	9[b]	6.27	2.40	0.33
*Permian	10	6.13	0.13	0.73
Permian	11	5.92	NR	NR
Permian	12	5.89	NR	NR
Permian	14	6.13	NR	NR
Permian	15	6.11	NR	NR
Permian	16	6.01	NR	NR
Permian	17	too few specimens	NR	NR
*Permian	18	6.20	none	0.34
*Permian	19	6.22	NR	NR
Permian	20	incomplete data	NR	NR
Triassic	21	6.17	1.50	ND
Triassic	22	6.25	1.70	0.70

NR--not reported in literature ND--not determined in present study
[a]Sublette Range localities
[b]Montpelier locality
*Phosphatic limestones rich in organic matter

other Permian lithologies, the average efficiency value of the assemblages found in phosphatic, carbonaceous strata is 6.19, in comparison to 6.02 for the ammonoid assemblages in light gray, crystalline carbonates.

Selected Lower Triassic (Scythian) ammonoid genera show (Figure 55) a strong correlation between efficiency value for calcium carbonate utilization and type of lithology. Lithology 21 is a coarsely-crystalline, shell-carbonate, and its ammonoids have a corresponding average efficiency value of 6.17. Lithology 22 is a phosphatic, fine-grained limestone, rich in organic matter, and its ammonoids have a corresponding weighted average efficiency value of 6.25. Because abundances and lithologic types are not available for other Triassic assemblages, no analysis involving published assemblages is possible.

A possible causal relationship appears to exist between efficiency in the utilization of calcium carbonate in the shell-coiling geometry of the more successful (abundant) species and oxygenation of the environment as reflected by presence or absence of organic matter and phosphate minerals in the associated lithology. Among Raup's (1967) factors which possibly influenced the autecology of ammonoids, the efficient utilization of calcium carbonate in the shell-coiling geometry is interpreted to be most reliable and readily applicable in the paleoecology of ammonoids. This is because it is the only factor considered for which lithological evidence may suggest the direction of selective pressure affecting these nekto-benthic organisms.

Mollusks, under conditions of low oxygen, will utilize calcium from their own shells as a metabolite. Although it is certainly not postulated here that ammonoids in the Phosphoria and Thaynes seas experienced periodic severe depletion of oxygen, these environments which supported ammonoids are considered to have been characterized by a lower oxygen level throughout the duration of these habitats. Furthermore, by analogy with the inferred occurrence of Nautilus on the soft substrates off the Fiji Islands (Ward and others, 1977, p. 387), even anoxic conditions limited to the sediment water interface would be detrimental to nektobenthic ammonoid existence. As to whether these conditions extended up into the water column cannot be determined, but fossil shark and skate tooth whorls found associated with the ammonoids indicate the possibility is not very likely.

Furthermore, Eosianites, Eothinites, Hoffmania, Celtites, and Columbites all possess very high efficiency of calcium carbonate utilization (6.75-7.25) and yet none of these are ever known to numerically dominate any assemblage. Raup has generated (Figures 45 and 46), by computer, efficiency values ranging up to 8.5, yet Eosianites with 7.25, was the highest observed in this study. Why are higher values not realized among ammonoids recovered from phosphatic, carbonaceous lithologies? Examination of the corresponding rotational stability values for these genera provides a possible answer. These stability values range from .04-.08. Higher efficiency values fall within the .04 rotational stability isopleth. It is the interpretation of the author that selective pressure for calcium carbonate efficiency, but

against rotational stability favored a coiling geometry with a W-D coordinate of 2.0 and 0.2. This coiling geometry provides optimum combination of calcium carbonate efficiency with a corresponding rotational stability.

SIZE-FREQUENCY DISTRIBUTIONS AND INFERENCES

Most, if not all, ammonoid faunas were recovered from dark, coarse-to-fine grained bituminous limestone nodules in phosphatic shales which lack an appreciable percentage of terrigenous detritus. This observation, in combination with the absence of various sedimentary texture and structures, i.e., cross-bedding, ripple marks, flute casts, scour marks, oolites, suggests that the ammonoid assemblages accumulated in environments where the mechanical destruction of shells and winnowing by currents was minimal. This means the possibility of recovering a life assemblage (catastrophic death or census assemblage), or at least an undisturbed death assemblage which accumulated over long intervals of time, increases considerably. The reliability of size-frequency distributions for the inferences concerning mortality rates is enhanced if the assemblage has not been transported or winnowed.

High organic and/or phosphate content of associated lithologies usually indicates a low oxygen content of the water immediately overlying the substrate and suggests low rate of sediment accumulation on the substrate. Species of the brachiopod genus Leiorhynchus are abundant in black shales and limestones throughout the upper Paleozoic, commonly unbroken and retaining both valves (Newell and others, 1953, p. 67). This genus is thought to have been well adapted to conditions of low oxygen. Alexander (personal communication, 1977) interprets the nearly perfect bilateral symmetry among all of the specimens of this

brachiopod to indicate a epiplanktonic mode of existence. Newell and others (1953, p. 198) indicated that most of the Permian, ammonoid-bearing limestones in the Guadalupe Mountains represent catastrophic death of entire communities by periodic upwelling of poisonous H_2S gas brought about by debris slides off the reef margins. Dinoflagellate blooms (red tides) also may have been responsible for mortality among ammonoids. When juveniles as well as adults are recovered, the probability that the assemblage was winnowed is diminished. Furthermore, Newell and others (1953, p. 198) stated that restricted horizontal distribution of the accumulations combined with the lack of sorting indicate that the shells did not float far after death.

Hallam (1972, p. 78) stated that the major factors molding unaltered size-frequency distributions are growth and mortality rates. He stated (1972, p. 72) that even without growth data, it must be concluded that mortality rates tend in general to decline from youth to maturity, although they may again increase at a later stage. Thus for a size-frequency distribution among invertebrates, moderately positive skewness is more common than strongly positive skewness. Normal distributions are unusual and negative skewness highly exceptional.

Strongly positive skewness represents low initial growth rate and high juvenile mortality rate which decreases with maturity. Negative skewness represents a high initial growth rate followed by increasing mortality rate with age.

An opportunistic species results in a prolific accumulation of dead individuals in a short time because of rapid maturation, high fecundity, and short generation time. The paleo-opportunistic species were not in equilibrium, i.e., they may dominate a fauna numerically in one stratum and may be rare or absent in all other beds. Presence of these species would be represented by a size-frequency distribution that is usually highly positively skewed. Average size is comparatively small relative to "equilibrium" species. This situation is exemplified by Cravenoceras from the Confusion Range and the lower zone of Kane Springs Wash, by Pseudogastrioceras, Medlicottia and Spirolegoceras from the Phosphoria Formation, and by Ophiceras from the Thaynes Formation (Figures 54-56).

In contrast, equilibrium species maintain fairly steady population size and are often present throughout a succession of layers. They inhabit environments of high stability and predictability, such as the deep ocean (Hallam, 1972, p. 74). They utilize available resources more efficiently, and expend less energy toward reproduction. These species commonly achieve a larger size and greater age. Growth rate is initially rapid through the vulnerable juvenile stage. When adulthood is attained, growth rate decreases considerably. Mortality rate increases with age (Hallam, 1972, p.72). Negative skewness would be more common in size-frequency distributions of equilibrium species, an observation reflecting increasing mortality rates later in life accompanied by decreasing growth rate.

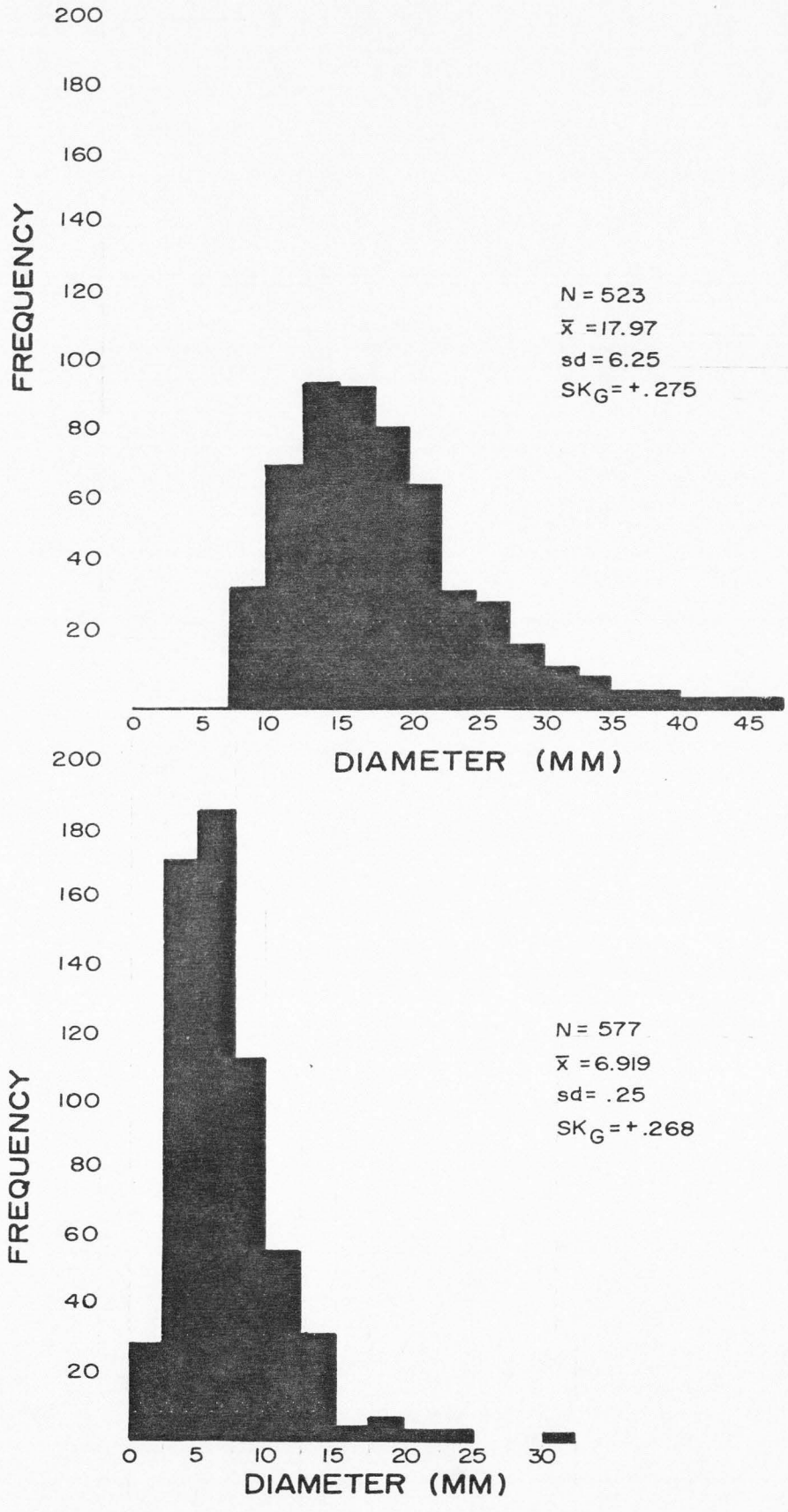

Figure 54. Size-frequency distributions for Cravenoceras sp. from Lithology 1 (above), and Lithology 2 (below). N = sample size, sd = standard deviation, $\bar{x}$ = average diameter, SK_G = skewness.

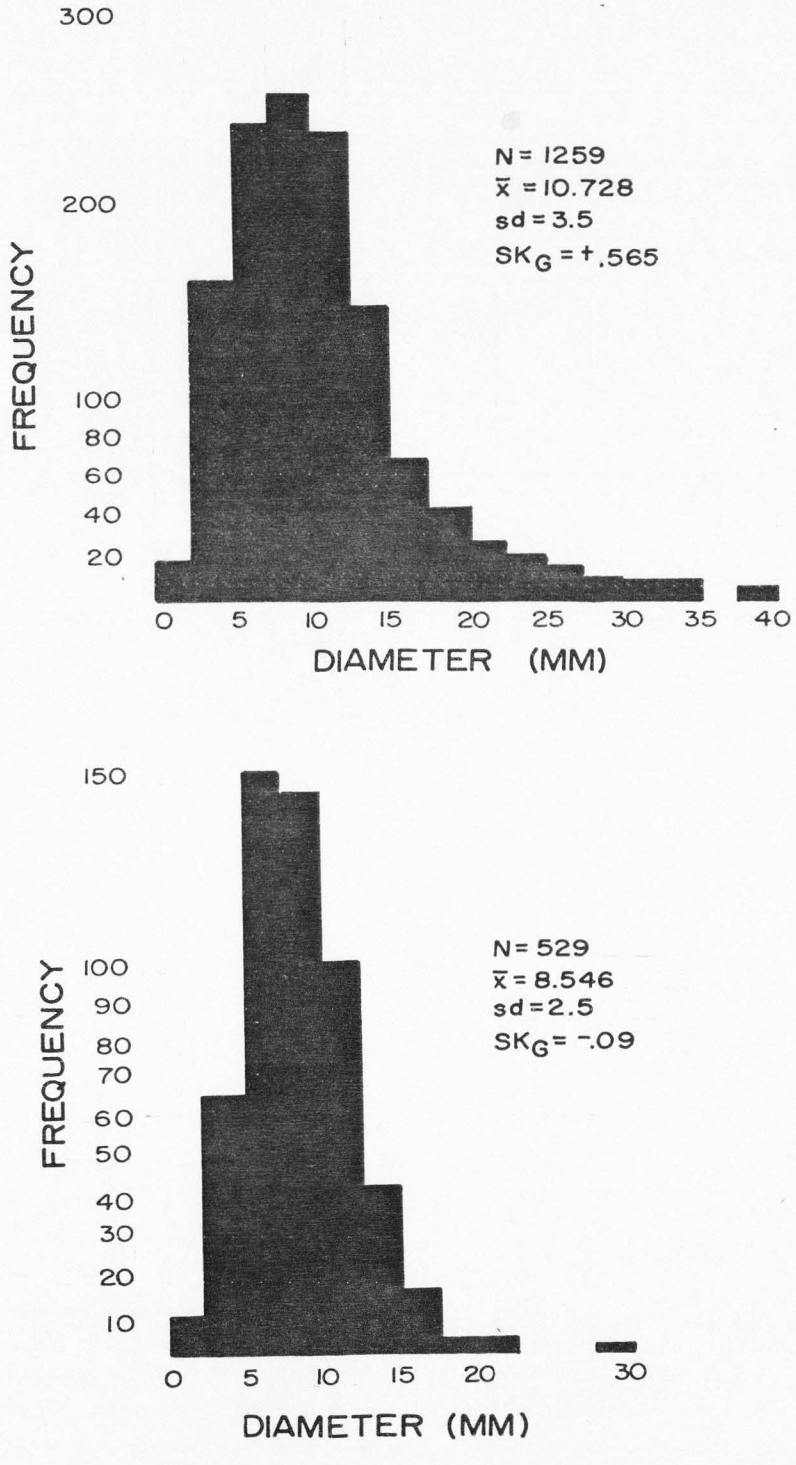

Figure 55. Size-frequency distributions for Pseudogastrioceras sp. from Raymond Canyon (above), and Layland Canyon (below), (Lithologies 9,13). N = sample size, $\bar{x}$ = average diameter, sd - standard deviation, SK_G = skewness.

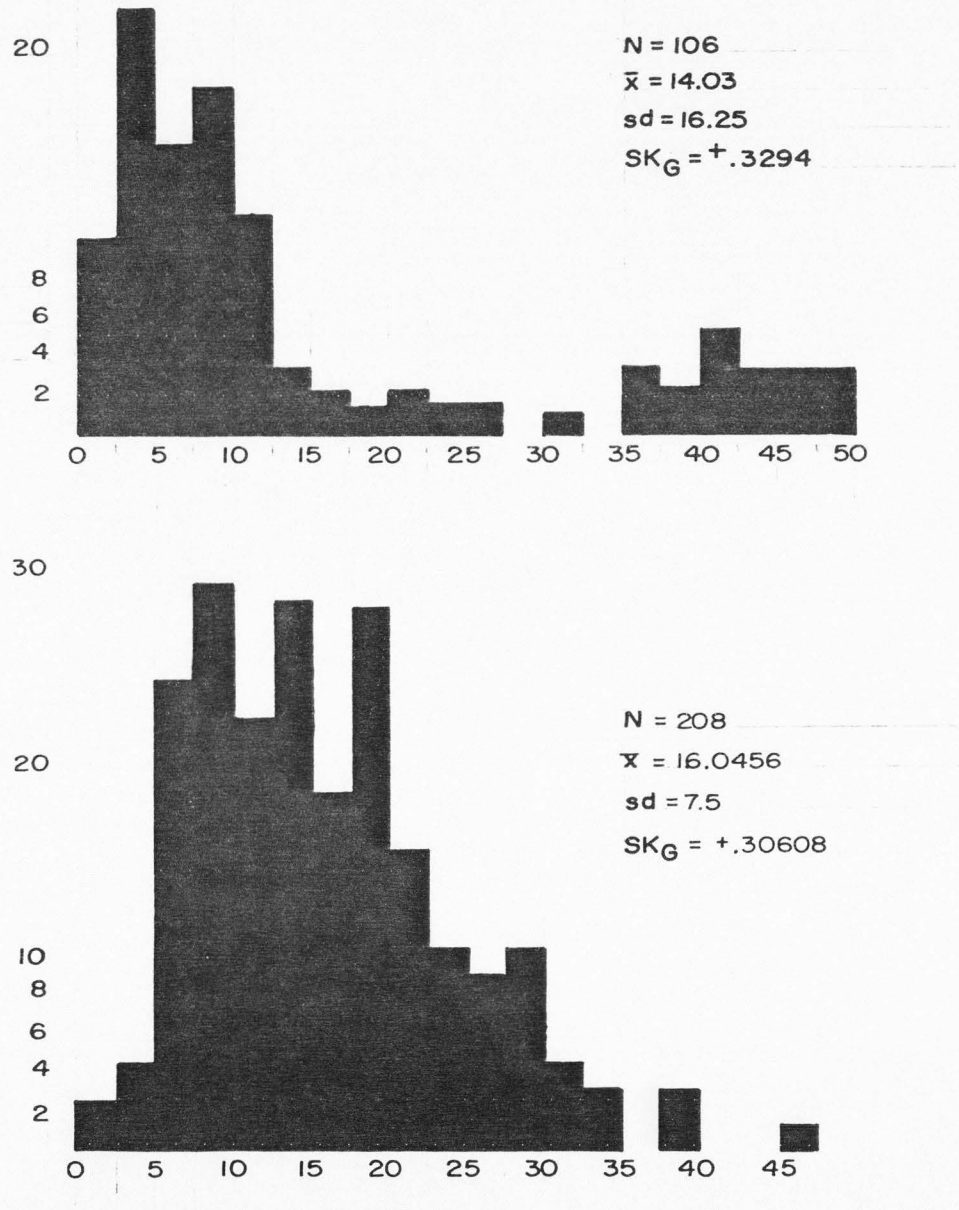

Figure 56. Size-frequency distributions for Medlicottia sp. (above), and Spirolegoceras sp. (below); from Lithologies 9,13. N = sample size, $\bar{x}$ = average diameter, sd = standard deviation, SK_G = skewness.

Cravenoceras (Figure 57) of the upper Kane Springs Wash zone exhibits nearly symmetrical size-frequency distribution whereas Columbites, and Meekoceras from the Thaynes Formation exhibit negative skewness (Figures 58 and 59). Favorable conditions of growth in the upper zone contrasting with the anoxic conditions of the lower zone at Kane Springs Wash are inferred from the radically different skewnesses observed in Cravenoceras versus Columbites and Meekoceras. The Phosphoria Formation, and locally the Chainman Shale, represent conditions which favored exploitation by opportunistic species of ammonoids. In contrast, the Thaynes Formation accumulated in seas that permitted opportunistic species to invade and coexist with equilibrium species (Figures 60 and 61).

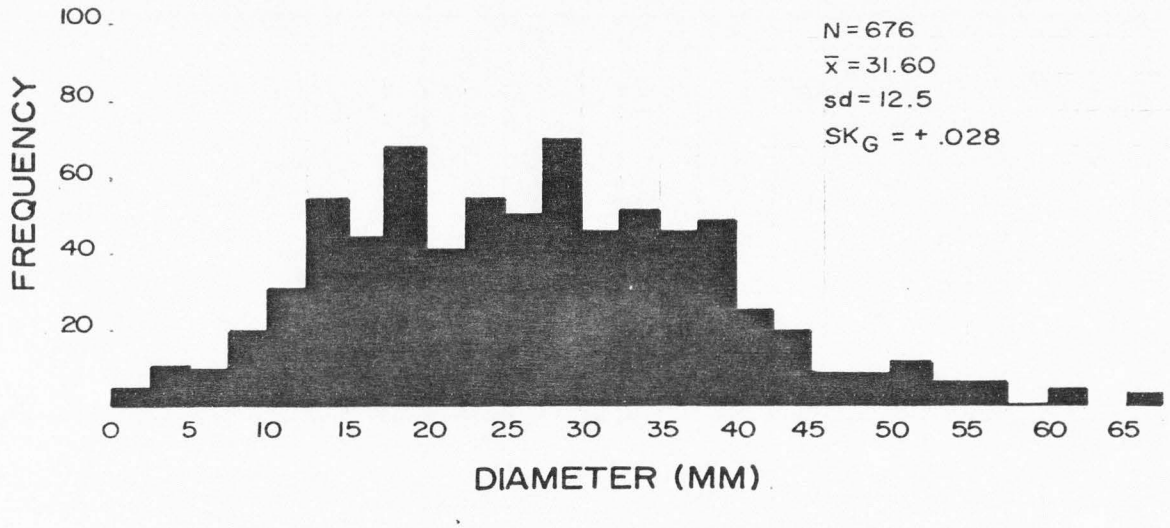

Figure 57. Size-frequency distributions for Cravenoceras sp. from Lithology 4. $\bar{x}$ = average diameter, N = sample size, sd = standard deviation, SK_G = skewness.

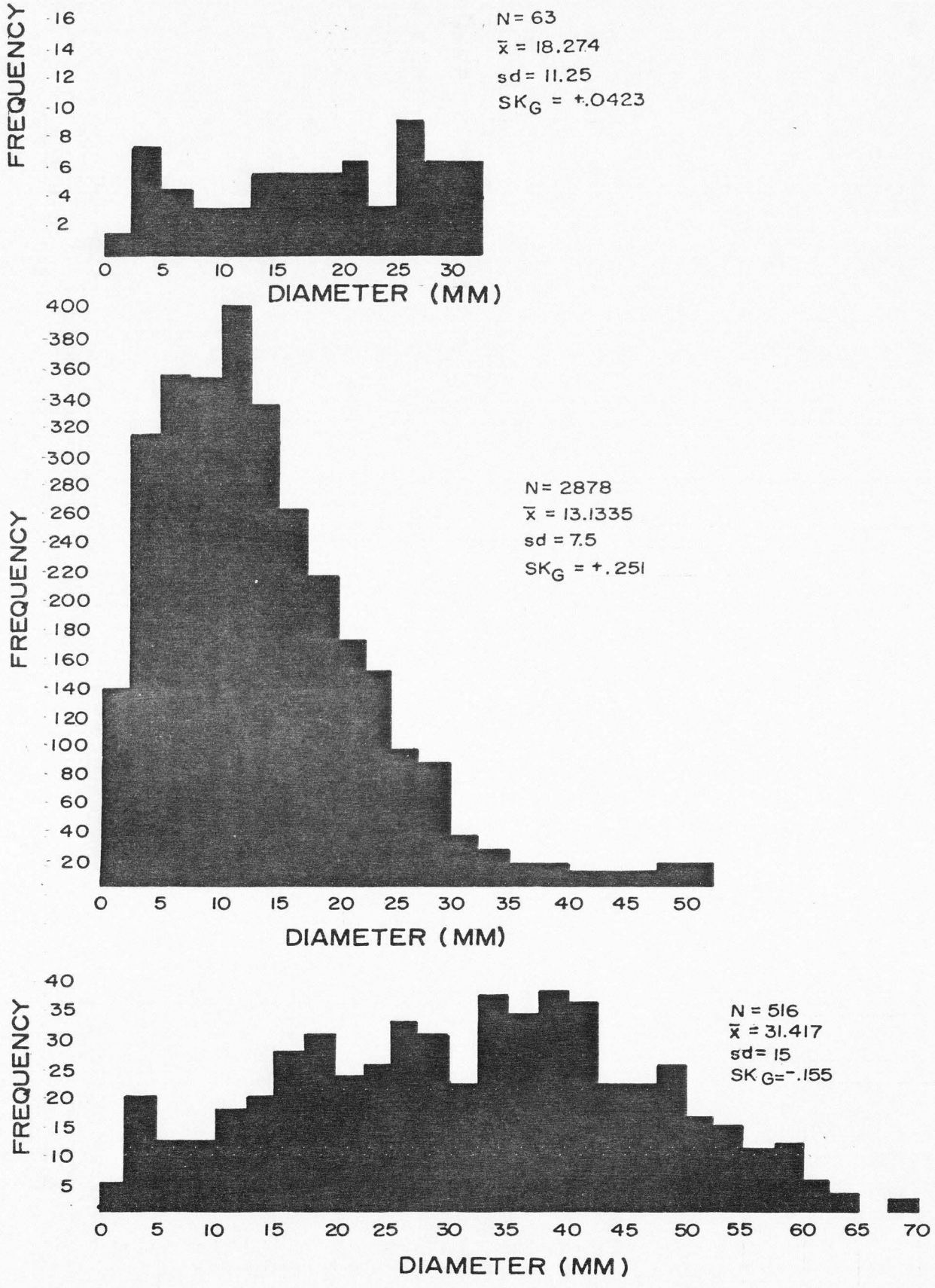

Figure 58. Size-frequency distributions for Celtites sp. (top. Ophiceras sp. (middle), and Columbites sp. (bottom) from Lithology 22. N = sample size, $\bar{x}$ = average diameter, sd = standard deviation, SK_G = skewness.

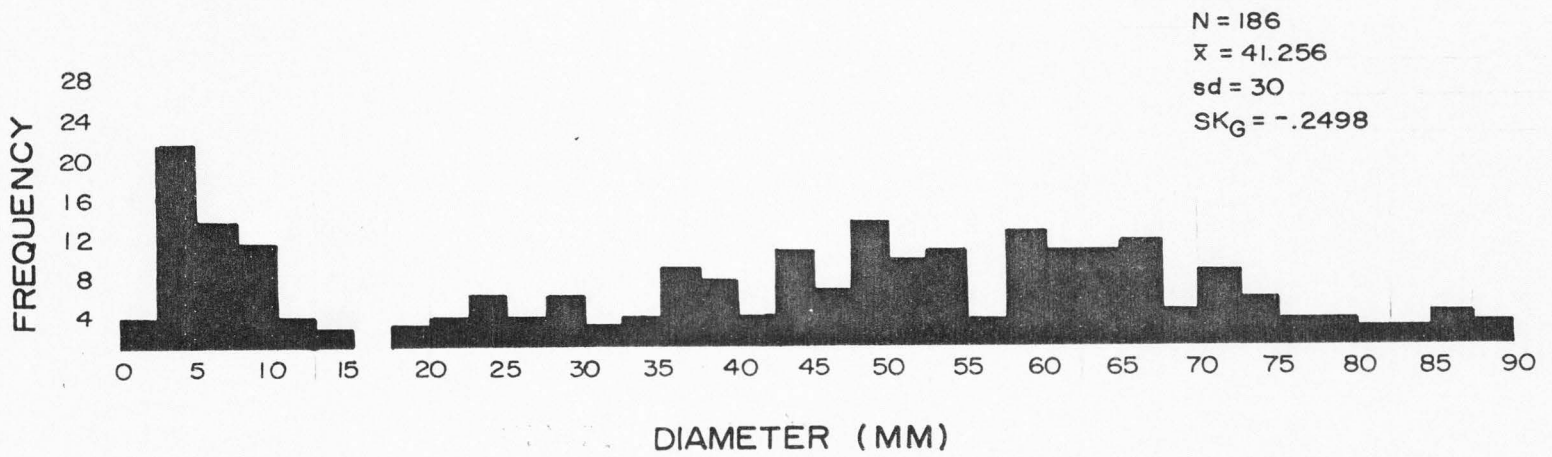

Figure 59. Size-frequency distribution for Meekoceras sp. from Lithology 22. N = sample size, $\bar{x}$ = average diameter, sd = standard deviation, SK_G = skewness.

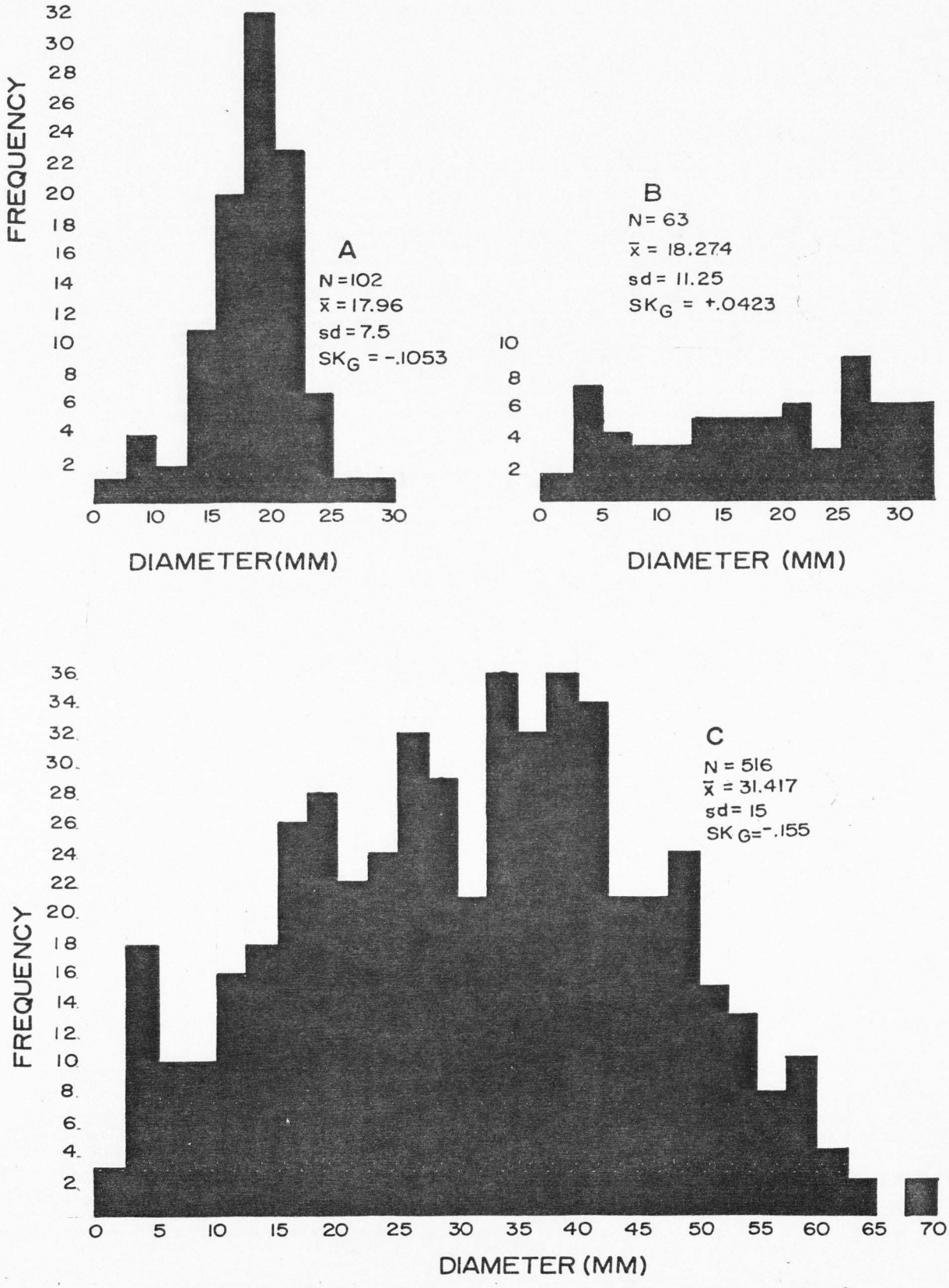

Figure 60. Size-frequency distributions for genera efficient in the utilization of calcium carbonate from Lithology 21, (A); and Lithology 22 (B,C). A = Juvenites sp., B = Celtites sp., C = Columbites sp. N = sample size, $\bar{x}$ = average diameter, sd = standard deviation, SK_G = skewness.

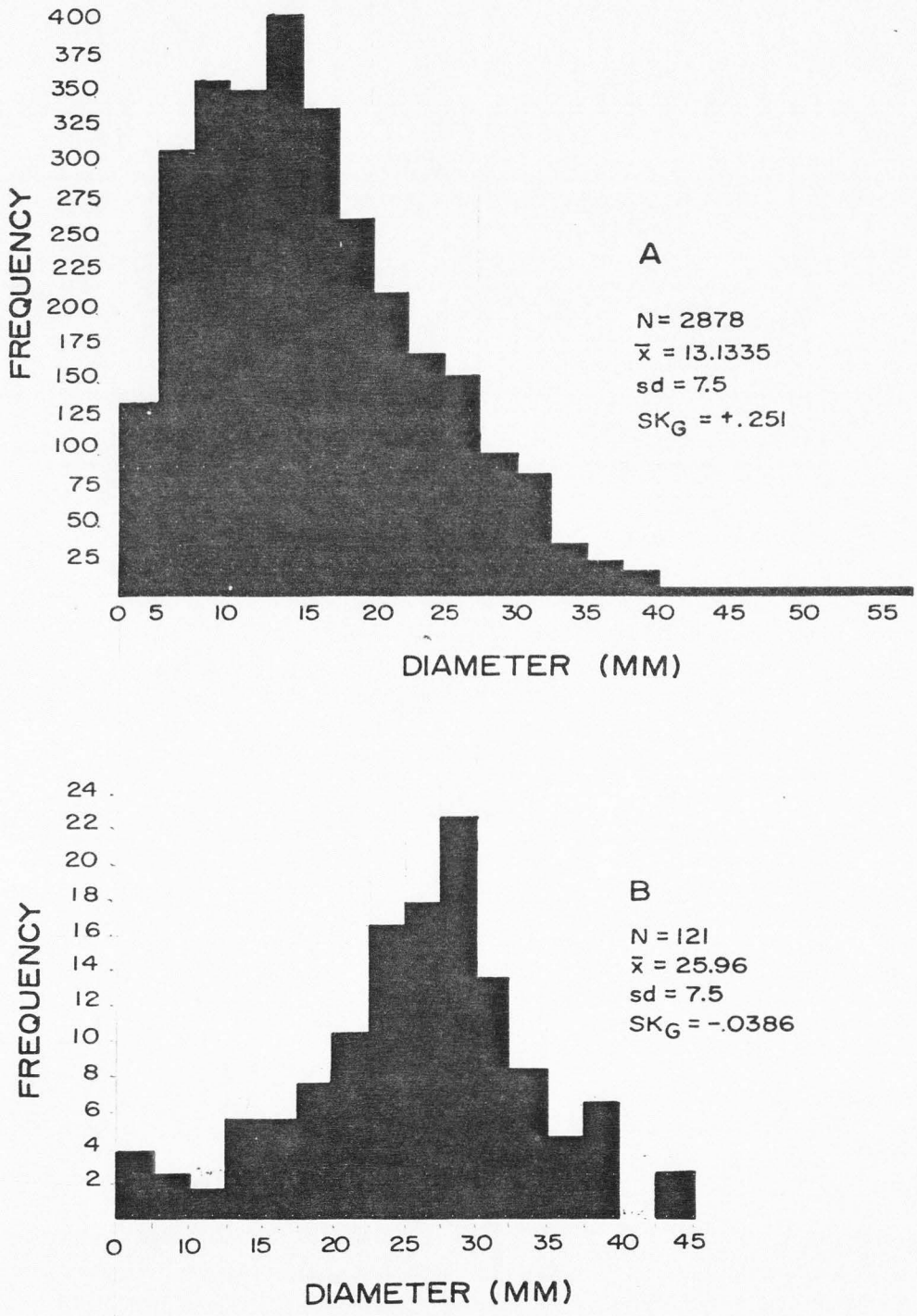

Figure 61. Size-frequency distributions for genera less efficient in the utilization of calcium carbonate from Lithology 21 (B), and Lithology 22 (A). A = Ophiceras sp., B = Prosphingites sp. N = sample size, $\bar{x}$ = average diameter, sd = standard deviation, SK_G = skewness.

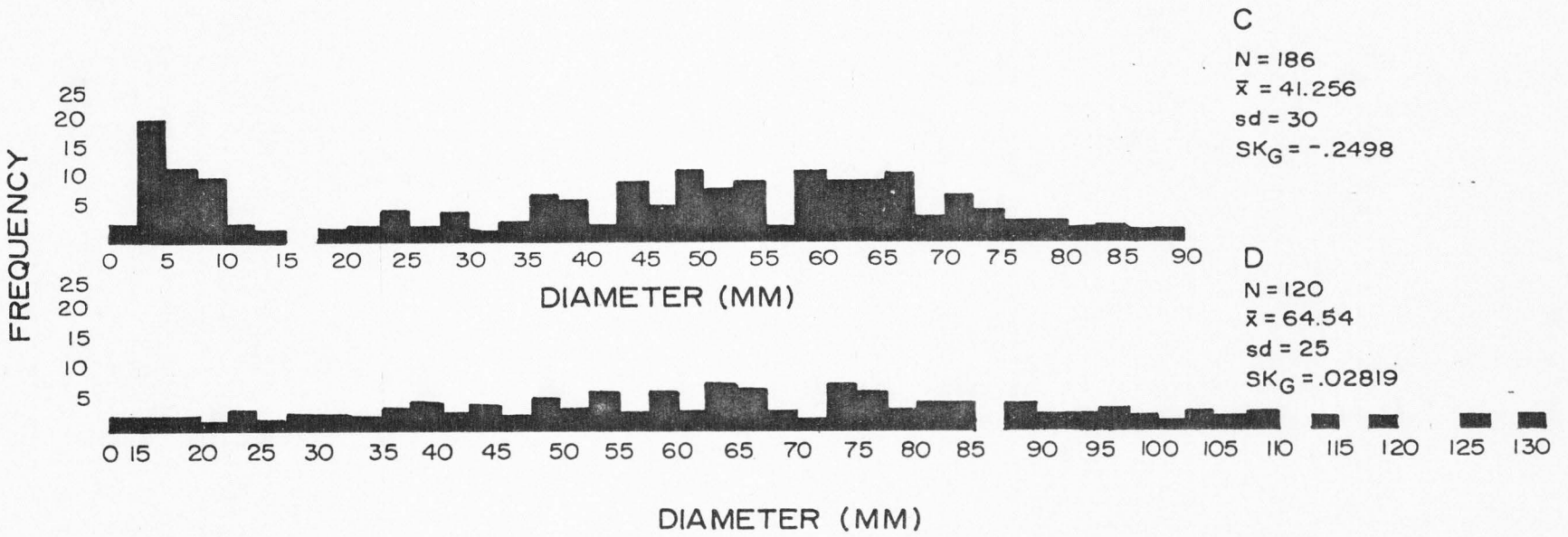

Figure 61. Continued. Size-frequency distributions for genera less efficient in the utilization of calcium carbonate from Lithology 21 (C), and Lithology 22 (D). C = Meekoceras sp., D = Meekoceras gracilitatus. N = sample size, $\bar{x}$ = average diamter, sd = standard deviation, SK_G = skewness.

BIOVOLUME DISTRIBUTIONS AND ANALYSIS

There are problems in the process of reconstructing ancient communities. In the case of nekto-benthonic "communities," soft-bodied forms can be ignored, though certain mobile coelenterates (jellyfish) were certainly present. A second problem (Ziegler and others, 1968, p. 4) concerns differential mortality rates among species. Obviously a species which had a longer life span and lower reproduction rate than another species would be represented in the assemblages by proportionally fewer numbers, relative to species with short generation time and high fecundity. This problem could be alleviated by determination of life span from growth-increment studies, but uniformity even within species is doubtful (see ontogenetic discussion). This biovolume analysis proceeds then on the inescapable assumption of proportional information loss from each community.

Estimates (Walker, 1972, p. 85) of absolute or relative abundance of preserved taxa of an ancient community must be determined in order to apply trophic group analysis. Although Walker (1972) was concerned wholly with benthic communities, his utilization of biovolume to that end is deemed applicable to studies of the nekto-benthos as well. Most modern ecologists use some measure of biomass as the stated unit of abundance (Walker, 1972, p. 85). Biomass cannot be determined for fossil taxa. Biovolume, which can be determined approximately for fossil taxa, is proportional to undecalcified biomass. Biovolume is, therefore, suggested as a paleontologic approximation of biomass.

The relative biovolume-dominance positions of the several most abundant taxa in the assemblage as determined probably reflect actual dominance within the former community.

For ammonoid faunas, whose component species have been analyzed with respect to their W and D morphologic variables, the biovolume-relative abundance distribution is calculated. Any faunal assemblage suspected of being reworked, transported, winnowed or containing non-indigenous, exotic species were not sampled and included in the biovolume analysis.

Biovolume, which forms the ordinate of the graph, is calculated as the difference in weight of an ammonoid fossil specimen when suspended on a fine thread immersed in water as opposed to its weight in air. This is the weight of the displaced water, which is numerically equal to the volume of the ammonoid shell (when the metric system is used). A balance with hundredths of a gram accuracy was used, and a constant density of internal matrix was assumed. Specimens with a diameter equal to the mean diameter value for the species were used to determine biovolume.

Relative abundance is used as the abscissa of the graph and is measured in powers of ten. It is the opinion of the author that such commonly used terms as rare, uncommon, common and abundant, which describe numerical abundance, can be roughly correlated with 10^0, 10^1, 10^2, and 10^3.

The following graphs (Figures 62-66) represent biovolume-relative abundance distributions for the analyzed assemblages on the North

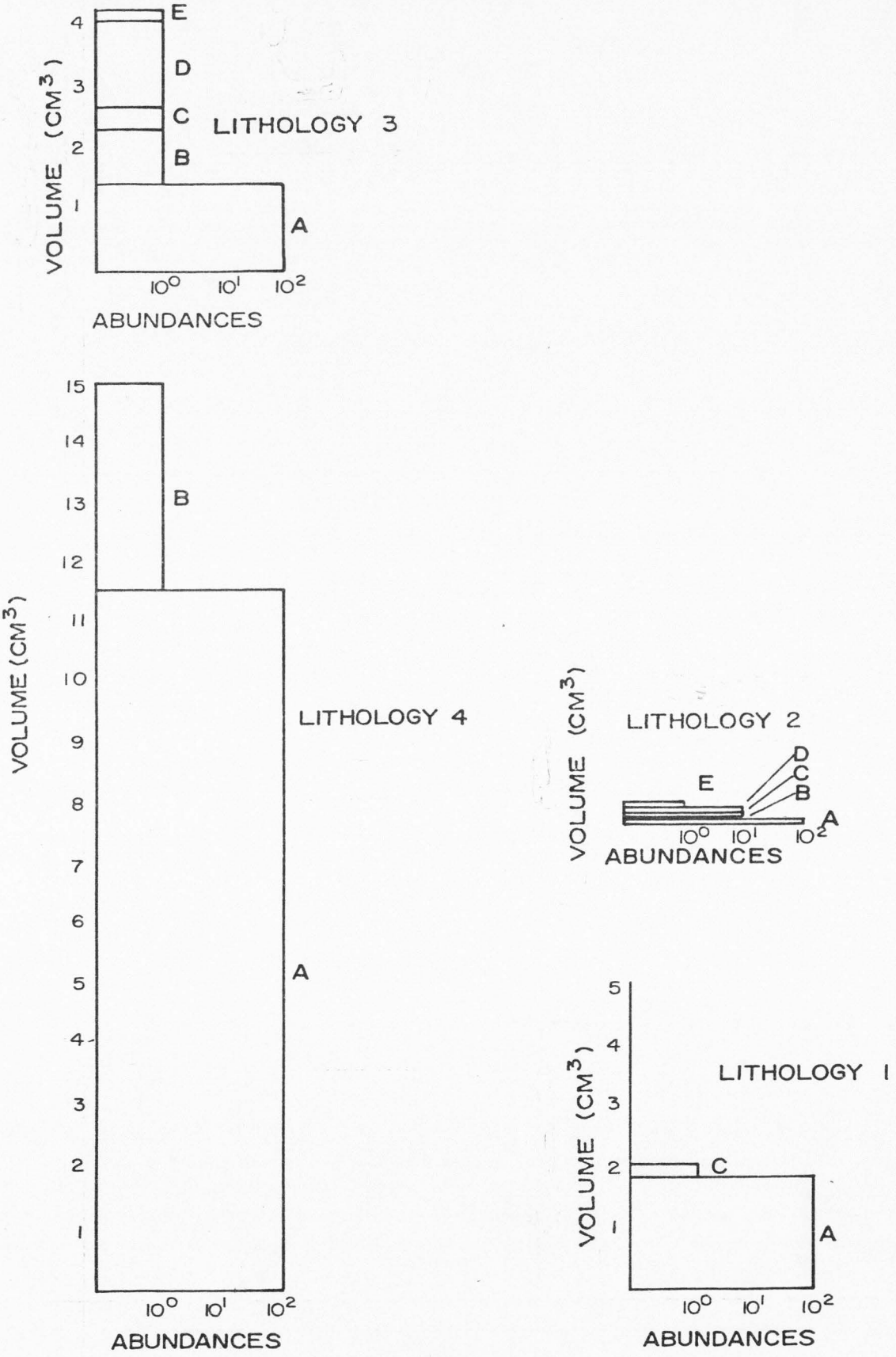

Figure 62. Biovolume-frequency distributions, selected Mississippian ammonoid assemblages.

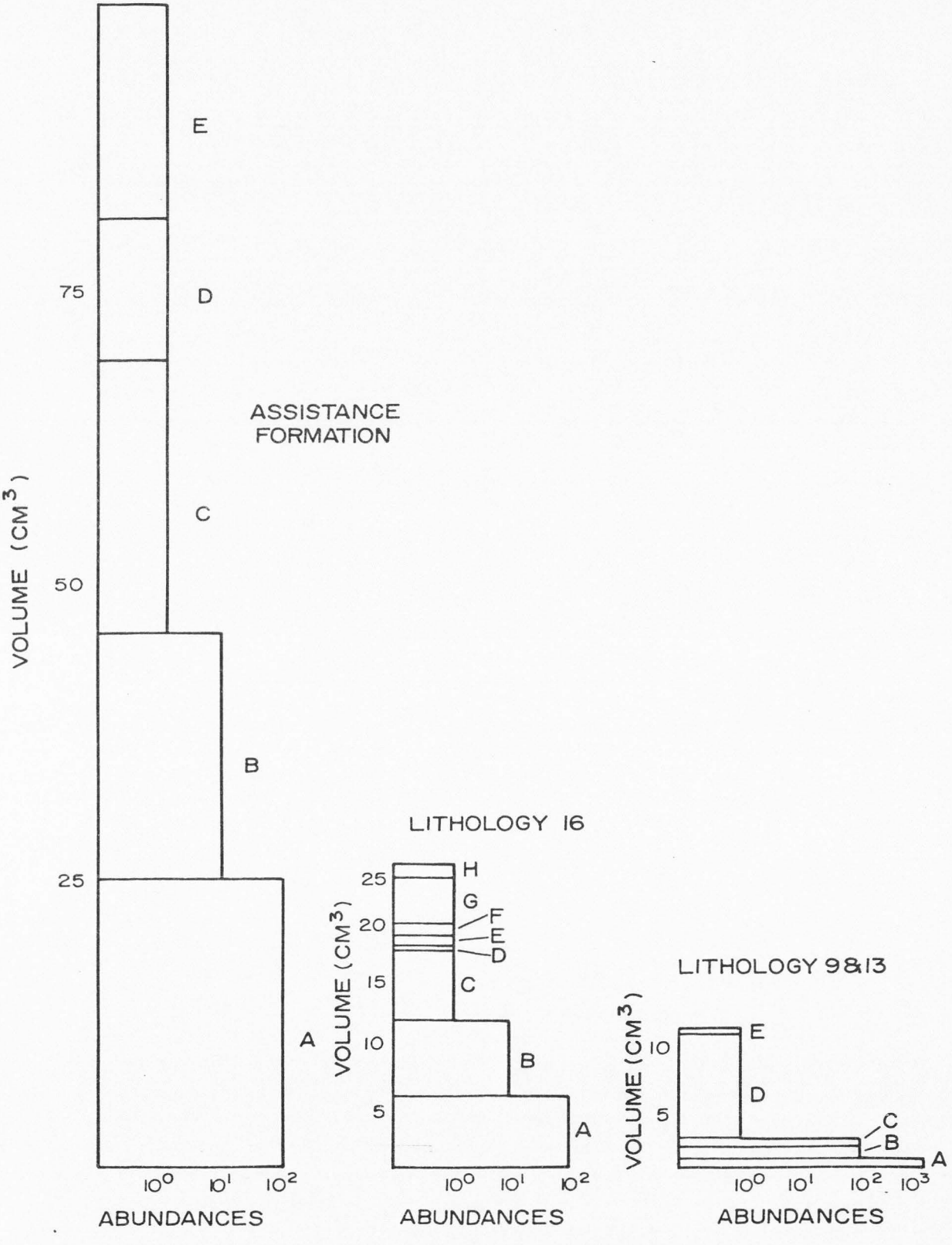

Figure 63. Biovolume-frequency distributions, selected Permian ammonoid assemblages.

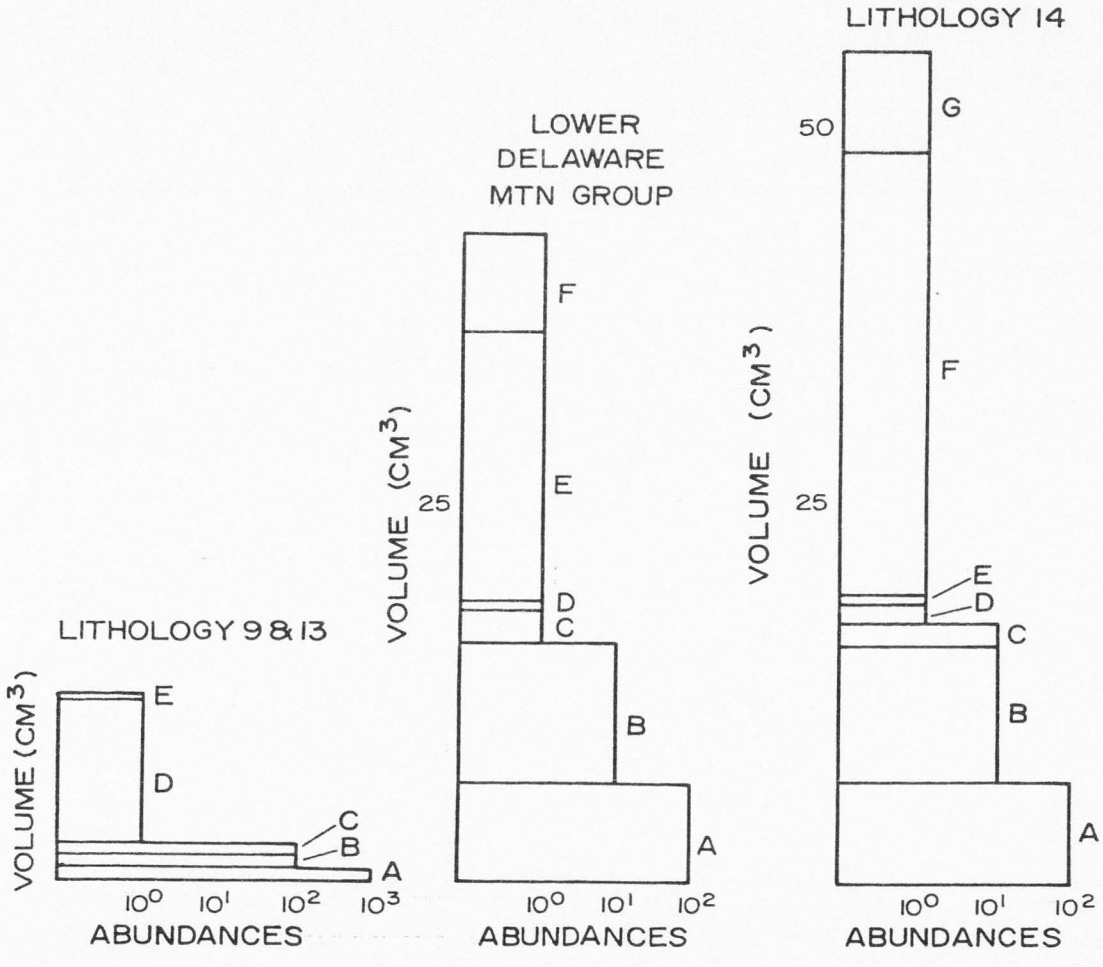

Figure 63. Continued.

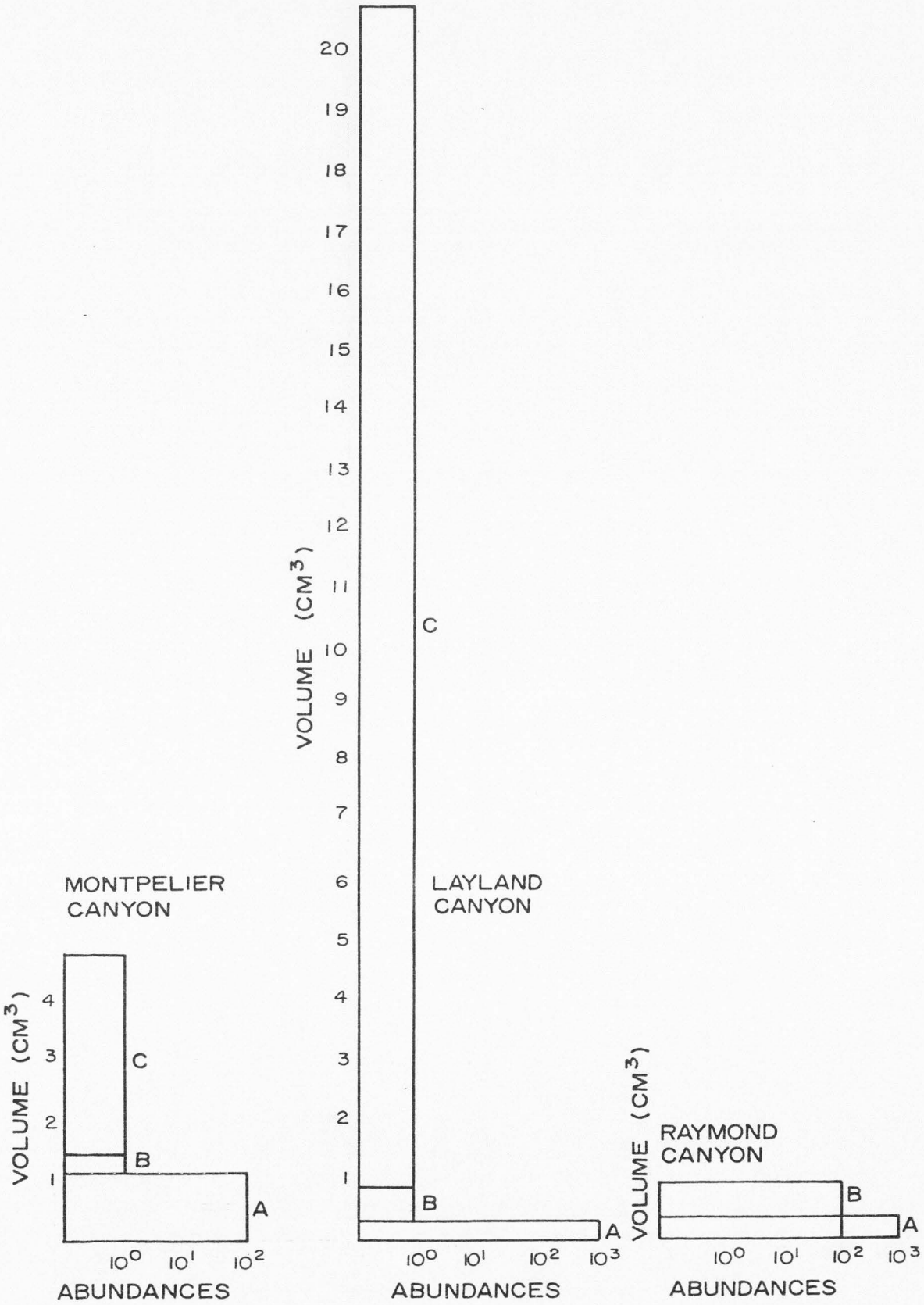

Figure 64. Biovolume-frequency distributions, ammonoid assemblages from the Permian Phosphoria Formation.

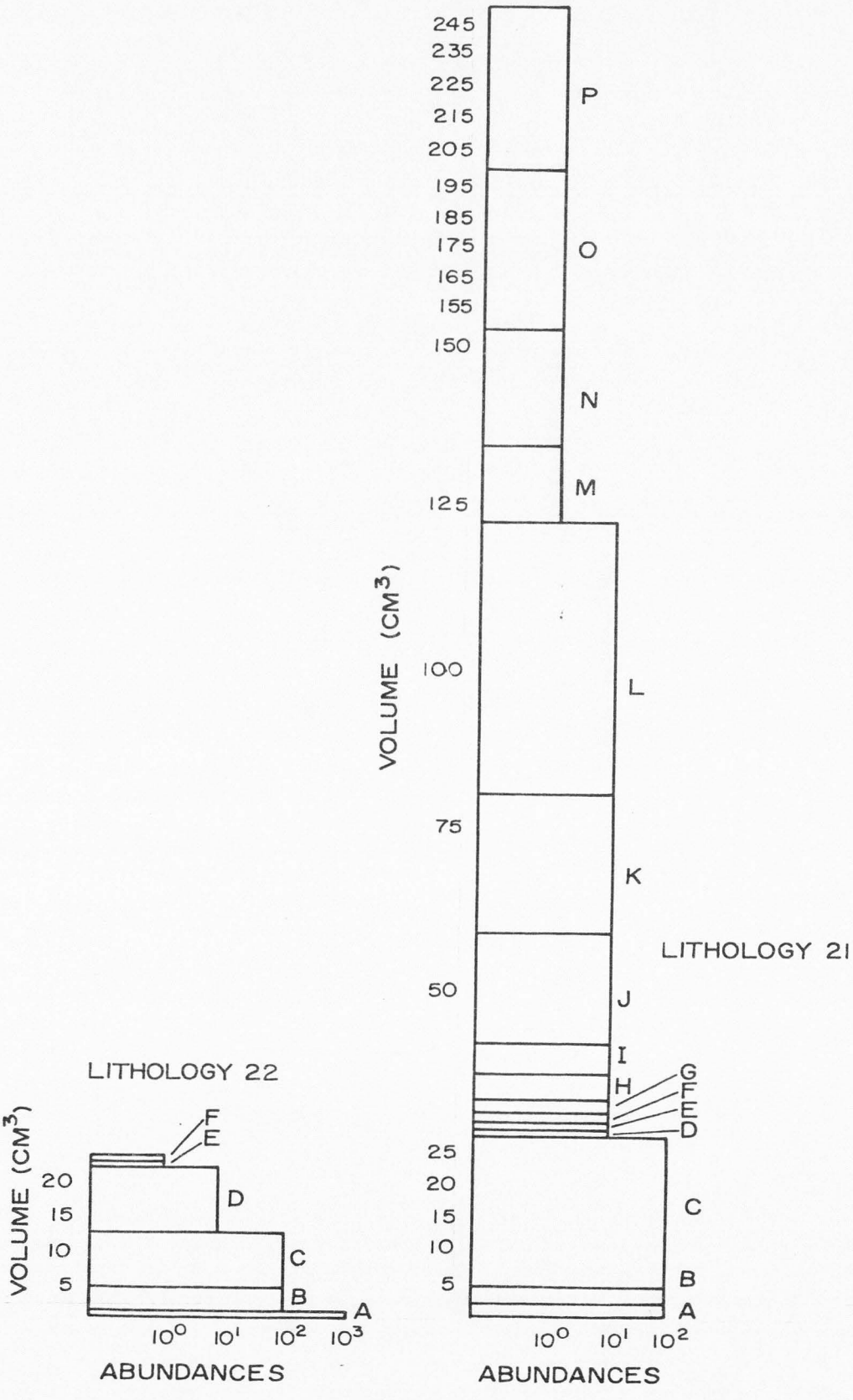

Figure 65. Biovolume-frequency distributions, ammonoid assemblages from the Triassic Thaynes Formation.

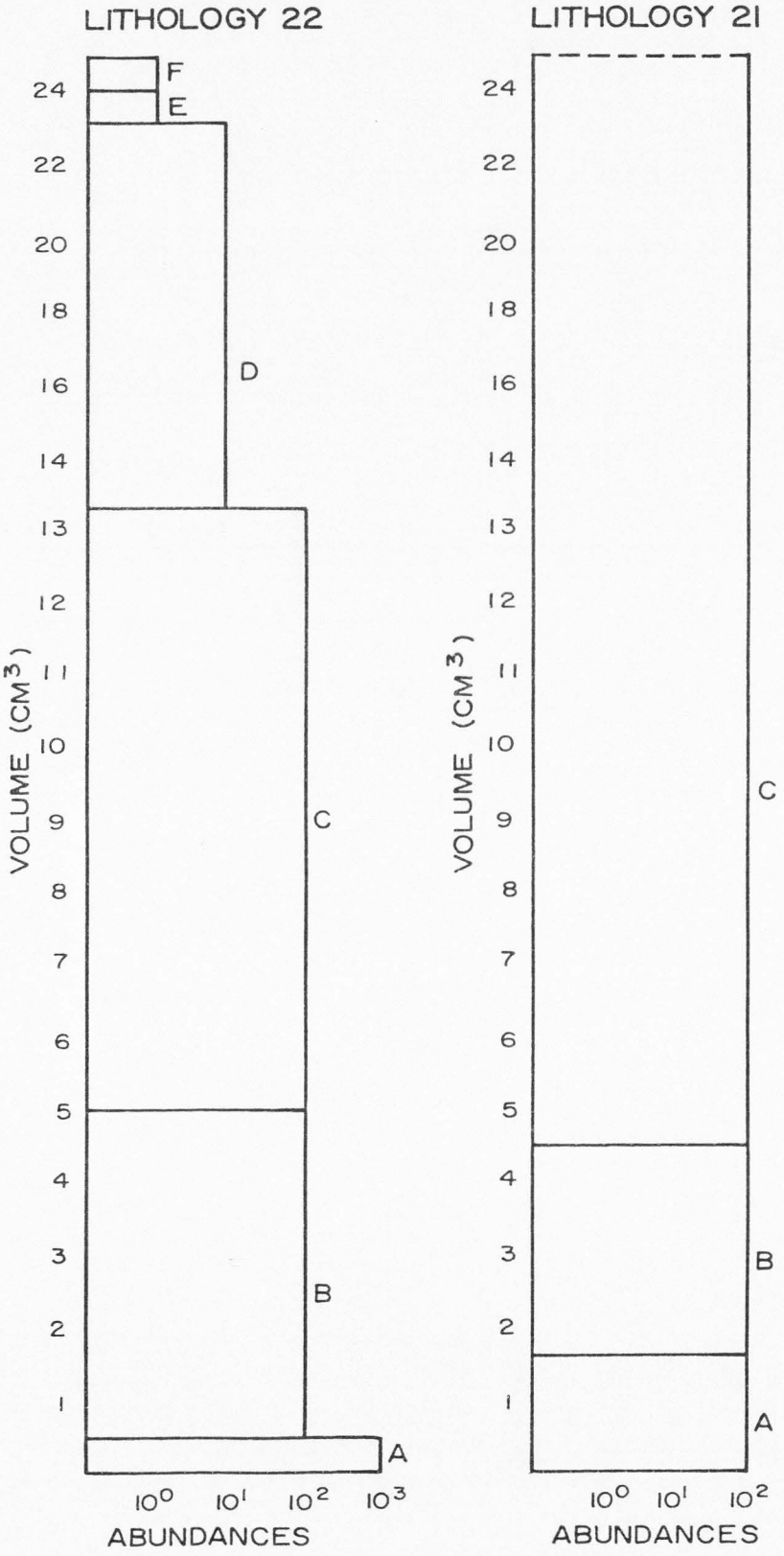

Figure 66. Biovolume-frequency distributions, ammonoid assemblages from the Triassic Thaynes Formation (expanded scale).

American continent (Figure 10). Lithologic character and mean diameters for these species are also recorded (Tables 7, 8, 9, 10).

Mississippian forms (Figure 62) reflect two extremes in carrying capacity of the water column above the substrate. The ammonoid assemblage from the Confusion Range (Lithology 2) displays the smallest biovolume values encountered, presumably attributable to a very poorly oxygenated habitat. This interpretation is supported by the high organic content of the associated lithology (Table 7). No selection for efficient utilization of calcium carbonate is observed among the ammonoid species. On the contrary, the least efficient form, Cravenoceras, reaches both the largest size and the greatest abundance. The success of Cravenoceras may be attributed to the globose whorls, which may have afforded greater bathymetric range (Westermann, 1971, p. 31). The ammonoid assemblage from the Panimint Range is of insufficient size to be quantitatively analyzed, but the ammonoid species have greater average biovolume, suggesting more oxygenated conditions in the water column. The assemblage from the Kane Springs Wash displays large average diameters, but a low species diversity. Because organic content of the associated lithology is low, well-oxygenated conditions conducive to favorable growth and attainment of large biovolume are inferred for the population. Under well oxygenated conditions, no selection toward efficient utilization of calcium carbomate is expected, and predictably none is seen.

Permian profiles (Figures 63 and 64) contain the most striking comparisons, which distinguish the Phosphoria faunal complex as one which

Table 7. Mississippian assemblages utilized in biovolume analysis

Designation	Lithology Number (Table 1)	Genus	Abundance	Average Diameter (mm)	Average Biovolume (cm^3)
A	3	Cravenoceras[a]	10^2	13.8	1.38
B	3	Eumorphoceras[a]	10^0	16.2	0.96
C	3	Anthracoceras[b]	10^0	15.6	0.40
D	3	Delpinoceras[b]	10^0	34.2	1.20
E	3	Prolecanites[a]	10^0	6.2	0.10
A	1,4	Cravenoceras[a]	10^2,10^2	17.5,35	1.74,11.56
B	1	Anthracoceras[b]	10^0	25.0	3.28
C	4	Pronorites[b]	10^0	10.0	0.12
A	2	Cravenoceras[a]	10^2	7.0	0.11
B	2	Eumorphoceras[a]	10^1	6.0	0.04
C	2	Dimorphoceras[b]	10^1	1.6	0.05
D	2	Epicanites[b]	10^1	3.6	0.03
E	2	Girtyoceras[2]	10^0	15.0	0.04

[a]After Gordon (1964)
[b]After Saunders (1973)

Table 8. Permian assemblages utilized in biovolume analysis

Designation	Lithology Number (Table 1)	Genus	Abundance	Average Diameter (mm)	Average Biovolume (cm^3)
A	Assistance Fm.	Daubichites[b]	10^2	59	25.60
B	Assistance Fm.	Sverdrupites[b]	10^1	45	20.90
C	Assistance Fm.	Synartinskia[b]	10^0	60	23.20
D	Assistance Fm.	Medlicottia[b]	10^0	50	11.70
E	Assistance Fm.	Popanoceras[b]	10^0	50	18.50
A	16	Waagenoceras[c]	10^2	30	6.47
B	16	Stacheoceras[c]	10^1	25	5.96
C	16	Martoceras[3]	10^0	26	5.96
D	16	Adrianites[c]	10^0	4	0.29
E	16	Hyattoceras[c]	10^0	12	0.81
F	16	Agathiceras[c]	10^0	12	0.82
G	16	Eumedlicottia[c]	10^0	38	4.31
H	16	Paraceltites[c]	10^0	22	1.19
A	9,13	Pseudogastrioceras[d]	10^3	11	0.38
B	9,13	Spirolegoceras[d]	10^2	16	1.14
C	9,13	Medlicottia[d]	10^2	14	0.58
D	9,13	Adrianites[d]	10^0	9	0.29
E	9,13	Paragastrioceras[d]	10^0	22,40	3.35,19.86

Table 8. Continued

Designation	Lithology Number (Table 1)	Genus	Abundance	Average Diameter (mm)	Average Biovolume (cm^3)
A	Lower Delaware Mtn. Group	Waagenoceras[a]	10^2	28	6.47
B	Lower Delaware	Pseudogastrioceras[a]	10^1	40	8.00
C	Lower Delaware	Cibolites[a]	10^0	27	1.76
D	Lower Delaware	Paraceltites[a]	10^0	13	0.34
E	Lower Delaware	Medlicottia[a]	10^0	60	18.00
F	Lower Delaware	Timorites[a]	10^0	32	6.47
A	18	Waagenoceras[a]	10^2	28	6.47
B	18	Pseudogastrioceras[a]	10^1	40	8.00
C	18	Xenaspis[a]	10^1	24	1.73
D	18	Cibolites[a]	10^0	27	1.76
E	18	Paraceltites[a]	10^0	13	0.34
F	18	Medlicottia[a]	10^0	80	30.27
G	18	Timorites[a]	10^0	30	6.47

[a]After Miller and Furnish (1940)
[b]After Nassichuk (1970)
[c]After Nassichuk (1977)
[d]Present study

Table 9. Triassic assemblages utilized in biovolume analysis

Designation	Lithology Number (Table 1)	Genus	Abundance	Average Diameter (mm)	Average Biovolume (cm^3)
	21	Lanceolites[b]	10^0	?	?
K	21	Pseudosageceras[b]	10^1	62	22.41
J	21	Paraussuria[b]	10^1	53	17.00
N	21	Pseudoaspidites[b]	10^0	52	17.00
D	21	Aspenites[b]	10^1	23	0.60
L	21	Arctoceras[b]	10^1	83	43.31
I	21	Owenites[b]	10^1	29	3.90
C	21	Meekoceras[b]	10^2	63	24.60
B	21	Prosphingites[b]	10^2	21	2.85
F	21	Parannites[b]	10^2	19	1.54
P	21	Flemingites[b]	10^0	90	50.00
O	21	Anaflemingites[b]	10^0	84	47.50
E,G	21	Dieneroceras[b]	10^1	21,26	0.89,1.80

Table 9. Continued

Designation	Lithology Number (Table 1)	Genus	Abundance	Average Diameter (mm)	Average Biovolume (cm^3)
M	21	*Xenoceltites*[b]	10^0	41	10.80
H	21	*Preflorianites*[2]	10^1	31	3.90
A	21	*Juvenites*[b]	10^2	18	1.50
A	22	*Ophiceras*[a]	10^3	13	0.38
B	22	*Columbites*[a]	10^2	33	4.47
C	22	*Meekoceras*[a]	10^2	35	8.30
D	22	*Pseudosageceras*[a]	10^1	50	10.14
E	22	*Celtites*[a]	10^1	18	1.12
F	22	*Cordillerites*[a]	10^0	18	0.50
	22	*Pseudoharpoceras*[a] (= *Hellenites*)	10^0	?	?
	22	*Tirolites*[a]	10^0	?	?

[a]After Kummel (1957)
[b]After Kummel and Steele (1962)

Table 10. Lithologic character and geochemical data derived from associated strata of ammonoid assemblages used in biovolume analysis

Geologic Period	Stratigraphic Unit (Lithology #)	Lithologic Character	% Insoluble	% Organic	% $Ca_3(PO_4)$	Accessory Minerals
Miss.	Chainman Fm.(#3)	Black,fine-grained,thin-bedded ls.	+	0.76	0.7	
Miss.	Perdido Fm. (#2)	Gray, fine-grained, thin-bedded ls.	+	NR	NR	
Miss.	Chainman Fm.(#1)	Black, phosphatic,nodular,limestone	+	+	23.2	
Miss.	Chainman Fm.(#4)	Arenaceous,ferruginous,claystone concretions	-	-	4.5	
Perm.	Phosphoria Fm. (#9,13)	Phosphatic,dolomitic,black limestone (Raymond Canyon, Layland Canyon)	15.96	0.95	1.2-2.5	
Perm.	Phosphoria Fm.	Phosphatic,nodular limestone (old mine near Montperlier)	9.34	0.34	2.5	
Perm.	Cherry Canyon Fm. (Getaway Mbr.)	Dark,fine-grained to granular ls.	13.71	0.10	1.0	Fe_2O_3,$MnCO_3$
Perm.	(South Wells Mbr.)	Black,dense,dolomitic,bituminous,ls.	21.83	0.29	-	Fe_2O_3,$MnCO_3$
Perm.	(Manzanita Mbr.)	Greenish-gray,earthy,dolomitic,ls.	21.70	0.11	-	Fe_2O_3,$MnCO_3$
Perm.	Bell Caryon Fm. (Hegler Mbr.)	Dark gray, fine-grained to granular, thin-bedded, limestone	12.00	0.34	-	Fe_2O_3,$MnCO_3$
Perm.	(Pinery Mbr.)	Granular,thick-bedded to massive, ls.	4.40	0.32	0.06	Fe_2O_3,$MnCO_3$

Table 10. Continued

Geologic Period	Stratigraphic Unit (Lithology #)	Lithologic Character	Insoluble	Organic	$Ca_3(PO_4)$	Accessory Minerals
Perm.	Rader Mbr.	Gray,granular,thick-bedded,limestone with dark gray,thin-bedded ls.	1.16	0.05	-	Fe_2O_3,$MnCO_3$
Perm.	Horsefeed Fm.	Silicified,bioclastic,grainstone	NR	NR	NR	
Perm.	Assistance Fm.	Glauconitic,sandy,clayey,limestone; with ironstone & sandstone concretions	NR	NR	NR	
Trias.	Thaynes Fm(#21)	Fine to coarsely crystalline, coquinoid,thick-bedded limestone	5?	-	1.50	Fe_2O_3
Trias.	Thaynes Fm.(#22)	Black, very fine-grained nodular to concretionary limestone	21.47	0.75	1.70	SiO_2

Lithologies used are referenced in text.
Insoluble residues were determined with 30% HCl.
$Ca_3(PO_4)_2$ percentages were provided by Dr. Donald Fiesinger and Bill Perkins using the ammonium molybdenate method.
Organic matter percentages were determined by weight loss from bleaching 100 gm powdered samples with hydrogen peroxide (3%).
Accessory minerals were identified by X-ray diffraction techniques or reported from the Literature.
(+) present in detectable amounts
(-) none detected.
NR = Not reported in literature

developed under oxygen-starved conditions, and had very low carrying capacity in the water column. Most associated, shelled invertebrates show this effect well; productid brachiopods lack prominent spines, and all brachiopods display thin shells, as do most of the mollusks.

The nautiloids and ammonoids are very small. Only one example of Pseudogastrioceras was found to approach the common size (approximately 40 mm in diameter) achieved by congeneric species from Texas. The Pseudogastrioceras specimens collected from the Phosphoria Formation had an average diameter of 11 mm. The largest Spirolegorceras collected from the Phosphoria Formation achieved a diameter of 34 mm. The largest contemporaneous arctic representative of Spirolegoceras, reassigned to Sverdrupites, was over 600 mm in diameter (Nassickuk, 1970, p. 27). Medlicottia is represented in the Phosphoria predominantly by juveniles, as are Adrianites and Paragastrioceras. One specimen of Paragastrioceras found in the Layland Canyon exposure of the Phosphoria does approach 50 mm, but the two other examples from Montpelier average only slightly over 20 mm. It is the presence of the Layland Canyon specimen which inflates the biovolume profile in comparison with the other biovolume-abundance distributions of the Permian period. Otherwise, the Phosphoria contains genera with a low biovolume range. This observation is harmonious with a high content of phosphate and organic matter in the associated lithology (Table 10). Despite low biovolume, Psuedogastrioceras and Spirolegoceras are very abundant at different levels in the strata of the Phosphoria Formation, and are inferred to have been opportunistic species of ammonoids. These forms represent more efficient

utilization of calcium carbonate in shell-coiling geometries than is displayed in most Permian assemblages. Thus, by keeping shells small, and coiling geometries efficient in calcium carbonate utilization, ammonoids were able to adapt to the anoxic conditions associated with the nektobenthic habitat of the Phosphoria sea. Because large numbers of juvenile forms are found, it is suspected that the juvenile ontogenetic stage was vulnerable to the stressed, anoxic environment. Mortality rate declined with age as evidenced by positively skewed distributions (Figures 55 and 56). Paleo-opportunistic species typically have high fecundity associated with short generation time, an observation which is congruent with the small size and number of juveniles found in Psuedogastrioceras and Spirolegoceras.

The other Permian assemblages, which are preserved in a wide variety of lithologies, are characterized by high species diversity, which suggests that the carrying capacity of the environment was high and nutrient resources stable. Because no geochemical data are available and because sampling is limited, this interpretation is not conclusive. Perrinites, Waagenoceras, and to a lesser extent Stacheoceras, are found in great numbers in many Permian faunas. These three abundant ammonoids, contemporaneous with the ammonoids of the Phosphoria Formation, display inefficient utilization of calcium carbonate. This may explain the fact that Perrinites and Waagenoceras are absent in Phosphoria altogether, and that Stacheoceras is represented by only four specimens which were described by Miller and Cline (1934, pp. 293, 295).

Triassic biovolume-abundance profiles (Figgures 65, 66) resemble slightly those of the Permian. The Columbites fauna displays a high content of organic matter and phosphate and a slightly smaller average diameter per species than is seen in the earlier Triassic Meekoceras fauna (Table 9). The most abundant shell-coiling geometries of the ammonoids of the Columbites Zone are efficient in the utilization of calcium carbonate, in fact, much more so than the Permian Phosphoria ammonoids. The greater efficiency in the utilization of calcium carbonate among ammonoids of the Columbites Zone relative to ammonoids of the Phosphoria Formation (Figure 54 vs. Figure 51) may explain the large biovolume (diameters) values attained by the ammonoids of the Columbites Zone in comparison to the ammonoids of Phosphoria Formation (Figure 66 vs. 64).

The Meekoceras fauna of Nevada has the highest biovolume values encountered within the investigation (Figure 65). Many different shell-coiling geometries developed, and selection for efficient utilization of calcium carbonate was low. This environment was probably very well oxygenated, and represented very favorable conditions which facilitated high ammonoid diversity.

ONTOGENETIC VARIATION

Raup (1967, p. 51-53) stated that ontogenetic variation in coiling geometry of a taxon produces a shift in the W and D values of successive age (size)--classes from one part of the ammonoid field to another. Such change is observed during growth in practically all ammonoid shells. In some species, the variability has produced more evolute shells, but in most taxa involute shells result. The change is usually gradual rather than sudden.

The above observation is not surprising, for Westermann (1971, pp. 12, 30) has demonstrated that increasing shell wall thickness, decreasing volume of body chamber, and decreasing length of body chamber occurred with increasing shell diameter in many ammonoids. This is because constant growth rates in ammonoid shells were rarely realized. Buranaby (1966, p. 405) stated that in many ammonoids the shape of the shell is only approximately represented by a logarithmic or equi-angular spiral curve. Complications such as contrasting cameral cross-section proportions at successive intervals of the shell developed, with the result that the venter and umbilical seam followed different spiral curves during growth.

Actually, three different phases of ontogeny are recognized (Treatise, 1957, p. 101L). The initial stage is represented by the protoconch, a mobile or planktonic form usually less than one millimeter

in size. During the second stage, which includes chambers of equal width following the protoconch, accretionary growth rates vary considerably between individuals of the same population. Morphologic variables observed in the second phase (such as appearance or disappearance of surface ornamentation) for two specimens of the same species often can be compared only if the individuals attained the same ontogenic stages, and rarely do the dimensions of the shells at these stages coincide.

The gerontic phase of ontogenetic growth is accompanied by a closer spacing of septal faces, crowding or an enlargement of ribs, and the appearance of apertural structures, such as lappets and rostra. These latter structures apparently compensated for the increased buoyancy which resulted from a decreased body chamber volume (Westermann, 1971, p. 30). The smaller dimensions of the body chamber are a result of the termination of adult body chamber construction before cessation of construction of the septal wall. These gerontic characteristics were not found in any ammonoids analyzed in this investigation.

Because ammonoids do not assume a constant growth rate, the "normal" planispiral ammonoid of Raup (1967, p. 44), which maintains essentially the same geometry throughout its growth, is idealized, but not realized in nature. Nevertheless, for the scope of this report, ontogenetic variation in W and D of analyzed genera will be plotted on the base-diagrams of Raup (1967, Figure, p. 56; Figure p. 60; Figure, p. 62; Figure, p. 63), with the assumption that these variables change at a constant rate.

The following figures (67-78) illustrate these plots by using W and D parameters with increasing diameters for the most abundant Permian and Triassic species, as well as variability for Paracravenoceras ozarkense, as displayed by Raup (1967, Figure, p. 54). The latter genus resembles very closely the Cravenoceras from Nevada. These ontogenetic variations in W and D coiling geometry parameters values are recorded in Tables 11 and 12.

Paracravenoceras (Figures 67-70) illustrates a gradual shift towards decreasing D values (more involute), but maintained very constant W values during ontogeny. It is noteworthy that Raup (1967, p. 53) believed this goniatite to exhibit more ontogenetic change than most goniatites and much more than non-goniatite ammonoids.

Medlicottia (Figures 71-74) displays obvious, visual ontogenetic change as individuals. Specimens less than three millimeters in diameter resemble Epicanites sp. and are highly evolute; those less than seven milimeters resemble Pronorites sp. and are slightly evolute; those less than twenty millimeters in diameter resemble Artinskia sp. and are moderately involute; those with diameters greater than twenty millimeters display the highly involute form of the adult Medlicottia.

Pseudogastrioceras (Figures 71-74) shows relative constancy in coiling geometry with most variation attributable to variable umbilical widths, which is often indicative of sexual dimorphism.

Spirolegoceras (Figures 71-74) is highly variable with respect to W and D, but in this case, a wide and narrow form as described by Nassichuk (1970, p. 88) has been used. Sexual dimorphism, rather than the existence of separate species, is suspected.

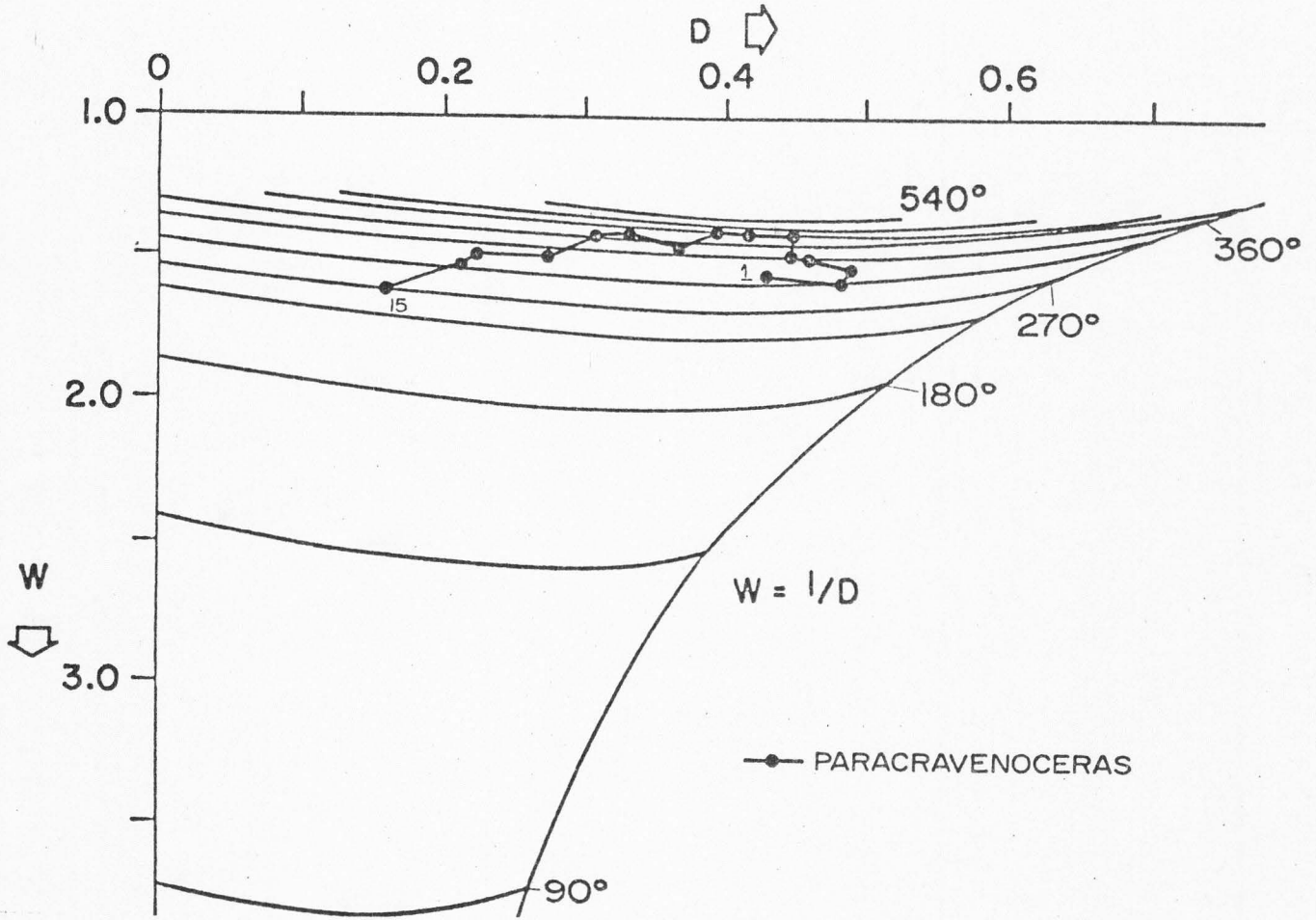

Figure 67. Ontogenetic variation in body-chamber length (in degrees) for the Mississippian genus Paracravenoceras sp.

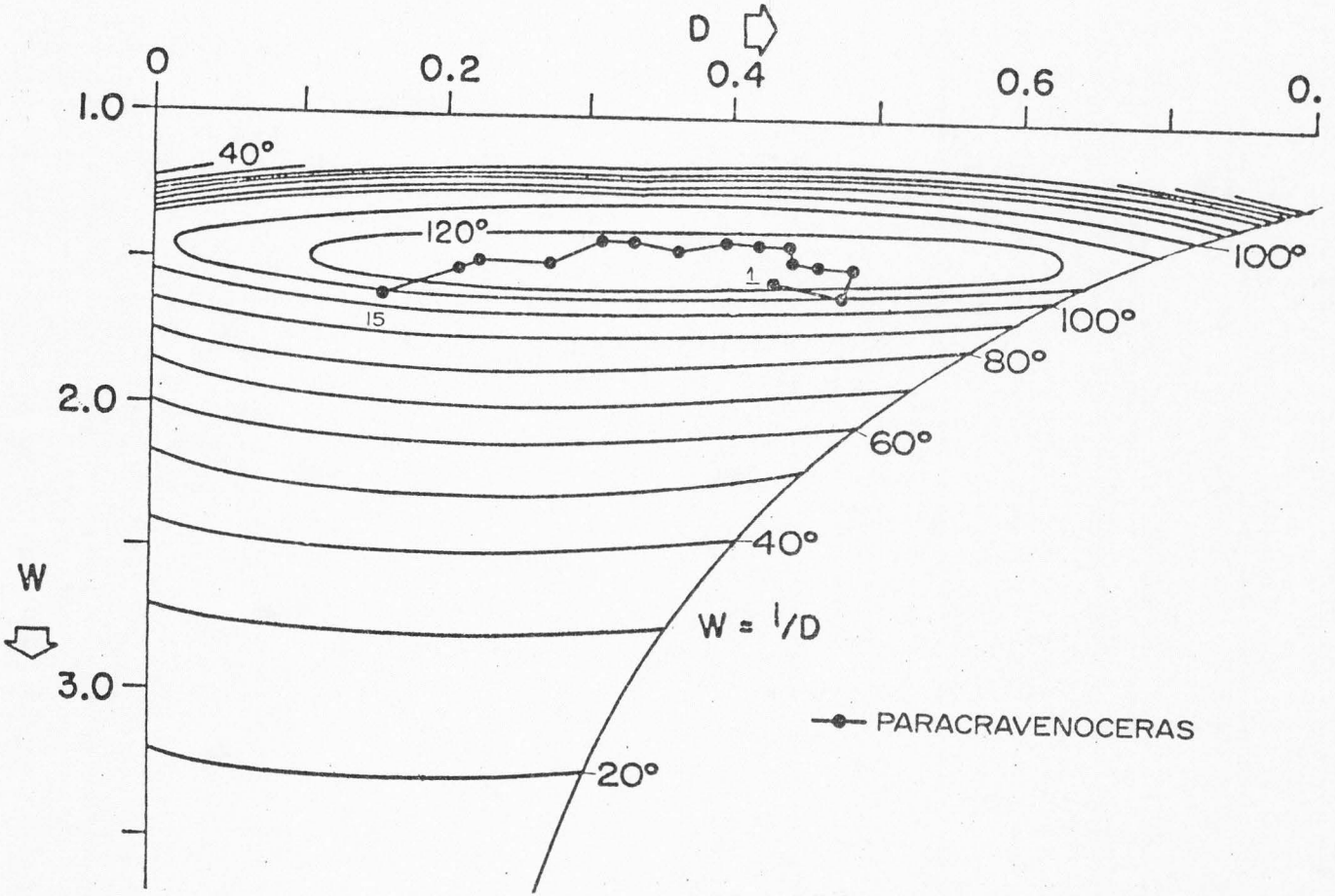

Figure 68. Ontogenetic variation in life-orientation for the Mississippian genus Paracravenoceras sp.

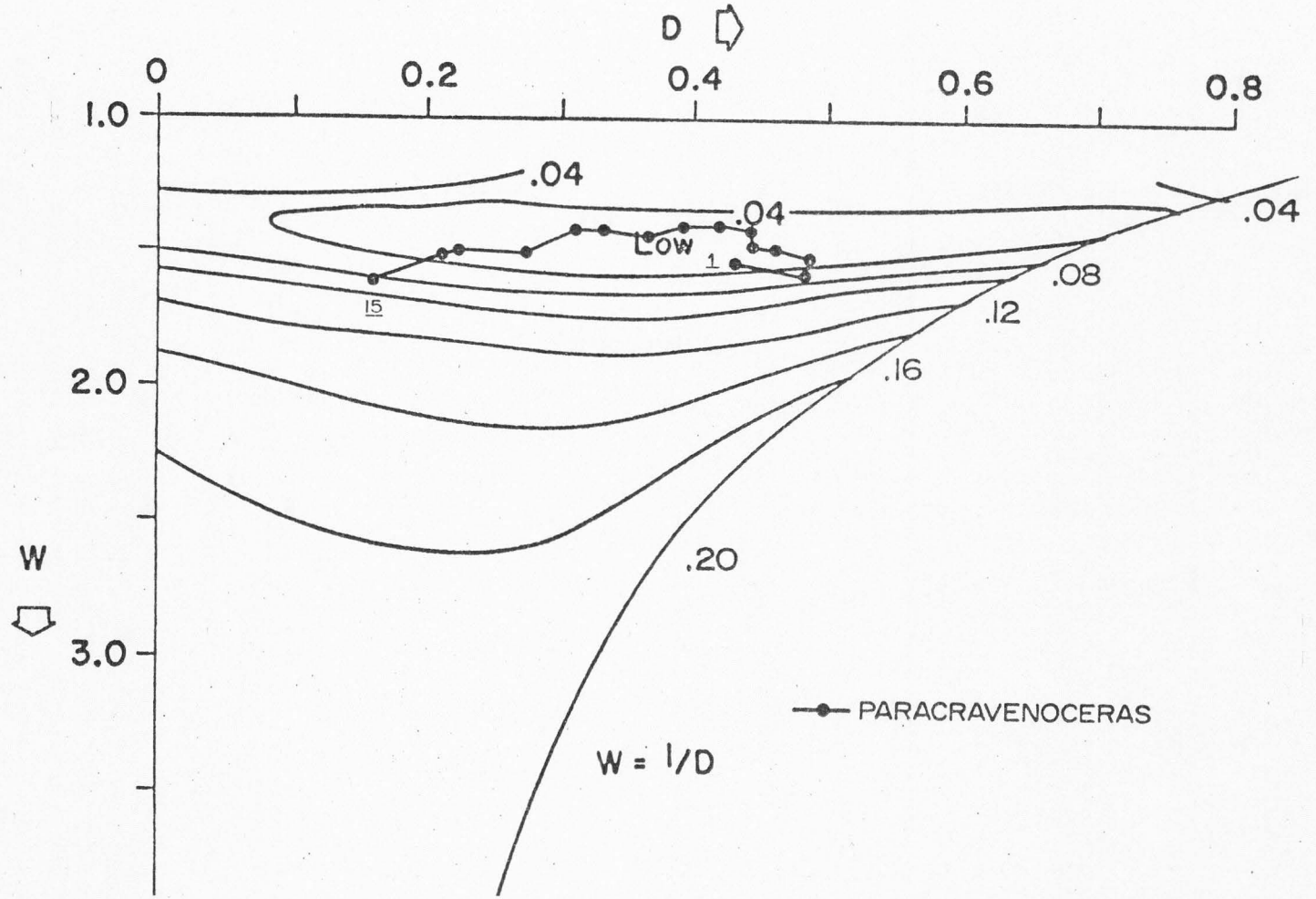

Figure 69. Ontogenetic variation in rotational stability for the Mississippian genus Paracravenoceras sp.

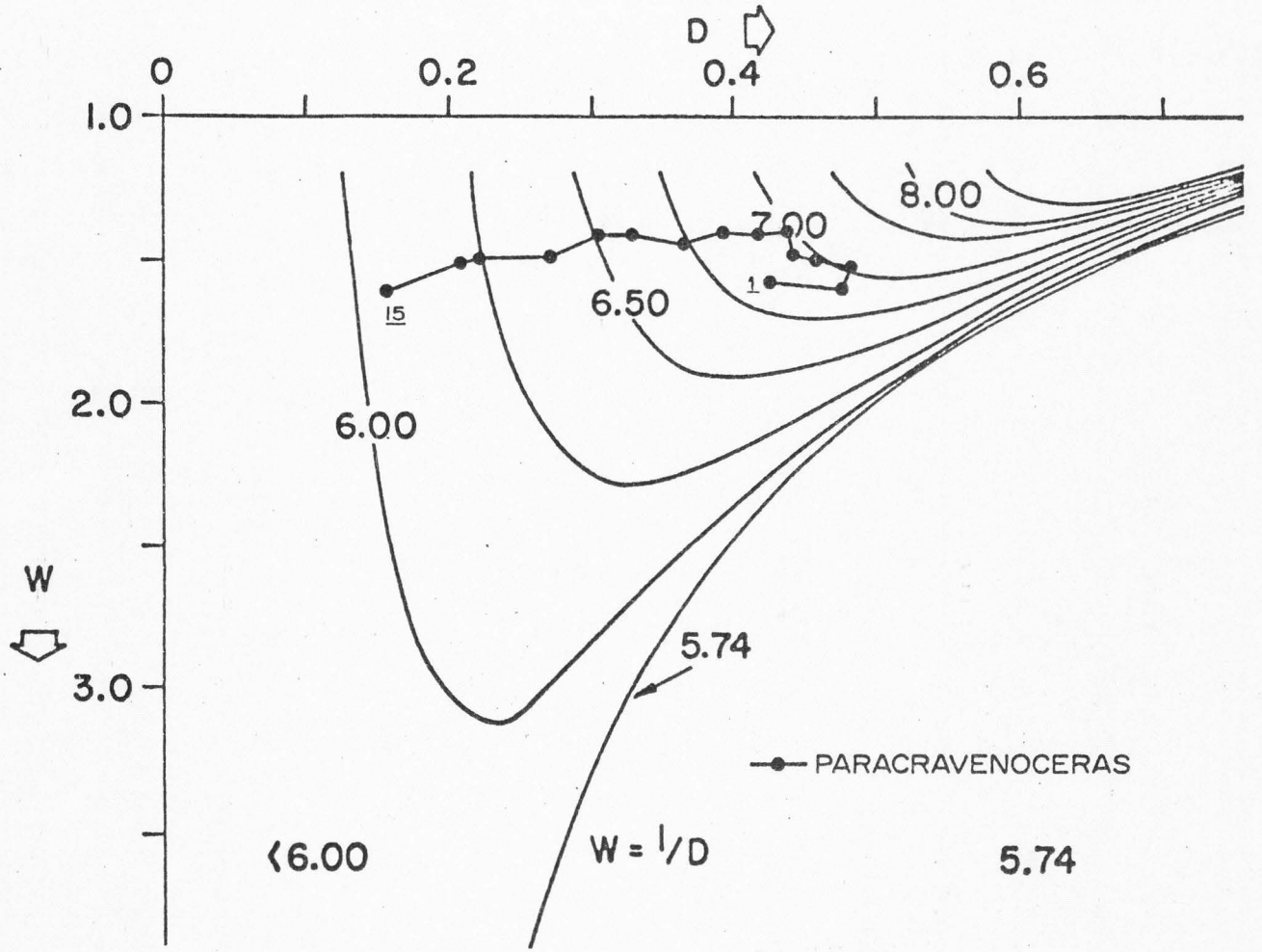

Figure 70. Ontogenetic variation in calcium carbonate efficiency for the Mississippian genus Paracravenoceras sp.

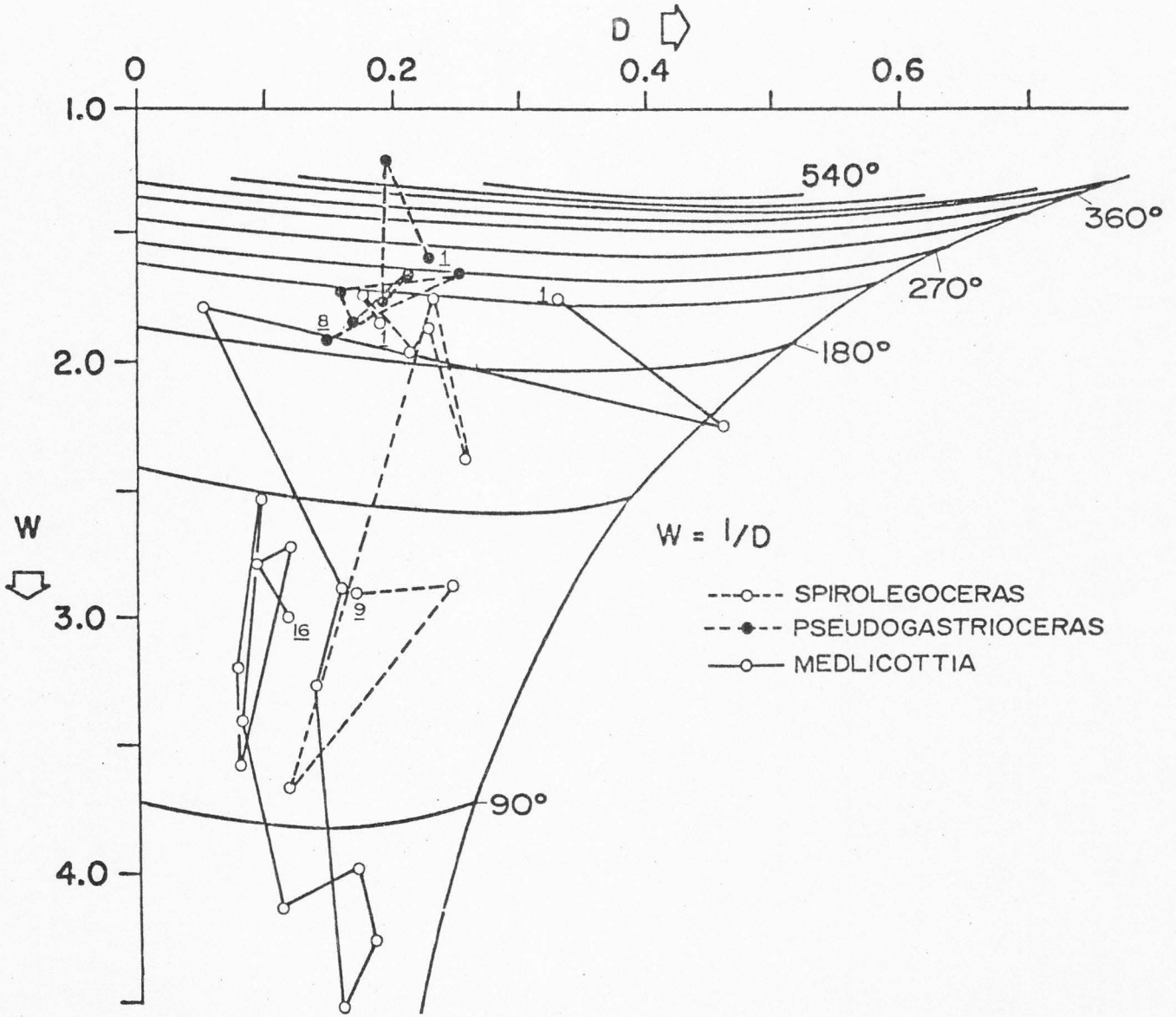

Figure 71. Ontogenetic variation in body-chamber length (in degrees) for selected Triassic ammonoid genera.

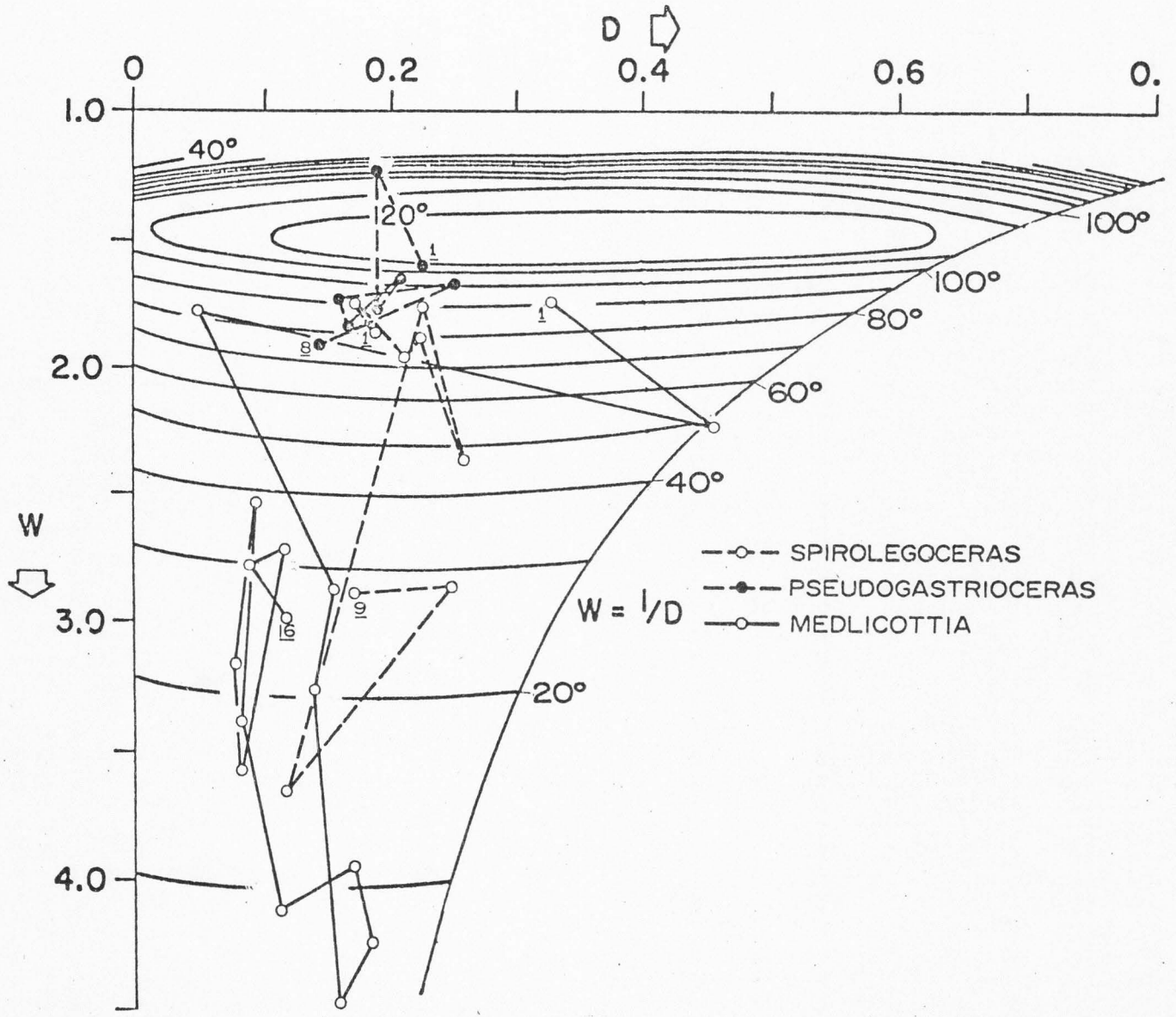

Figure 72. Ontogenetic variation in life-orientation for selected Permian ammonoid genera.

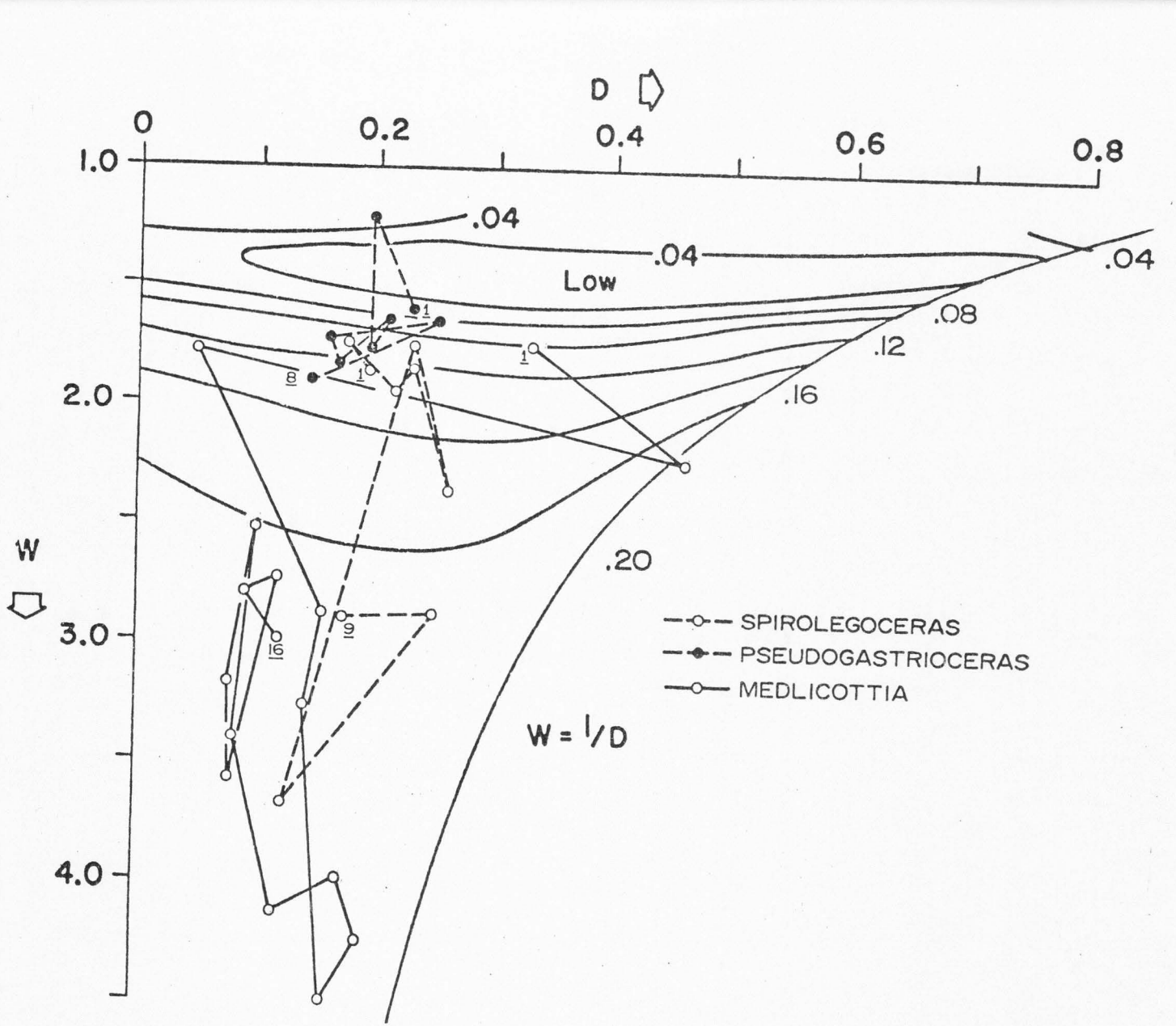

Figure 73. Ontogenetic variation in rotational stability for selected Permian ammonoid genera.

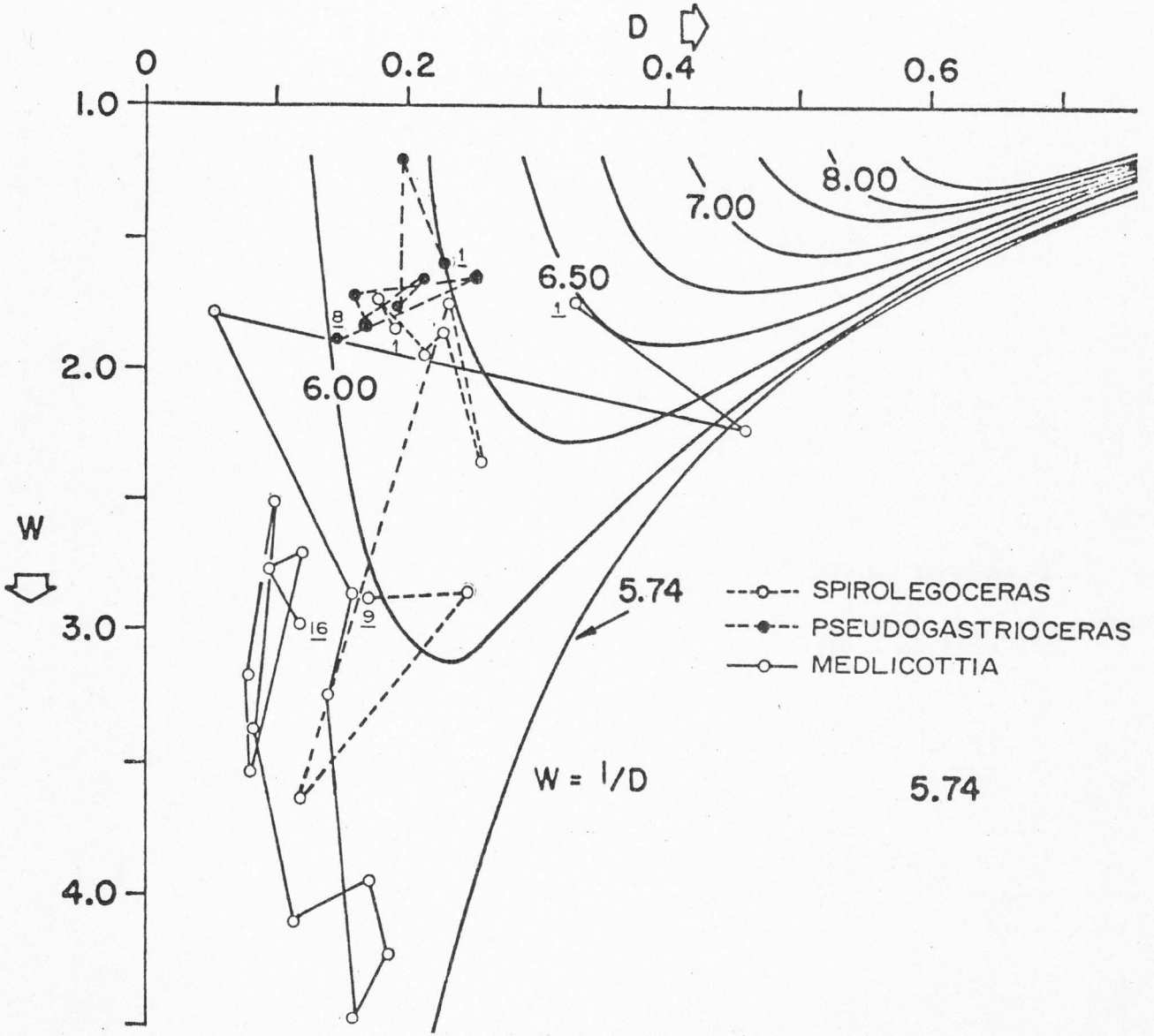

Figure 74. Ontogenetic variation in calcium carbonate efficiency for selected Permian ammonoid genera.

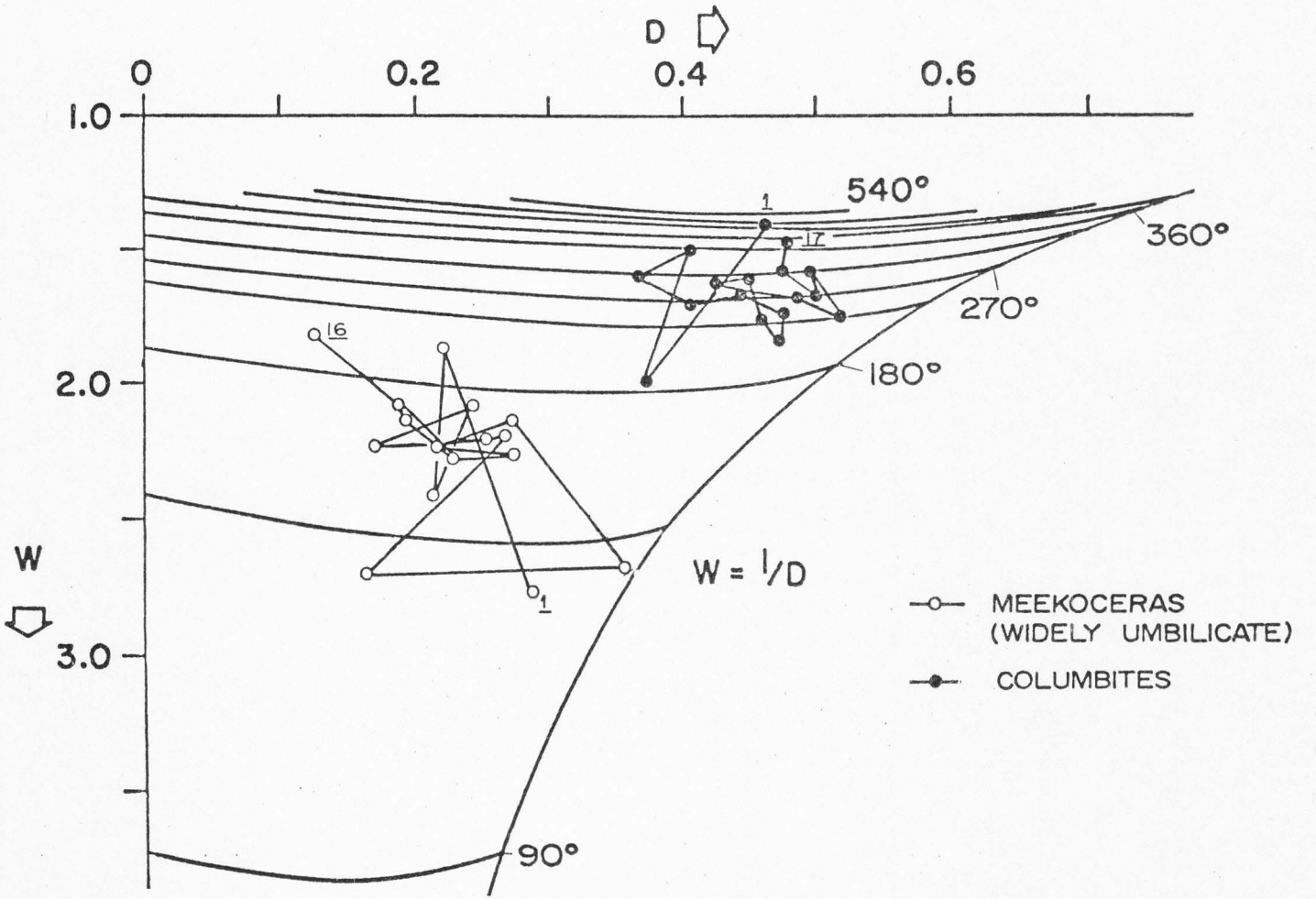

Figure 75. Ontogenetic variation in body-chamber length (in degrees) for selected Triassic ammonoid genera.

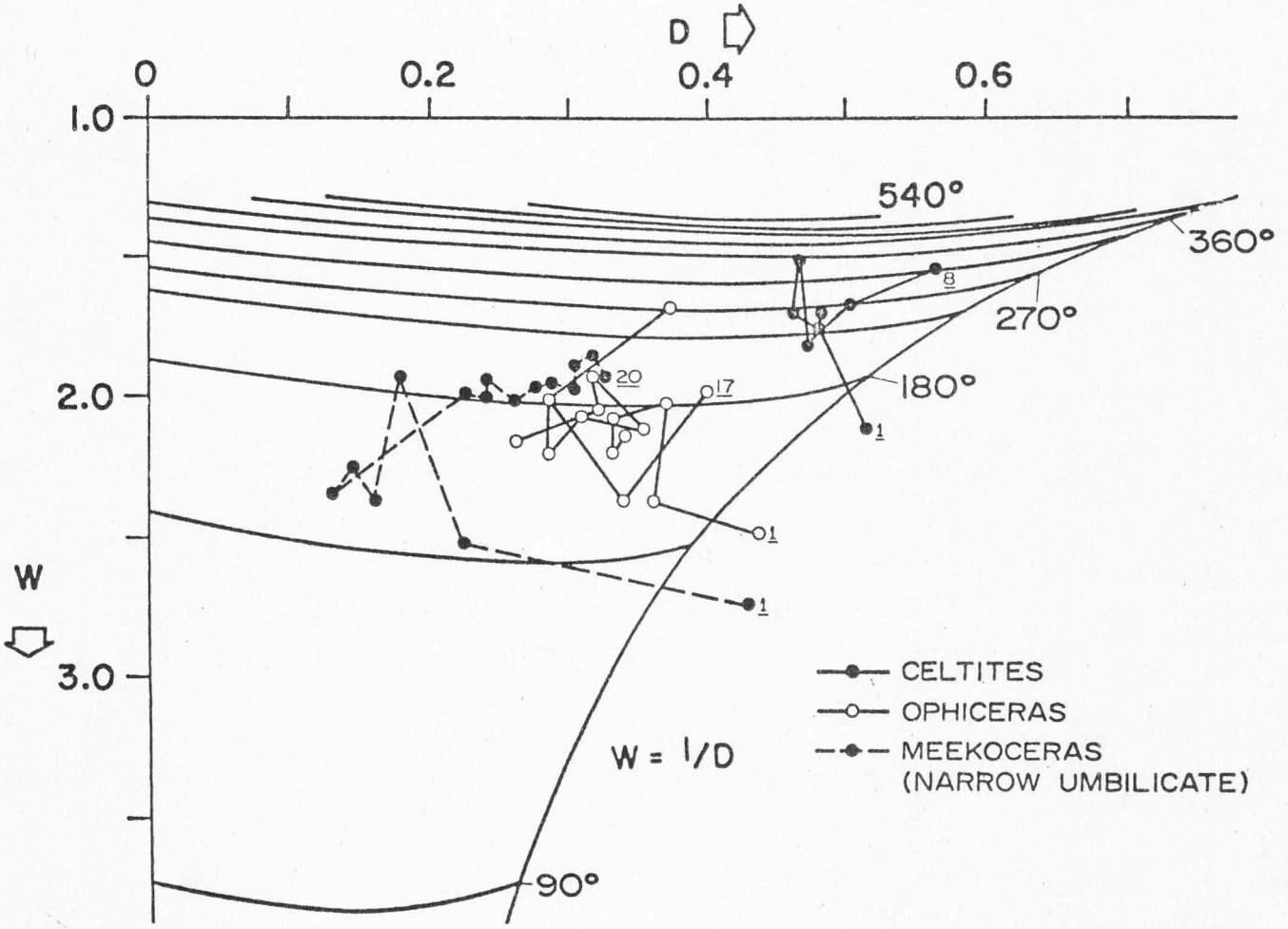

Figure 75. Continued.

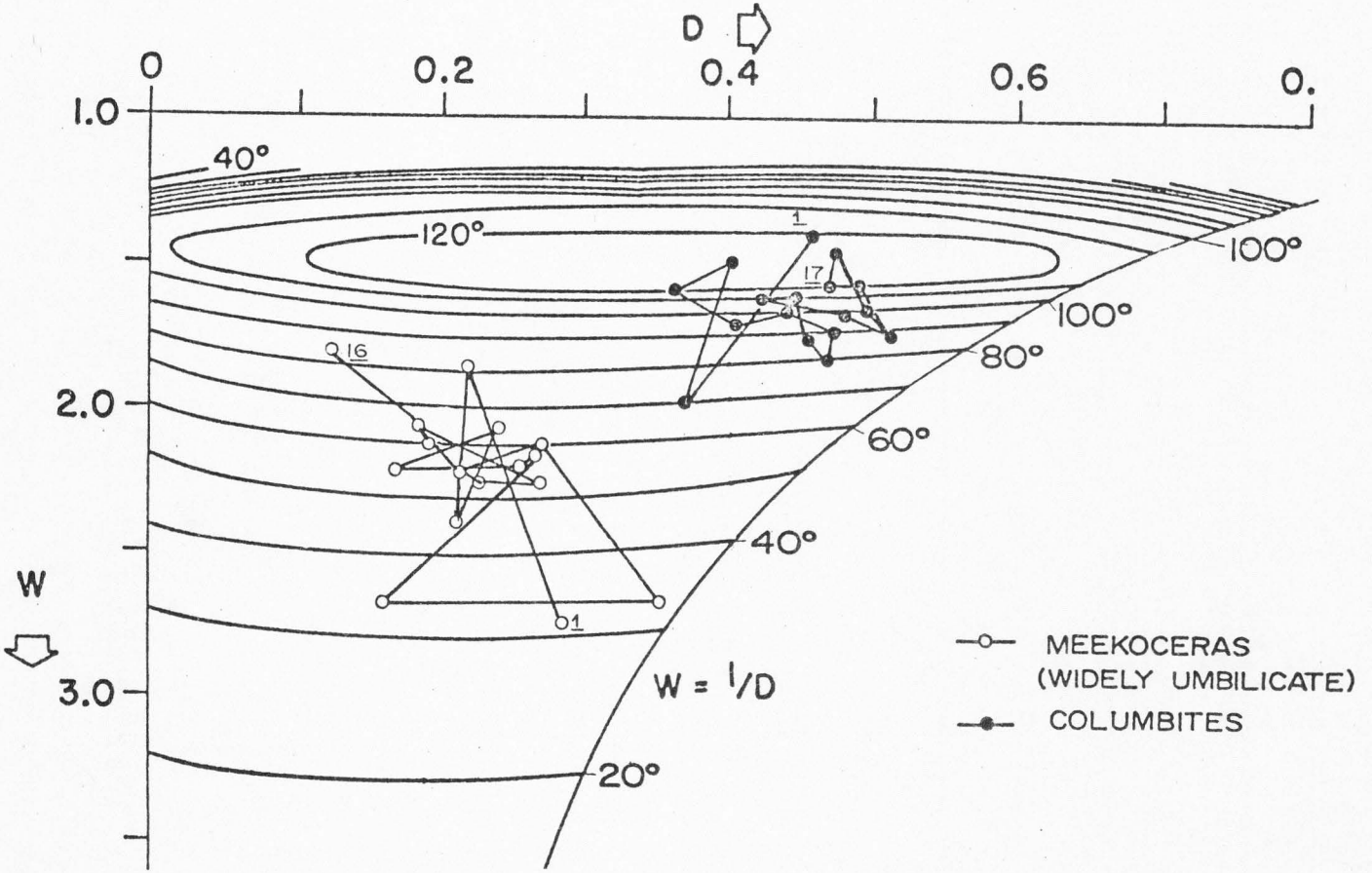

Figure 76. Ontogenetic variation in life-orientation for selected Triassic ammonoid genera.

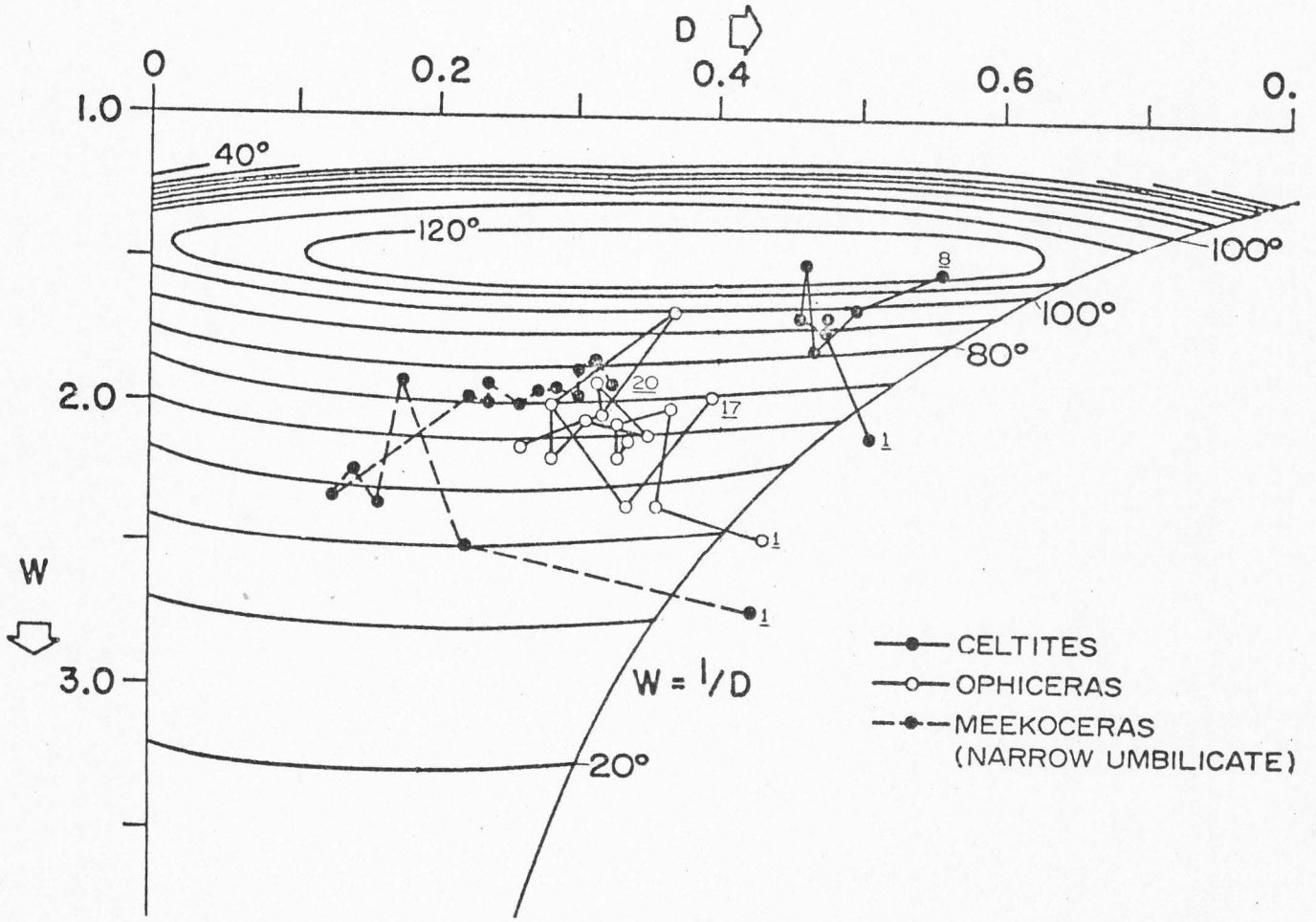

Figure 76. Continued.

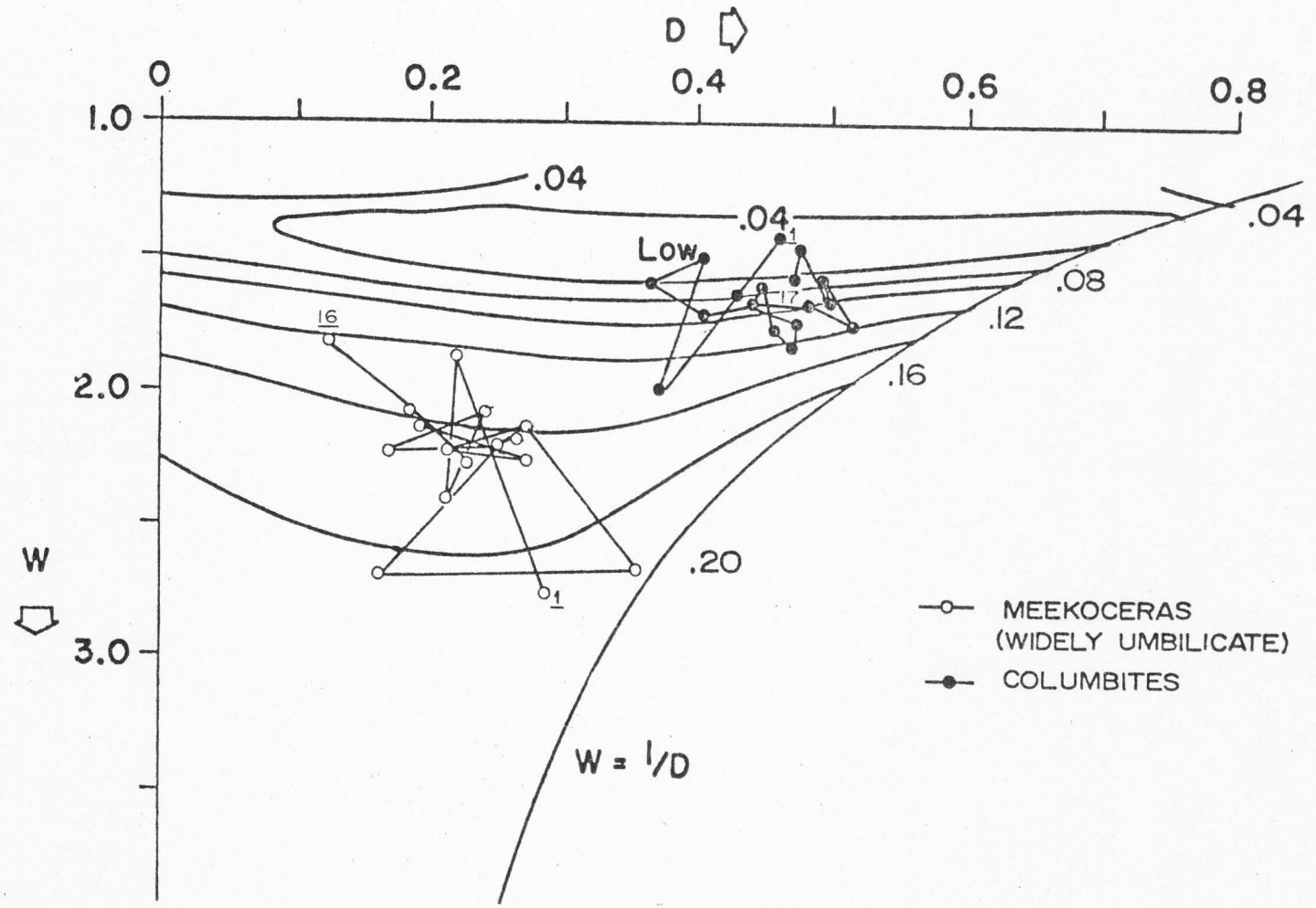

Figure 77. Ontogenetic variation in rotational stability for selected Triassic ammonoid genera.

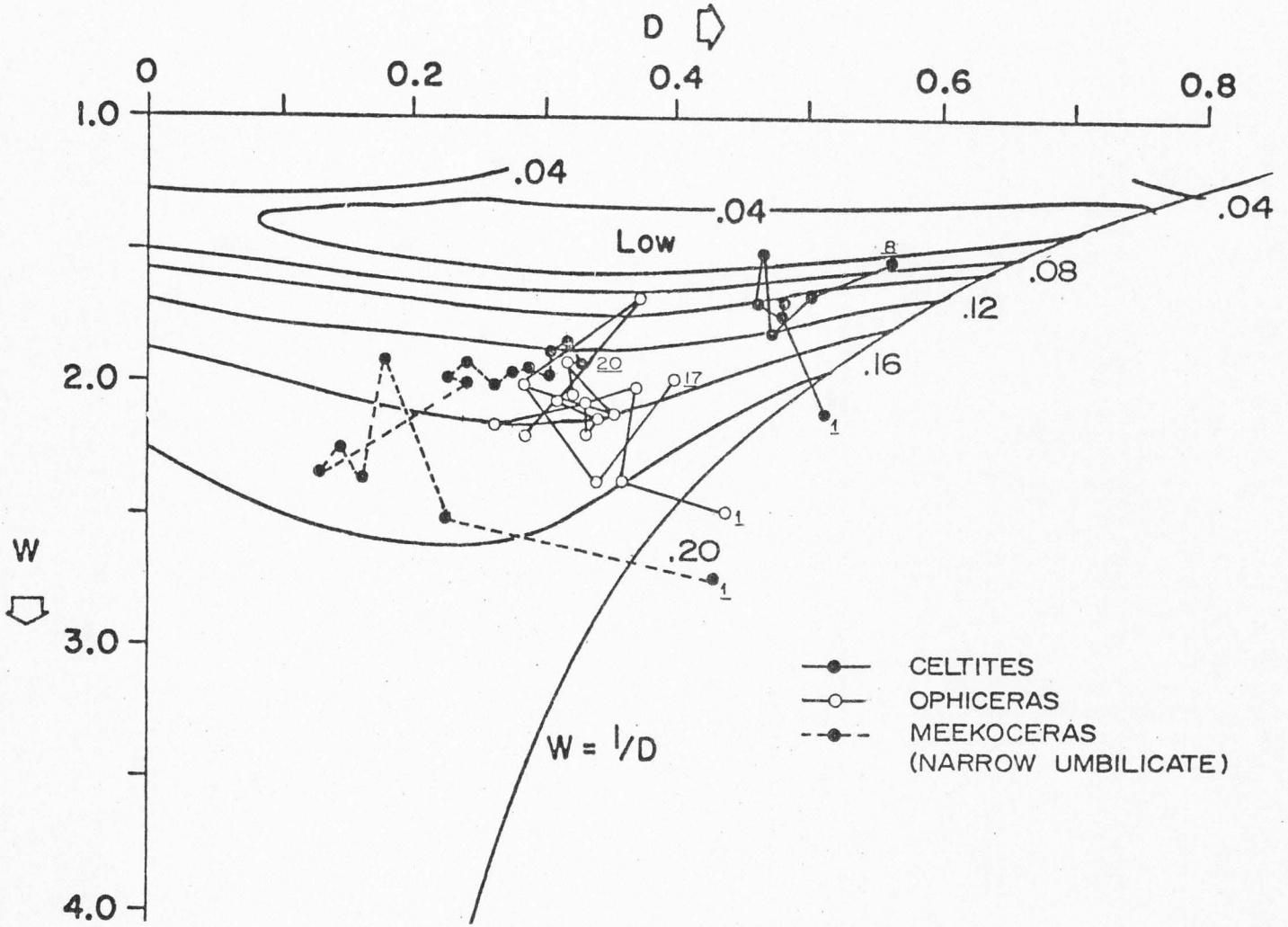

Figure 77. Continued.

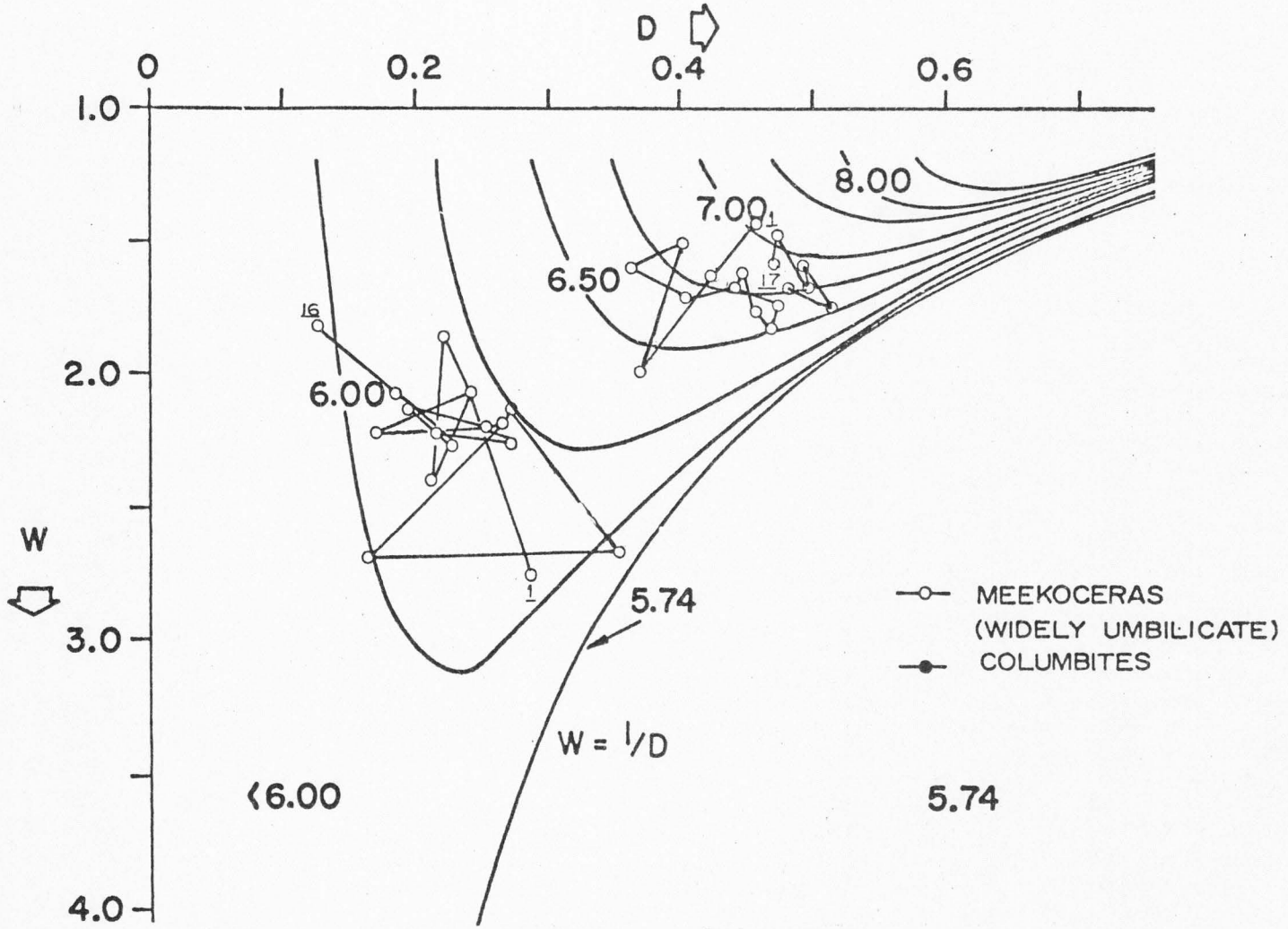

Figure 78. Ontogenetic variation in calcium carbonate efficiency for selected Triassic ammonoid genera.

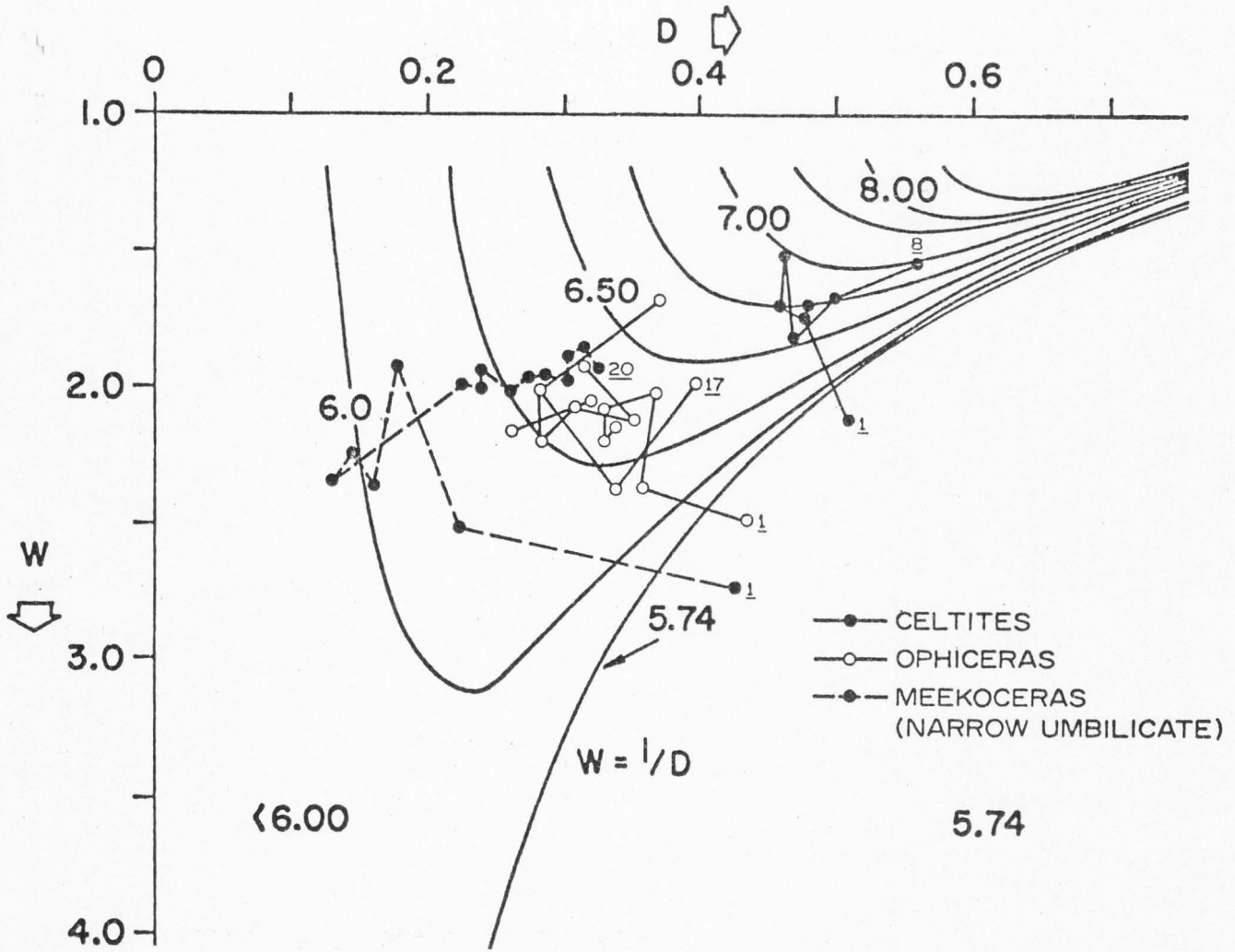

Figure 78. Continued.

Table 11. Ontogenetic variation in parametric values for coiling geometry in selected Permian ammonoid genera of the Phosphoria Formation

No.	Diameter (mm)	d	e	a	$(d/e)^2=W$		d-a/d=D	
			Medlicottia c.f. M. whitneyi					
1	2.0	1.2	0.9	0.8	1.78		0.3330	
2	2.5	1.5	1.0	0.8	2.25		0.4660	
3	4.2	2.1	1.8	2.0	1.36		0.0476	
4	4.7	2.9	1.7	2.4	2.91		0.1724	
5	6.8	4.0	2.2	3.4	3.31		0.1500	
6	7.6	5.1	2.4	4.0	4.52		0.1764	
7	8.5	5.4	2.6	4.4	4.31		0.1851	
8	9.3	5.8	2.9	4.8	4.00		0.1724	
9	9.5	6.1	3.0	5.4	4.13		0.1206	
10	10.2	6.5	3.5	6.0	3.45		0.0769	
11	10.2	6.4	4.0	5.8	2.56		0.0937	
12	11.5	7.0	3.9	6.4	3.22		0.0857	
13	12.3	7.2	3.8	6.6	3.59		0.0833	
14	16.2	9.6	5.8	8.5	2.74		0.1145	
15	37.5	23.5	14.0	22.2	2.82		0.0553	
16	52.5	33.0	19.0	30.0	3.01		0.0909	
			Pseudogastrioceras simulator					
1	3.5	1.8	1.7	1.6	1.75	1.59	0.0555	0.227
	4.5	2.7	1.9	1.9	2.01		0.2962	
	5.2	3.3	2.3	2.6	1.61		0.3030	
	4.8	2.8	2.0	2.6	1.16		0.2857	
	5.1	3.1	2.5	2.2	1.99		0.1935	
2	9.5	6.2	6.2	5.5	1.27	1.20	0.0161	0.194
	9.5	5.5	4.5	5.0	1.21		0.1818	
	9.6	6.0	4.4	5.5	1.18		0.2626	
	9.9	6.1	4.2	5.7	1.15		0.3114	
3	13.7	8.1	6.4	6.4	1.60	1.78	0.2098	0.1895
	13.6	7.9	6.3	6.4	1.52		0.2025	
	15.4	8.5	7.3	6.6	1.66		0.1411	
	13.3	8.5	6.8	6.3	1.82		0.2000	
	15.0	10.3	8.3	6.7	2.36		0.1941	
4	18.5	11.2	8.2	9.0	1.54	1.63	0.2678	0.2108
	19.0	11.1	8.5	8.7	1.63		0.2342	
	20.6	11.5	9.8	9.0	1.61		0.1478	
	21.4	12.4	10.0	9.5	1.70		0.1936	
5	24.5	14.4	12.3	9.5	2.30	1.85	0.1458	0.1731
	24.5	13.3	11.1	10.9	1.44		0.1654	
	24.5	14.4	11.4	10.5	1.90		0.2083	
6	30.5	19.2	16.0	14.6	1.74		0.1666	
7	40.0	23.5	17.8	18.3	1.65		0.2425	
8	50.5	29.5	25.3	21.4	1.90		0.1423	

Table 11. Continued

No.	Diameter (mm)	d	e	a	$(d/e)^2=W$		d-a/d=D	
				Spirolegoceras fischeri				
1	5.5	2.8	2.0	2.6	1.96		0.0714	
2	8.3	4.5	4.0	4.0	1.27	1.83	0.1111	0.1930
	9.5	6.5	3.8	4.0	2.92		0.3846	
	9.5	5.5	4.5	5.0	1.49		0.0909	
	9.8	6.0	4.4	5.0	1.86		0.1666	
	8.8	5.0	3.5	4.2	2.04		0.1600	
	9.0	5.3	4.5	4.0	1.39		0.2452	
3	10.0	5.8	4.5	4.6	1.66	1.73	0.2069	0.1806
	10.0	5.0	4.5	4.8	1.23		0.0400	
	11.4	6.6	5.5	5.6	1.44		0.1515	
	11.3	7.0	4.8	5.1	2.13		0.2714	
	11.8	7.0	5.0	5.8	1.96		0.1714	
	12.0	7.0	5.0	5.3	1.96		0.2428	
4	13.0	7.0	4.5	6.0	2.42	1.97	0.1428	0.2084
	13.4	8.0	6.8	6.0	1.38		0.2500	
	13.4	7.6	5.0	6.0	2.31		0.2100	
	14.0	8.0	5.0	6.0	2.56		0.2500	
	13.0	7.4	6.8	6.0	1.18		0.1891	
5	15.3	9.0	6.5	7.0	1.92	1.86	0.2222	0.2275
	15.4	8.3	6.7	7.0	1.53		0.1566	
	15.8	9.0	7.0	7.4	1.65		0.1770	
	16.0	10.0	7.5	7.5	1.77		0.2500	
	16.0	9.7	6.4	7.0	2.30		0.1750	
	16.2	10.6	7.6	7.4	1.95		0.3960	
	16.7	9.7	7.0	7.6	1.92		0.2164	
6	17.4	10.6	8.0	9.8	1.75	2.39	0.0750	0.2572
	18.7	11.4	6.6	7.6	2.98		0.3333	
	19.0	11.0	7.0	7.0	2.47		0.3630	
7	20.0	12.3	9.2	9.5	1.79		0.2276	
8	24.0	12.5	9.0	11.0	3.68		0.1200	
9	30.5	18.0	11.5	13.4	2.87		0.2550	

All dimensions were measured with a vernier calipers.

Table 12. Ontogenetic variation in parametric values for coiling geometry in selected Triassic ammonoid genera in the Columbites Zone

No.	Diameter (mm)	d	e	a	$(d/e)^2=W$		d-a/d=D	
				Ophiceras sp.				
1	3.4	2.1	1.1	1.0	2.62	2.48	0.5328	0.4430
	2.4	1.5	1.0	0.9	2.49		0.4000	
	2.3	1.5	0.9	0.9	2.91		0.4480	
	3.5	2.0	1.5	1.2	1.90		0.4000	
2	5.0	2.7	2.2	1.6	1.75	2.36	0.4560	0.3660
	5.9	3.6	2.3	2.4	2.45		0.3333	
	6.1	3.6	2.2	2.2	2.67		0.3880	
	6.2	3.7	2.1	2.5	3.10		0.3240	
	6.2	3.6	2.4	2.4	2.25		0.3333	
	6.3	3.7	2.6	2.4	2.03		0.3640	
3	8.0	4.7	3.3	2.8	1.53	2.02	0.4040	0.3680
	8.0	7.3	5.2	5.5	1.97		0.2465	
	8.3	5.0	3.5	3.3	2.04		0.4600	
	9.2	5.5	3.9	3.4	1.99		0.3818	
	9.5	5.5	3.6	3.6	2.33		0.3450	
	9.8	6.2	4.1	3.9	2.29		0.3709	
4	10.8	6.7	4.8	4.5	1.95	2.04	0.3280	0.3230
	11.2	6.8	4.6	4.4	2.10		0.3520	
	11.6	6.9	4.9	4.9	1.98		0.2890	
5	12.9	7.7	5.0	5.1	2.37	2.19	0.3376	0.3341
	13.0	7.8	5.3	5.2	2.16		0.3333	
	14.2	8.1	5.8	5.6	1.95		0.3086	
	14.3	8.5	5.9	6.1	2.35		0.3640	
	14.4	8.3	5.9	5.6	1.98		0.3250	
	15.0	9.2	6.0	6.1	2.35		0.3369	
6	15.6	9.6	6.3	6.0	2.32	2.15	0.3750	0.3406
	16.0	9.2	6.2	6.0	2.20		0.3470	
	17.5	10.3	7.4	7.2	1.93		0.3000	
7	20.6	11.9	8.9	8.6	1.79	2.10	0.2773	0.3064
	20.8	12.2	8.7	8.5	1.97		0.3030	
	21.5	12.3	8.7	8.4	1.99		0.3170	
	21.8	13.0	8.9	8.7	2.13		0.3300	
	22.0	12.8	9.0	8.8	1.96		0.3015	
	22.1	14.0	9.2	9.4	2.31		0.3280	
	22.5	13.5	8.4	9.6	2.58		0.2880	
8	23.8	13.4	9.0	9.8	2.22		0.2680	
9	25.0	14.4	9.1	9.9	2.50	2.06	0.3120	0.3240
	25.5	14.1	10.7	9.7	1.74		0.3120	
	26.0	14.9	10.5	10.9	1.97		0.2850	
	27.5	16.0	11.2	9.8	2.04		0.3870	
10	28.7	17.2	12.1	12.0	2.02	1.94	0.3023	0.3178
	29.0	16.7	12.3	11.7	1.84		0.2990	
	29.0	16.5	12.0	10.5	1.89		0.3630	
	30.0	18.5	12.6	13.8	2.15		0.2540	
	30.2	17.5	13.0	11.0	1.81		0.3710	

Table 12. Continued

No.	Diameter (mm)	d	e	a	$(d/e)^2=W$		d-a/d=D	
				Ophiceras sp.				
11	32.0	18.7	13.0	12.1	2.13		0.3530	
12	36.4	21.0	15.0	14.8	1.96	1.96	0.2952	0.2901
	36.4	21.0	15.3	15.0	1.96		0.2850	
13	43.0	25.3	17.0	18.2	2.21		0.2806	
14	43.8	24.5	19.0	15.2	1.66		0.3790	
15	46.3	26.5	18.8	16.8	1.99		0.2900	
16	47.8	27.0	20.0	17.5	2.38		0.3510	
17	53.0	30.0	21.2	18.0	2.00		0.4000	
				Columbites sp.				
1	3.0	1.0	0.9	0.7	1.23	1.43	0.3000	0.4540
	4.0	2.3	1.8	0.9	1.63		0.6080	
2	14.0	7.8	5.5	4.9	2.02		0.3730	
3	17.5	9.2	7.5	5.5	1.50		0.4020	
4	19.1	10.0	8.0	7.0	1.56	1.59	0.3000	0.3628
	19.3	10.5	8.7	6.5	1.44		0.3800	
	20.0	11.5	8.6	6.8	1.78		0.4086	
5	23.3	13.0	10.0	7.8	1.69		0.4000	
6	25.0	14.3	11.0	8.4	1.69	1.65	0.4120	0.4360
	26.8	15.0	11.8	8.1	1.61		0.4600	
7	27.8	15.7	12.2	8.8	1.65	1.62	0.4390	0.4380
	28.5	16.0	12.7	9.0	1.59		0.4370	
8	32.5	18.0	13.2	9.5	1.86	1.77	0.4720	0.4580
	34.5	19.3	14.9	10.7	1.68		0.4450	
9	36.0	21.2	15.4	10.4	1.89	1.79	0.4190	0.4720
	36.3	21.0	15.8	12.2	1.77		0.4900	
	36.9	20.8	15.8	11.2	1.73		0.4840	
10	38.5	21.9	16.0	11.3	1.87	1.69	0.5090	0.4735
	39.0	22.3	18.0	11.5	1.53		0.4560	
	40.0	22.4	18.0	11.0	1.55		0.4840	
11	43.3	24.0	18.8	13.6	1.63		0.4330	
12	46.0	25.3	19.6	13.0	1.66	1.66	0.4610	0.4740
	47.0	26.4	19.9	13.8	1.76		0.4860	
	47.0	26.6	21.2	13.3	1.57		0.4770	
13	49.0	27.0	21.5	13.0	1.58	1.74	0.5180	0.5090
	50.0	29.0	21.0	16.0	1.90		0.5000	
14	54.5	31.0	24.5	15.7	1.60		0.4930	
15	56.4	32.0	23.7	15.8	1.82	1.66	0.5060	0.4980
	57.0	31.0	25.4	15.8	1.49		0.4900	
16	60.3	32.3	26.1	16.6	1.53	1.48	0.4860	0.4710
	61.4	33.7	28.2	18.3	1.43		0.4560	
17	68.0	37.4	30.0	21.3	1.56		0.4320	

Table 12. Continued

No.	Diameter (mm)	d	e	a	$(d/e)^2=W$		d-a/d=D	
				Celtites sp.				
1	7.0	4.5	3.1	2.2	2.11	2.12	0.5110	0.5160
	7.8	4.4	3.0	2.1	2.14		0.5220	
2	11.0	6.7	4.6	3.3	2.12	1.69	0.5070	0.4860
	11.3	6.2	5.3	2.2	1.39		0.6450	
	12.4	6.9	5.5	4.2	1.57		0.3070	
3	15.0	7.5	6.0	3.5	1.77	1.72	0.5410	0.4920
	15.5	8.3	7.0	4.5	1.41		0.4570	
	16.0	8.8	6.6	4.4	1.77		0.5000	
	16.2	10.0	7.2	5.3	1.93		0.4700	
4	17.4	9.8	7.5	5.2	1.70		0.4690	
5	20.0	12.0	9.0	5.5	1.40	1.51	0.4570	0.4730
	20.5	11.4	9.2	6.3	1.54		0.4470	
	20.6	11.4	9.1	5.5	1.57		0.5170	
6	22.4	12.5	9.3	6.5	1.81		0.4800	
7	25.5	14.3	10.7	7.2	1.79	1.67	0.4960	0.5040
	26.0	15.0	11.8	7.2	1.56		0.5000	
	26.0	14.6	11.4	7.4	1.64		0.4930	
	26.6	14.6	11.5	7.5	1.61		0.4860	
	27.5	15.5	12.3	7.7	1.58		0.5200	
	27.5	15.9	12.0	7.8	1.75		0.5090	
	28.0	15.8	11.9	7.5	1.76		0.5250	
8	30.0	17.0	14.0	7.1	1.47	1.55	0.5820	0.5648
	30.5	16.5	13.7	7.0	1.45		0.5750	
	31.9	18.1	13.8	8.3	1.72		0.5410	
	32.0	17.0	14.0	8.0	1.47		0.5820	
	32.3	18.0	14.0	8.2	1.65		0.5440	
				Meekoceras sp. (widely umbilicate)				
1	6.0	3.5	2.1	2.5	2.75		0.2850	
2	21.5	12.8	9.4	10.0	1.84		0.2180	
3	26.5	15.5	10.0	12.2	2.40		0.2120	
4	28.0	16.5	11.5	12.6	2.05		0.2420	
5	29.5	17.5	11.8	14.5	2.19		0.1710	
6	36.0	21.5	14.5	16.0	2.20		0.2560	
7	39.0	23.0	15.5	17.0	2.19		0.2600	
8	43.5	26.5	16.5	22.5	2.58		0.1500	
9	56.4	27.0	16.6	20.0	2.64		0.3500	
10	49.5	29.4	20.0	21.5	2.16	2.20	0.2680	0.2460
	50.5	29.5	19.7	23.1	2.22		0.2160	
11	54.5	32.3	22.0	23.6	2.22		0.2690	
12	61.2	37.4	26.5	30.5	2.13	2.10	0.1840	0.2030
	62.0	36.0	24.0	28.0	2.25		0.2222	
13	66.5	38.5	26.5	30.5	2.13		0.1840	
14	71.8	41.0	30.5	36.0	1.80		0.1210	

Table 12. Continued

No.	Diameter (mm)	d	e	a	$(d/e)^2=W$		d=a/d=D	
			Meekoceras sp. (narrowly umbilicate)					
1	2.8	1.8	1.1	1.0	2.77		0.4280	
2	7.2	4.3	2.3	3.6	3.49		0.1620	
3	8.3	5.2	3.3	4.2	2.57	2.53	0.1920	0.2250
	8.3	5.4	3.4	4.1	2.52		0.2900	
	9.8	5.7	3.6	4.6	2.50		0.1929	
4	21.9	13.2	9.0	10.8	2.15		0.1818	
5	23.5	13.9	9.4	10.6	2.18	1.97	0.2370	0.1850
	24.0	14.0	10.0	11.2	1.96		0.2000	
	22.9	12.8	9.6	11.3	1.77		0.1170	
6	26.3	15.8	10.2	12.0	2.39	2.38	0.2020	0.1690
	27.4	16.8	10.9	14.5	2.37		0.1360	
7	29.1	17.7	11.4	14.3	2.41		0.1920	
8	32.3	18.9	12.5	16.0	2.29		0.1530	
9	35.1	20.5	13.4	17.8	2.34		0.1317	
10	43.0	25.2	17.4	18.9	2.10	2.04	0.2500	0.2400
	44.0	26.0	18.5	20.0	1.97		0.2300	
11	45.0	27.0	19.5	20.5	1.92		0.2400	
12	48.0	28.0	20.0	22.0	1.96	2.01	0.2140	0.2360
	48.5	29.0	20.2	21.5	2.06		0.2580	
13	54.0	31.0	22.0	22.8	1.99		0.2640	
14	60.0	34.5	24.0	25.2	2.06	1.96	0.2690	0.2820
	63.0	35.5	26.0	25.0	1.86		0.2950	
15	66.0	39.5	28.0	27.3	1.99		0.3080	
16	70.0	41.0	30.0	28.6	1.87		0.3020	
17	75.0	43.8	32.0	30.0	1.87		0.3150	
18	80.0	46.5	32.0	33.0	2.11	2.07	0.2900	0.3150
	82.5	47.0	33.0	31.0	2.02		0.3400	

All dimensions were measured with a vernier calipers.

Ophiceras, Columbites, and Celtites (Figures 75-78) show a tight cluster of W and D values with increasing diameters, though a few divergent values are encountered.

Meekoceras (Figures 75-78) displays a wide range of W and D values. The existence of a widely umbilicate form, M. curticostatum of Smith (1932, p. 11), and a narrowly umbilicate form, M. micromphalus of Smith (1932, p. 11) accounts for much of the variability. For all analyzed ammonoids, a range of variability in W and D parameters is encountered with increasing diameters. Sexual dimorphism within the same species could result in differences in W and D parameters comparable to those encountered between different species of the same genus. This observation supports the author's preference for morphologic analysis of genera rather than species. Stanton and Evans (1972, p. 848) stated the genus is the working unit of paleoecology, the utility of the species having been vitiated by subjective taxonomy.

Among the previous ammonoid genera analyzed for ontogenetic variation in W and D, a correlation is suggested between ontogenetic trends in W and D and mortality inferred from size frequency distributions. The trend toward more involute shell-coiling geometries during ontogeny, and a corresponding greater inefficiency in the utilization of calcium carbonate, may result in increased mortality rate among adults. The best example of this possible correlation between ontogenetic variation and mortality rate is Medlicottia, which proliferated in the poorly-oxygenated Phosphoria sea. During ontogeny, a more involute coiling geometry developed (Figure 73). The corresponding

size-frequency distribution (Figure 56) suggests increasing mortality during the adult stage.

CONCLUSIONS

Though Raup published his concept and development of W and D shell-coiling geometry parameters over 11 years ago, to date no published study known to the author has yet applied Raup's technique to ammonoid assemblages. The application of Raup's technique to ammonoid assemblages from Mississippian to Triassic age involves autecological interpretation from trends observed in length of body chamber, life orientation, rotational stability, and efficiency in the utilization of calcium carbonate.

Average length of body chamber in ammonoids is observed to decrease from 297° to 209° from Mississippian to Triassic time. An increase in apertural area accompanied this trend, and a possible consequence was that a greater range of prey sizes was afforded ammonoids with shorter body chambers.

Reconstruction of life-orientation of ammonoids has been over-simplified in the computer-analysis of Raup (1967), who considered only shape and other geometrical aspects of the shell in his calculations. Recent findings on Nautilus with additional evidence from fossil epizoan encrustations on ammonoid shells suggest that the ability of the organism to adjust its attitude may not be readily discernable from preserved morphology alone. Consequently, from the Mississippian to Triassic time, no trends in reconstructed life-orientations can be substantiated based solely on W and D values.

Rotational stability is an important characteristic in that it affected the energy expended by the organism during locomotion. Because ammonoids were most likely carnivorous, and had a high metabolic rate, high rotational stability would conserve energy in the search for prey, and be selectively advantageous. A trend of increasing average rotational stability is observed for ammonoids from Mississippian to Triassic time (.07 and .10), possibly in response to the appearance of marine, vertebrate predators on ammonoids.

Efficiency in the utilization of calcium carbonate may be selectively advantageous and therefore well-established among ammonoids from black, phosphatic limestones rich in organic matter. This hypothesis is very well supported by the data. The Permian genera Pseudogastrioceras and Spirolegoceras, and the Triassic genera Ophiceras and Columbites all display efficiency values greater than 6.2, and they numerically dominate their respective ammonoid assemblages in the phosphatic, organic rich intervals of the Phosphoria and Thaynes Formations. In correlative ammonoid assemblages from light-gray, crystalline carbonates, no such correlation between efficiency in the utilization of calcium carbonate and abundance is observed.

Size-frequency distributions are utilized in recognition of opportunistic species of ammonoids. High numerical abundance, high mortality rate of juveniles, small size and conservation of calcium carbonate typifies the paleo-opportunistic species Cravenoceras, Psuedogastrioceras and Ophiceras.

Biovolume-relative abundance distributions are useful in discerning the carrying capacity of the habitat both in number of individuals and species diversity; a large area under the biovolume-relative abundance profile indicates diversification under optimum environmental conditions; a small area under the profile indicates colonization of a stressful habitat. The Chainman, Phosphoria and Thaynes (Columbites Zone) Formations have ammonoid assemblages which show small areas under the biovolume-relative abundance profile, characteristics of anoxic environmental stress. The Permian stratigraphic units correlative with the Phosphoria Formation have ammonoid assemblages which show large areas under the profile and the associated lithologies, i.e., light gray crystalline carbonates, suggest environments which could support a diversified ammonoid fauna, including large-sized species. Ontogenetic variation produces changes in the body chamber length, life orientation, rotational stability, and utilization of calcium carbonate of the analyzed genera of ammonoids. These ontogenetic variations usually resulted in the development of more involute shell-coiling geometries. Corresponding size-frequency distributions suggest increased mortality rates during ontogeny for some genera (Paracravenoceras, Medlicottia, Figures 70, 74) which show decreasing efficiency in the utilization of calcium carbonate with age.

Despite the obvious advantages afforded an ammonoid which possessed very high rotational stability (.16 or higher), or very high efficiency in the utilization of calcium carbonate (8.00 or higher) these values were not determined among ammonoids analyzed in this study. This deficiency resulted from selection on a variety of morphologic

characteristics which are frequently inter-related and possibly genetically coupled. In the field of coiling geometries, high rotational stability values correspond with low efficiency in the utilization of calcium carbonate values, and high efficiency values fall in the low stability range. The distribution of ammonoid genera in all analyzed assemblages suggests that the optimum morphology attained under the stressful conditions of anoxic habitats is a coiling geometry that displays moderately high efficiency in the utilization of calcium carbonate and only average rotational stability. Although both rotational stability and efficiency in the utilization of calcium carbonate conserve energy in the budget of the ammonoid, a premium was placed on efficiency in utilization of calcium carbonate under inferred anoxic stress, whereas in inferentially well-oxygenated habitats, selection for increased rotational stability is observed in evolutionary trends.

REFERENCES CITED

Burnaby, T. P. 1966. Allometric growth of ammonoid shells: A generalization of the logarithmic spiral. Nature 209:904-906.

Chamberlain, J. A. 1976. Flow patterns and drag coefficients of cephalopod shells. Palaeontology 19:539-563.

Collinson, J. W. 1968. Permian and Triassic biostratigraphy of the Medicine Range, northeastern Nevada. Earth Sci. Bull. Wyoming Geol. Assoc. 1:25-45.

Denton, E. J. 1974. On buoyancy and the lives of Modern and Fossil cephalopods. Proc. Royal Soc. London B185:273-299.

Dunbar, C. O. and K. M. Waage. 1969. Historical Geology. John Wiley and Sons, Inc., New York. 556 p.

Fenton, C. L. and M. A. Fenton. 1958. The Fossil Book. Doubleday and Company, Inc., Garden City, New York. 482 p.

Girty, G. H. 1910. The fauna of the phosphate beds of the Park City Formation in Idaho, Wyoming and Utah. U. S. Dept. Int. Geol. Survey Bull. 436. 82 p.

Gordon, M. Jr., R. K. Hose, and C. A. Repenning. 1957. Goniatite zones in the Chainman Shale equivalents (Mississippian), western Utah (Abstract): Geol. Soc. America Bull. 68. p. 1737.

Gordon, M. Jr. 1964. California Carboniferous cephalopods. U. S. Dept. Int. Geol. Survey Prof. Paper 483-A. 27 p.

Hallam, A. 1972. Models involving population dynamics. pp. 67-80 In T. J. M. Schopf (Ed.). Models in Paleobiology. Freeman, Cooper and Co., San Francisco. 250 p.

Heptonstall, W. B. 1970. Buoyancy control in ammonoids. Lethaia 3:317-328.

King, P. B. 1930. Geology of the Glass Mountains, Texas. Part I, Descriptive Geology. Univ. of Texas, Bureau of Econ. Geol. Bull. 3038. 167 p.

King, P. B. 1937. Geology of the Marathon Region. U. S. Dept. Int. Geol. Survey Prof. Paper 187. 148 p.

King, P. B. 1958. Geology of the Southern Guadalupe Mountains, Texas. U. S. Dept. Int. Geol. Survey Prof. Paper 215. 138 p.

King, R. E., C. O. Dunbar, C. Preston, Jr., and A. K. Miller. 1944. Geology and Paleontology of the Permian Area northwest of Las Delicias, southwestern Coahuila, Mexico. Geol. Soc. America Spec. Paper 52. 172 p.

Kummell, B. 1954. Triassic stratigraphy of southeastern Idaho and adjacent areas. U. S. Dept. Int. Geol. Survey Prof. Paper 254-H. 29 p.

Kummell, B. 1957. Paleoecology of Lower Triassic Formations of southeastern Idaho and adjacent areas. pp. 437-368. In H. S. Ladd (Ed.). Treatise on Marine Ecology and Paleoecology, Vol. 2. Geol. Soc. America. Mem. 67.

Kummel, B. and G. Steele. 1962. Ammonoids from the Meekoceras graciliatus Zone at Crittenden Spring, Elko County, Nevada Jour. Paleontology 36:638-703.

McCaleb, J. A. 1968. Lower Pennsylvanian ammonoids from the Bloyd Formation of Arkansas and Oklahoma. Geol. Soc. America. Spec. Paper 96. 123 p.

Miller, A. K. and L. M. Cline. 1934. The Cephalopods of the Phosphoria Formation of northwestern United States. Jour. Paleontology 8:281-302.

Miller, A. K. and W. M. Furnish. 1940. Permian ammonoids of the Guadalupe Mountain region and adjacent areas. Geol. Soc. America Spec. Paper 26. 242 p.

Miller, A. K. and E. J. Parizek. 1948. A lower Permian ammonoid fauna from New Mexico. Jour. Paleontology 22:350-358.

Miller, A. K., H. R. Downs and W. Youngquist. 1949. Some Mississippian cephalopods from Central and Western United States. Jour. Paleontology 23:600-612.

Miller, A. K., W. M. Furnish and O. H. Schindewolf. 1957a. In R. C. Moore (Ed.). Treatise on Invertebrate Paleontology, Pt. L., Mollusca 4. Geol. Soc. America and Univ. Kansas Press, Lawrence, Kansas. 490 p.

Moore, R. C., J. D. Frie, J. M. Jewett, L. Wallace and H. G. O'Connor. 1951. The Kansas Rock Column. Kansas St. Geol. Survey Bull. 89. 123 p.

Moore, R. C., C. G. Lalicker and A. F. Fischer. 1952. Invertebrate Fossils. McGraw-Hill Book Co., Inc., New York. 766 p.

Nassichuk, W. W., W. M. Furnish and B. F. Glenister. 1965. The Permian ammonoids of Arctic Canada. Geol. Survey. Canada Dept. Mines Tech. Surveys Bull. 131. 56 p.

Nassichuk, W. W. 1970. Permian ammonoids from Devon and Melville Islands, Canadian Arctic Archipelago. Jour. Paleontology 44:77-97.

Nassichuk, W. W. 1977. Upper Permian ammonoids from the Cache Creek group in Western Canada. Jour. Paleontology 51:557-590.

Newell, N. D., J. K. Rigby, A. G. Fischer, A. J. Whiteman, J. E. Hickox and J. S. Bradley. 1953. The Permian reef complex of the Guadalupe Mountains Region, Texas and New Mexico. W. H. Freeman and Co., San Francisco. 236 p.

Newell, N. D. 1957. Supposed Permian tillites in northern Mexico are submarine slide deposits. Geol. Soc. America Bull. 68:1569-1576.

Peterson, M. D. 1975. Upper Devonian (Famennian) ammonoids from the Canning basin, western Australia. Jour. Paleontology 49.

Plummber, F. B. and G. Scott. 1937. Upper Paleozoic ammonites in Texas. Univ. Texas Bureau Econ. Bull. 3701. 516 p.

Raup, D. M. 1967. Geometric analysis of shell coiling: Coiling in ammonoids. Jour. Paleontology 41:43-65.

Saunders, W. B. 1973. Upper Mississippian ammonoids from Arkansas and Oklahoma. Geol. Soc. America Spec. Paper 145. 110 p.

Seilacher, A. 1960. Epizoans as a key to ammonoid ecology. Jour Paleontology 34:189-193.

Sellards, E. H., W. S. Adkins and F. B. Plummer. 1932. The Geology of Texas. Vol. 1. Stratigraphy. Univ. Texas Bureau Econ. Geol. Bull. 3232. 818 p.

Smith, J. P. 1927. Upper Triassic marine invertebrate faunas of North America. U. S. Dept. Int. Geol. Survey Prof. Paper 141. 262 p.

Smith, J. P. 1932. Lower Triassic ammonoids of North America. U. S. Dept. Int. Geol. Survey Prof. Paper 167. 199 p.

Spinosa, C., W. M. Furnish and B. F. Glenister. 1970. Araxoceratidae, Upper Permian ammonoids from the western hemisphere. Jour. Paleontology 44:730-739.

Spinosa, C., W. M. Furnish and B. F. Glenister. 1975. The Xenodiscidae, Permian ceratoid ammonoids. Jour. Paleontology 49:239-283.

Stanton, R. J., Jr. and I Evans. 1972. Community structure and sampling requirement in paleoecology. Jour. Paleontology 46: 845-858.

Tasch, P. 1973. Paleobiology of the invertebrates. John Wiley and Sons Inc., New York. 923 p.

Tozer, E. T. 1965. Latest Lower Triassic ammonoids from Ellesmere Island and northeastern British Columbia. Geol. Survey Can. Dept. Mines Tech. Surveys Bull. 123. 45 p.

Trueman, A. E. 1941. The ammonite body chamber with special reference to the buoyancy and mode of life of the living ammonite. Quar. Jour. Geol. Soc. London 96:339-383.

Walker, K. R. 1972. Trophic analysis: A method for studying the function of ancient communities. Jour. Paleontology 46:82-93.

Ward, P., R. Stone, G. Westermann, and A. Martin. 1977. Notes on animal weight, cameral fluids, swimming speed and color polymorphism of the cephalopod Nautilus pompilius in the Fiji Islands. Paleobiology 3:377-388.

Webster, G. D. 1969. Chester through Derry conodonts and stratigraphy of northern Clark and Southern Lincoln Counties, Nevada. Univ. Calif. Pub. Geol. Sciences, Vol. 79, 107 p.

Westermann, G. E. G. 1971. Form, structure and function of shell and siphuncle in coiled mesozoic ammonoids. Life Science Contr. Royal Ont. Mus. 78. 39 p.

Yancey, T. E. 1975. Permian marine biotic provinces in North America. Jour Paleontology 49:758-766.

Youngquist, W. 1949. The cephalopod fauna of the White Pine Shale of Nevada. Jour. Paleontology 23:276-305.

Youngquist, W. 1949. The cephalopod fauna of the White Pine Shale of Nevada: Supplement Jour. Paleontology 23:613-616.

Ziegler, A. M., L. R. M. Cocks and R. V. Bambach. 1968. The composition and structure of Lower Silurian marine communities. Lethaia 1:1-27.